UNIVERSITY OF DURBAN-WESTVILLE

DEPARTMENT OF CHEMICAL ENGINEERING

MATHEMATICAL MODELLING OF THE DYNAMICAL INTERACTIONS BETWEEN KILLER AND SENSITIVE WINE YEAST SUBJECTED TO NUTRITIONAL STRESS

A. S. Vadasz

December 2000

MATHEMATICAL MODELLING OF THE DYNAMICAL INTERACTIONS BETWEEN KILLER AND SENSITIVE WINE YEAST SUBJECTED TO NUTRITIONAL STRESS

Alisa S. Vadasz

MATHEMATICAL MODELLING OF THE DYNAMICAL INTERACTIONS BETWEEN KILLER AND SENSITIVE WINE YEAST SUBJECTED TO NUTRITIONAL STRESS

by

Alisa S. Vadasz

Submitted in partial fulfilment of the requirements for the degree of

Master of Science in Bio-Chemical Engineering

MSc. Eng.

in the Department of Chemical Engineering in the

Faculty of Science and Engineering, at the University of Durban–Westville.

Supervisor: **Prof. M.E.E. Abashar**

Joint supervisor: **Prof. A. S. Gupthar**

December 2000

DECLARATION

I, Alisa S. Vadasz

REG. NO: 9509479

Hereby declare that the dissertation/thesis entitled

Mathematical modelling of the dynamical interactions between killer and sensitive wine yeast subjected to nutritional stress

is the result of my own investigation and research and that it has not been submitted in part or in full for any other degree or to any other university.

Alisa Vadasz

15 December 2000

ACKNOWLEDGEMENTS

I wish to express my sincere gratitude to all those who provided me encouragement and assistance during the course of this study. Special appreciation is extended to:

Professor M.E.E. Abashar of the Chemical Engineering Department and Professor A.S. Gupthar of the Biochemistry Department for their invaluable guidance and advice as supervisors of this research.

Professor P. Vadasz of the Mechanical Engineering Department, my husband and advisor, for his constant enthusiastic involvement, support, guidance, and assistance.

Professor M. Ariatti of the Biochemistry Department for his sustained interest, support and assistance whenever it was required.

Dr. Michael Gregory and Dr. Yougasphree Naidoo of the Electron Microscopy Unit for their assistance in producing the micrographs.

Mr Asok Rajh, the photographer of the Science Faculty, for assistance in his field.

My dear endless supporting and encouraging family, Peter, my husband, and Johnathan, Nataly and Gabriel, my children.

CONTENTS

LIST OF FIGURES AND TABLES

PAGE

PAGE

SYNOPSIS

A new mathematical model is proposed for the recovery of the complete dynamical interactions of cell growth of single wine yeast strains of *Saccharomyces cerevisiae*. This new model is extended and applied for two species competing over a common ecological niche, revealing theoretical and experimental evidence of extinction and coexistence during batch fermentation. The computational results were shown to compare well with the new experiments conducted for both the pure and mixed cultures. The results of the proposed model show that the batch yeast growth in a limited nutrient media (5% grape juice and pure water) is associated with substantial oscillations, which damp out over time, allowing the cell concentration to stabilise at the stationary equilibrium. In addition, the proposed model recovers effects that are frequently encountered in experiments such as a "*lag phase*" as well as an inflection point in the "*ln curve*" of the cell concentration. The proposed model also recovers the Logistic Growth Curve as a special case.

Keywords: Yeast growth; Nutritional stress; Population dynamics; Competitive exclusion.

CHAPTER 1

INTRODUCTION

1.1 Background

The significant importance of mathematical modelling in food microbiology was discussed extensively by Roberts, (1995) and Baranyi and Roberts, (1995). In particular, the growth of yeast is reported widely in connection with classical as well as more modern developments of mathematical models. From the very early stages of the application of models in population dynamics, yeast growth was used in their validation.

The choice of modelling approach depends on the purpose of the model. A common view in (evolutionary) biology is that mathematical models are mainly useful for making predictions that can be used in experimental work. However, the testable predictions of a model are not necessarily its main contribution to science. Insights, quantitative as well as qualitative aspects, provided by models, their ability to train ones intuition about complex phenomena, to provide a framework for studying such phenomena, and to identify key components in complex systems, are at least as important as specific predictions. For these purposes, the most useful tools are simple models and metaphors.

There are inconsistent theoretical results that, in some cases, recover excellently the growth curve of microorganisms (Pearl, 1927) while other cases show substantial qualitative as well as quantitative discrepancies (Baranyi and Roberts, 1994). Some of these discrepancies are the existence of a *"lag phase"*, the existence of an inflection point on the *"log curve"* of the cell concentration, and the existence of overshooting and an oscillatory mode of growth. Figure **1.1** (Vadasz, A.S., 1999) reveals few of the unrecovered characteristics of batch yeast growth under nutritional stress, such as the existence of an inflection point on the *"log curve"* of the cell concentration, a possible

existence of overshooting and an oscillatory mode of growth. These indicate the limitations of the existing models to capture all the possibilities of the macro growth nature, which is affected by various dynamical internal and external conditions. These facts motivate the current study.

Mathematical models of populations (plants and organisms) aim to understand the way different kinds of biological and physical interactions affect the dynamics of the various species. There are many important elements to consider in constructing mathematical models, such as factors that determine the numerical magnitude of the population, parameters that determine the time scale of an adaptive response to environmental changes, and accordingly the type of response, tracing the environmental variations or averaging over them (May, 1981).

There are two broad categories of models. The first, spatially homogeneous (when the population concentration distribution in space is assumed to be uniform), deals with the dependence of population changes over time such as continuous, discrete or delay. (Krebs, 1978; May, 1981; Edelstein-Keshet, 1988). The second, spatially heterogeneous, deals with spatial distribution of population concentrations and includes types as "spatio-temporal" or "patches" (Krebs, 1978; May, 1981; Edelstein-Keshet, 1988). At one extreme, continuous growth is when there is a complete overlap between generations and the population changes continuously in time. At the opposite extreme, discrete growth is where there is no overlapping between generations, the population growth occurs in discrete time steps and reproduce at fixed intervals. Most real life regulatory mechanisms are likely to operate with some built-in delay, therefore, delay models were developed, first introduced by Hutchinson, (1948) (May, 1975). Spatially heterogeneous models are concerned with the distribution over space and time.

(a)

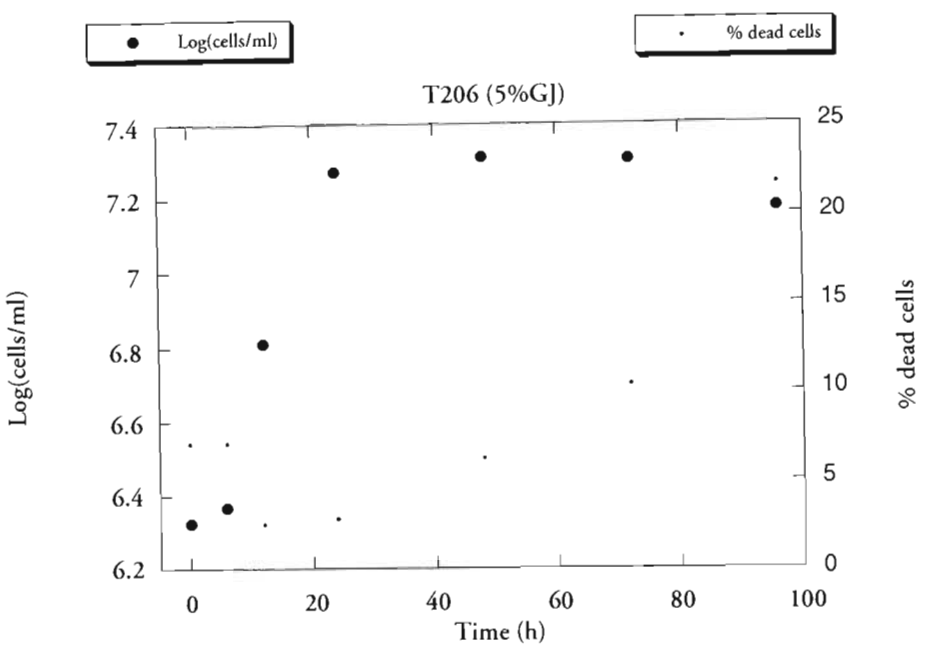

(b)

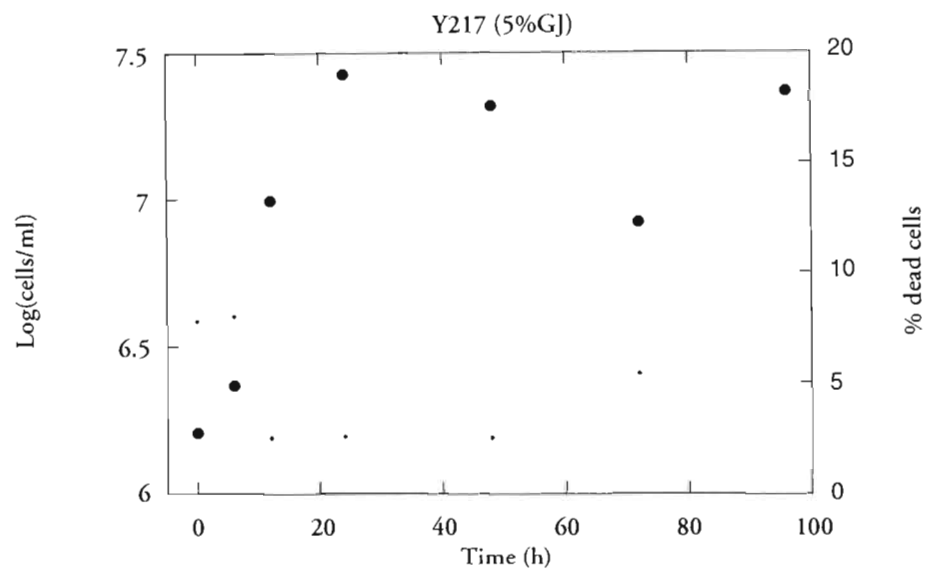

Figure **1.1** Log of cell number per ml and % dead cells of microscale batch fermentation involving single cultures of *Saccharomyces cerevisiae* (a) a sensitive strain, Y217 and (b) a K_2 killer strain, T206, growing in 5% grape juice (GJ).

1.2 Literature review

1.2.1 Discrete versus continuous modelling

Both discrete and continuous models of population growth studied so far, deal with a population as a continuous, rather than discrete variable, where n denotes a population size and $x = n / A$ where A is area, or $x = n / V$ where V is volume. When the size of a population is large, the approximation of a continuous n is reasonable especially when one normalises it: $n_* = n / n_{\max}$. Therefore, the distinction between continuous and discrete models refers to continuous and discrete in time and both consider the population size as a continuous variable. While for some species their reproduction habits are season-linked, for others they are not. For those which exhibit affinity to seasons, a discrete model in time indicating the reproduction rate from one reproduction season to another is possible, and most probably more accurate than the model that is continuous in time. However, for the others a continuous model in time seems more appropriate.

1.2.2 Continuous modelling of an isolated species

1.2.2.1 A pure culture

Naturally, populations of plants and organisms tend to interact with their biological and physical environment. Simple models of environmentally controlled single species capture the general principles of behavioural patterns.

1.2.2.1.1 Malthus' model (Simple birth and death)

This model applies in an unlimited habitat (a suitable ecological environment).

Life support system (LSS) is defined as the collection of all *life support elements* in the culture environment, allowing for active growth. These include nutrition, temperature and a vital range of pH levels. Pertinent to active growth, the following parameters are considered:

Natural birth rate: ax where a is the specific (relative) natality rate.

Natural death rate: bx where b is the specific (relative) morality rate.

The rate of change of the population size x is

$$\frac{dx}{dt} = (a-b)x \tag{1-1}$$

The specific (relative) growth rate, μ, is defined in the form

$$\mu = (a-b) \tag{1-2}$$

Substituting (1-2) into (1-1)

$$\frac{dx}{dt} = \mu x \tag{1-3}$$

This is an equation for a single species without competition and with an unlimited supply of life support elements.

The solution of (1-3) is obtained via direct integration

$$x = x_0 e^{\mu t} \tag{1-4}$$

where x_0 is the initial cell concentration, i.e. at $t = 0$. This solution is presented graphically in Figure **1.2**.

From (1-3) one can observe that

$$\frac{1}{x}\frac{dx}{dt} = \mu \tag{1-5}$$

Therefore, μ, indeed represents the relative (or specific) growth rate.

Another form of equation (1-5) is

$$\frac{d(\ln x)}{dt} = \mu \tag{1-6}$$

suggesting the introduction of a new variable, y_K

$$y_K = \ln x \tag{1-7}$$

Then equation (1-6) becomes

$$\frac{dy_K}{dt} = \mu \tag{1-8}$$

leading to the solution

$$y_K = \mu t + y_{K_0} \tag{1-9}$$

Where y_{K_0} is the initial value of y_K, i.e. at $t = 0$.

The major problem with *Malthus' model* is that the solution is not bound as $t \to \infty$, for $\mu > 0$. The solution (1-3) yields the following limits:

as $t \to \infty \Rightarrow x \to \infty$ for $\mu > 0$, and $x = 0$ for $\mu < 0$ (as $t \to \infty$) (1-10)

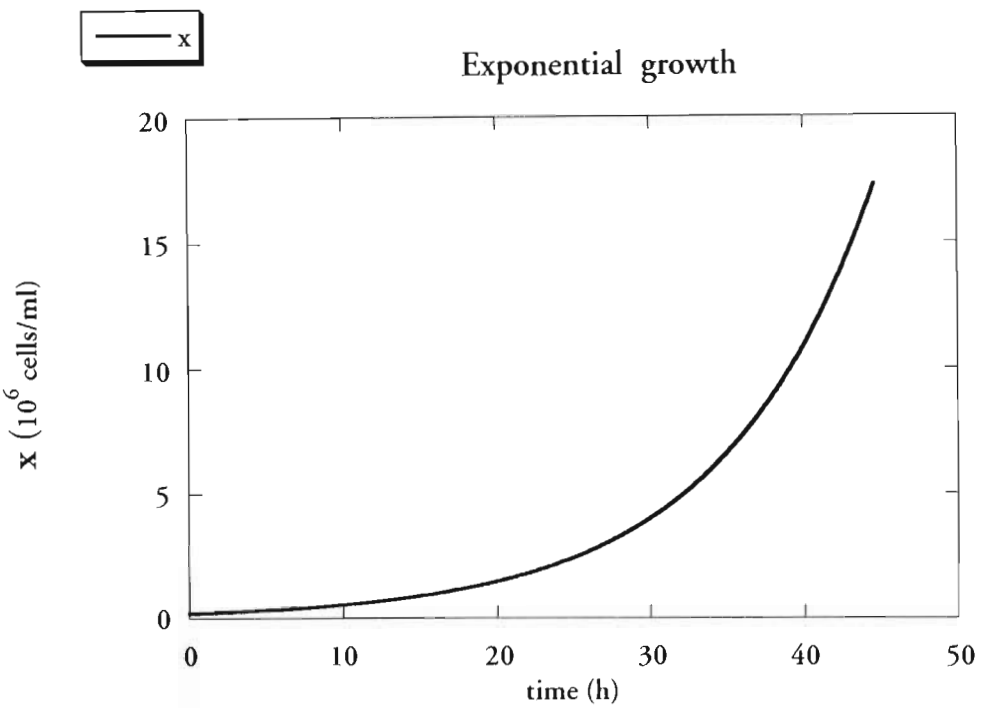

Figure **1.2** Exponential growth following equation (1-4), $x_0 = 0.2 \times 10^6$ (cells / ml), $\mu > 0$.

1.2.2.1.2 Pearl - Verhulst model (Logistic growth model or LGM)

In order to obtain a more realistic representation of the dynamics of the interaction between the yeast population and its habitat, one needs to consider a finite size of the habitat. In a finite habitat (ecological environment), it is expected that crowding somehow affects the relative growth rate, e.g. by exerting excessive demands upon food supply and thereby decreasing fecundity or even causing starvation. In other words, the relative growth rate, μ in equation (1-3), should, therefore, be decreased by a term proportional to the population size or its concentration;

$$\frac{dx}{dt} = (\mu - \beta x)x \qquad (1\text{-}11)$$

This is an equation for a single species (strain) without competition from other species (strains), but including internal competition on the source of LSS (*1.2.2.1.1*).

Integrating equation (1-11)

$$\frac{dx}{(\mu - \beta x)x} = \int dt + C_0 \qquad (1\text{-}12)$$

yields

$$x = \frac{\mu e^{\mu t}}{\beta e^{\mu t} + C} \quad (for\ \mu \neq 0) \qquad (1\text{-}13)$$

where

$$C = \frac{\mu - \beta x_0}{x_0} \qquad (1\text{-}14)$$

Substituting equation (1-14) into (1-13) yields

$$x = \frac{x_0 \mu e^{\mu t}}{\beta x_0 \left(e^{\mu t} - 1\right) + \mu} \quad (for\ \mu \neq 0) \tag{1-15}$$

The stationary points (or steady state solutions) of equation (1-11) are obtained by setting $dx/dt = 0$ in equation (1-11), in the form

$$x = 0 \quad \text{and} \quad x = \frac{\mu}{\beta} \tag{1-16}$$

One can observe from equation (1-15) that for an initial condition $x_0 = 0$ the solution (1-15) is $x = 0$ for all values of t. However, for any other value of x_0, one can observe the long term solution by representing equation (1-15) after dividing both numerator and denominator by $e^{\mu t}$, to obtain

$$x = \frac{x_0 \mu}{\beta x_0 + (\mu - \beta x_0) e^{-\mu t}} \tag{1-17}$$

From equation (1-17) one clearly obtains

$$x = \frac{x_0 \mu}{x_0 \beta} \qquad as\ \ t \to \infty \tag{1-18}$$

or

$$x = \frac{\mu}{\beta} \qquad as\ \ t \to \infty \quad for \quad x_0 \neq 0 \tag{1-19}$$

Therefore, the steady-state solution $x = 0$ is obtained only when the initial conditions are $x_0 = 0$, i.e. in absence of x-yeast at $t = 0$. The steady-state solution $x = \mu/\beta$ is obtained for any other initial conditions (naturally $x > 0$). The linear stability analysis of these two

steady-state solutions is presented in Appendix A.1 (A.1.1). This analysis concludes that the steady-state solution $x = \mu/\beta$ is stable and $x = 0$ is unstable if $\mu > 0$, while $x = \mu/\beta$ becomes unstable and $x = 0$ becomes stable if $\mu < 0$.

As the case when $\mu > 0$ is the one of relevance to this study, it is convenient to use the notation

$$\delta = \frac{\mu}{\beta} \tag{1-20}$$

Therefore, equation (1-11) can be presented in the form

$$\frac{dx}{dt} = \mu x\left(1 - \frac{x}{\delta}\right) \tag{1-21}$$

For $\mu > 0$ the effective growth rate, $\left(1 - \frac{x}{\delta}\right)$, is positive if $x < \delta$, and negative if $x > \delta$. It leads to a globally stable equilibrium point at $x = \delta$. This value $x = \delta = \mu/\beta$ may be thought of as the *"carrying capacity of the habitat (environment)"*, as determined by the life support system (LSS).

The solution (1-15) can be presented in terms of δ in the form

$$x = \frac{\delta e^{\mu t}}{\left(e^{\mu t} + \frac{\delta}{x_0} - 1\right)} \tag{1-22}$$

or

$$x = \frac{\delta}{1 + \left(\frac{\delta}{x_0} - 1\right) e^{-\mu t}} \tag{1-23}$$

with $x = \delta$ as $t \to \infty$ $(for \quad x_0 \neq 0)$.

At $t = 0$

$$\left(\frac{dx}{dt}\right)_{t=0} = \mu x_0\left(1 - \frac{x_0}{\delta}\right) \tag{1-24}$$

and at $t \to \infty$

$$\left(\frac{dx}{dt}\right)_{t\to\infty} = 0 \qquad [(1-21) \quad and \quad x = \delta] \tag{1-25}$$

From eq. (1-24) it is clear that the only cases when the initial slope of the growth curve is zero are (i) when $x_0 = \delta$ or (ii) when $x_0 = 0$. Otherwise, the initial slope of the growth curve is positive if $x_0 < \delta$ or negative if $x_0 > \delta$. The inflection point of the growth curve represents the point where the curve changes its shape from concave to convex. Applying the second derivative of x on equation (1-21) and equating to zero gives the inflection points in the resulting solution $x(t)$

$$\frac{d^2x}{dt^2} = \mu - 2\frac{\mu}{\delta}x = 0$$

$$\frac{d^2x}{dt^2} = \mu\left(1 - 2\frac{x}{\delta}\right) = 0 \tag{1-26}$$

$$x_{infl.pt.} = \frac{\delta}{2} = \frac{\mu}{2\beta} \tag{1-27}$$

which upon substitution in (1-23) yields

$$\left[1 + \left(\frac{\delta}{x_0} - 1\right)e^{-\mu t}\right]\frac{\delta}{2} = \delta$$

$$\left[1+\left(\frac{\delta}{x_0}-1\right)e^{-\mu t}\right]=2$$

$$\left(\frac{\delta}{x_0}-1\right)e^{-\mu t}=1$$

$$e^{\mu t}=\frac{\delta}{x_0}-1$$

$$\mu t=\ln\left(\frac{\delta}{x_0}-1\right)$$

$$t_{infl.pt.}=\ln\left(\frac{\delta}{x_0}-1\right)^{-\mu} \qquad (1\text{-}28)$$

The solution (1-22) or (1-23) represents a sigmoid as presented graphically in Figure **1.3**, for different values of K_o, ($\mu = 0.2\ s^{-1}$). From equations (1-27) and (1-28), one observes that while the value of x at the inflection point is independent of the initial conditions ($x_{infl.pt.}$ does not depend on x_0), the time value when the inflection point occurs does depend on the initial conditions (i.e., $t_{infl.pt.}$ does depend on x_0).

For initial conditions $x_0 > \delta/2$ the solution does not pass through an inflection point (the inflection point occurs then at $t<0$). Furthermore, for $x_0 > \delta$, at $t=0$: $t=0 \quad \frac{dx}{dt}<0$, and the solution (1-13) $x=\delta/\left[1-\left(1-\delta/x_0\right)e^{-\mu t}\right]$, can be represented graphically as shown in Figure **1.3** by the top two curves.

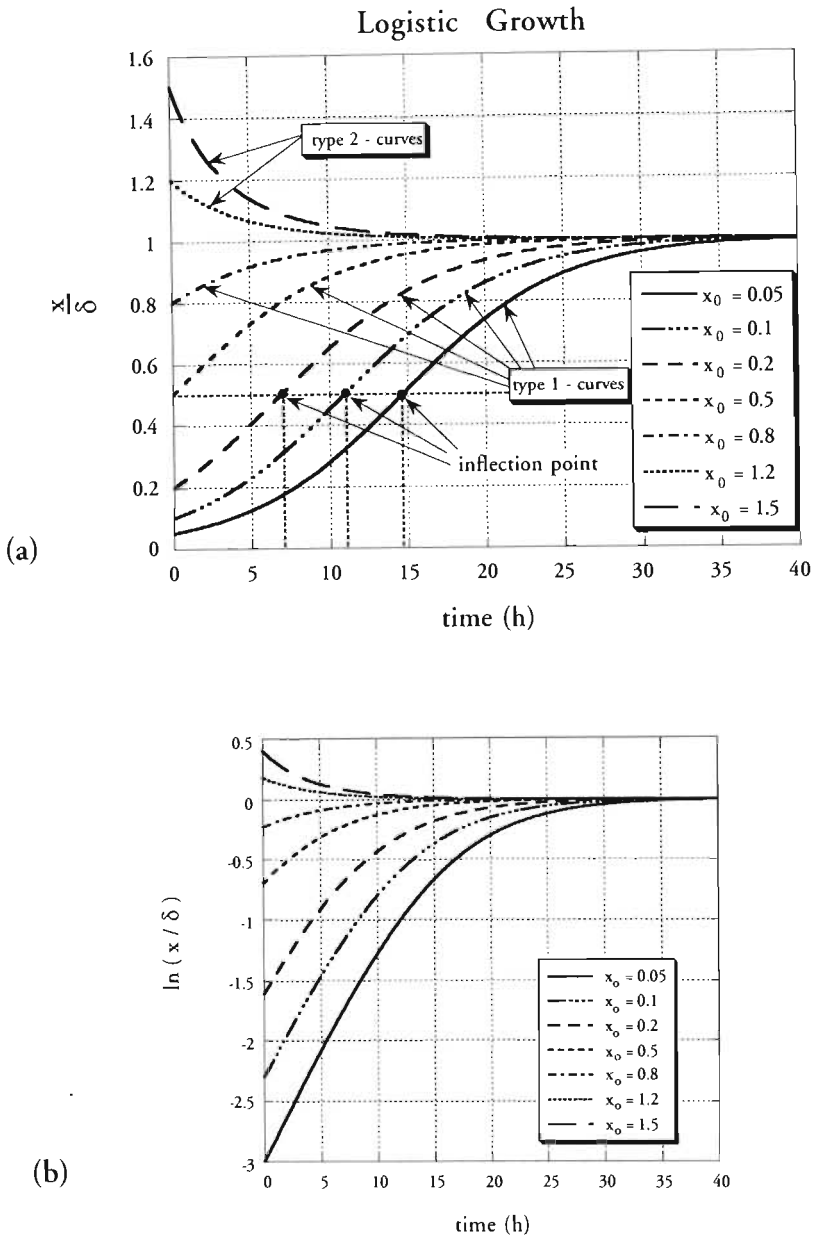

Figure **1.3** Graphical description of the family of Logistic Growth curves corresponding to the analytical solution, equation (1-23), of the Logistic Growth Model (LGM), equation (1-24). (a) The family of curves for cell concentration versus time, and (b) the family of *ln curves* of the cell concentration versus time.

A slightly more general class of equations proposed by Blumberg (1968) gives the possibility to adjust the inflection point according to the specific population growth characteristics. It should be realised that the right hand side of equation (1-11) could be the first terms of a *Taylor expansion* of a function $f(x)$ as indicated by Edelstein-Keshet, (1988), e.g.

$$\frac{dx}{dt} = f(x) \qquad \text{where} \qquad f(x) = C_0 + C_1 x + C_2 x^2 + C_3 x^3 + \ldots$$

As the growth rate is zero when $x = 0$, since at least one individual must exist for the population to grow at all, thus $C_0 = 0$.

There are at least two qualitative discrepancies between this model and the experimental evidence in the growth of yeast:

1. The present model does not recover the "lag" phase of the growth dynamics curve.

2. The present model does not recover the inflection point on the "ln curve" of the cell concentration.

1.2.2.1.3 Hutchinson model (Logistic population growth with delay)

In the attempt to address the first qualitative discrepancy indicated previously, i.e. the lack of a "lag" phase (where $x = \text{constant}$, i.e. $dx/dt = 0$) in the logistic population growth solution, one can introduce a correction to the *Pearl – Verhulst model.*

The *Hutchinson model* was developed in an attempt to correct the fact that in equation (1-21) the density (concentration) dependent regulatory mechanism as represented by the factor $(1 - x/\delta)$ operates instantaneously. By considering that these regulatory effects are

likely to operate with some built-in time lag, whose characteristic magnitude may be denoted by τ, one can incorporate such time delays in equation (1-21) in the form of

$$\frac{dx}{dt} = \mu x\left[1 - \frac{x(t-\tau)}{\delta}\right] \tag{1-29}$$

This delay-differential equation was first introduced into ecology by Hutchinson, (1948) and Wangersky and Cunningham, (1957) and reviewed by May, (1975). More realistically, the regulatory term is likely to depend not on the population at a time exactly τ minutes (or other time units) earlier, but rather on some smooth average over past populations (e.g. May, 1973)

$$\frac{dx}{dt} = \mu x\left[1 - \int_{-\infty}^{t} Q(t-t')\,x(t')\,dt'\right] \tag{1-30}$$

Equation (1-29) is the special case when Q is a delta-function $Q(t) = \Delta(t-\tau)/\delta$.

1.2.2.2 Continuous modelling of two species competing over a common ecological niche

Some strains of yeast, called "killer", secrete into the growth medium toxins, which are lethal for other yeast strains, called "sensitive". The killer yeast is immune to the toxin it releases. Viral RNA, which inhabits the killer yeast encodes the killer toxin. This may suggest that the virus that produces the mycotoxin lives in a mutual - symbiotic relationship with its yeast host (Wickner, 1976).

The model of competition to be developed in this study is applied to the interaction between a killer and a sensitive strain of yeast growing in a mixed culture, as well as to the interaction between two different sensitive strains of yeast.

There are two general approaches in attempting modelling of physical phenomena. The first is the "microscopic" approach, which tends to describe mathematically all possible known effects up to most of the relevant details. The second is a "macroscopic" approach, which attempts to find the simplest possible mathematical representation of a physical reality and introduce lumped parameters into the latter in order to represent the global impact of the more complicated "microscopic" details on the system.

The first approach was used, for example by Ramon-Portugal *et al.* (1997) for modelling the interaction between one killer and one sensitive strain of yeast growing in a mixed culture. They formulated their mathematical model by expressing rate equations for the evolution of the killer toxin concentration as well as the interaction and growth between the killer and sensitive strains of yeast. They obtained eventually a set of five non-linear ordinary differential equations and solved the system numerically. An even more microscopic approach to the same problem would require including in the model the mutually symbiotic relationship between the virus and killer-yeast host.

The second approach is applied in this study, where an attempt is made to represent the effect of the killer-toxin as a lumped parameter in a model of two species competing over a common ecological niche. The logical derivation of the model is provided along with a critical review of the fundamental competition models, starting with the classical competition model of Lotka-Volterra. The relevance and possible introduction of the killer-toxin effect in such models is introduced along with the presentation of this critical review.

1.2.2.2.1 *Classical model for two species (sensitive or killer)* **competing over a common ecological niche**

The classical model for two species competing over a common ecological niche was introduced as an extension of the Logistic Growth Model (LGM), which applies for one species in isolation and in an homogenous habitat. Considering x_1 and x_2 to represent the concentration of these two different species (in the present case the two strains of yeast), respectively, then μ_1 and μ_2 represent their corresponding maximum specific growth rates in isolation. The quantity of available nutrition will diminish in proportion to the total population size (or cell concentration). However, the two different species (strains) affect the food supply in different degrees. The first species, carrying the index 1, diminishes the nutrition supply by $h_1 x_1$ per unit time while the second species, carrying the index 2, diminishes the nutrition supply by $h_2 x_2$, giving a total nutrition consumption rate of $(h_1 x_1 + h_2 x_2) > 0$ ($h_1 > 0$ and $h_2 > 0$). The diminished nutrition supply affects the specific growth rates at different degrees depending on the effectiveness of food utilisation of each species. Introducing these considerations into the Logistic Growth Model yields the following classical system of equations

$$\frac{\mathrm{d}x_1}{\mathrm{d}t} = \left[\mu_1 - \gamma_1(h_1 x_1 + h_2 x_2)\right] x_1 \qquad (1\text{-}31)$$

$$\frac{\mathrm{d}x_2}{\mathrm{d}t} = \left[\mu_2 - \gamma_2(h_1 x_1 + h_2 x_2)\right] x_2 \qquad (1\text{-}32)$$

where γ_1 and γ_2 are food utilisation factors for each species, which depends for example on the species metabolism and its consequent level of effectiveness in utilising the available nutrition for growth. The system of equations (1-31)-(1-32) can be presented in the following equivalent form

$$\frac{\mathrm{d}\,x_1}{\mathrm{d}\,t} = \gamma_1\left[\phi_1 - \left(h_1 x_1 + h_2 x_2\right)\right] x_1 \tag{1-33}$$

$$\frac{\mathrm{d}\,x_2}{\mathrm{d}\,t} = \gamma_2\left[\phi_2 - \left(h_1 x_1 + h_2 x_2\right)\right] x_2 \tag{1-34}$$

where the following notation is introduced. A further notation will be used later

$$\phi_1 = \frac{\mu_1}{\gamma_1} \;\; ; \quad \phi_2 = \frac{\mu_2}{\gamma_2} \;\; ; \qquad \beta_1 = \gamma_1 h_1 \;\; ; \qquad \beta_2 = \gamma_2 h_2 \;\; ; \tag{1-35}$$

The steady state solutions of the system of equations (1-33)-(1-34) are obtained by setting $\left(\mathrm{d}\,x_1/\mathrm{d}\,t\right) = \left(\mathrm{d}\,x_2/\mathrm{d}\,t\right) = 0$ and obtain

$$\left[\phi_1 - \left(h_1 x_1 + h_2 x_2\right)\right] x_1 = 0 \tag{1-36}$$

$$\left[\phi_2 - \left(h_1 x_1 + h_2 x_2\right)\right] x_2 = 0 \tag{1-37}$$

Solving the algebraic system of equations (1-36) and (1-37) provides the following steady state solutions

S1: $\quad x_{st1} = 0 \quad$ and $\quad x_{st2} = 0$ (1-38)

S2: $\quad x_{st1} = 0 \quad$ and $\quad x_{st2} = \dfrac{\phi_2}{h_2} = \dfrac{\mu_2}{\beta_2} = \delta_2$ (1-39)

S3: $\quad x_{st1} = \dfrac{\phi_1}{h_1} = \dfrac{\mu_1}{\beta_1} = \delta_1 \quad$ and $\quad x_{st2} = 0$ (1-40)

S4: $$\begin{cases} h_1 x_1 + h_2 x_2 = \phi_1 \\ h_1 x_1 + h_2 x_2 = \phi_2 \end{cases} \tag{1-41}$$

The steady states S1-S3 are stationary points, while S4 is a stationary line. The latter is the solution of the linear system

$$\begin{bmatrix} h_1 ; h_2 \\ h_1 ; h_2 \end{bmatrix} \begin{bmatrix} x_{st1} \\ x_{st2} \end{bmatrix} = \begin{bmatrix} \phi_1 \\ \phi_2 \end{bmatrix} \tag{1-42}$$

It is obvious from equation (1-42) that the determinant of the coefficients' matrix H vanishes, i.e. $\det[H] = h_1 h_2 - h_1 h_2 = 0$. Therefore, the only possible solution for S4 corresponds to the necessary condition $\phi_1 = \phi_2 = \phi$. Then, the solution lies on the straight line expressed by

$$h_1 x_{st1} + h_2 x_{st2} = \phi \tag{1-43}$$

The linear stability of these steady states is presented in Appendix A.1 (A.1.2), and they are summarised in the following Table **1.1**.

Table **1.1** Linear stability of steady state solutions for the classical model of competition

Steady State Solution	Linear Stability Conditions
S1 $x_{1S} = 0$ & $x_{2S} = 0$	$\mu_1 < 0$ & $\mu_2 < 0$
S2 $x_{1S} = 0$ & $x_{2S} = \delta_2$	$h_1\delta_1 < h_2\delta_2$ & $\mu_2 > 0$
S3 $x_{1S} = \delta_1$ & $x_{2S} = 0$	$h_1\delta_1 > h_2\delta_2$ & $\mu_1 > 0$
S4 $h_1 x_{1S} + h_2 x_{2S} = \phi$	Globally Stable if $\mu_1 > 0$ & $\mu_2 > 0$ subject to $\phi_1 = \phi_2 = \phi$.

The results expressed by the steady states S1-S3 introduced "Volterra's Competitive Exclusion Principle" which can be formulated in the following form: "If two species are competing over a common ecological niche and $h_1\delta_1 < h_2\delta_2$, then the first species (carrying the index 1) is doomed to extinction, and the second species (carrying the index 2) survives and attains a limit population size of $x_{2S} = \delta_2$". In all these cases, the marginal stability is monotonic and neither periodic solutions nor overshooting are, therefore, possible.

The only possibility of coexistence of the two species occurs if the steady state S4 materialises. The condition for its existence, i.e. $\phi_1 = \phi_2 = \phi$, is extremely limiting and implies that both species behave similarly as far as their growth to food utilisation ratio is concerned. Nevertheless, in nature, there are plenty of examples where coexistence of species does occur in the same habitat. The latter motivated DeBach, (1966) to reformulate the "Competitive Exclusion Principle" and present it as the "Coexistence Principle" in the form: "Different species which coexist indefinitely in the same habitat must have different ecological niches, that is they must not be ecological homologues". Furthermore, the concept of niches within the same habitat was developed substantially (MacArthur, 1968). Excellent reviews of the niche theory and niche overlap is presented by May, (1981b) and Pianka, (1981). Furthermore, May, (1981b) suggests that a major motivation for investigations along the lines of the niche theory was driven by the need to estimate the values of the coefficients h_1 and h_2 in equations (1-31)-(1-34).

Yet, the experimental results of two yeast strains grown in a mixed culture in pure water (see section 3.3.4.2 and Figures **3.36-3.46**) show that for initial conditions at a ratio of 1:1 between each two strains considered, the result was always one of coexistence. It is very unlikely to believe that in the pure water habitat there is a multiplicity of different ecological niches, nor that the very stringent condition corresponding to the steady state

solution S4 above is fulfilled by all yeast strains used in the experiments. Since the reason for the very stringent condition of coexistence in the classical model presented above is the fact that $\det[H] = h_1 h_2 - h_1 h_2 = 0$. A modification of the classical model is, therefore, needed by imposing the requirement $\det[H] \neq 0$ that may accommodate coexistence subject to less stringent conditions.

A mycovirus-cured derivative of the killer yeast *Saccharomyces cerevisiae* T206 was produced by cycloheximide treatment (Fink and Styles, 1972) and used as the killer control (3.2.2.2). This treatment or curing of the killer yeast deletes its ability to produce and release toxin.

The complete and correct modelling of the interaction between killer and sensitive cells needs to take into consideration the individual dynamics of the killer and sensitive yeast in isolation, as well as the additional component of the killer-toxin effects on the sensitive yeast population (Chapter 3).

The killer toxin has the ability to perforate the cell wall of the sensitive cells (Vadasz, A.S. 1999; Vadasz *et al.*, 2000), and this can be the reason for adding vital nutrients from within the killed cells. Although the toxin destruction of the sensitive cells was observed while growing under conditions of extreme limiting vital nutrients, the percent of sensitive dead cells was relatively low in comparison with cells growing in a rich medium. Growing under nutritional stress affects the levels of production and activity of the killer toxin. Also, examination of cells under electron microscopy revealed that healthy cells develop physical protective structures (Vadasz, A.S. 1999; Vadasz *et al.*, 2000).

1.3 Unanswered questions and motivation for the proposed research

Pearl, (1927), whose Logistic Growth Model (LGM) is still widely used, reported experimental results of yeast growth based on Carlson, (1913) and compared them to his proposed Logistic Growth Model (LGM) results. The experimental results fitted excellently with Pearl's logistic curve that represented the solution of the LGM. Pearl, (1927) suggested the LGM as a universal model for population growth and not only for yeast. However, experiments carried out in populations other than yeast indicated that the LGM does not recover essential features and, therefore, might not be appropriate in all cases, reducing its general applicability as well as the claim of its universality. In some cases, a strong point was made in favour of using models that are discrete rather than continuous in time, even in spatially-homogeneous media (May, 1995). Excellent reviews of this and other relevant topics are presented by Pielou, (1969), Krebs, (1978), May, (1975, 1981) and Edelstein-Keshet, (1988).

The two most common substantial qualitative features that the LGM does not recover but they appear in experiments is the existence of a *"Lag Phase"* at the initial stage, and the existence of an inflection point on the *"ln curve"* of the cell concentration (or *"log curve"*). Baranyi and Roberts, (1994) provide an excellent explanation of the reason why the LGM can not recover the inflection point on the *"ln curve"* of the cell concentration in the cases where a *"Lag Phase"* is present. The inability of the LGM to recover the two basic qualitative features mentioned above (i.e. the existence of the *"Lag Phase"* and the existence of an inflection point in the *"ln curve"* of the cell concentration) provided a strong motivation to develop other models that resolve these discrepancies. Baranyi and Roberts, (1994) report such a new model proposed by Baranyi *et al.*, (1993). Their new model is essentially an extended non-autonomous version of the Logistic Growth Model (LGM). Non-autonomous models are indeed acceptable in natural environments where

diurnal or other time variations of temperature, pH as well as other medium parameters occur, therefore, imposing on the growth parameters a time dependence. There is substantial experimental evidence that the latter parameters affect substantially the results. However, the motivation provided by Baranyi and Roberts, (1994) for suggesting a non-autonomous model was for recovering the microbial growth in a well-controlled batch culture experiment for a constant environment, and in particular, in recovering the *"lag phase"*. Their argument is that the *"lag phase"* is a result of the "*inertia*" that the cell population possesses from growing previously in another environment, prior to being inoculated and grown in the actual environment. This is indeed the process that typical batch experiments follow. However, other explanations for the existence of the *"lag phase"* support the view that it is essentially linked to the time delay needed for the cells to transfer available nutrition from the medium into the cell before they can use it for growth and cell division.

There are additional qualitative as well as quantitative discrepancies between the LGM solution and experimental results. More recent experimental results suggest the existence of overshooting and oscillations either in spatially homogeneous yeast growth media (Davey *et al.*, 1996) as well as in spatio-temporal experiments of Boiteaux and Hess, (1978) and Haken, (1979). While there are a large number of reports which suggest that oscillations in the enzyme and metabolite concentrations are linked to the cells' growth (e.g. De la Funte, 1999; Wolf and Heinrich, 1997), very limited results suggest the existence of oscillations in the cell concentration itself. The former results are controlled by autocatalytic chemical reactions that are known to exhibit oscillations. The latter correspond to measuring the yeast growth in continuous cultures.

The aim of this study is to present a new autonomous, dynamical growth model. The proposed model is compared with new experimental results in order to confirm the

existence of overshooting as well as oscillations during the batch yeast growth of *Saccharomyces cerevisiae* in pure and mixed cultures, subjected to nutritional stress (5% grape juice and pure water). Furthermore, the new autonomous, dynamical model needs to recover all the qualitative features that the LGM fails short, and to present the LGM solution as one optional solution of the model.

CHAPTER 2

PROBLEM FORMULATION

2.1 Problem formulation for a single species

Some repetition of matters discussed in Chapter 1 is required in order to formulate the present problem and to place it in proper context.

Pearl, (1927) suggested an extraordinarily simple model for population growth and applied it for a wide variety of experimental data, indicating in most cases an outstanding fit. While there were substantial challenges to fitting his model as a universal law, he showed in the case of yeast an excellent match with experimental results based on Carlson, (1913). The Logistic Growth Model (LGM) suggested independently by Pearl, (1927) was derived earlier also by Verhulst, (1838) but was practically forgotten and overlooked for almost ninety years. It essentially suggests that the concentration of a particular population, yeast cells in our case, is governed by the following equation

$$\frac{\mathrm{d}x}{\mathrm{d}t} = \mu\left(1-\frac{x}{\delta}\right)x \quad , \tag{2-1}$$

where x is the viable cell concentration, δ is the carrying capacity of the environment, and μ, the maximum specific growth rate.

The analytical solution to Equation (2-1) expressed in the form,

$$x = \frac{\delta}{1+\left(\frac{\delta}{x_o}-1\right)\mathrm{e}^{-\mu t}} \quad , \tag{2-2}$$

where x_o is the initial cell concentration, yields the familiar "*S*" shaped logistic curve. The family of curves represented by the solution (2-2) of the LGM equation (2-1) is presented in Figure **1.3a**. From the figure, it can be observed that there are two types of curves corresponding to whether $x_o < \delta$, or whether $x_o > \delta$. It seems that there is no experimental evidence that recovered the type of curve associated with $x_o > \delta$. It has been shown, and it can be observed in Figure **1.3a** that for initial conditions corresponding to $x_o < \delta/2$ (for $\mu > 0$) an inflection point exists in the logistic curve solution $x(t)$ according to equation (2-2). The inflection point is recovered at a value of $x = x_{infl.\ point} = \delta/2$. However, when a logarithm of this solution is presented, i.e. $\ln(x(t))$ or $\log(x(t))$, this inflection point disappears, i.e. the logarithm of the cell count concentration according to the LGM's solution (2-2) can not recover an inflection point, as can be observed in Figure **1.3b**. Actually, these are convex curves monotonically increasing (for $x_o < \delta/2 < \delta$) and stabilizing at the non-trivial stationary value $x = \delta$. The trivial stationary value $x = 0$ is unstable for $\mu > 0$. Pearl, (1927) showed an excellent match between the LGM solution expressed by equation (2-2) and experimental results reported by Carlson, (1913).

On the other hand, there is substantial evidence from other, more recent, experimental results indicating that an inflection point is recovered on the logarithm of the cell-concentration graph (Baranyi and Roberts, 1994).

One way to incorporate a *"Lag Phase"* in a Logistic Growth Model was proposed by Hutchinson, (1948) and Wangersky and Cunningham, (1957). Hutchinson's model was developed in an attempt to correct the fact that in equation (2-2) the concentration dependent regulatory mechanism represented by the factor $[1 - x/\delta]$ operates instantaneously. By considering that these regulatory effects are likely to operate with

some built-in time lag, τ, one can incorporate such time delays in the LGM equation as suggested in equations (1-29) and (1-30).

The major objection to using the **delay-models** proposed in equations (1-29) and (1-30) is the fact that if there is a regulatory delay mechanism in the system it should be recovered as part of the solution and not provided as part of the input data or parameters. The time delay, τ, or the delay delta function, Q, become input parameters in the delay models.

Other formulations of growth models were proposed as variations of the LGM equation (2-1) by considering different forms of the specific growth rate. In general, this can be presented in the form

$$\frac{\mathrm{d}x}{\mathrm{d}t} = x\mu f(x) \quad , \tag{2-3}$$

where $\mu f(x)$ is the relative growth rate and different forms of the function $f(x)$ have been proposed. Edelstein-Keshet, (1988) proposes for a sufficiently smooth function to consider its Taylor series form $f(x) = a_1 x + a_2 x^2 + a_3 x^3 + a_4 x^4 + \ldots$. The reason that the right hand side of equation (1-30) does not include a free constant term is motivated by the requirement that $(\mathrm{d}x/\mathrm{d}t)_{x=0} = 0$ in order "to dismiss the possibility of *spontaneous generation* of living organisms from inanimate matter". The latter is referred by Edelstein-Keshet (1988) as the "*Axiom of Parenthood*: every organism must have parents". Baranyi and Roberts (1994), for example, preferred to use a Richards' family of growth curves in the form $f(x) = \left[1 - (x/\delta)^m\right]$.

Baranyi and Roberts, (1994) suggested a new model to resolve the problem of lack of recovery of a "*lag phase*" and an inflection point in the logarithm of the cell concentration curve by the LGM and its different variations. They realised that the only

way that a recovery of both the *lag phase* and the inflection point on the logarithm of the cell concentration curve can be accomplished is via a non-autonomous model. They, therefore, suggested including a time-dependent adjustment function $\alpha(t)$ in the form

$$\frac{\mathrm{d}x}{\mathrm{d}t} = x\mu\alpha(t)f(x) \quad , \tag{2-4}$$

where $f(x)$ takes one of the forms of the Richards' family of growth curves discussed above. They present different forms of the adjustment function, $\alpha(t)$ which recover different forms of previously proposed models as well as the *Lag Phase* and the inflection point on the logarithm of the cell concentration curve. The major limitation of this proposed model is the fact that it is non-autonomous, i.e. it requires for each experiment to evaluate an adjustment function, which depends on time explicitly, rather than a series of constants.

The question that arises is how to derive an autonomous model that captures inherently the fact that "the environment may be changing during the growth" as suggested by Baranyi and Roberts (1994). The answer to the latter question forms the objective of the present study. One is faced with substantial experimental evidence that shows excellent qualitative and quantitative match with the solution of the LGM on one hand. On the other hand, other experimental results indicate substantial qualitative and quantitative discrepancies between the LGM solution and the experimental data, such as the lack of recovery of a *lag phase* and an inflection point on the logarithm of the cell concentration curve.

2.2 Problem formulation for interaction between two competitive species: the modified classical model for two species competing over a common ecological niche

The *"modified classical model"* was introduced for example by Pielou, (1969) as well as May, (1981b) as an extension of the *"classical model"* (presented in section *1.2.2.2.1*) and was motivated by pure mathematical arguments of generality. Vadasz P. and Vadasz A.S. (2000) are showing that the same model is derived from first principles if environmental pollution (deterioration) due to metabolic waste or other natural and virulent toxins are being considered. Their arguments lead to the unavoidable conclusion that the h's in the coefficients' matrix H usually carry four unequal values, i.e. h_{11}, h_{12}, h_{21} and h_{22}, transforming equations (1-31) and (1-32) into the modified classical form

$$\frac{\mathrm{d}x_1}{\mathrm{d}t} = \left[\mu_1 - \gamma_1\left(h_{11}x_1 + h_{12}x_2\right)\right] x_1 \tag{2-5}$$

$$\frac{\mathrm{d}x_2}{\mathrm{d}t} = \left[\mu_2 - \gamma_2\left(h_{21}x_1 + h_{22}x_2\right)\right] x_2 \tag{2-6}$$

The terms $\left(h_{11}x_1 + h_{12}x_2\right)$ and $\left(h_{21}x_1 + h_{22}x_2\right)$ in equations (2-5) and (2-6), respectively, do not represent anymore only the nutrition depletion rate but rather a more complex impact of both nutrition depletion as well as environmental pollution on the birth and death rates of the respective species. The environmental deterioration due to metabolic as well as other sources of toxin released into the environment is particularly essential in batch growth typical to some laboratory experiments as the ones conducted in this study. If for example the killer strain of yeast is allocated the index 1, then the impact of its toxin on a sensitive yeast strain (carrying the index 2) will be reflected in the value of the coefficient h_{21}. When the metabolic waste released by the sensitive yeast strain is affecting the killer

strain, it is reflected in the value of the coefficient h_{12}. It is sensible to assume that under conditions when the killer strain is effective in the competition with the sensitive one because of its toxin the condition $h_{21} >> h_{12}$ applies. Since now the impact of γ_1 and γ_2 is more subtle that in the previous classical case it is convenient to combine the coefficients by using the following notation

$$\beta_{11} = \gamma_1 h_{11} \qquad \beta_{12} = \gamma_1 h_{12} \qquad \beta_{21} = \gamma_1 h_{21} \qquad \beta_{22} = \gamma_1 h_{22} \tag{2-7}$$

and represent equations (2-5) and (2-6) in the form

$$\frac{\mathrm{d}\, x_1}{\mathrm{d}\, t} = \left[\mu_1 - \beta_{11} x_1 - \beta_{12} x_2\right] x_1 \tag{2-8}$$

$$\frac{\mathrm{d}\, x_2}{\mathrm{d}\, t} = \left[\mu_2 - \beta_{21} x_1 - \beta_{22} x_2\right] x_2 \tag{2-9}$$

The steady states of the modified classical model (2-8) and (2-9) are obtained by setting $\left(\mathrm{d}\, x_1/\mathrm{d}\, t\right) = \left(\mathrm{d}\, x_2/\mathrm{d}\, t\right) = 0$, and yield

$$\left[\mu_1 - \beta_{11} x_1 - \beta_{12} x_2\right] x_1 = 0 \tag{2-10}$$

$$\left[\mu_2 - \beta_{21} x_1 - \beta_{22} x_2\right] x_2 = 0 \tag{2-11}$$

Solving the algebraic system of equations (2-10) and (2-11) provides the following steady state solutions

S1: $\quad x_{st1} = 0 \quad$ and $\quad x_{st2} = 0$ (2-12)

S2: $\quad x_{st1} = 0 \quad$ and $\quad x_{st2} = \dfrac{\phi_2}{h_2} = \dfrac{\mu_2}{\beta_{22}} = \delta_2$ (2-13)

S3: $\quad x_{st1} = \dfrac{\mu_1}{\beta_{11}} = \delta_1 \quad$ and $\quad x_{st2} = 0$ (2-14)

$$\text{S4:} \quad \begin{cases} \beta_{11}x_1 + \beta_{12}x_2 = \mu_1 \\ \beta_{21}x_1 + \beta_{22}x_2 = \mu_2 \end{cases} \tag{2-15}$$

The stationary point S4 is obtained as the solution to the system of linear equations

$$\begin{bmatrix} \beta_{11} & ; & \beta_{12} \\ \beta_{21} & ; & \beta_{22} \end{bmatrix} \begin{bmatrix} x_{st1} \\ x_{st2} \end{bmatrix} = \begin{bmatrix} \mu_1 \\ \mu_2 \end{bmatrix} \tag{2-16}$$

and yields

$$\text{S4:} \qquad x_{st1} = \frac{\mu_1\beta_{22} - \mu_2\beta_{12}}{\Delta} \quad ; \qquad x_{st2} = \frac{\mu_2\beta_{11} - \mu_1\beta_{21}}{\Delta} \tag{2-17}$$

where $\Delta = \det[H] = \beta_{11}\beta_{22} - \beta_{12}\beta_{21}$. Vadasz, P. and Vadasz, A.S. (2000) presented a non-linear global stability analysis of the stationary points S1-S4, which is summarised in Table **2.2**.

Table **2.2** Global stability conditions of the stationary points for the modified classical model (Vadasz, P. and Vadasz, A.S., 2000)

Steady State Solution	**Global Stability Conditions**
S1 $x_{1S} = 0$ & $x_{2S} = 0$	$\mu_1 < 0$ & $\mu_2 < 0$
S2 $x_{1S} = 0$ & $x_{2S} = \delta_2$	$\left(\Delta > 0 \ \& \ \frac{\delta_2}{\delta_1} > \frac{\beta_{11}}{\beta_{12}}\right)$ or $\left(\Delta < 0 \ \& \ \frac{\delta_2}{\delta_1} > \frac{\beta_{21}}{\beta_{22}}\right)$
S3 $x_{1S} = \delta_1$ & $x_{2S} = 0$	$\left(\Delta < 0 \ \& \ \frac{\delta_2}{\delta_1} > \frac{\beta_{11}}{\beta_{12}}\right)$ or $\left(\Delta > 0 \ \& \ \frac{\delta_2}{\delta_1} > \frac{\beta_{21}}{\beta_{22}}\right)$
S4 $h_1x_{1S} + h_2x_{2S} = \phi$	$\frac{\beta_{21}}{\beta_{22}} < \frac{\delta_2}{\delta_1} < \frac{\beta_{11}}{\beta_{12}}$ (implies also $\Delta > 0$)

In addition, S2 and S3 can be locally stable if $(\beta_{11}/\beta_{12}) < (\delta_2/\delta_1) < (\beta_{21}/\beta_{22})$ (implies also $\Delta < 0$). For this case, the choice between whether S2 or S3 are stable depends on the initial conditions.

From Table **2.2**, it is obvious that coexistence is possible within a wide range of parameter values. The stability condition of the coexistence stationary point, S4, does not limit substantially the values of the parameters as in the classical model. In addition, extinction of one species or the other can be obtained depending on the values of the parameters, and for parameters' values that fulfil the inequality $(\beta_{11}/\beta_{12}) < (\delta_2/\delta_1) < (\beta_{21}/\beta_{22})$, the extinction of one or the other species depends on the initial conditions. In all cases, the solution reaches a stationary point monotonically; i.e. no oscillations, nor overshooting seem possible, in contrast to experimental evidence presented in Chapter 3. The latter forms another objective of the present study.

CHAPTER 3

NEW EXPERIMENTS OF YEAST GROWTH UNDER EXTREME NUTRITIONAL STRESS

3.1 Background

Yeast, unicellular eukaryotes, are used widely as a model system in basic and applied fields of life science, medicine and biotechnology, and almost certainly, have been used by humans since the dawn of civilisation. Yeast, a typical fungus, has fundamentally the same sub-cellular structure as higher animal and plant cells. The cell wall is the sole yeast structure lacking in animal cells. It is significant, and in keeping with the genetically dependent cell shape, that the cell wall is situated on the outer surface of the cell, and it plays an important role in the transport of materials into and out of the cell (Klis, 1994). The cell wall is the first line of specific recognition, cell-to-cell communication and protection.

Ascomycetous yeast strains are noted particularly for their ability to ferment carbohydrates; hence, the name Saccharomycetes. Fermentation was a welcome discovery because it has the effect of preservation by lowering the pH and, in some cases, producing alcohol, in conditions, which few microorganisms prosper. Because of this property and the resultant alcohol and carbon dioxide produced, brewers, wine makers, distillers and bakers employ yeast in their industries. It was only relatively recently in the fermentation history that the yeast 'function' came to be understood (Pasteur, 1866). Since that time progress in the knowledge of yeast has been rapid, driven in part by the great economic importance of the organisms. Many commercial strains available had been placed in the *Saccharomyces cerevisiae* group.

Strains of *Saccharomyces cerevisiae* survive and proliferate in their natural habitats through constant adaptation within the constraints of a dynamic ecosystem. This facultative anaerobic organism has the ability to select from its environment those food sources that will enable it the best possible chance of surviving. *S. cerevisiae*, like many other microorganisms, is able to adjust its enzymatic composition according to the quality of its food sources. Expression of genes for utilisation of food sources is induced by these sources, and is highly regulated. The tight gene regulation encoding such enzymes in *S. cerevisiae* is reviewed by Johnston and Carlson, (1992), Magasanik, (1992), Hinnebusch, (1992) and Paltauf *et al.*, (1992), for the assimilation of carbon, nitrogen, amino acids and lipid sources, respectively.

Growth and reproduction patterns in yeast are inherited, and are reviewed by Herskowits and Oshima (1981), Herskowitz *et al.*,(1992) and Sprague and Thorner, (1992). A strain-inherited basal growth pattern, that is not affected by the available nutrition, but by cell specific properties, cell inertia and storage energy (Lillie and Pringle, 1980; Barton *et al.*, 1982; Hartig *et al.*, 1990; Binder *et al.*, 1991; Herskowitz *et al.*, 1992; Sprague and Thorner, 1992; Waterham *et al.*, 1993; Klis, 1994; Osumi, 1998) should be known when growing a particular strain in the absence of nutrients, but pure water.

Growth of yeast cells cannot easily be separated from the fermentation process and is pertinent to both substrate assimilation and production of the fermentation end-product. The control of fermentation is achieved by monitoring the changes in the fermentation medium resulting from the metabolic activities of the proliferating yeast cells. During fermentation, environmental factors affecting the yeast growth tend to vary. In mixed cultures, it may include the effect of a mycoviral toxin, which is produced by killer strains (reviewed by Wickner, 1976, 1986, 1992) against a sensitive strain (Hutchins and Bussey, 1983; Bussey, 1991; Van Vuuren and Jacobs, 1992; Carrau *et al.*, 1993; Franken

et al., 1998; Ahmed *et al.*, 1999; Vadasz *et al.*, 2000), and may adversely affect the production of the final desired product.

In general, the aim of fermentation, like any other industrial process, is to obtain the highest efficiency in the use of raw materials and the production plant without distorting the quality of the end product. Thus, the most important properties for fermenting yeast are:

- A rapid fermentation rate without excessive yeast growth;
- An efficient utilisation of a carbon source with good conversion to the desired product;
- An ability to withstand the stresses imposed by the alcohol concentrations and osmotic pressures encountered during fermentation;
- A reproducible production of the correct levels of flavour and aroma compounds;
- An ideal flocculation character for the process employed;
- Good 'handling' characters such as retention of viability during storage and genetic stability.

The basic growth pattern of wine strains of *Saccharomyces cerevisiae* under extreme nutritional stress media (5% grape juice and pure water) is examined in this study in order to develop a model simulating the dynamical interactions of killer and sensitive yeast strains in single and mixed cultures. Therefore, the aim is in understanding of the macro qualitative features controlling the dynamics of these interactions. Cycloheximide-curing of the M dsRNA viral genome in a killer yeast yields a non-toxin producing derivative which can be is used as the killer control (3.2.2.2).

3.2 Materials and methods

3.2.1 Yeast strains and materials

3.2.1.1 Yeast strains

Sensitive wine strains of *Saccharomyces cerevisiae* VIN7 and CSIR Y217 were obtained from the Institute for Wine Biotechnology, University of Stellenbosch, South Africa and from the Council for Scientific and Industrial Research (CSIR), Pretoria, South Africa, respectively. The killer strain of *S. cerevisiae* T206 was obtained from the Department of Microbiology and Biochemistry, University of Pretoria, South Africa.

3.2.1.2 Materials

Yeast extract, malt extract, D - glucose, peptones, agar, $(NH_4)_2$ HPO_4 ,NaH_2PO_4 , citric acid, absolute ethanol, sea sand (grade GR), paraformaldehyde, glutaraldehyde, sodium cacodylate and NaOH were purchased from Merck, Darmstadt. WLN (Bacto W.L. Nutrient) medium was purchased from Difco laboratories, Detroit, Michigan, USA. Hanepoot white grape juice (Ceres, South Africa) was used. Loeffer's methylene blue and cycloheximide were obtained from BDH Chemicals, Poole, UK. Acetic acid, ammonia, ethanol and glycerol test kits were obtained from Boehringer Mannheim GmbH, FRG (Appendix A.3). DNase I (Grade I) and bovine pancreatic Ribonuclease A (Type I-AS, protease free), agarose (DNA Grade), molecular weight marker III were also obtained from Boehringer Mannheim GmbH, FRG. Ethidium bromide was from Sigma Chemical Company, St. Louis, MO, USA. All other reagents used were of analytical grade. Millex-GS and HA type filters (0.22 and 0.45µm pore size) were purchased from Millipore Corporation, MA, USA.

3.2.2 Experimental methods

The preparation of the different chemical solutions and media are presented in Appendix A.2.

3.2.2.1 Maintenance of *Saccharomyces cerevisiae* cultures

Saccharomyces cerevisiae strains, VIN 7, CSIR Y217, T206 and T206q, were grown on yeast malt extract agar (YMA) plates (Appendix A.2) stored at 4°C and sub-cultured according to the work process, every 2-3 weeks. Cultures were activated by re-streaking on freshly prepared sterile YMA-plates and incubated for 4 days at 25°C prior to experimental work.

3.2.2.2 Curing the killer yeast, *S. cerevisiae* T206

The K_2 killer T206 strain from freshly prepared 4 days old YMA plates was re-streaking on YMA_{cyc} plates (Appendix A.2) containing cycloheximide (Fink and Styles, 1972) in ratio of 1µg cycloheximide per 4ml YMA volume and incubated for 7 days at 25°C. From these, a minute inoculum was passed on YMA_{cyc} plates of the same constituents and further re-streaked on YMA_{cyc} plates of the same and increasing cycloheximide : YMA ratio (Appendix A.2). Re-streaked plates were incubated as described above.

The success of the curing process was regularly tested (3.2.2.9) on methylene blue agar plates (Appendix A.2). Also, nucleic acids from both killer (T206) and killer-cured (T206q) strains were isolated in order to observe if the mycoviral double - stranded RNA species would be recovered (3.2.2.3).

3.2.2.3 Isolation of the mycoviral double - stranded RNA

Total yeast nucleic acids were isolated from *Saccharomyces cerevisiae* T206 and T206 cured, T206q, by modifying the method of Fried and Fink, (1978). Triplicates of 200ml YMB medium (Appendix A.2) in 500ml Erlenmeyer flasks were inoculated aseptically with a loopful of 4 days re-activated T206 and T206q cultures, respectively. These were incubated in an incubator shaker (New Brunswick Scientific, classic series C24, Edison, NJ, USA) set at 80 oscillations per minute, (rpm) and 25^{0}C for 24 hours. Then, cells were harvested by centrifugation at 4000rpm for 30 minutes (Hettich Universal centrifuge), and pellets of three flasks were combined. Each of the combined pellets (T206 and T206q separately) were washed by different solutions, each treatment followed by centrifuged as described above and the washing discarded. Firstly, pellets were washed twice with 100ml autoclaved sterile distilled water, followed a wash with TE buffer (pH 7.5) (Appendix A.2), then re-suspended in 20ml Tris - mercaptoethanol buffer (pH 8.7) (Appendix A.2) for 20 minutes at room temperature, and washed twice with sterile Tris - H_2SO_4 (pH 9.3) (Appendix A.2). TSE buffer (pH 7.5) (Appendix A.2) was added to pellets (1ml per gram of wet weight of the cells). These suspensions were pipetted into chilled porcelain mortars pre-washed with TE buffer (pH 7.5) and situated on crushed ice. Wet sterile sea sand (approximately 4-5g) (Appendix A.2) was added to each of the mortars, and cells were firmly ground in a circular motion with a chilled pestle, until cell homogenates became slightly viscous. This required a few minutes, depending on the force applied to a certain amount of cells. Cell slurries were separated from the sea sand, each was transferred to 250ml Erlenmeyer flasks and mixed with TSE + SDS buffer (Appendix A.2) and phenol (Appendix A.2) at the ratio of 1:4:4 (v/v/v), respectively. These flasks were rotated (80 rpm) in an incubator shaker for 2 hours at 25^{0}C, and then centrifuged as described above. The upper aqueous phase containing the nucleic acids

was removed and adjusted to 0.7M NaCl. Two and a half volumes of chilled absolute ethanol were added to these aqueous solutions, where nucleic acids were precipitated for12 hours at minus 20^{0}C, then centrifuged at 27000rpm for 30 minutes (Beckman L5-65 ultracentrifuge, USA), using type 40 rotor and polyallomer centrifuge tubes. Each pellet was re-suspended in a total volume of 100µl TE buffer (pH 7.5). Diluted samples (with TE buffer, depending on each sample concentration) of these were examined spectrophotometrically (Shimadzu UV-160A ultraviolet/visible wavelength spectrophotometer) between wavelengths of 210 to 310nm in order to estimate the purity and amount of the isolated nucleic acids. The rest of isolated samples were used for agarose gel electrophoresis analyses and stored at 0^{0}C until required for further examinations.

3.2.2.4 Agarose gel electrophoresis analyses

Equal aliquots of the isolated nucleic acids from *Saccharomyces cerevisiae* T206 cured, T206q and T206 were treated as indicated in Table **3.1**.

A gel (70x100x3mm^2) was made up of ultra pure DNA grade agarose suspension (1% w/v) that was heated to boiling while being stirred continuously, until it became translucent. Electrophoresis-buffer (10x) (Appendix A.2) was added to the solution (10% v/v) when it was cooled to about 75^{0}C. At 60^{0}C it was poured into a clean, dry, level surface ultraviolet light translucent plastic (UVTP) casting tray with an 8 well-former comb placed in approximately 1cm from the top position (cathode end). After 2 hours of gel setting, the tray was placed into a horizontal electrophoresis apparatus (Bio-Rad mini sub DNA cell apparatus), and filled with electrophoresis-buffer (1x) (Appendix A.2) up to 5mm above the gel surface. A peristaltic pump (Gilson Minipuls 2, France) was connected to the sub-cell buffer compartments to re-circulate the buffer. Then, wells were

loaded with 8µl of the total volume obtained from the treated DNA Marker III (*Eco*RI-*Hin*dIII λ digest), undigested and endonuclease-digested isolated nucleic acid samples, as indicated in Table **3.1.** Electrophoresis was carried out at a constant 40 volts current (Consort model E455, microcomputer electrophoresis power supply) for about 3 hours or until the blue colour gel loading buffer (Appendix A.2) had traversed about two third of the gel.

When the electrophoresis procedure ceased, the gel was stained in ethidium bromide solution (1.0µg/ml) for about a hour. The separation of the DNA fragments was observed under UV_{254nm} illumination and printed (White/UV Transilluminator video graphic monitor and printer, Sony). Photographs were taken using a red filter (screw-in-type, Marumi, 55mm R2) fitted to the camera lens (MINOLTA, MD Zoom 35-70mm 1:3.5, 55mm, Japan).

Table **3.1** Endonuclease digestion analyses of the isolated nucleic acids from *Saccharomyces cerevisiae* T206q and T206

Lanes	**1**	**T206q**			**T206**			**8**
		2	**3**	**4**	**5**	**6**	**7**	
DNA Marker III* (0.25mg/ml)	6µl							6µl
Isolated nucleic acids		10µl	10µl	10µl	20µl	20µl	20µl	
Bovine pancreatic DNase I (1mg/ml)		2µl			2µl			
Bovine pancreatic RNase A (1mg/ml)			2µl			2µl		
Incubation for one hour: Solutions contained RNase ⇨ 37°C, DNase (and all the rest) ⇨ 4°C								
EDTA (100mM)		2µl	2µl	2µl	2µl	2µl	2µl	
Gel loading buffer	3µl	3µl	3µl	3µl	3µl	3µl	3µl	3µl
Total volume	9µl	17µl	17µl	17µl	27µl	27µl	27µl	9µl
Volume loaded	8µl	8µl	8µl	8µl	8µl	8µl	8µl	8µl

* DNA Marker III (*Eco*RI-*Hind*III λ digest), Boehringer Mannheim GmbH, FRG.

3.2.2.5 Determination of the biomass of yeast cells

Saccharomyces cerevisiae VIN7, Y217, T206 and T206q cultures were prepared by inoculating a superficial loopful 4 days old culture from YMA medium into 50ml G-medium (Appendix A.2) in 125ml Erlenmeyer flasks. These cultures were built up at about 20 - 23^{0}C, 80 rpm, in an incubator shaker (New Brunswick Scientific, classic series C24, Edison, NJ, USA) over 24 hours. From these, fermentation inocula were adjusted to 10^6 viable cells / ml using a Bright Line haemacytometer (American Optical Co. New York, USA). Dead cells were differentiated from viable ones by staining in 0.1% methylene blue stain. Fermentation were performed in triplicates using 300ml stressed (5% grape juice) and complex (G-medium) media (Appendix A.2) in 500ml Erlenmeyer flasks in the shaker as described but for 96 hours. Aliquots of 2ml from each suspension were withdrawn aseptically at different times during the fermentation. Cells were harvested by micro-centrifugation (Micro Centaur, MSE, Sanyo, UK) at 12000rpm for 15 minutes, and supernatant discarded. Cell pellets were washed three times, re - suspended in 2ml 20^{0}C autoclaved sterile distilled water and re-centrifuged as described above. Thereafter, washed cells were re - suspended as above and the optical densities of the cells were obtained at wavelength of 600nm, using distilled water as blank. These cell suspensions were passed (1ml x 2 per sample) through a wet (1ml distilled water) pre - weighed dry nitrocellular filter (HA type 0.45µm pore size), using a syringe and a plastic filter holder. Fine forceps were used to remove the filters with the cells from the filter holder. Filters were placed in a 105^{0}C pre - heated oven for about 10 - 15 minutes to dry, then cooled in a desiccator for a few minutes, weighed, put back in the oven for another 5 -10 minutes, and so on, until each sample reached a constant mass value. The cell biomass was estimated in duplicate by deducting the dry mass of the filter from the constant mass value of the filter with the cells. Correction for the maximum medium-

components, was achieved with cell free aliquots as described and reduced from the biomass values. However, no correction was achieved for metabolites accumulated during fermentation, which possibly dried at 105^{0}C as a solute. For each strain, results were recorded separately, as cell biomass (g/l) versus the optical density (OD_{600nm}) plots, for both media.

3.2.2.6 Fermentation

Saccharomyces cerevisiae strains VIN7, Y217, T206 and T206q cultures were prepared by inoculating a superficial loopful of 4 days old culture from YMA medium into 25ml of stressed media, 20^{0}C autoclaved distilled water and filter-sterilised (0.22μm pore size) 5% grape juice (Appendix A.2), respectively. The cells were collected by centrifugation (2500rpm for 3 minutes), then twice washed with 10ml of the respective medium. These washed cells were re-suspended in 20ml of the respective new media. From these, inocula were adjusted to a total of 10^6 (and to 10^7 when examined the affect of initial concentration on the steady state phase) viable cells / ml using a haemacytometer. Dead cells were stained blue (0.1% methylene) and thus differentiated from viable ones.

Pure (single strain or control) and mixed batch fermentation were performed in triplicates using 300ml of both distilled water and 5% grape juice media, respectively, in 500ml Erlenmeyer flasks at 25^{0}C, 80rpm, in an incubator shaker over 350 hours. The flasks were unflushed and fitted with cotton wool bungs.

The sensitive wine-yeast strains (S), VIN7 and Y217, were challenged at the early logarithmic phase of growth (T_{9h}) and at T_{0h} with the K_2 killer yeast T206 (K) and the killer-cured derivative (Kq), T206q, separately, at a killer : sensitive (K/S) and killer cured : sensitive (Kq/S) cell ratio of approximately 1:100 and 1:1, respectively. Also,

examined cultures of the killer yeast T206 (K) challenge at T_{9h} its cured derivative (Kq) at ratio 1:100 (K/Kq) and two sensitive strains, VIN7 and Y217, mixed at T_{0h} at ratio 1:1.

Aliquots of 0.1ml fermentation medium were withdrawn aseptically for counting the viable and dead cells at relatively short time intervals at different periods of growth (15-30 minutes and 2-3 hours) until it was estimated that a steady state was reached. Aliquots of 3ml were withdrawn once a day and every second or third day at the stationary phase for further analyses. In total, the aliquots withdrawn comprised of less than 9% of the initial volume.

Inoculating the samples on WLN plates (Appendix A.2) yielded the survival ratio of the strains in mixed cultures, and methylene blue agar plates (Appendix A.2) monitored the killer toxin effect and the efficiency of the curing process. Boehringer Mannheim (FRG) kits were used to evaluate the concentrations of acetic acid (Cat. No. 542946), ammonia (Cat. No. 542946), ethanol (Cat. No. 176290) and glycerol (Cat. No. 148270). The instructions to these diagnostic kits are given in Appendix A.3. Reducing sugar concentration (DNS technique) and pH of media were also monitored.

3.2.2.7 Determination of residual sugar (DNS technique)

Redusing grape juice sugar (mainly D-fructose) concentrations were determined spectrophotometrically by a modification (Gupthar, 1987) of the dinitrosalicylic acid method of Miller, (1959). Standard curves of optical densities versus D-fructose standard and diluted grape juice were compared (Vadasz, A.S., 1999). Sterile triplicate samples of 0.0, 0.05, 0.1, 0.2, 0.3, 0.5, 0.7 and 1.0% w/v D-fructose, and diluted Hanepoot grape juice (Ceres, SA) containing expected sugar levels (Vadasz, A.S., 1999) of 0.0, 0.5, 1.0, 2.0, 4.0, 5.0 and 10 g /litre were used. To 25µl sample (of the standard curves and yeast fermenting media) was added 2475µl autoclaved distilled water (dH_2O). The control

(0.0% w/v) sample was used to zero the spectrophotometer. To each sample was added 250µl 2N NaOH and 250µl DNS reagent (Appendix A.2). The samples were mixed and incubated for 5 minutes at 85^{0}C. After heating, 2.5ml dH_2O was added per sample and samples were allowed to cool at room temperature. Optical densities of samples were read against the control at 540nm using a spectrophotometer. In order to estimate reducing sugar concentrations of control and challenged fermentations investigated, their absorption results were compared with the results obtained for the reliable standard grape-juice sugar curve.

3.2.2.8 **WLN** (Bacto Wallerstein Laboratory Nutrient) **differential medium**

Four days re-activated yeast cultures growing on YMA plates were inoculated on WLN medium plates (Appendix A.2). Plates were inoculated with small inocula of sensitive wine yeast strains, VIN 7 and Y217, the killer strain T206 and, the killer-cured, T206q, respectively. Plates were incubated at 25^{0}C for 4-5 days. These were used in order to identify the typical colony of each strain.

Samples of these strains growing in pure dH_2O (section 3.2.2.6) were diluted in autoclaved 20^{0}C distilled water (dH_2O) to a viable cell concentration of about 10^1 cells per ml after cell counting. These diluted samples were filtered through Milipore filters (type HA, 0.22µm pore size), and washed with cooled autoclaved distilled water (1ml x2). Then, with 1ml dH_2O cells were washed off the filter onto the WLN plates, spread on the medium surface, allowed to be absorbed for 1 hour, and then incubated as described above.

Samples were withdrawn from pure and mixed cultures at the same times. The pure cultures were used as the controls of the mixed ones in order to differentiate the relative

survival of each strain in the mixed cultures, while growing in the exact set of conditions. The filtration aimed to wash out spores, possibly liberated from asci.

3.2.2.9 Methylene blue agar: a medium for the killer phenotype test

A loopful of K^-R^- cells of VIN 7and Y217, was added separately to autoclaved cooled 20ml distilled water. An optical density of about 0.6 at 600nm was adjusted for the cell suspensions. Aliquots of 0.1ml per plate were spread onto methylene blue agar plates (Appendix A.2). The K^-R^- cell suspensions were allowed to absorb for 1 hour. Thereafter, a thin but heavily inoculated streak of both, the designated K_2 killer T206 (K^+R^+) and its cured strain, T206q (K^-R^+), respectively, were applied separately on these plates. The methylene blue agar plates were incubated at 25^0C for 3-4 days to observe the killer toxin effect and the success of the curing. T206 and T206q, from freshly prepared YMA plates (4 days), were used as the killer and killer-cured controls, respectively. Samples of the sensitive, killer and killer cured strains growing in pure dH_2O (section 3.2.2.6) were plated on methylene blue agar plates at the inception, mid-stream and at the end of the experimental duration, where sensitive cells were challenged by both T206 and T206q as described above.

3.2.2.10 Electron microscopy

3.2.2.10.1 Preparation for scanning electron microscopy (SEM)

Agar medium

Sensitive wine strains VIN7 and Y217 were spread inoculated on 3% (v/v) grape juice agar plates (Appendix A.2). An hour after the inoculation, both were challenged (section 3.2.2.9) with the killer T206, and incubated 7 days at 25^{0}C. Plates were flooded with 3% Karnovskys fixative (1:3 dilution of stock containing 5% (w/v) paraformaldehyde and 4% (v/v) glutaraldehyde) in 0.2M sodium cacodylate buffer (pH 7.2) at room temperature (about 25^{0}C) for an hour. After removing the fixative, the agar was washed with 0.2M sodium cacodylate buffer for 15 minutes. Wedges of agar, incorporating part of the concentric growth inhibition (clearing) zone induced by the toxin (section 3.3.2.1), followed by a flanking region of superficial growth, were removed from the plates, immersed in 1% aqueous osmium tetroxide (OsO_4) (Appendix A.2) at "room temperature" (*ca.* 25^{0}C) in a dark cupboard for 30 minutes. The material was washed with buffer as described and dehydrated through a graded series of ethanol (i.e. 20 minutes each in 50%, 70%, 90% ethanol, and 3 changes of 30 minutes each in 100% ethanol, using 'dry' alcohol for the last change). Thereafter, critical point drying was achieved with liquid CO_2 in a Biorad CPD 750 critical point dryer. Dried samples were attached to brass stubs using a double-sided sticky carbon conductive tape. Growth was uppermost, and edges of the agar blocks were firmly pressed onto the surfaces of the stubs. Samples were coated with 10nm gold in an atmosphere of argon in a Polaron Sputter E5000 coating unit for 5 minutes at 30-40 amps. Specimens were viewed in a Philips SEM 500 at 6-12kV.

Liquid medium

Cells were harvested from fermentation medium (5% grape juice) by centrifugation at 6000 rpm for 5 minutes and washed twice in 0.89% saline. Cells were similarly treated as those from the 3% grape juice agar plates till the last change of 100% 'dry' alcohol, as described above, with centrifugation to re-pellet. Cells were gently spread with a drop of 100% alcohol on thin round pieces of glass, which were attached to fitted brass stubs using the same double-sided sticky carbon conductive tape, then sputter coated with gold and examined as described above for the solid medium (Vadasz *et al.*, 2000).

3.2.2.10.2 Preparation for transmission electron microscopy (TEM)

Cell pellets (*3.2.2.10.1*, liquid medium) were flooded with 3% Karnovskys fixative in 0.2M sodium cacodylate buffer (pH 7.2) at room temperature for an hour, then centrifuged. After removing the supernatants, the pellets were washed well with 0.2M sodium cacodylate buffer for 10 minutes, then re- centrifuged. Pellets were re-suspended in 1% aqueous osmium tetroxide (OsO_4) (Appendix A.2) at "room temperature" (*ca.* 25^0C) in a dark cupboard for an hour. Then, they were washed twice with the buffer as described above, and dehydrated through a graded series of ethanol (i.e. 30 minutes each in 50% and 70%, twice in 90% ethanol and 3 changes in 100% ethanol, using 'dry' alcohol for the last change). The samples were re-suspended in 3 changes of propylene oxide for 20 minutes each and taken through increasing concentrations of low viscosity resin of Spurr (1969) (Appendix A.3), diluted with propylene oxide (i.e. 50% - 12h, 75% - 12h and 100% - 24h at room temperature) leaving the lids open in a fume extractor cupboard. Drops of the pellets were transferred into labelled Beem capsules were 100% Spurr' resin polymerised for 48h at 60^0C under vacuum (Vadasz *et al.*, 2000). Ultra-thin sections were cut with Drukker diamond knife using a Reichert OMU2 ultramicrotome

and collected on uncoated 200-square mesh copper grids and were post-stained with 2% aqueous uranyl acetate (Appendix A.2) for 7 minutes followed by lead citrate (Appendix A.2) for 7 minutes. Sections were observed and photographed with a Philips 301 transmission electron microscopy (TEM).

3.3 RESULTS AND DISCUSSION

3.3.1 Analyses of the killer and killer-cured nucleic acids

Most strains of *Saccharomyces cerevisiae* carry one or more double-stranded RNA (dsRNA) viruses (Wickner, 1992). Killer strains secrete virally-encoded protein toxins that are lethal to strains, which lack the toxin specific immunity. The exceptions are the killer and neutral strains that are carrying that specific immunity genome. This confers a growth advantage to its host, increasing its survival in ecosystems of clinical, environmental and industrial significance (Starmer *et al.*, 1992; Wickner, 1996; Magliani *et al.*; 1997). Commercial fermentation exploits killer strains (Van Vuuren and Jacobs, 1992) that may influence the pathophysiology of opportunistic infections (Pettoello-Mantovani *et al.*, 1995), and offer candidates for novel antimycotic medications (Polonelli *et al.*, 1986). Yeast viruses show striking parallels to pathogenic dsRNA viruses of higher eukaryotes (Cheng *et al.*, 1994).

The killer phenomenon in *S. cerevisiae* strains is controlled by two types of cytoplasmically inherited dsRNA plasmids (Ramon-Portugal *et al.*, 1997) separately encapsulated in virus-like particles (VLPs), which show neither an infective nor lytic cycle. Therefore, they are termed (Lemke, 1977) latent mycoviruses. VLPs contain the L (large) and M (medium) dsRNA genome (Herring and Bevan, 1974).

The L-dsRNA molecules are approximately 5.1 kilobases (kb) in size (Van Vuuren and Wingfield, 1986; Franken *et al.*, 1998), linear and code for an RNA polymerase which produces single stranded transcripts that encode the protein coat of the VLPs (Tipper and Bostian, 1984). There are also indications that this polymerase is involved in replication of both L and M genomes.

The M-dsRNA genome codes for the toxin and a related immunity factor. K_1 and K_2 toxins are encoded by variant M_1 (about 1.8 kb) and M_2 (about 2.0 kb) dsRNAs, respectively. The size of these two M-dsRNAs varies rapidly by up to 300bp (base pairs) without affecting the copy number, the toxin production or the immunity. The site of this variation is probably the poly rA/poly rU region. The K_2 phenotype of strain T206 (Van Vuuren & Wingfield, 1986) is found almost exclusively among fermentation contaminants.

Genetic evidence clearly demonstrates that M-dsRNA is the determinant of both toxin production and immunity (Wickner, 1976). A schematic model for the preprotoxin maturation via the yeast secretion pathway has been proposed by Tipper and Bostian, (1984). Immunity to the toxin is conferred by the toxin precursor and its open reading frame is sufficient. The immunity component could compete with a required toxin receptor, or interact with the toxin to prevent lethal channel formation (Bussey, 1991). Boone and co-workers, (1986) had shown that the immunity is conferred by the precursor protein that can act as a competitive inhibitor of the mature toxin, by saturating a cell membrane receptor that normally mediates toxin action. Genetic deletion of *TOK1*, which encodes a potassium selective ion channel in the plasma membrane, confers K_1 toxin resistance, where over expression increases susceptibility (Ahmed *et al.*, 1999).

Hutchins and Bussey, (1983) reported that after a certain lag period the killer toxin is bound to a cell wall receptor, that is β-1,6-D-glucan for K_1 and K_2 killer yeast cells on both sensitive and killer strains. It appears that the killing process involved two components for toxin action, one is the cell-wall receptor and the other is a receptor involved on the plasma membrane. The events occurring after the binding of the toxin to the plasma membrane remain unclear. They assumed that toxin binding of cell membrane receptors results in the liberation of K^+ ions, ATP and other metabolites, leading to destruction of the cellular membrane pH gradient.

In this study the K_2 killer yeast *S. cerevisiae* T206 strain was cured of its killer phenotype by treatment with cycloheximide, modifying Fink and Styles' (1972) method (section 3.2.2.2). Nucleic acids from both killer (T206) and killer cured (T206q) strains were isolated (3.2.2.3) and examined spectrophotometrically (Figures **3.1** and **3.2**). Peaks were observed at wavelength of 259.4 and 257.8nm, and valleys at 232.7 and 232.3nm, respectively. A_{260}/A_{280} ratios were 1.895 and 1.947, respectively, indicating that the nucleic acid extracts were relatively highly purified or free of excessive protein contamination. From about 4g wet cells approximately 3.74 and 2.34mg/ml, respectively of the nucleic acids were isolated.

The success of the curing process was assessed by agarose gel electrophoresis (Figure **3.3**). *S. cerevisiae* T206 and T206q genomic DNA bands were found in both undigested and bovine pancreatic RNase-digested samples of the isolated nucleic acids, but not in DNase I-digested samples, as expected, and migrated alongside the 21.2kb *Eco*RI-*Hin*dIII digest λ DNA marker band. Undigested and DNase I digested samples marked the isolated RNAs on the gel. The killer T206 strain yielded both L and M_2 dsRNA species, estimated to be approximately 5.0 and 2.0kb, respectively (Figure **3.3**). Only L dsRNAs band was observed for the killer cured (T206q) strain. The deletion of the M

viral genome using cycloheximide treatments is well documented (Fink and Styles, 1972).

Low molecular weight nucleic acids (<0.83kb) were found to be susceptible to bovine pancreatic RNase (absent in lanes 4 and 7), but not to DNase I (observed in lanes 2 and 3 and more pronounced in lanes 6 and 7). Considering the relative high concentration of nucleic acids of the killer samples compared with that of those applied for the killer-cured, the amount of L dsRNA of the cured strain seemed to be relatively larger and of slightly higher molecular weight (5.1kb). It is a well known phenomenon that killer-cured strains, devoid of M-dsRNA, generally show increased L -dsRNA copy number (Radler *et al.*, 1992; Wickner, 1986).

nm	λ	nm	λ
310.0	0.086	305.0	0.083
300.0	0.084	295.0	0.116
290.0	0.176	285.0	0.256
280.0	0.380	275.0	0.513
270.0	0.629	265.0	0.698
260.0	0.720	255.0	0.690
250.0	0.617	245.0	0.517
240.0	0.418	235.0	0.354
230.0	0.346	225.0	0.453
220.0	0.692	215.0	0.935
210.0	1.060		

*** PEAK-PICK ***

-- PEAK --		-- VALLEY --	
λ	ABS	λ	ABS
259.4	0.723	232.7	0.340

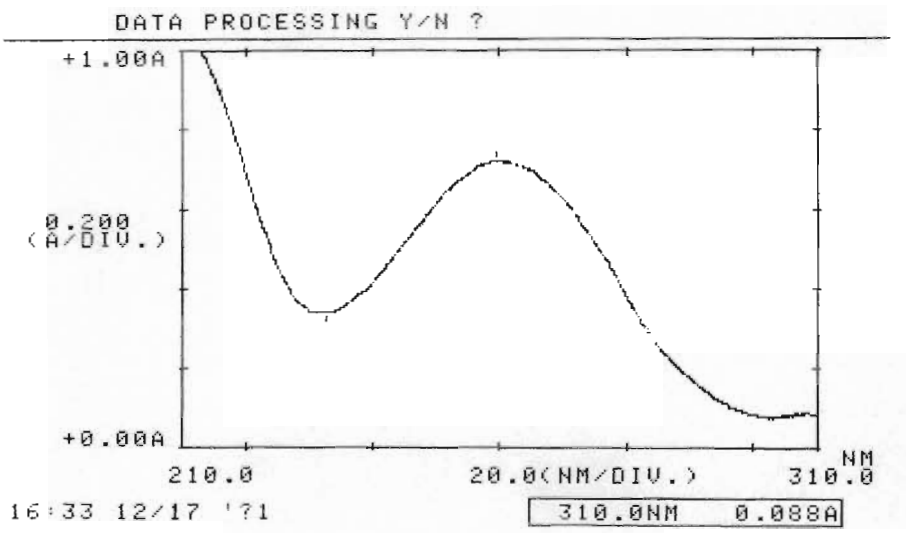

Figure **3.1** Spectrophotometric analysis of the total nucleic acids isolated from *Saccharomyces cerevisiae* T206 (K^+R^+), the K_2 killer strain.

nm	λ	nm	λ
310.0	0.141	305.0	0.152
300.0	0.196	295.0	0.319
290.0	0.528	285.0	0.822
280.0	1.185	275.0	1.567
270.0	1.926	265.0	2.187
260.0	2.339	255.0	2.319
250.0	2.111	245.0	1.780
240.0	1.456	235.0	1.243
230.0	1.203	225.0	1.406
220.0	1.789	215.0	1.976
210.0	1.856		

*** PEAK-PICK ***

-- PEAK --		-- VALLEY --	
λ	ABS	λ	ABS
257.8	2.364	232.3	1.198
215.4	1.977		

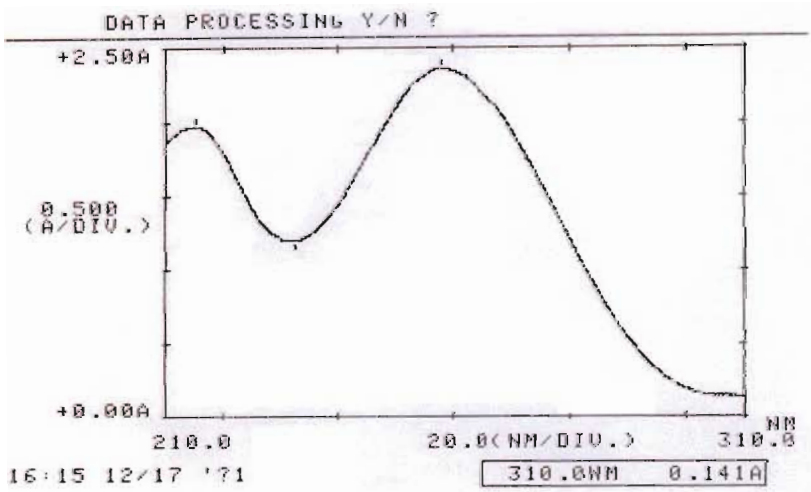

Figure **3.2** Spectrophotometric analysis of the total nucleic acids isolated from *Saccharomyces cerevisiae* T206q, the cured-killer derivative of strain T206.

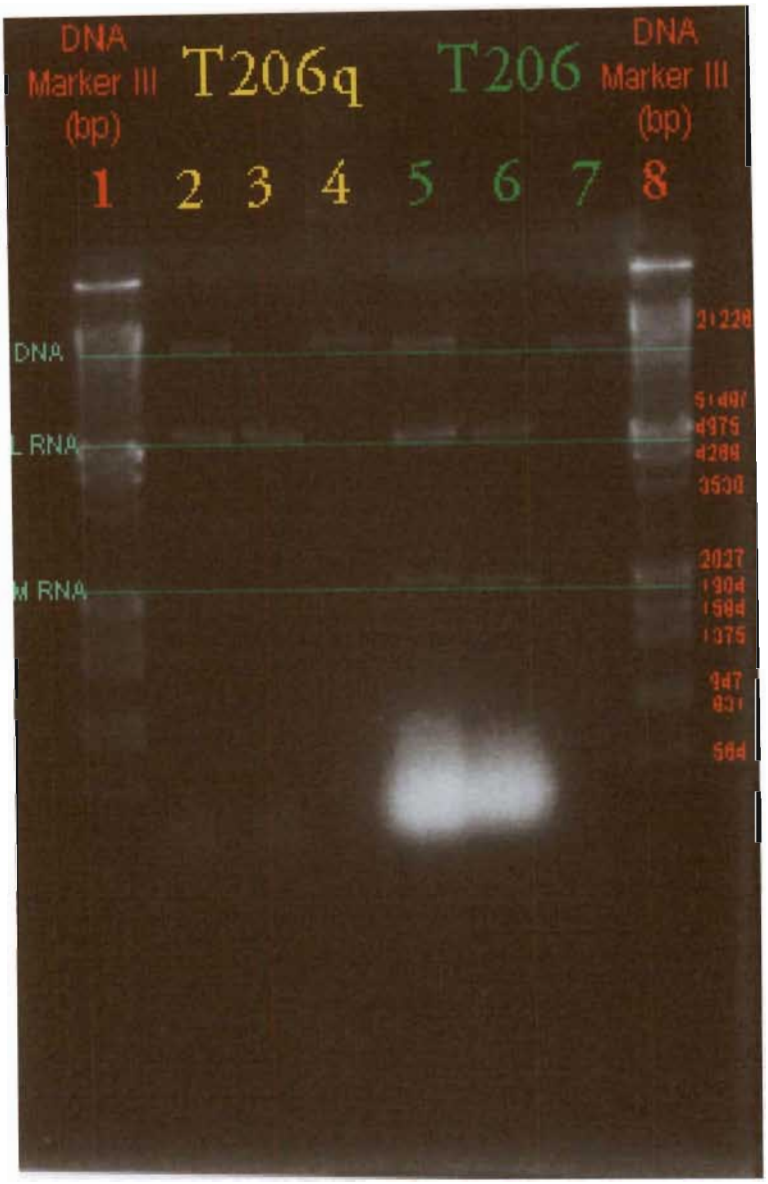

Figure **3.3** Agarose gel electrophoresis of total nucleic acids of the K_2 killer strain *Saccharomyces cerevisiae* T206 and its cured derivative, T206q.

Lanes 1 and 8: DNA marker III (*Eco*R1-*Hin*dIII λ digest). Lanes 2 and 5: undigested nucleic acid samples, lanes 3 and 6: DNase I digest, and lanes 4 and 7: bovine pancreatic RNase digest, of the killer-cured and killer strains' nucleic acids, respectively.

3.3.2 Yeast strain identification

3.3.2.1 Medium identifies the killer phenomenon

The killer-cured strain could easily regain its killer nature on contact with the killer strain (Wickner, 1986). Therefore, working with these two strains required a simple test reassuring their purification, by testing the killer effect on sensitive strains. The success of the curing process was regularly tested on methylene blue agar plates (3.2.2.9) (Figure **3.4**) of spread-inoculated sensitive cells (wine yeast strains, VIN7 and Y217) challenged by both the killer (T206) and its cured derivative, T206q (Figure **3.4**: 1.1, 2.1). Daily observations revealed the killer effect. Within a few days, presumably dependent on the relative strength and amount of the toxin released by the killer yeast, killer colonies were surrounded by a clearing zone in which no growth of the seeded sensitive strains occurred (Figure **3.4**: 1.2, 2.2). Also, a zone of dead sensitive cells became pronounced, staining dark blue in the presence of the methylene blue around the zone of clearing (Figure **3.4**: 1.3, 2.3). Killer colonies continued to grow, showing a progressive "white line" away from the killer inocula keeping a zone of clearance while further killing sensitive cells beyond the zone of clearing. The killer phenomenon was observed with the K_2 killer yeast T206 but not with the killer-cured strain T206q (Figure **3.4**). Different factors could influence the sensitivity of the assay. The ratio of cell concentration between the killer and the sensitive strains; the initial concentration, cell specific growth rate at a certain set of conditions, cell growth phase on production of or exposure to the killer toxin and the degree of sensitivity of specific sensitive cells to a certain mycotoxin. The clearing (inhibition) zone was found to be directly proportional to the activity of the killer toxins (Radler and Knoll, 1988; Ramon-Portugal *et al.*, 1997).

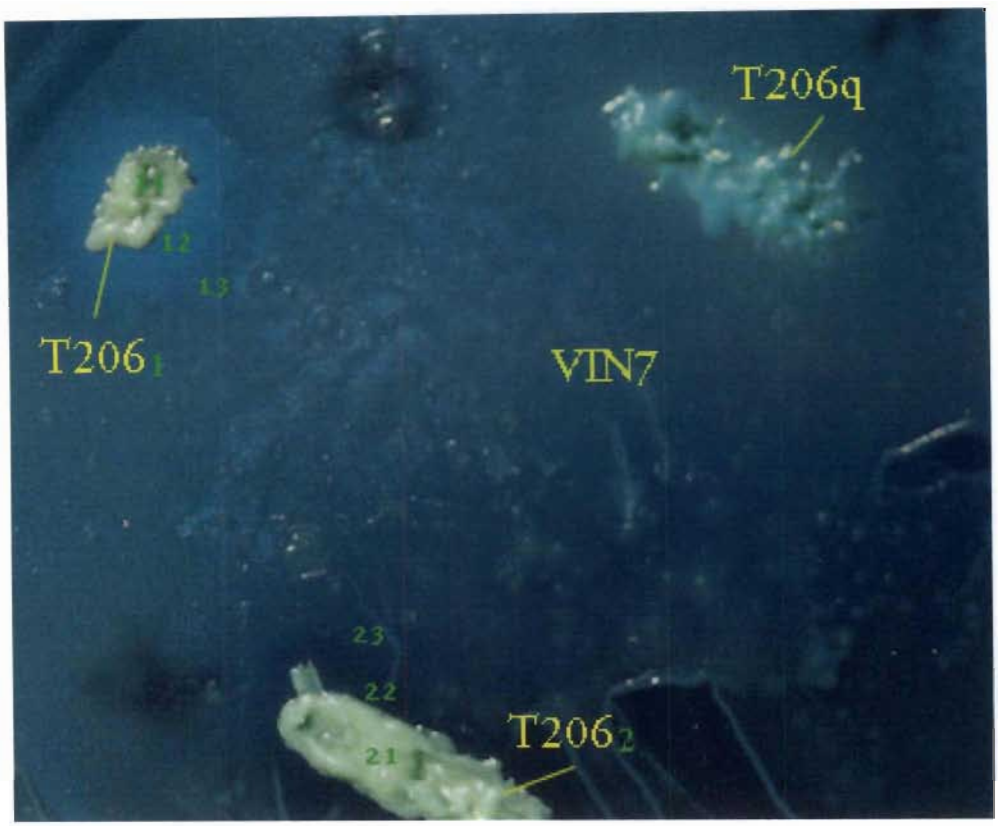

Figure **3.4** A methylene blue agar plate of the sensitive strain VIN7 challenged by both $T206_1$ and T206q growing in the liquid media (3.2.2.6). $T206_2$ sample taken from a YMA plate. $T206_1$ and $T206_2$ showed the same growth pattern of the killer toxin effect, which was not observed for the cured strain, T206q.

1.1 and 2.1 are the killer growing colonies, 1.2 and 2.2 are the typical clear zones of growth inhibition, and 1.3 and 2.3 are the darker stained rings around the clearing zones of the dead cells of the sensitive strain (VIN7).

3.3.2.2 Medium differentiates yeast strains

WLN is a very hygroscopic medium recommended for the cultivation of yeast and bacteria encountered in brewing and industrial fermentation process. It contains Bacto-bromcresol green that characterises the green colour of the medium, and is considered as a differential medium for sensitive and killer strains of *S. cerevisiae*.

The WLN plates (3.2.2.8) containing single (Figure **3.5**) and mixed of two (Figure **3.46**) strain cultures of the sensitive wine yeast strains, VIN7 and Y217, killer strain T206 and killer-cured T206q had grown strain typical colonies within 4 days of inoculation. The medium gradually lost its intense green colour and became totally clear after about 4-5 days. In 7 to 10 days of inoculation, growing cultures also gradually changed their typical colony phenotypes, staining with intensity. Therefore, it was necessary to sample pure cultures on this differentiating medium as controls, parallel to the sampling of the mixed ones.

The colonies of all four wine-yeast strains had a round configuration, smooth margins and convex elevation, but each had a unique staining appearance. The colonies of the killer T206 strain (Figure **3.5a**) showed a gradient of yellowish to dark green- at the top and a cream opaque to transparent appearance at the circumference. All killer-cured T206q colonies (Figure **3.5b**) were whitish with typical light yellowish-stained tops.

The phenotypes of sensitive yeast colonies were strain-specific. VIN7 (Figure **3.5c**) produced colonies of pointed yellowish evergreen stained tops, and relative to the killer strain, had larger whitish circumferences. Y217 (Figure **3.5d**) produced grey-evergreen colonies with centres of cream-opaque in colour, and circumferences opaque to transparent.

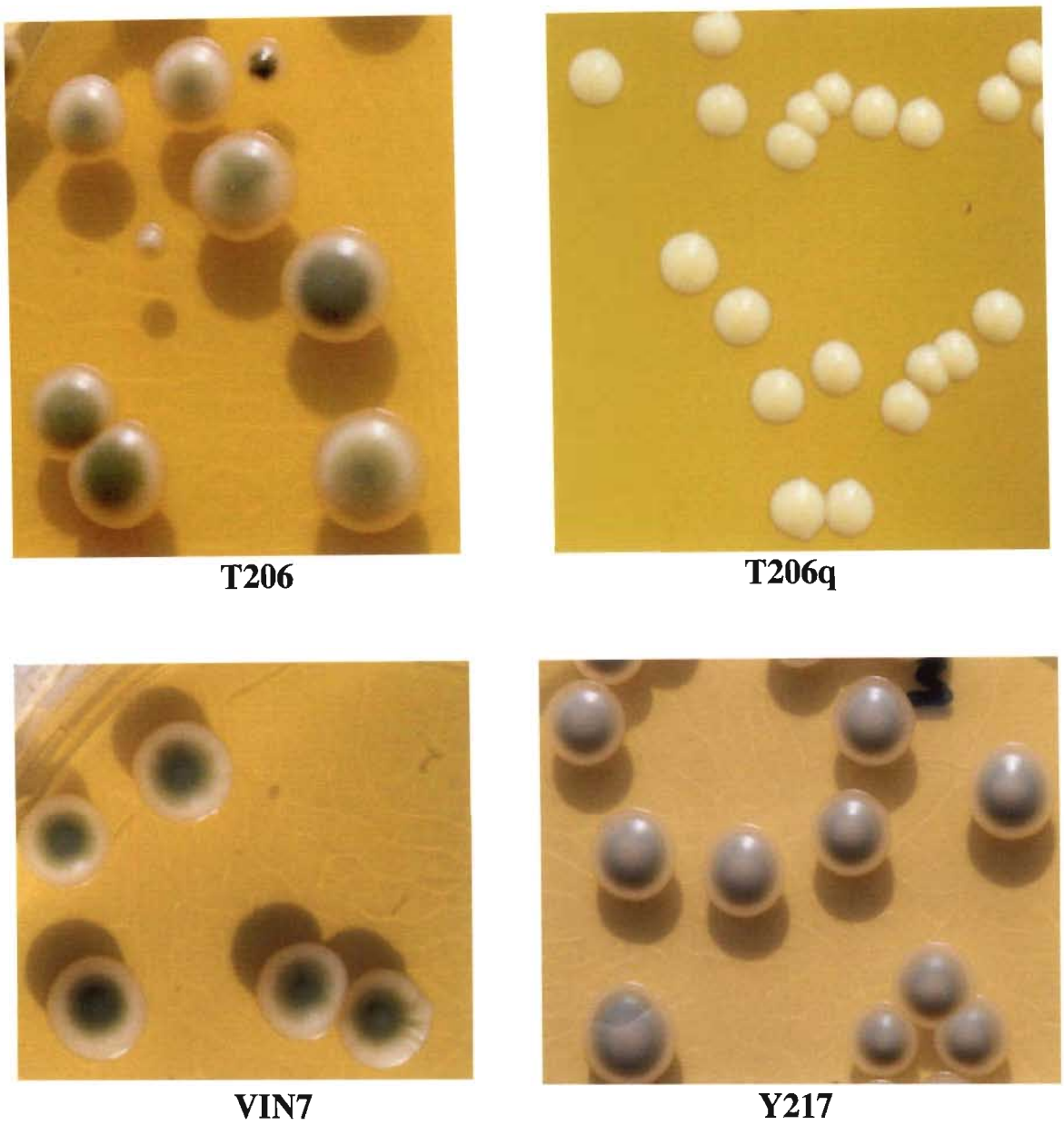

Figure **3.5** Typical colonies of *Saccharomyces cerevisiae* strains T206, T206q, VIN7 and Y217, respectively, growing on WLN differentiation medium.

3.3.3 Biomass of the yeast cells

Biomasses of pure cultures of *Saccharomyces cerevisiae* VIN7, Y217, T206 and T206q, growing in stressed (5% grape juice) and complex (G-medium) media (Appendix A.2) were estimated using a gravimetric technique (section 3.2.2.5). For each strain, results were recorded as cell biomass (g/l) versus the optical density (OD_{600nm}) plots, using both media separately (Figures **3.6** to **3.9**). Cell biomass found to be directly proportional to the cell turbidity, which was measured as optical density at a wavelength of 600nm. Cell biomass also found to be strain specific, correlating with the physical cell size, increasing in this order: Y217 < T206q < T206 < VIN7, as regularly observed under the light microscope. T206 biomass was slightly larger than that of T206q, which could be due to the presence of the VLPs in the killer strain.

But cells growing in the rich medium were found to have a relative higher specific biomass than those growing in the stressed medium. That could be explained by the changes occurring to the physical cell size. Cells, growing in the rich medium, reached the maximum potential size at specific growth conditions and while those growing in the stressed medium did not. Cells, growing in the rich medium, presumably stored excess consumed nutrients, while those growing under extreme nutritional limitations used their potential stored energies. Different cell sizes could be observed. Also, the cell shape switched from a typical spheroid shape to an elongated one and unicellular cells aggregated, showing a pseudohyphae growth pattern as could be observed under the light microscope (see 3.3.5 Electron microscopy).

Spore staining revealed that the degree of sporulation of cells growing under nutritional stress was much more pronounced than that occurring rich medium (3.3.4.1), although some germination and budding did occur. This could also affect the absorbance readings and, therefore, the biomass versus the optical density values.

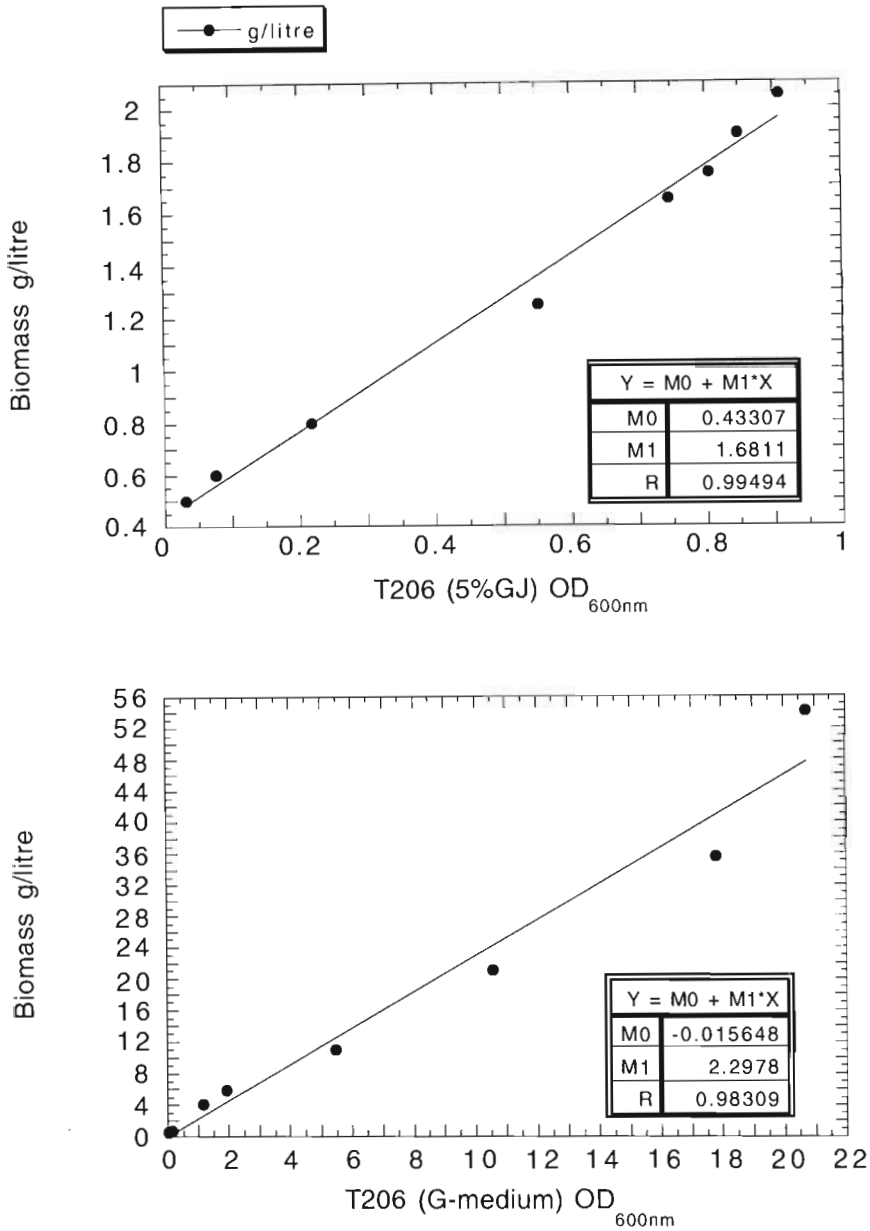

Figure **3.6** The biomass (g/l) versus OD_{600nm} of *Saccharomyces cerevisiae* T206 growing in 5% grape juice and G- media, respectively.

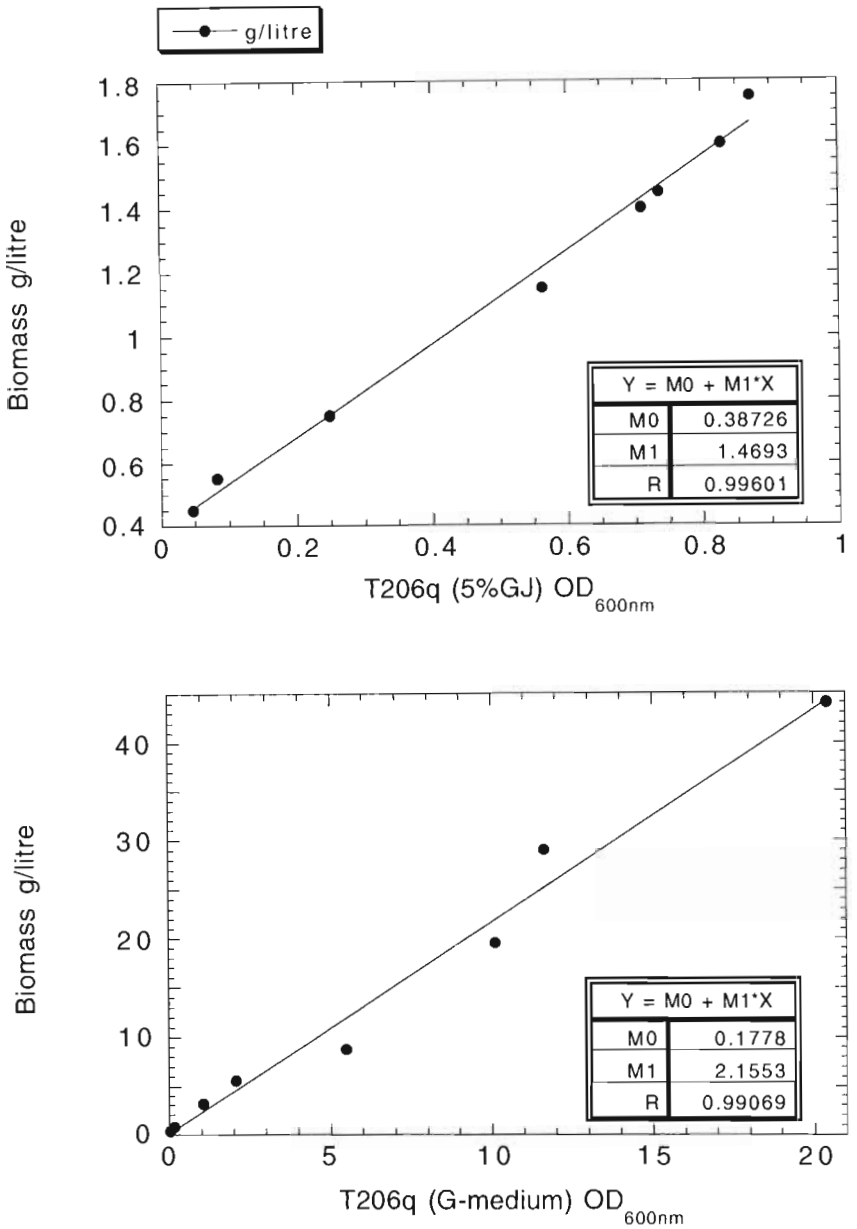

Figure **3.7** The biomass (g/l) versus OD_{600nm} of *Saccharomyces cerevisiae* T206q growing in 5% grape juice and G- media, respectively.

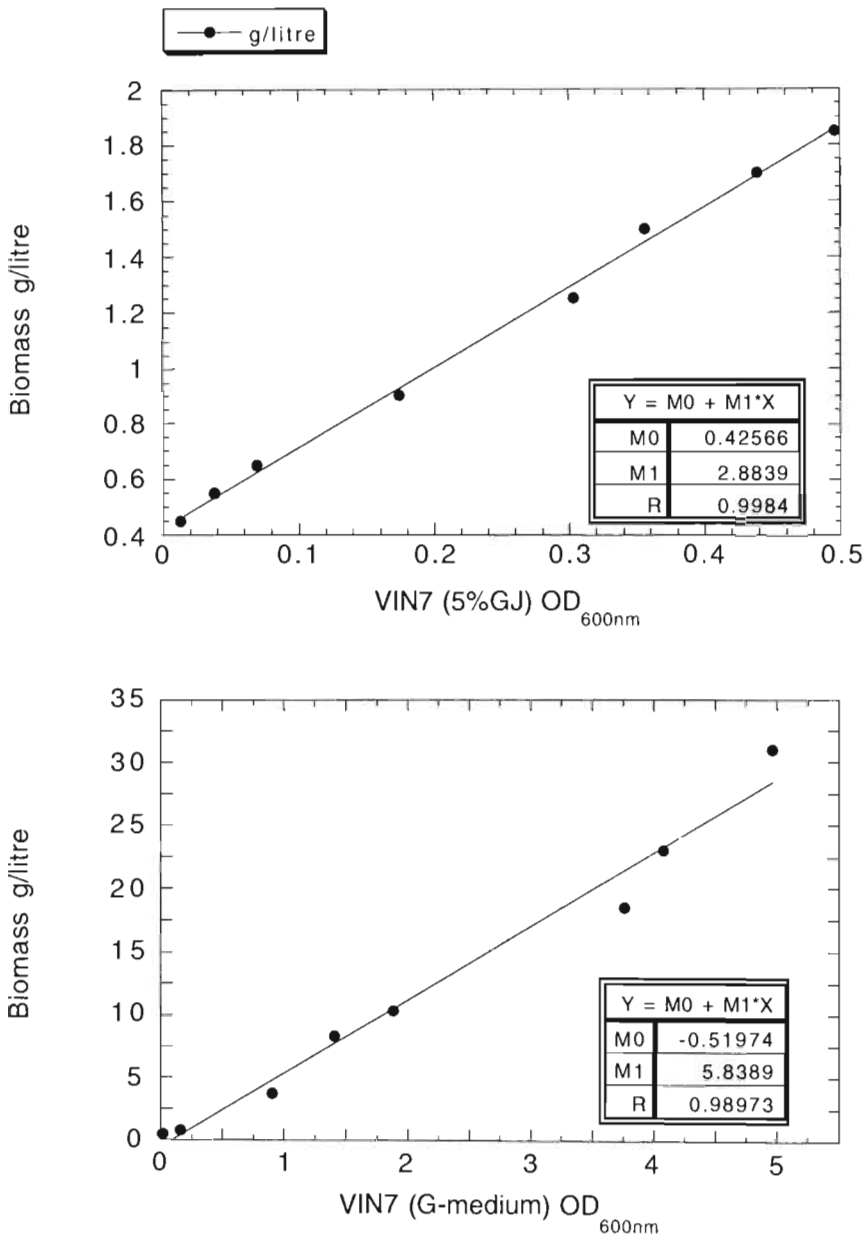

Figure **3.8** The biomass (g/l) versus OD_{600nm} of *Saccharomyces cerevisiae* VIN7 growing in 5% grape juice and G- media, respectively.

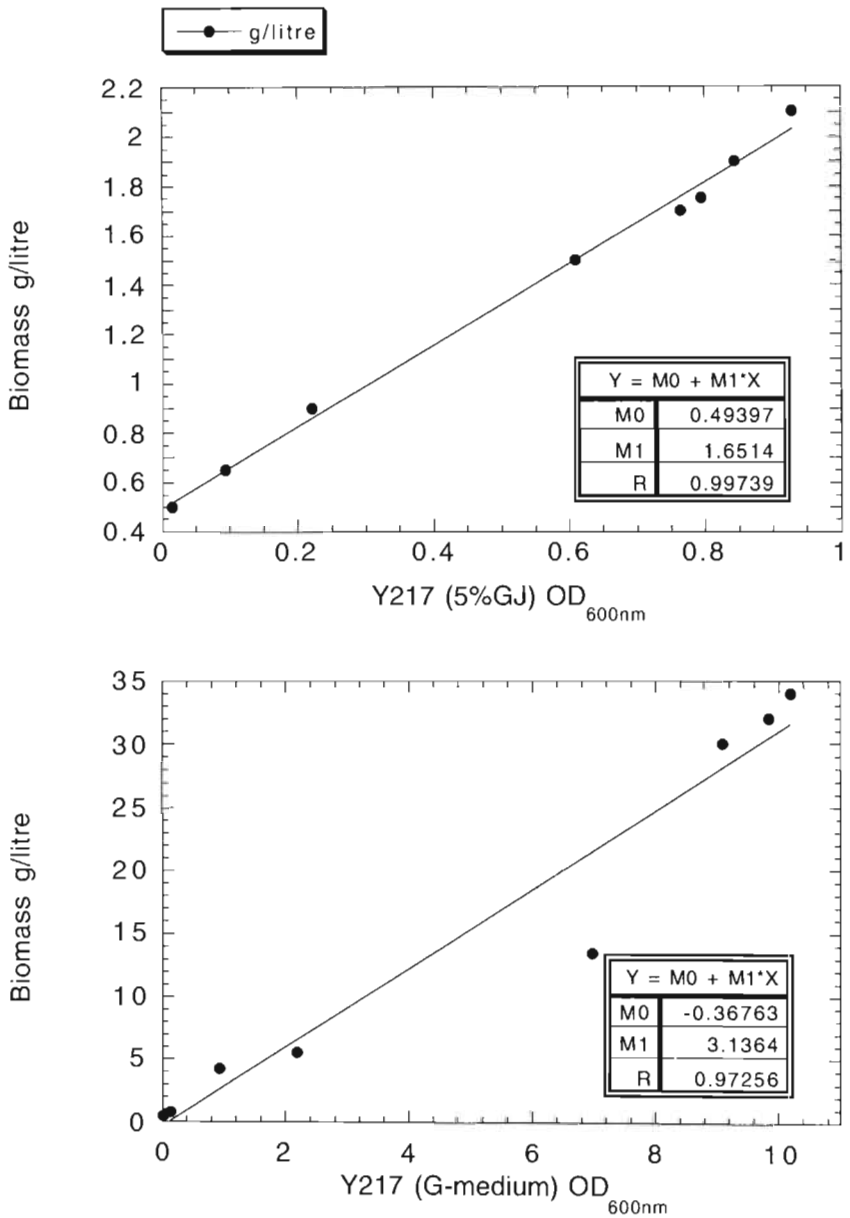

Figure **3.9** The biomass (g/l) versus OD_{600nm} of *Saccharomyces cerevisiae* Y217 growing in 5% grape juice and G- media, respectively.

Strain specific ratios of biomass obtained for stressed medium versus the ones obtained for the rich medium dependent on physical cell size and its specific growth rate (increased in this order: VIN7 < T206 < T206q ≤ Y217), and was found to decrease in this order: T206 > T206q > Y217 > VIN7, respectively.

3.3.4 Analyses of microscale vinifications

3.3.4.1 Cell growth pattern

The growth results of pure cultures are presented in Figures **3.10** to **3.25**. For initial cell concentration of about 10^6 cells/ml, cell counts and % dead cells are presented in Figures **3.10** to **3.13** and ln of cell counts in Figures **3.14** to **3.21**. Figures **3.18** to **3.21** present the ln of cell growth from inoculation throughout the log phase till stationary phase was obtained, yielding a typical sigmoidal pattern. Growth results for initial approximate cell concentration of 10^7 cells/ml, cell counts and % dead cells are presented in Figures **3.22** to **3.23** and ln of cell counts in Figures **3.24** to **3.25**.

All mixed cultures presented here were growing in pure water at the initial cell concentration of 10^6 cells/ml. The results of cell counts and % dead cells of sensitive cultures challenged by a killer (T206) and its cured derivative (T206q), separately, at ratios of 1:100 and 1:1 are presented in Figures **3.26-3.27** and **3.28-3.29**, respectively. Their Ln forms are presented in Figures **3.30-3.31** and **3.32-3.33**, respectively, and their relative survivals growing on WLN plates are presented in Figures **3.36-3.39** and **3.40-3.43**, respectively. Also are presented results of the killer, challenged its killer-cured derivative at ratio of 1:100 (Figures **3.34** and **3.44**) and a mixture (1:1) of two sensitive strains (VIN7 and Y217) (Figures **3.35** and **3.45**).

(a)

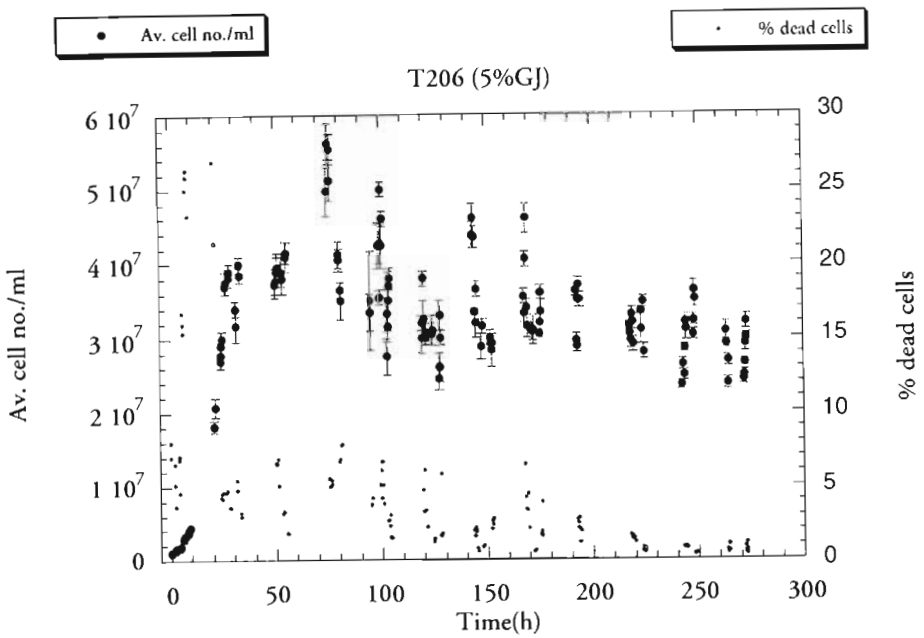

(b)

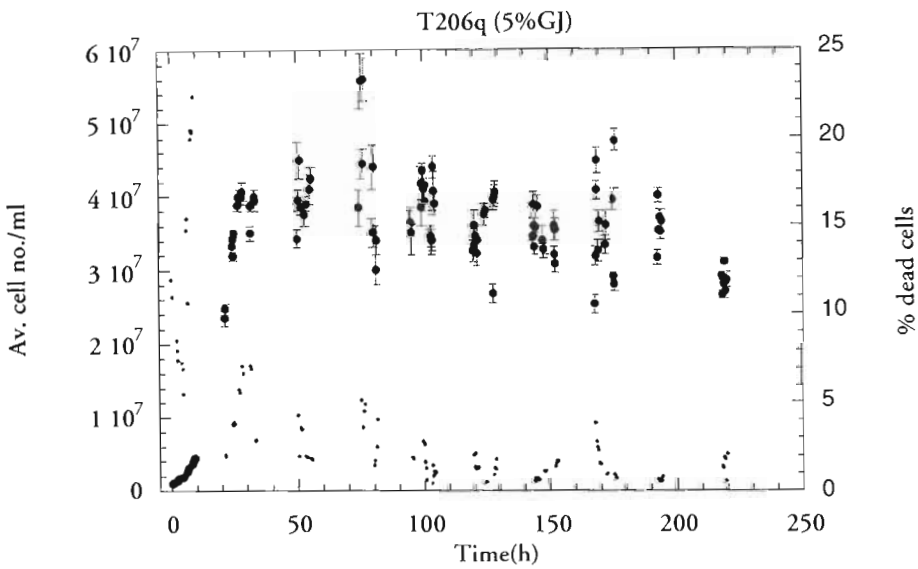

Figure **3.10** Mean cell number per ml and % dead cells of microscale batch fermentation involving single cultures of *Saccharomyces cerevisiae*, (a) the killer strain T206 and (b) its cured derivative, T206q, growing in 5% grape juice (GJ).

(a)

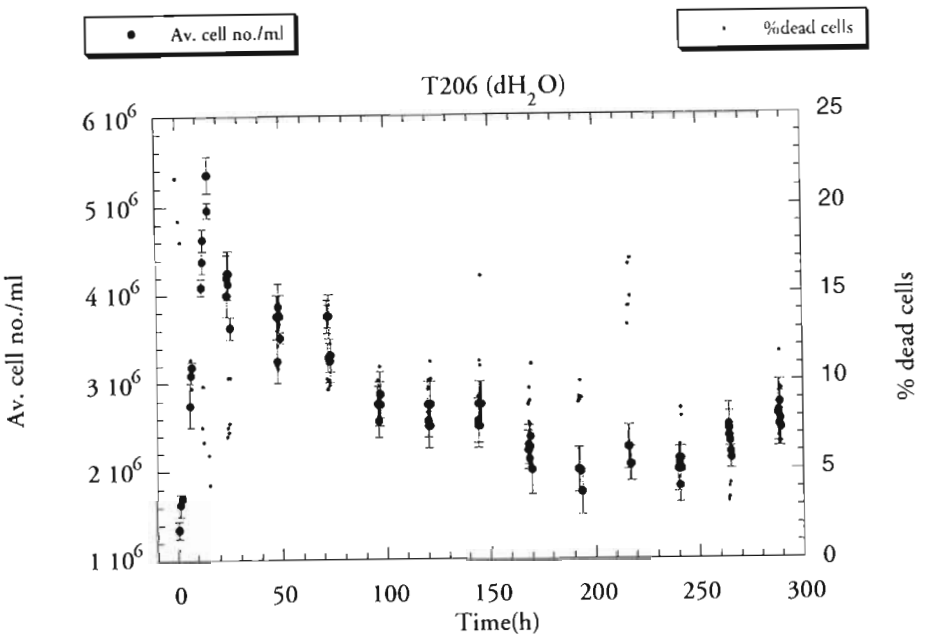

(b)

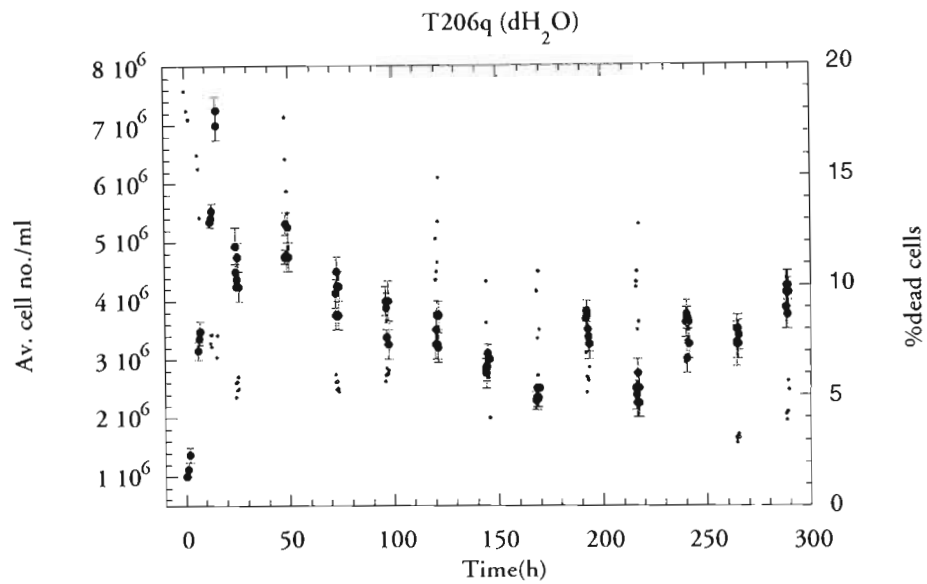

Figure **3.11** Mean cell number per ml and % dead cells of microscale batch growth involving single cultures of *Saccharomyces cerevisiae*, (a) the killer strain T206 and (b) its cured derivative, T206q, in pure water (dH_2O).

(a)

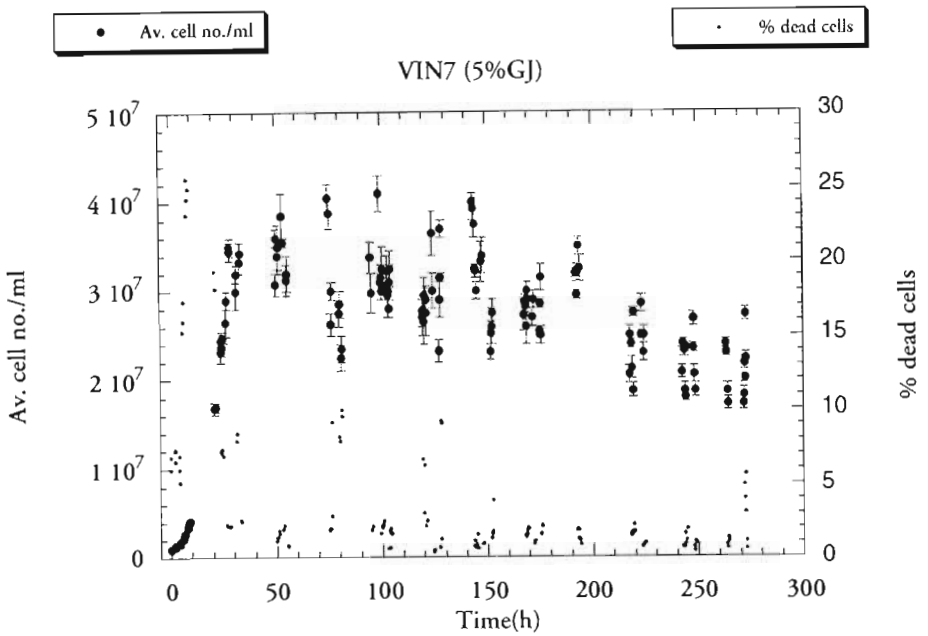

(b)

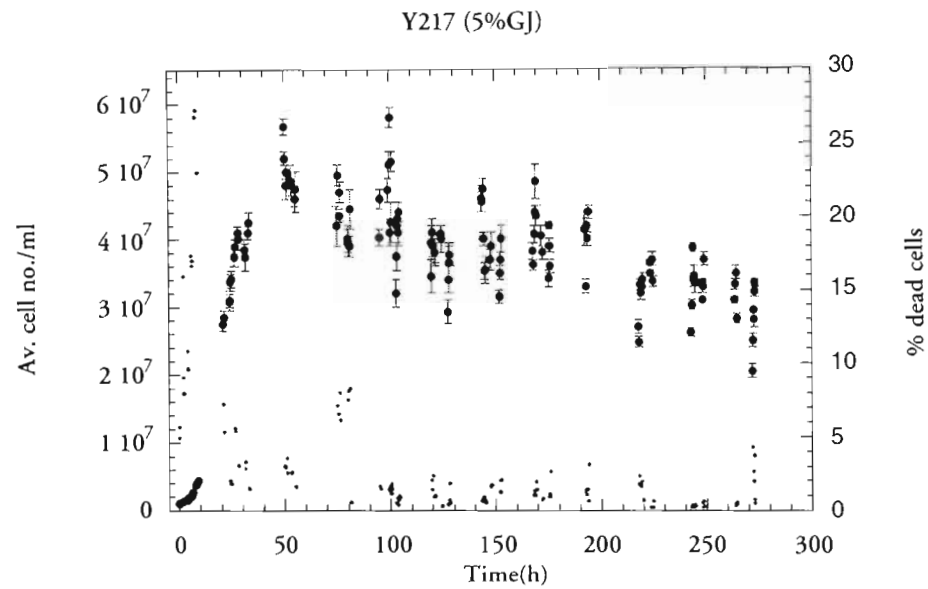

Figure **3.12** Mean cell number per ml and % dead cells of microscale batch fermentation involving single cultures of *Saccharomyces cerevisiae* sensitive strains, (a) VIN7 and (b) Y217, growing in 5% grape juice (GJ).

(a)

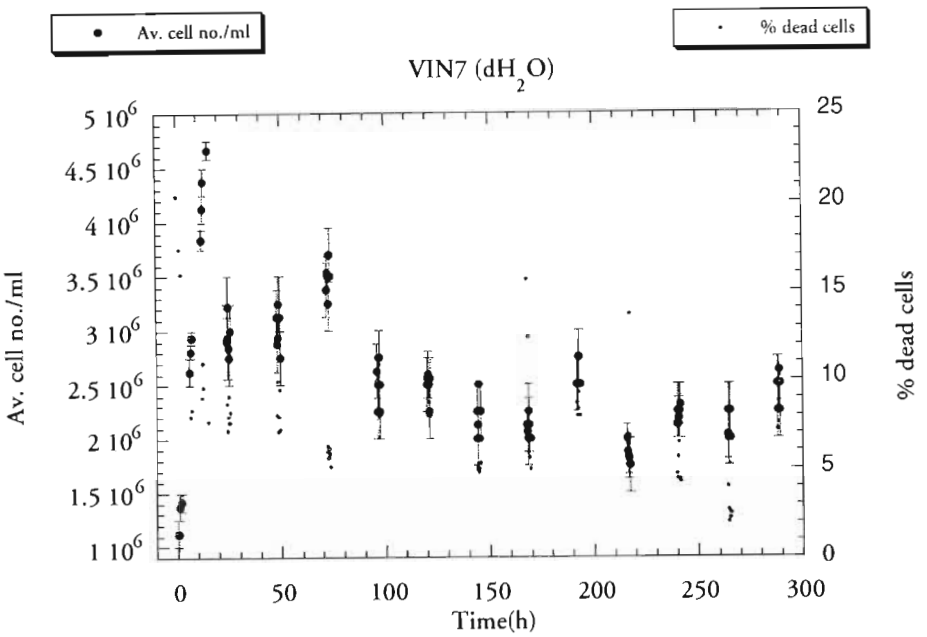

(b)

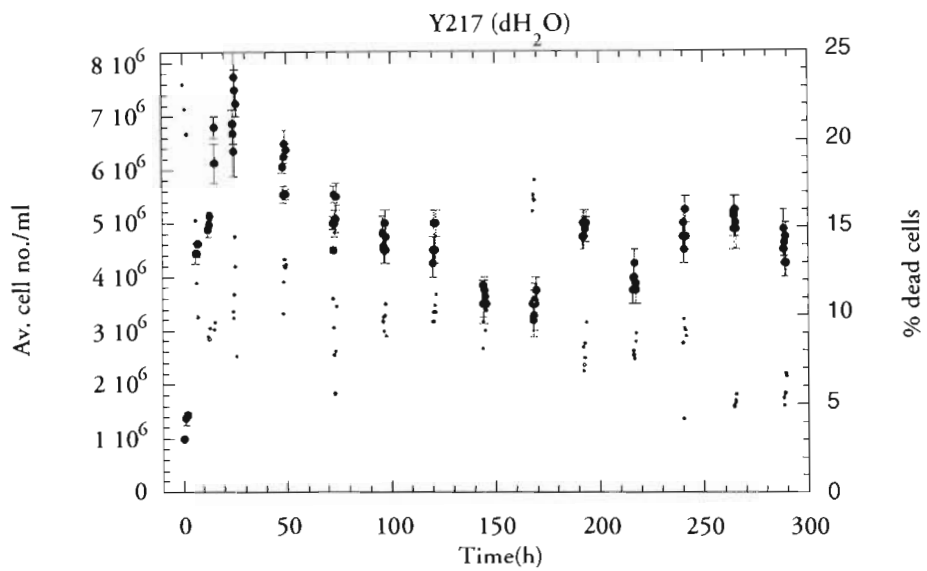

Figure **3.13** Mean cell number per ml and % dead cells of microscale batch growth involving single cultures of *Saccharomyces cerevisiae* sensitive strains, (a) VIN7 and (b) Y217, in pure water (dH_2O).

(a)

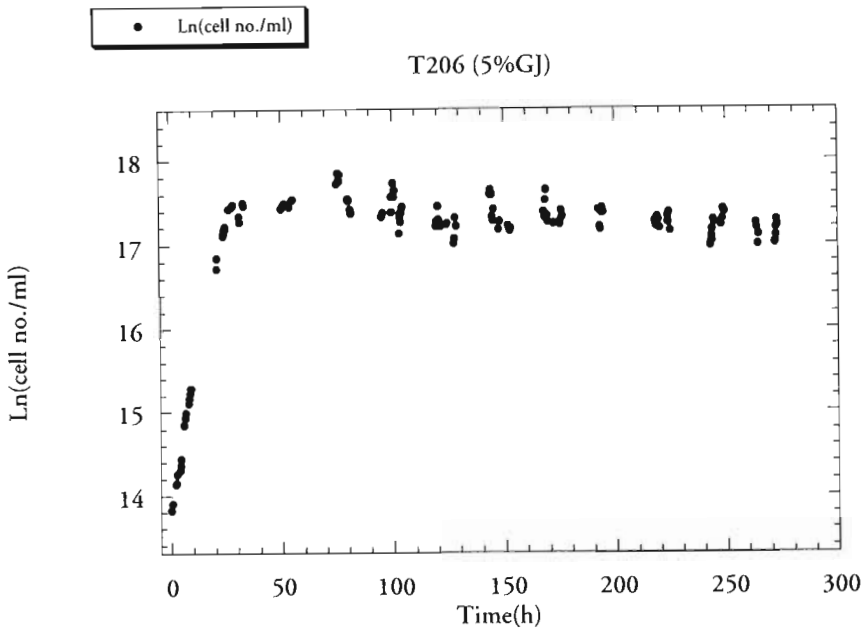

(b)

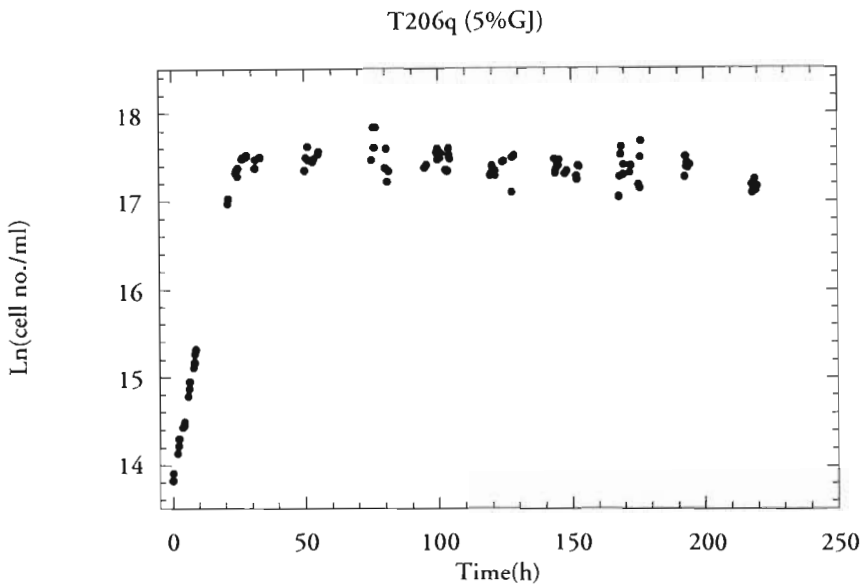

Figure **3.14** Ln of cell number per ml of microscale batch fermentation of single cultures of *Saccharomyces cerevisiae*, (a) the killer strain T206 and (b) its cured derivative, T206q, growing 5% grape juice (GJ).

(a)

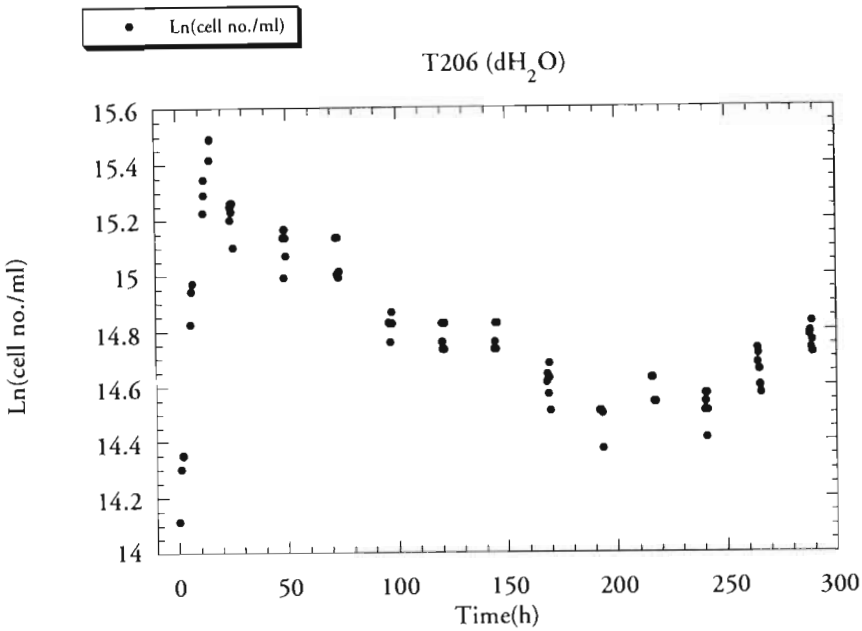

(b)

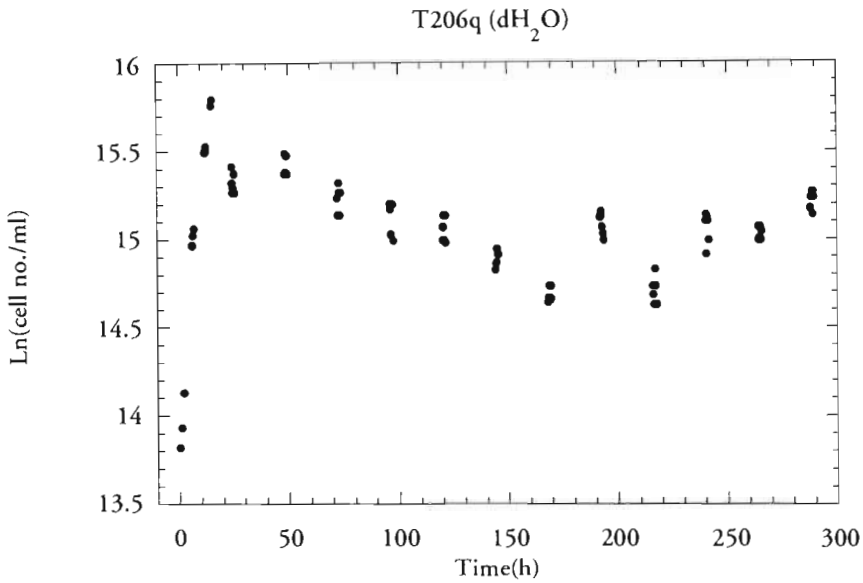

Figure **3.15** Ln of cell number per ml of microscale batch growth involving single cultures of *Saccharomyces cerevisiae*, (a) the killer strain T206 and (b) its cured derivative, T206q, in pure water (dH_2O).

(a)

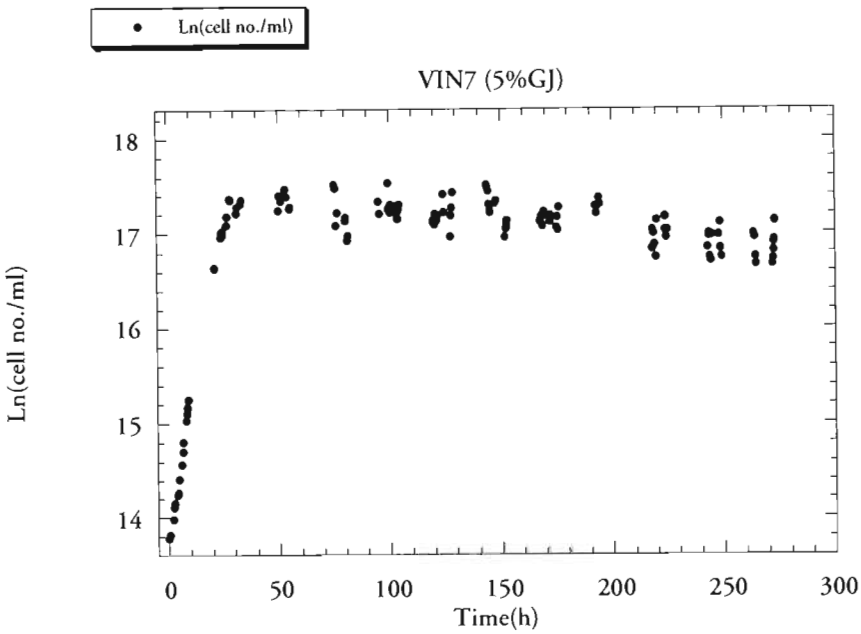

(b)

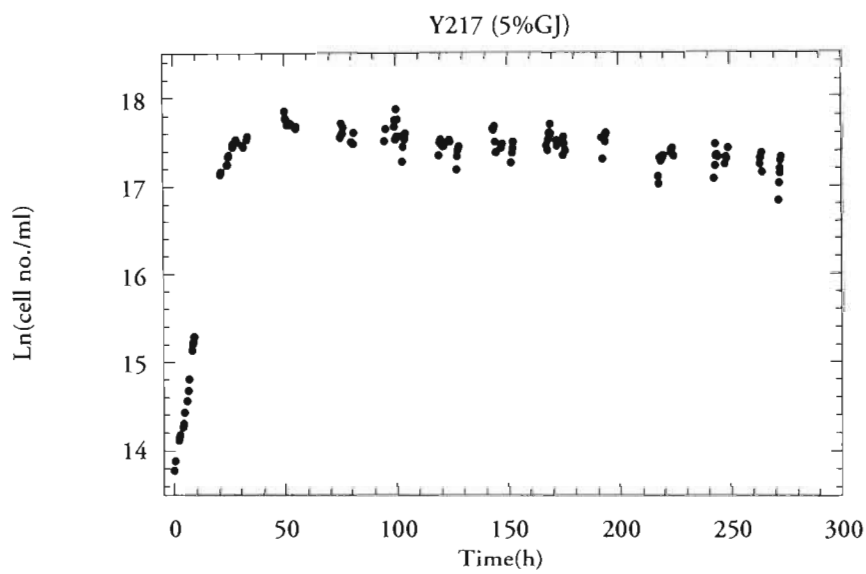

Figure **3.16** Ln of cell number per ml of microscale batch fermentation involving single cultures of *Saccharomyces cerevisiae* sensitive strains (a) VIN7 and (b) Y217, growing in 5% grape juice (GJ).

(a)

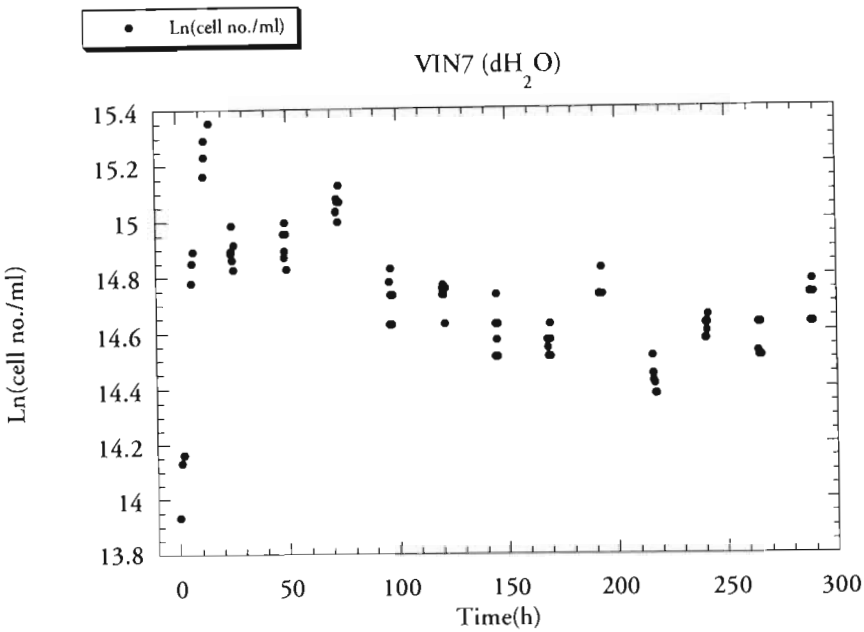

(b)

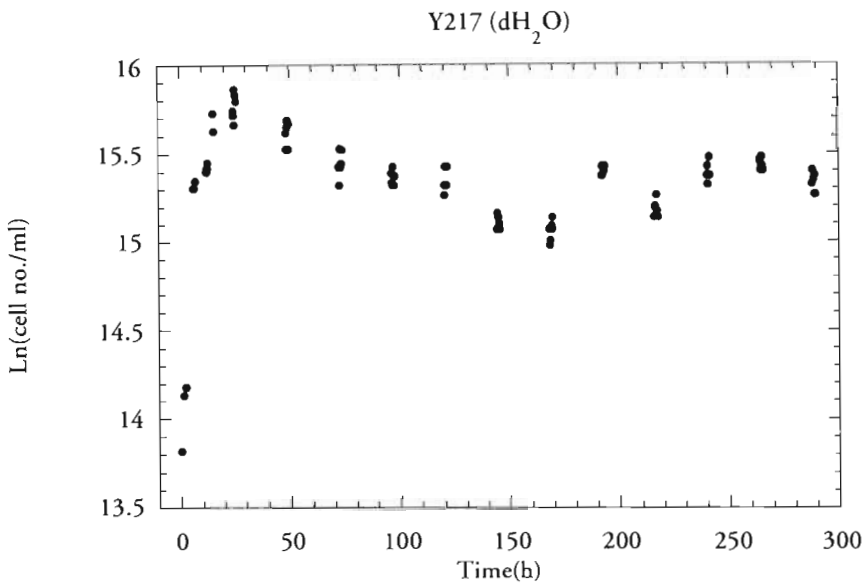

Figure **3.17** Ln of cell number per ml of microscale batch growth involving single cultures of *Saccharomyces cerevisiae* sensitive strains, (a) VIN7 and (b) Y217, in pure water (dH_2O).

(a)

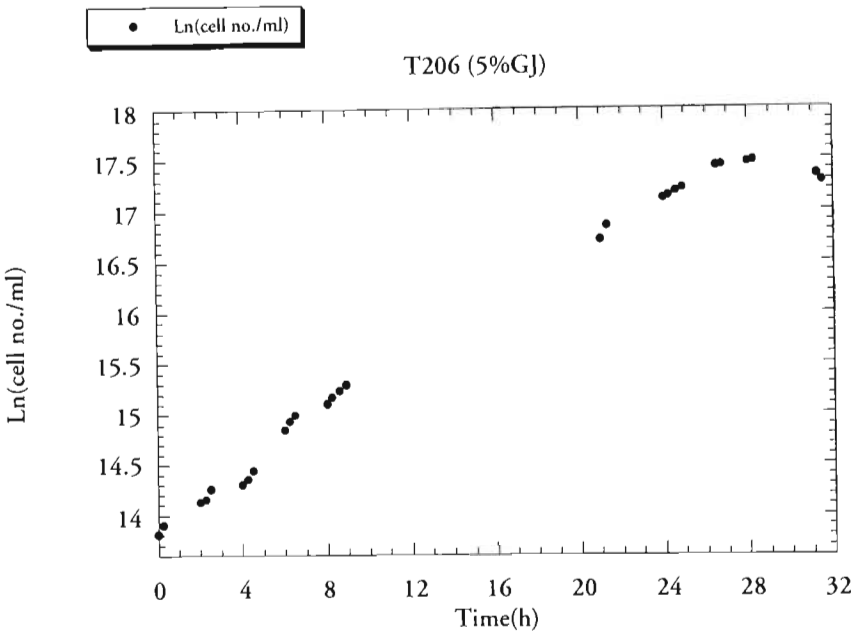

(b)

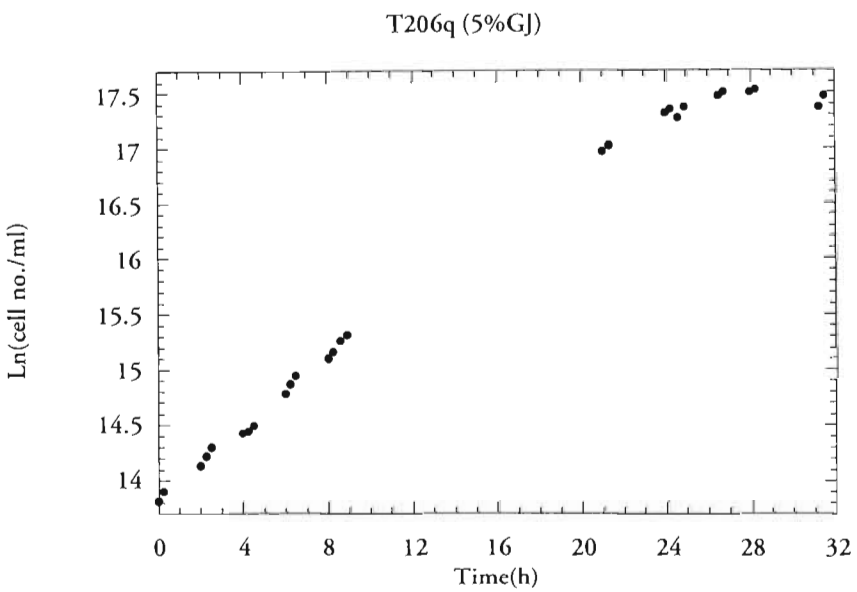

Figure **3.18** Ln of cell number per ml of microscale batch fermentation involving single cultures of *Saccharomyces cerevisiae*, (a) the killer strain T206 and (b) its cured derivative, T206q, growing in 5% grape juice (GJ) zooming into the log phase of growth.

(a)

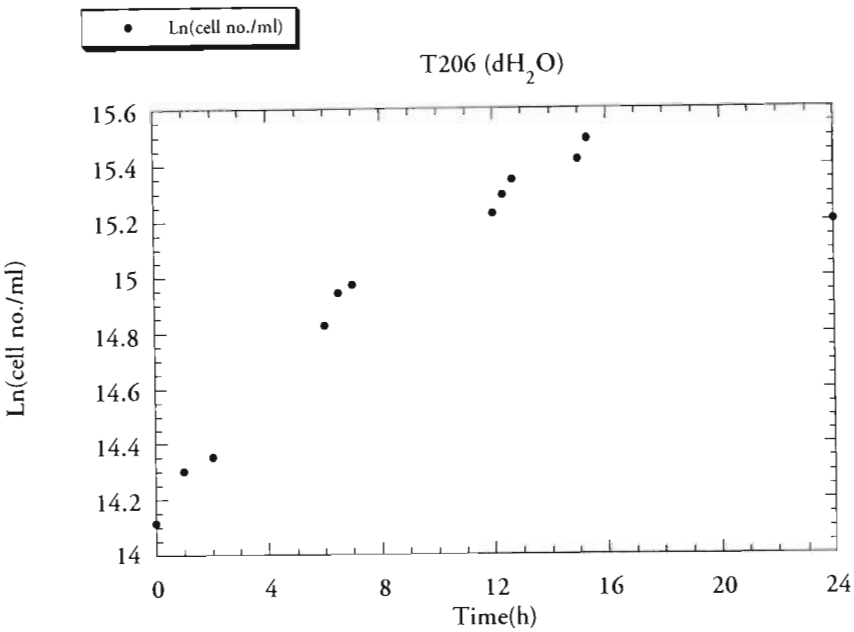

(b)

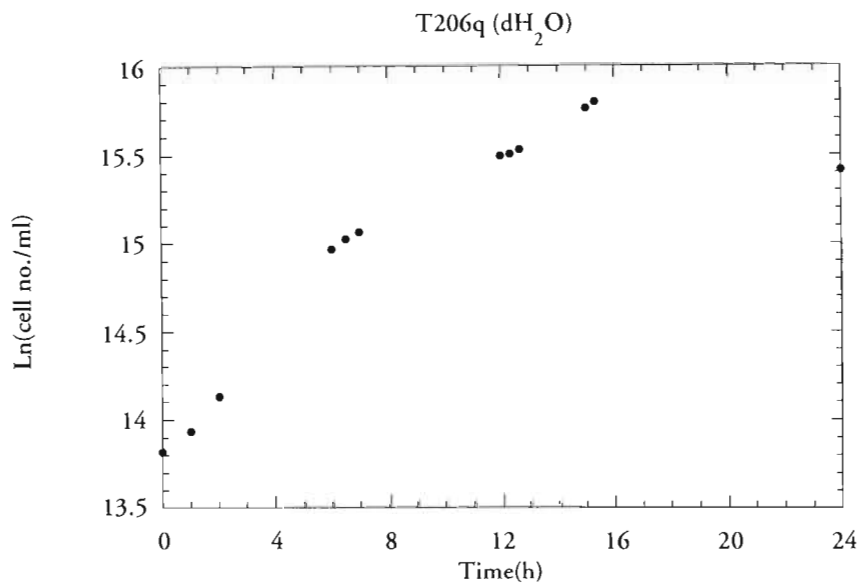

Figure **3.19** Ln of cell number per ml of microscale batch growth involving single cultures of *Saccharomyces cerevisiae*, (a) the killer strain T206 and (b) its cured derivative, T206q, in pure water (dH_2O) zooming into the log phase of growth.

(a)

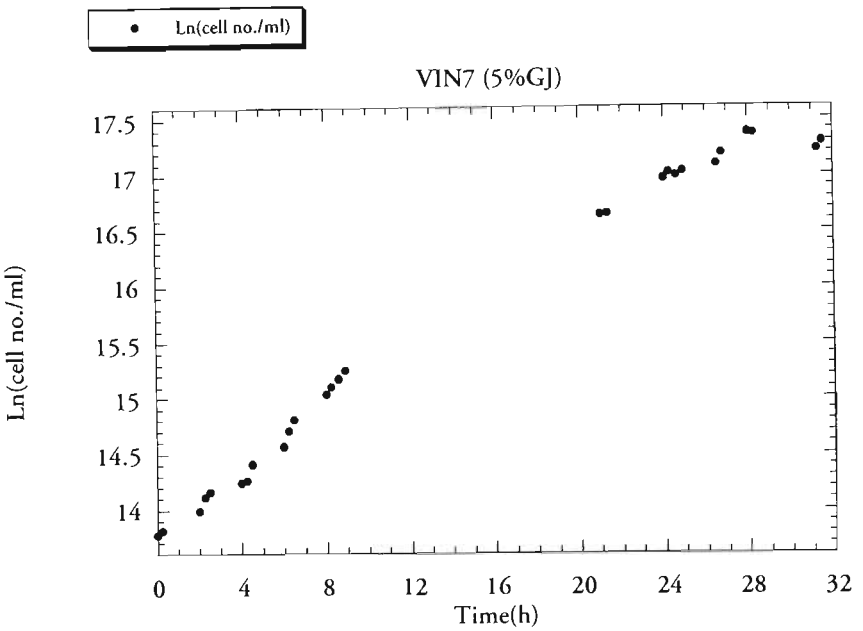

(b)

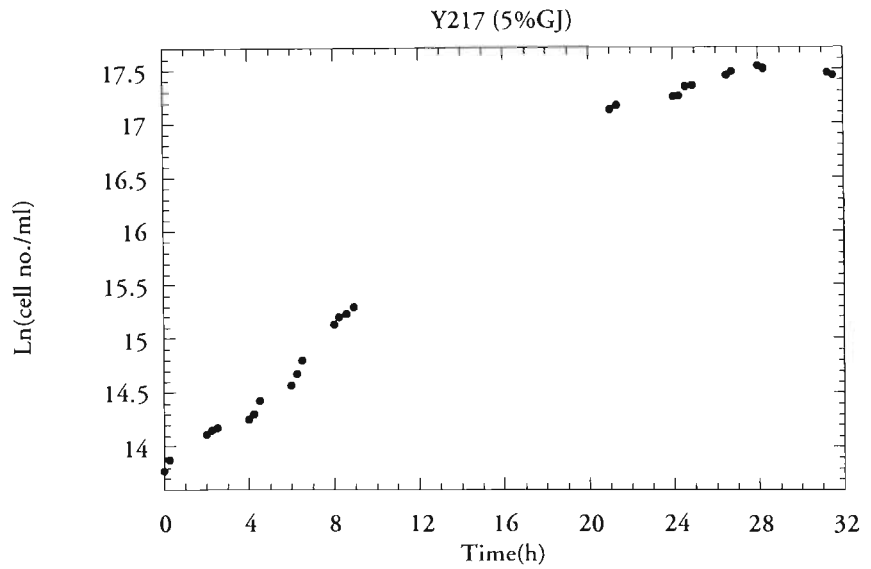

Figure **3.20** Ln of cell number per ml of microscale batch fermentation involving single cultures of *Saccharomyces cerevisiae* sensitive strains, (a) VIN7 and (b) Y217, growing in 5% grape juice (GJ) zooming into the log phase of growth.

(a)

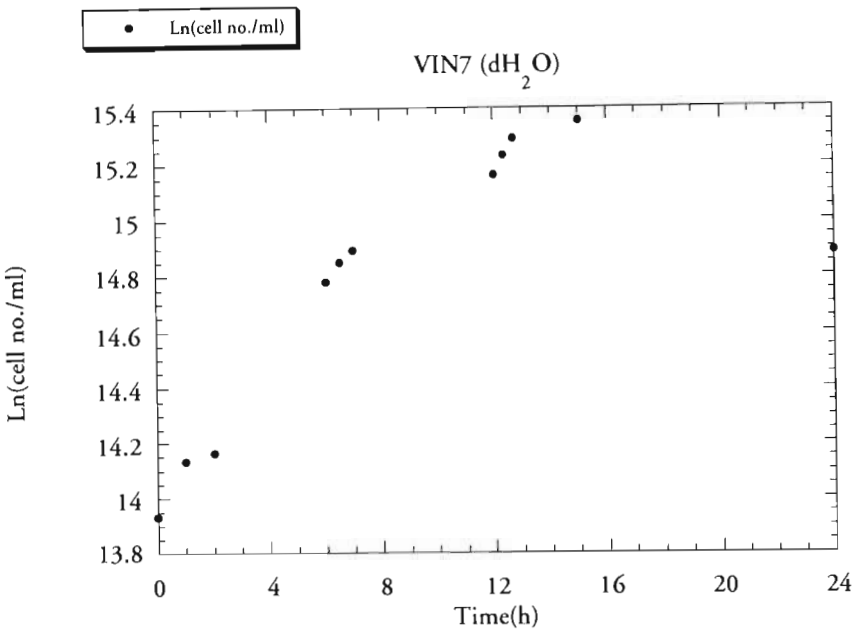

(b)

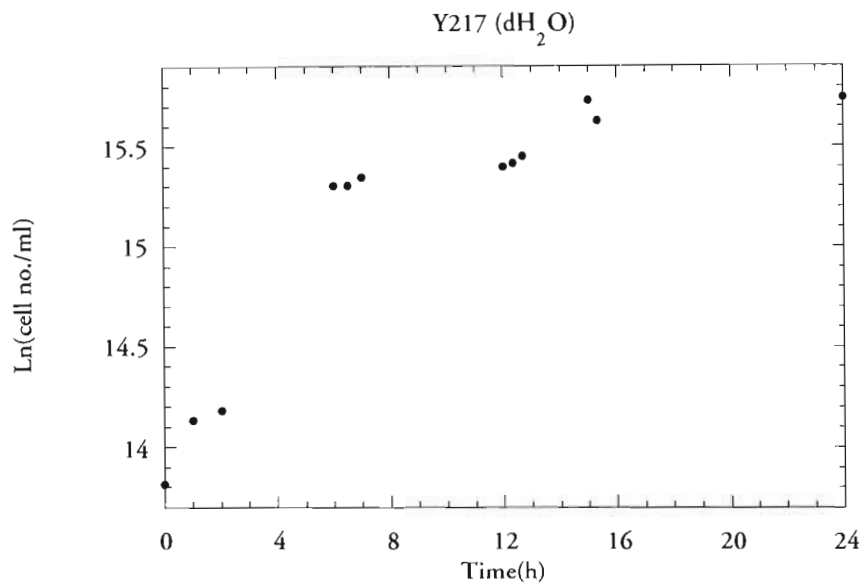

Figure **3.21** Ln of cell number per ml of microscale batch growth involving single cultures of *Saccharomyces cerevisiae* sensitive strains, (a) VIN7 and (b) Y217, in pure water (dH_2O) zooming into the log phase of growth.

(a)

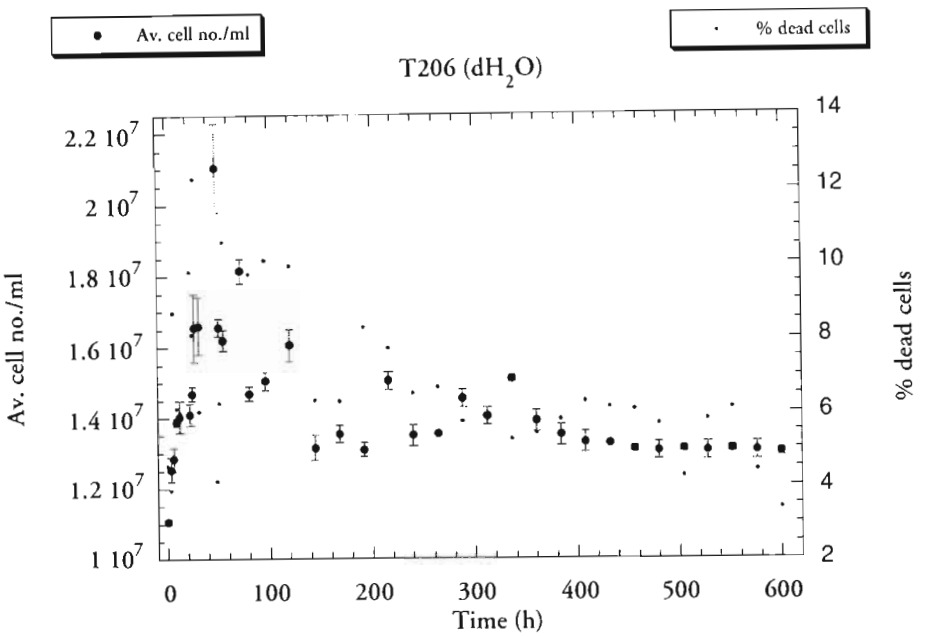

(b)

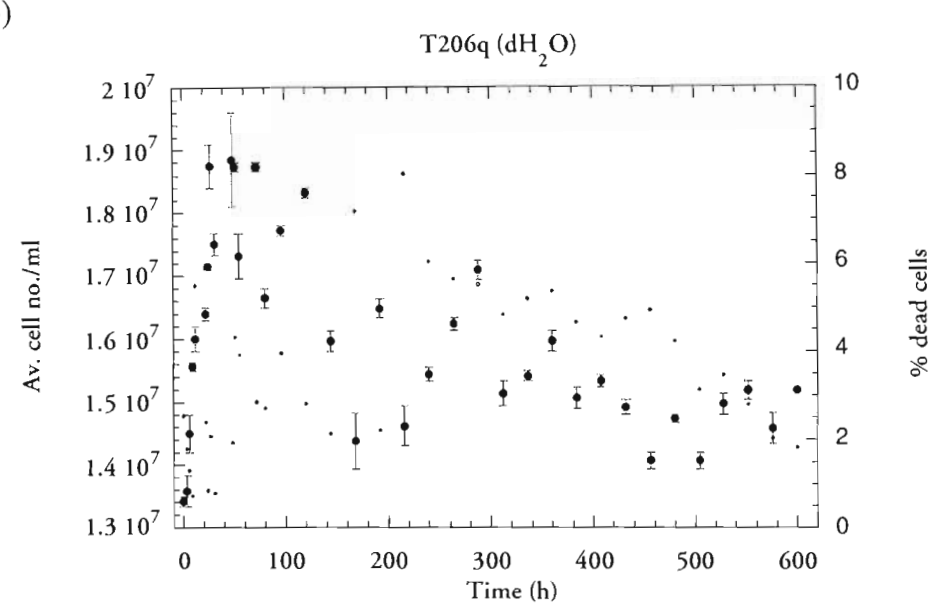

Figure **3.22** Mean cell number per ml and % dead cells of microscale batch growth involving single cultures of *Saccharomyces cerevisiae*, (a) the killer strain T206 and (b) its cured derivative, T206q, each inoculated at initial approximate cell concentration of 10^7cells/ml in pure water (dH_2O).

(a)

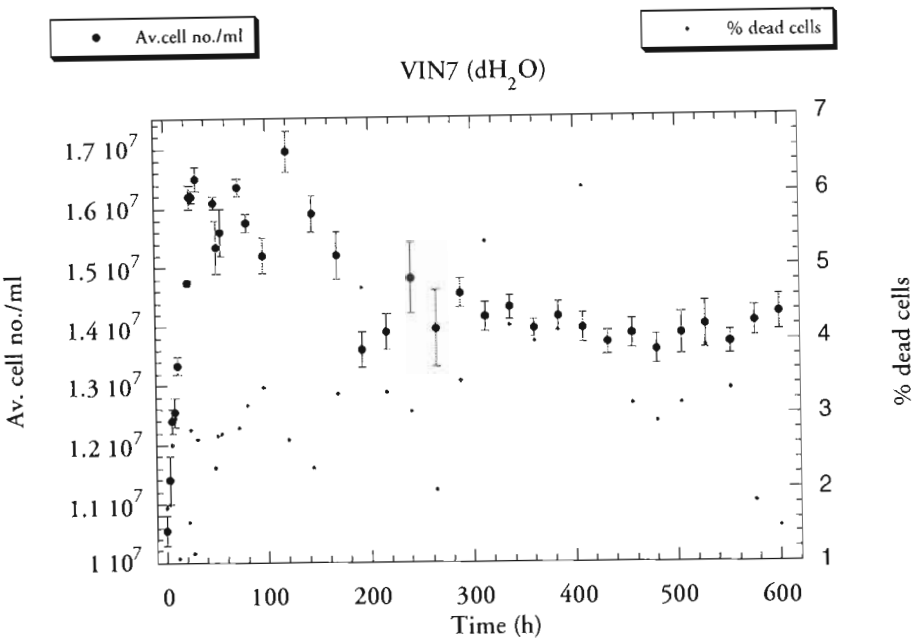

(b)

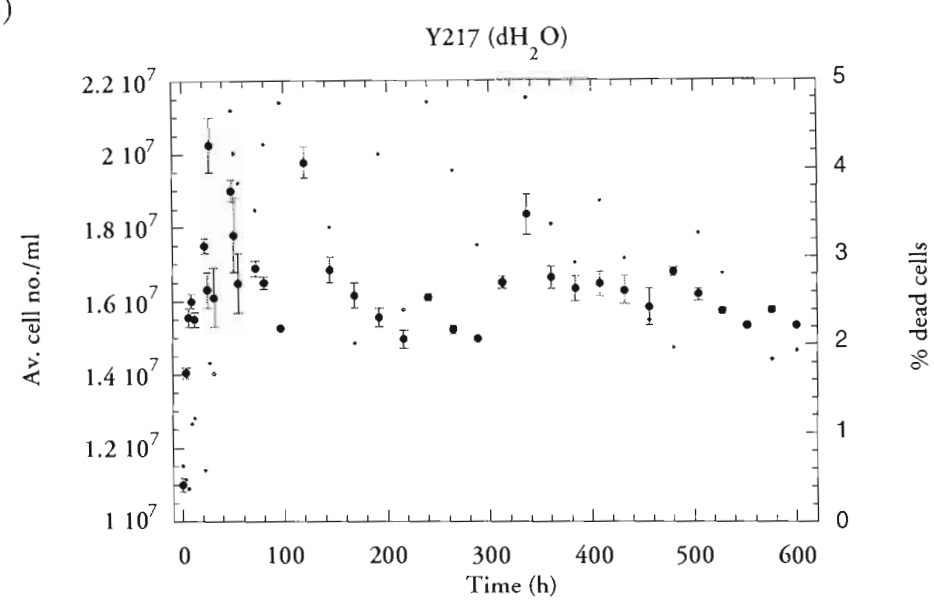

Figure **3.23** Mean cell number per ml and % dead cells of microscale batch growth involving single cultures of *Saccharomyces cerevisiae* sensitive strains, (a) VIN7 and (b) Y217, each inoculated at an initial approximate cell concentration of 10^7cells/ml in pure water (dH_2O).

(a)

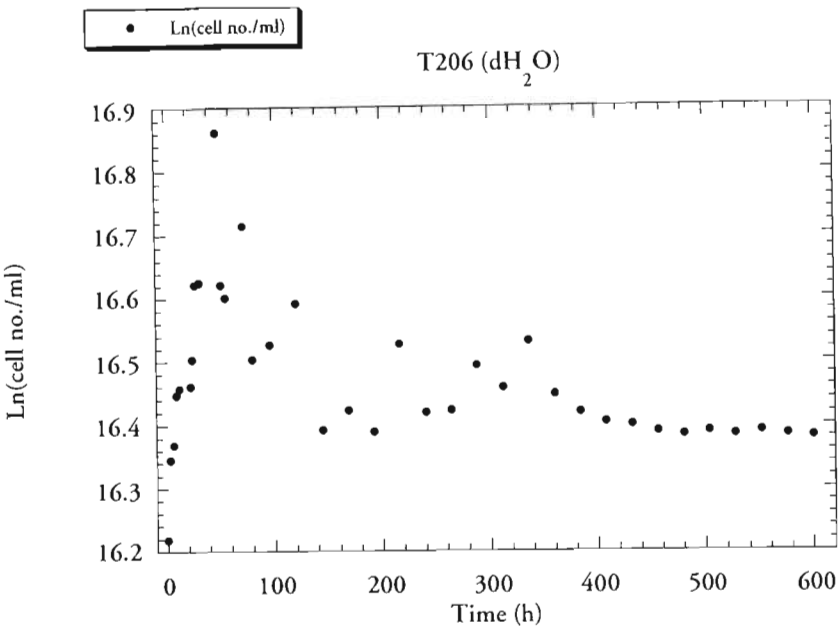

(b)

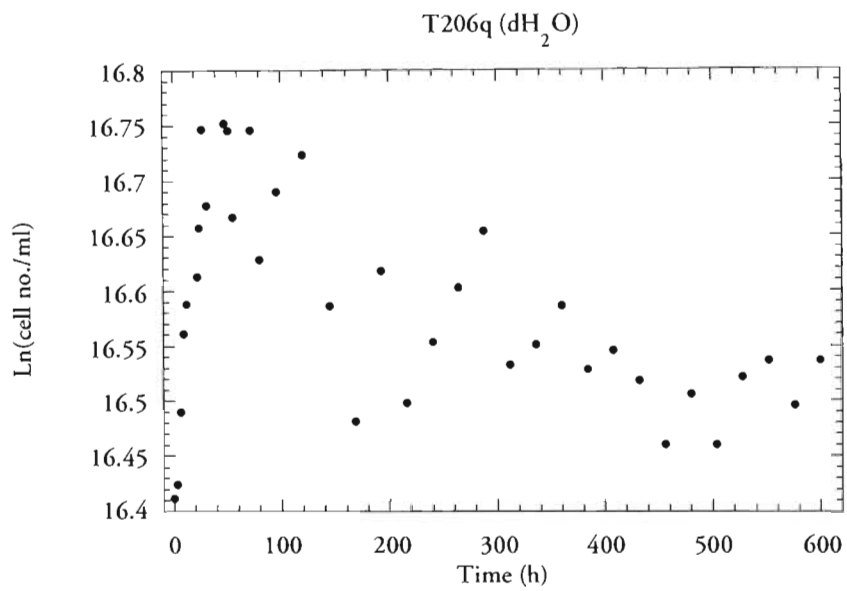

Figure **3.24** Ln of cell number per ml of microscale batch growth involving single cultures of *Saccharomyces cerevisiae*, (a) the killer strain T206 and (b) its cured derivative, T206q, each inoculated at an initial approximate cell concentration of 10^7 cells/ml in pure water (dH_2O).

(a)

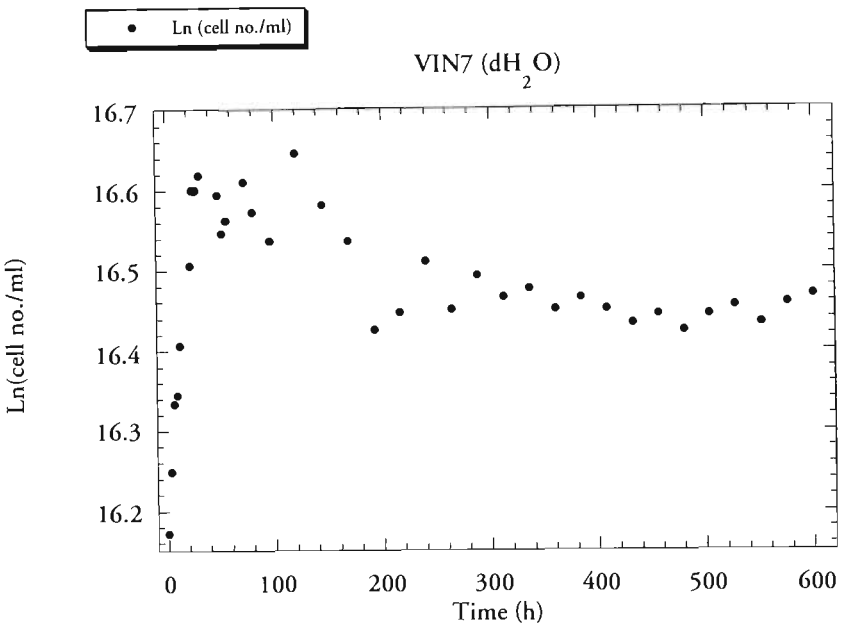

(b)

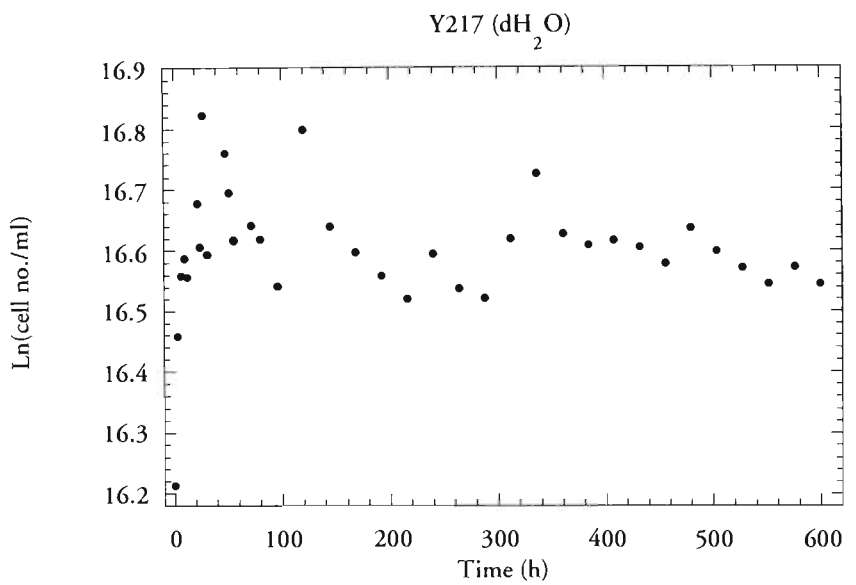

Figure **3.25** Ln of cell number per ml of microscale batch growth involving single cultures of *Saccharomyces cerevisiae* sensitive strains, (a) VIN7 and (b)Y217, each inoculated at an initial approximate cell concentration of 10^7 cells/ml in pure water (dH_2O).

(a)

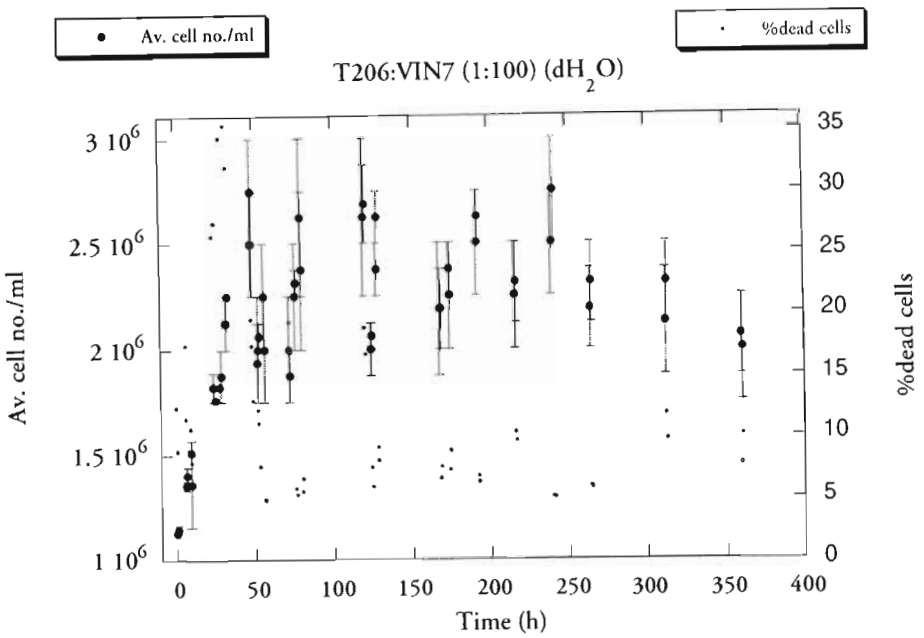

(b)

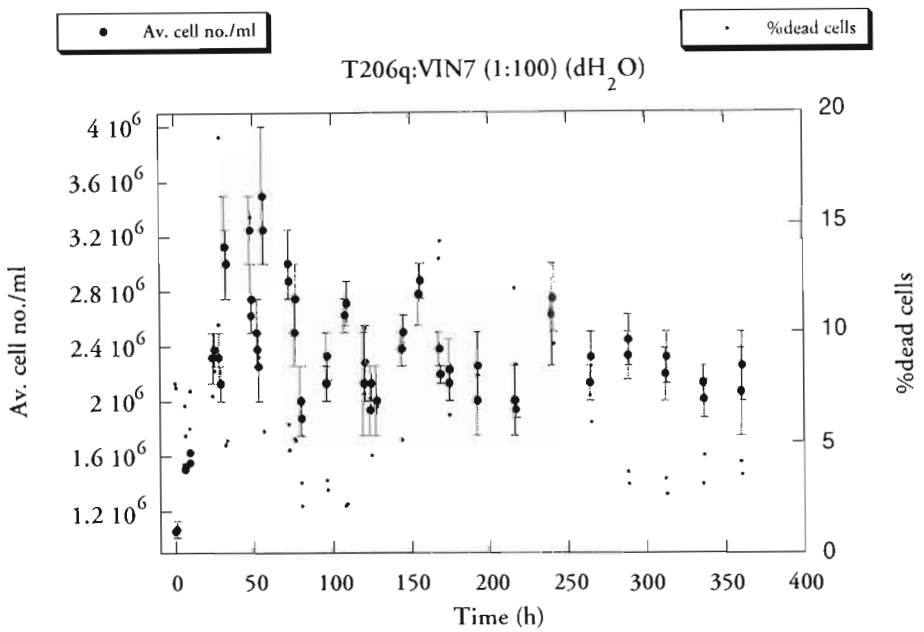

Figure **3.26** Mean cell number per ml and % dead cells of microscale batch growth in pure water (dH_2O) of mixed cultures of *Saccharomyces cerevisiae*, (a) killer strain T206 (K) and (b) its cured derivative T206q (Kq), separately challenging the sensitive strain VIN7 (Sv) at a K or Kq:Sv cell ratio of 1:100.

(a)

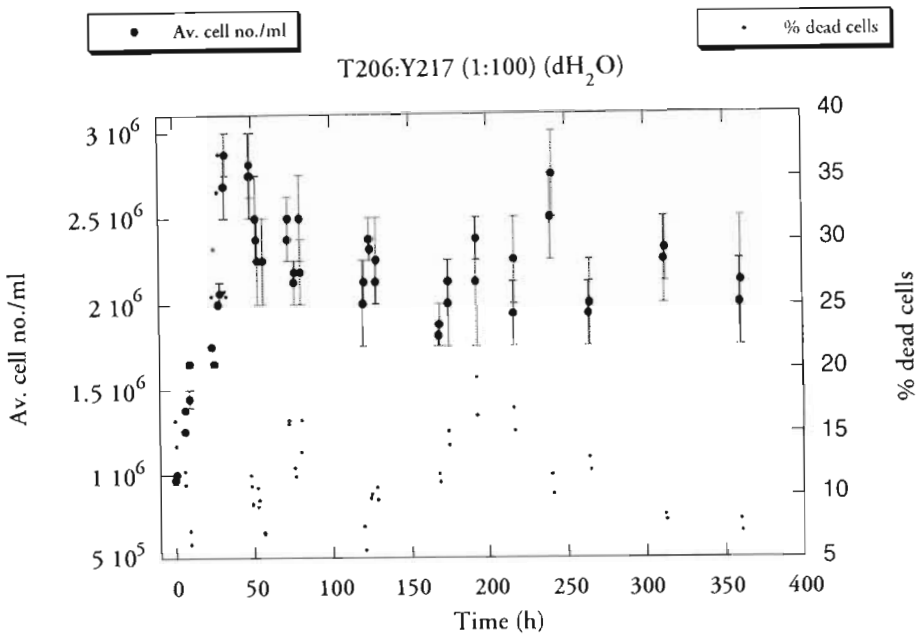

(b)

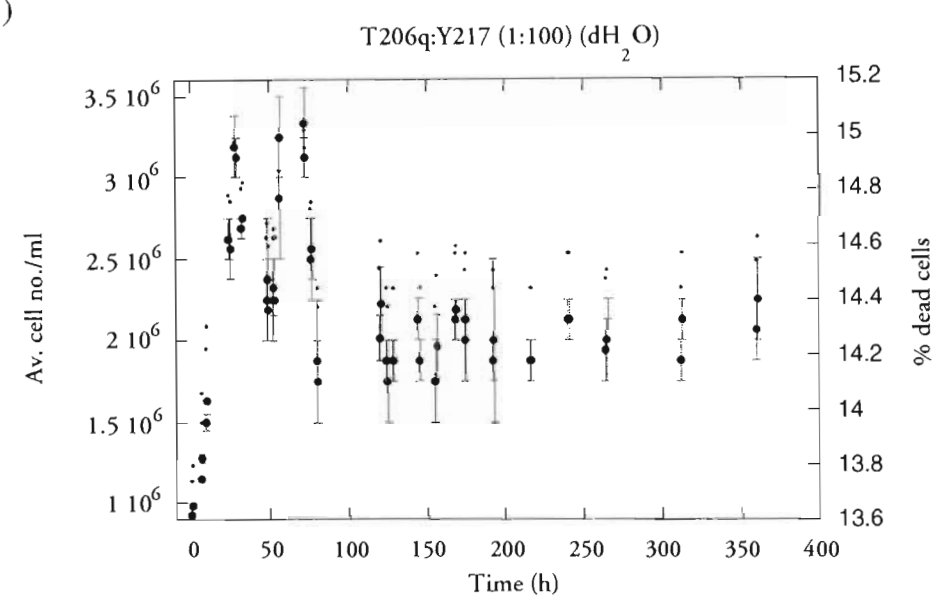

Figure **3.27** Mean cell number per ml and % dead cells of microscale batch growth in pure water (dH_2O) of mixed cultures of *Saccharomyces cerevisiae,* (a) killer strain T206 (K) and (b) its cured derivative T206q (Kq), separately challenging the sensitive strain Y217 (Sy) at a K or Kq:Sy cell ratio of 1:100.

(a)

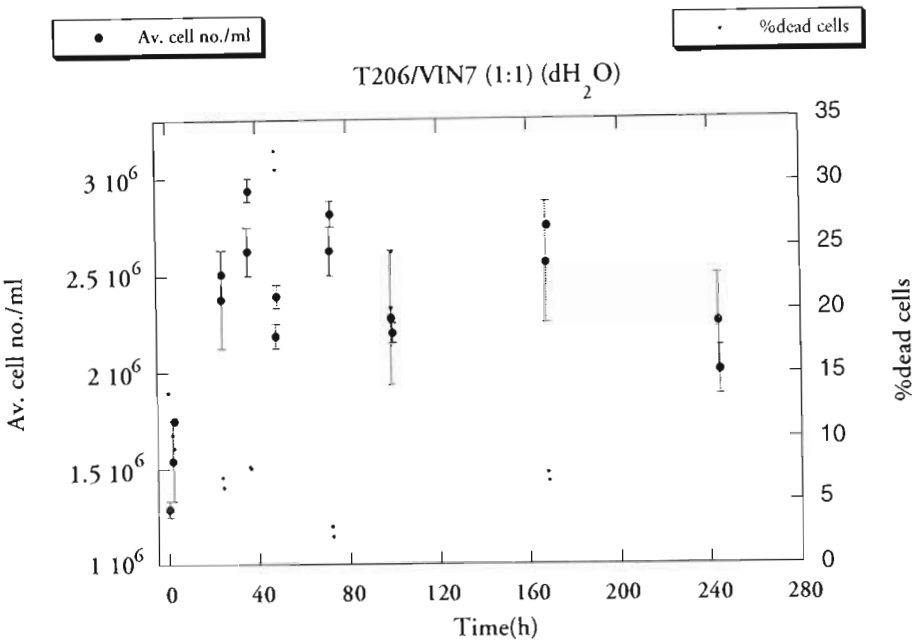

(b)

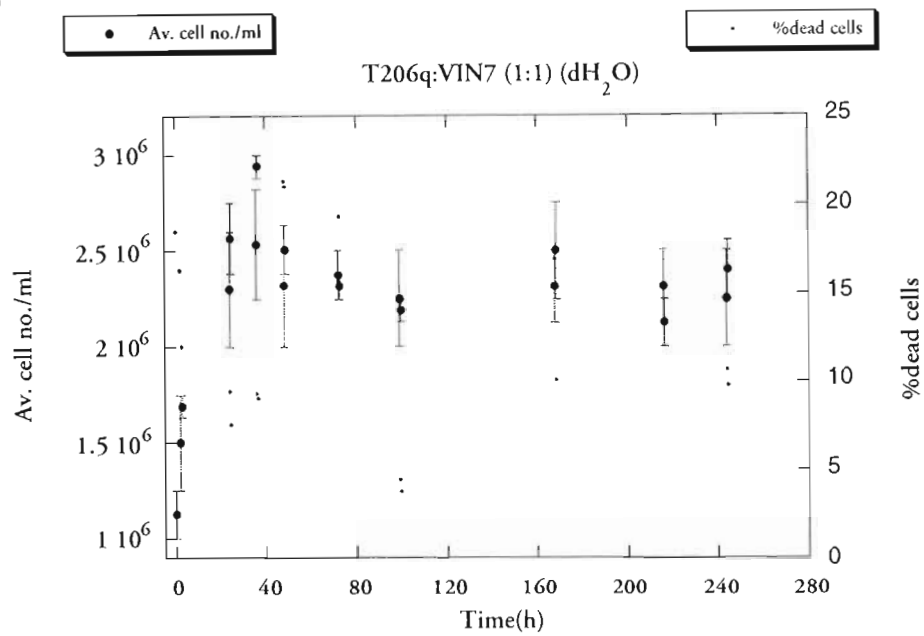

Figure **3.28** Mean cell number per ml and % dead cells of microscale batch growth in pure water (dH_2O) of mixed cultures of *Saccharomyces cerevisiae,* (a) killer strain T206 (K) and (b) its cured derivative T206q (Kq), separately challenging the sensitive strain VIN7 (Sv) at a K or Kq:Sv cell ratio of 1:1.

(a)

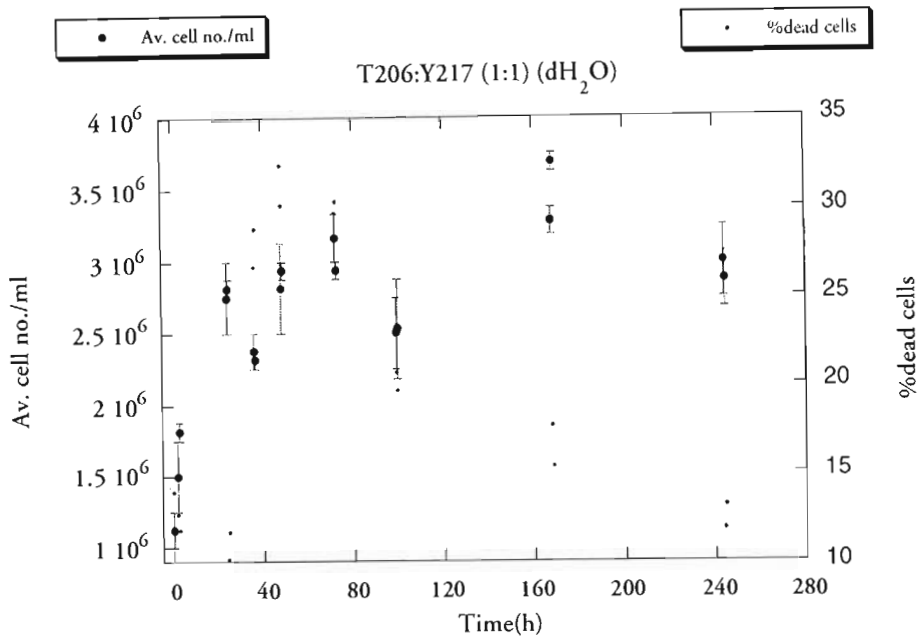

(b)

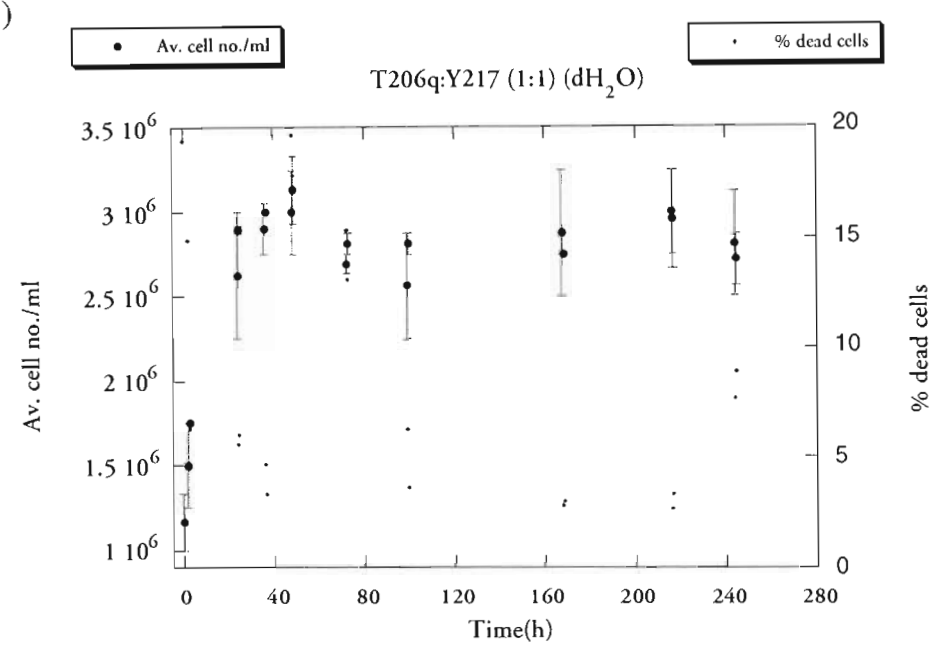

Figure **3.29** Mean cell number per ml and % dead cells of microscale batch growth in pure water (dH_2O) of mixed cultures of *Saccharomyces cerevisiae,* (a) killer strain T206 (K) and (b) its cured derivative T206q (Kq), separately challenging the sensitive strain Y217 (Sy) at a K or Kq:Sy cell ratio of 1:1.

(a)

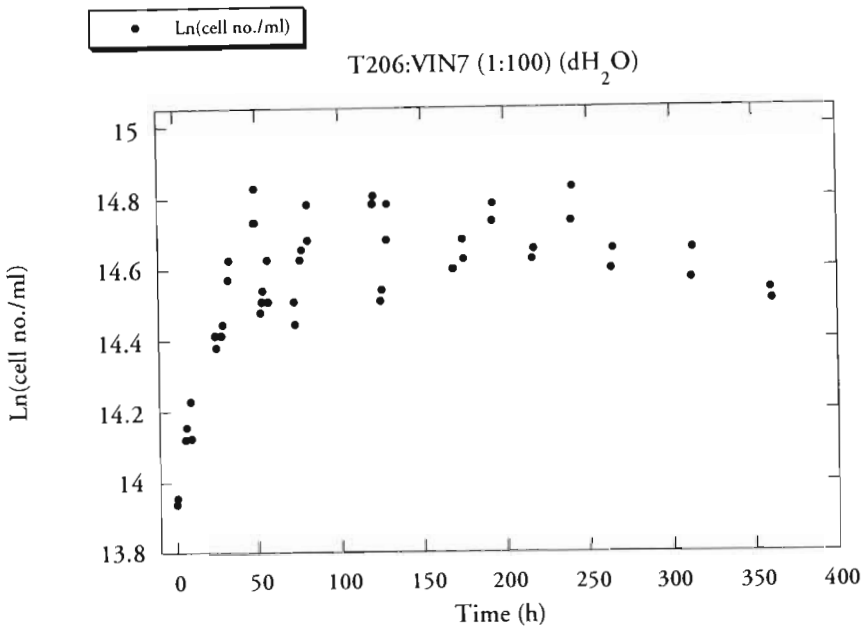

(b)

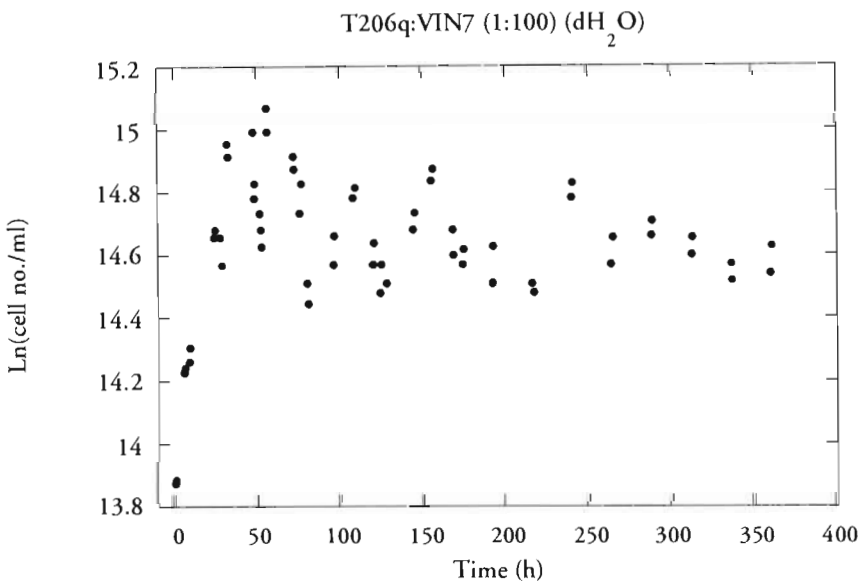

Figure **3.30** Ln of cell number per ml of microscale batch growth in pure water (dH_2O) of mixed cultures of *Saccharomyces cerevisiae,* (a) killer strain T206 (K) and (b) its cured derivative T206q (Kq), separately challenging the sensitive strain VIN7 (Sv) at a K or Kq:Sv cell ratio of 1:100.

(a)

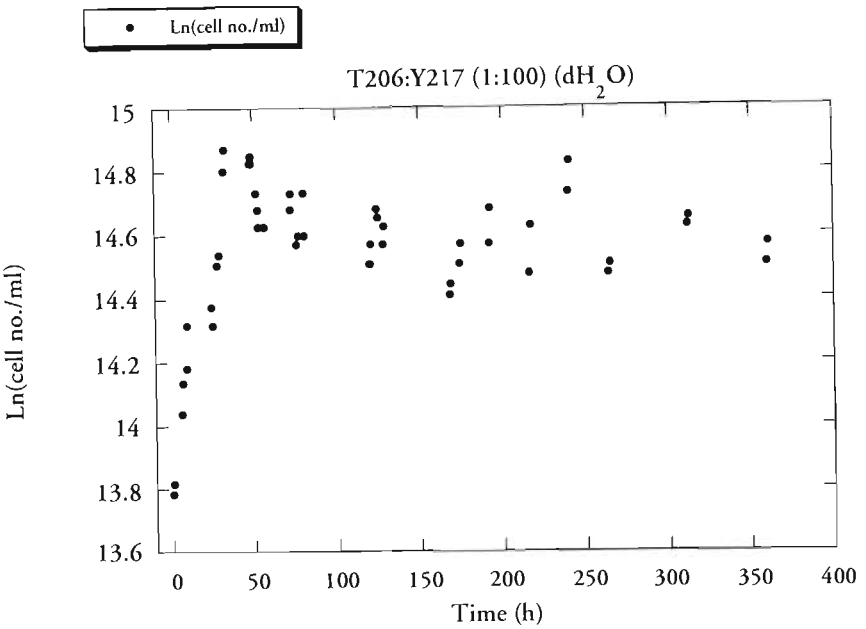

(b)

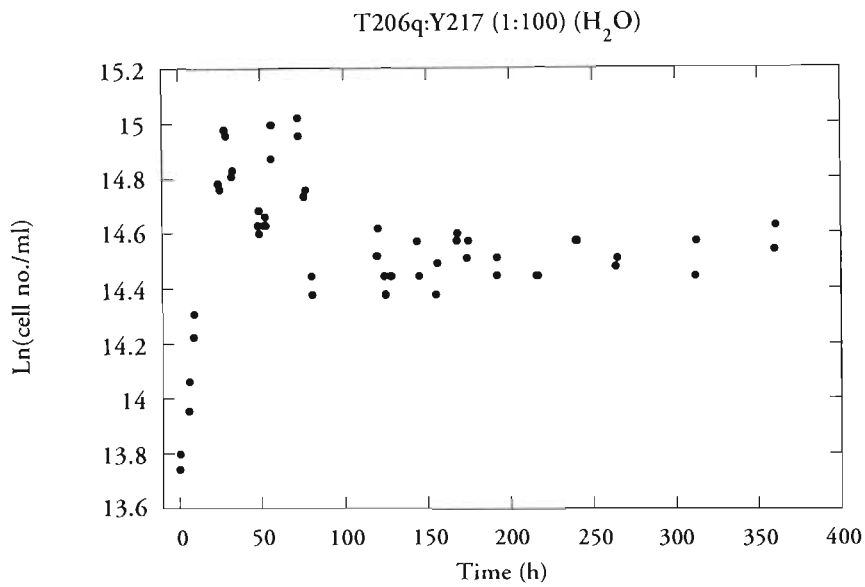

Figure **3.31** Ln of cell number per ml of microscale batch growth in pure water (dH_2O) of mixed cultures of *Saccharomyces cerevisiae*, (a) killer strain T206 (K) and (b) its cured derivative T206q (Kq), separately challenging the sensitive strain Y217 (Sy) at a K or Kq:Sy cell ratio of 1:100.

(a)

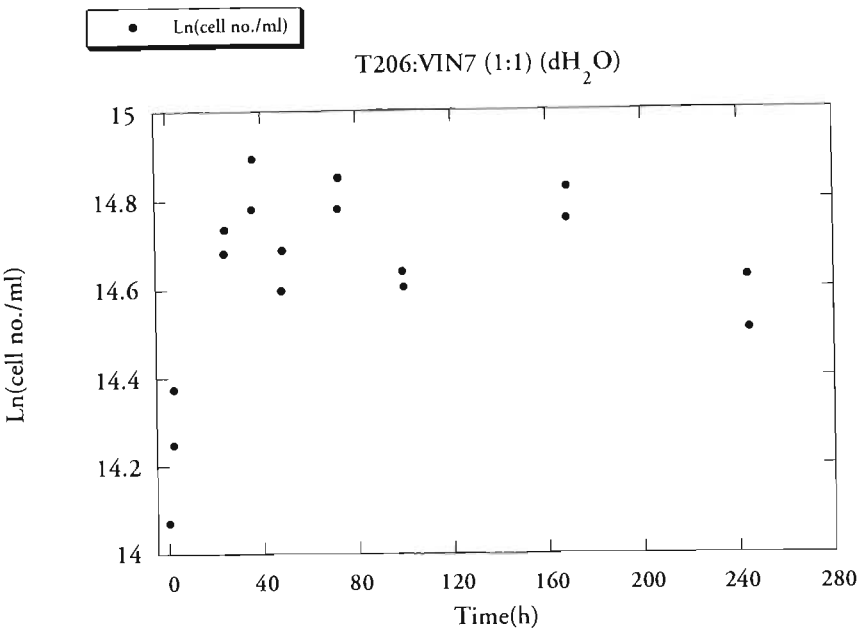

(b)

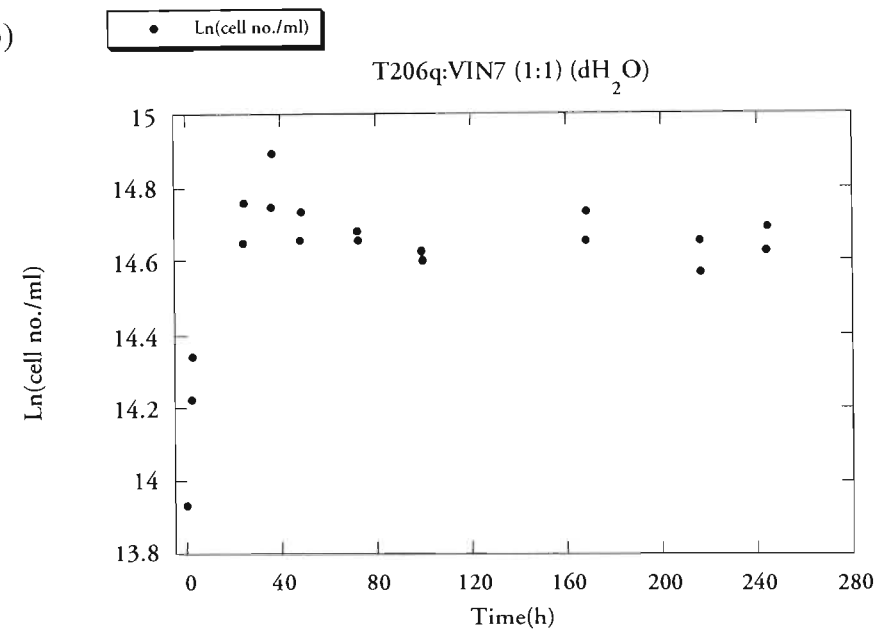

Figure **3.32** Ln of cell number per ml of microscale batch growth in pure water (dH_2O) of mixed cultures of *Saccharomyces cerevisiae*, (a) killer strain T206 (K) and (b) its cured derivative T206q (Kq), separately challenging the sensitive strain VIN7 (Sv) at a K or Kq:Sv cell ratio of 1:1.

(a)

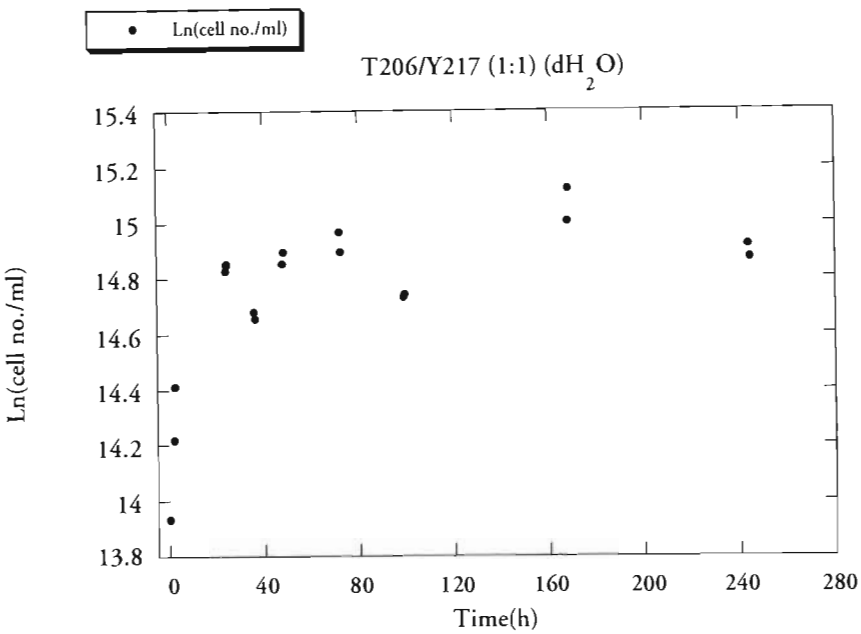

(b)

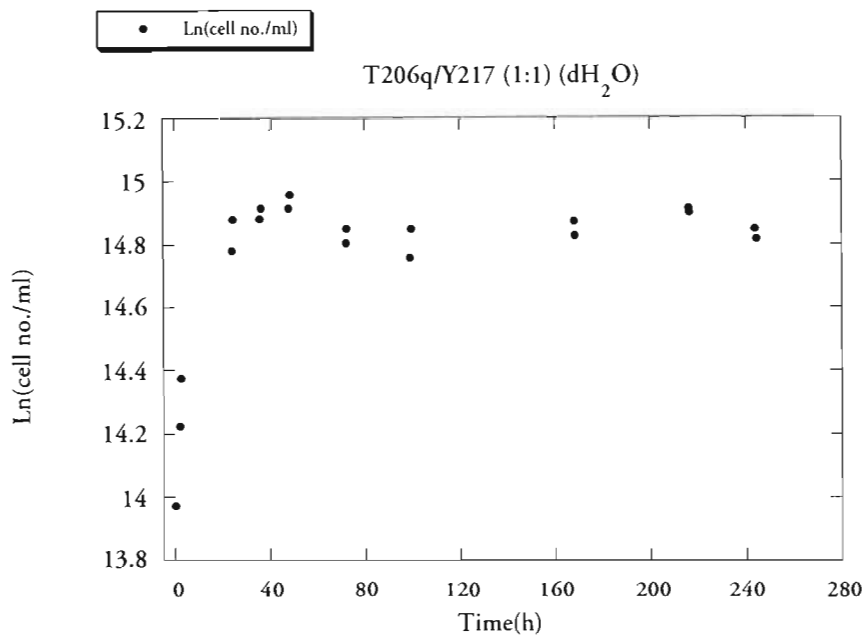

Figure **3.33** Ln of cell number per ml of microscale batch growth in pure water (dH_2O) of mixed cultures of *Saccharomyces cerevisiae,* (a) killer strain T206 (K) and (b) its cured derivative T206q (Kq), separately challenging the sensitive strain Y217 (Sy) at a K or Kq:Sy cell ratio of 1:1.

(a)

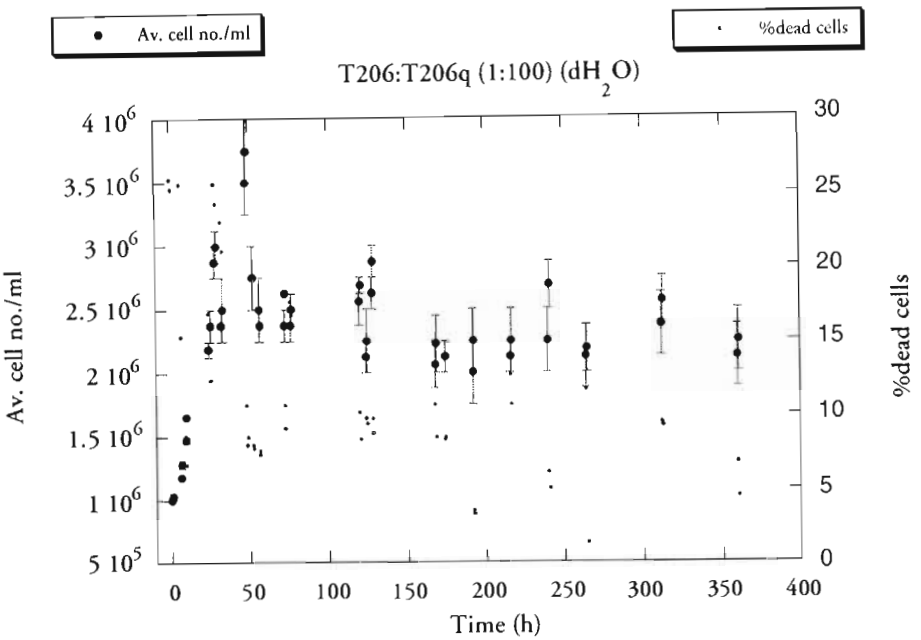

(b)

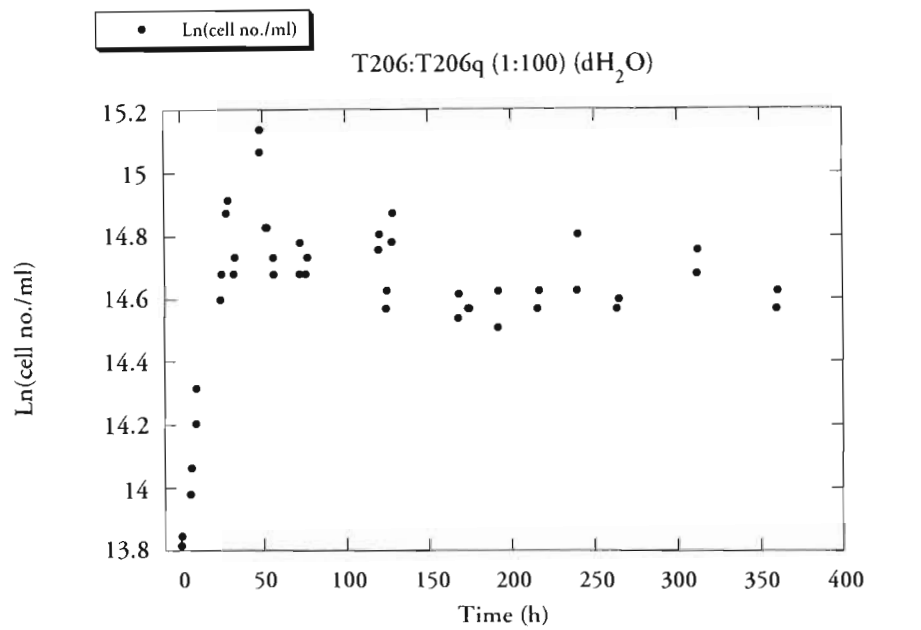

Figure **3.34** (a) Mean cell number per ml and % dead cells and (b) ln of cell number per ml of microscale batch growth in pure water (dH_2O) of mixed cultures of *Saccharomyces cerevisiae* killer cured derivative T206q (Kq) challenged by the killer strain T206 (K) at a K:Kq cell ratio of 1:100.

(a)

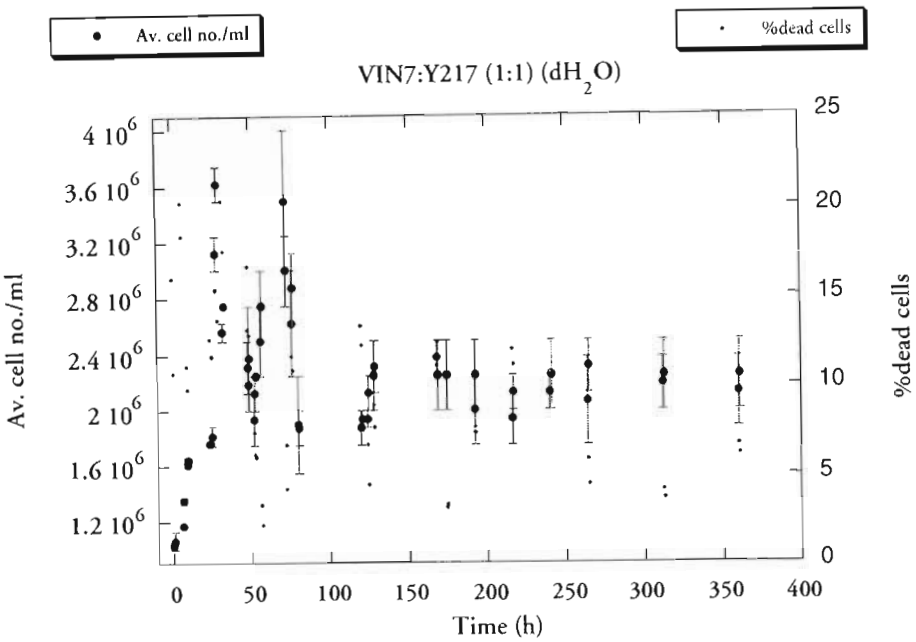

(b)

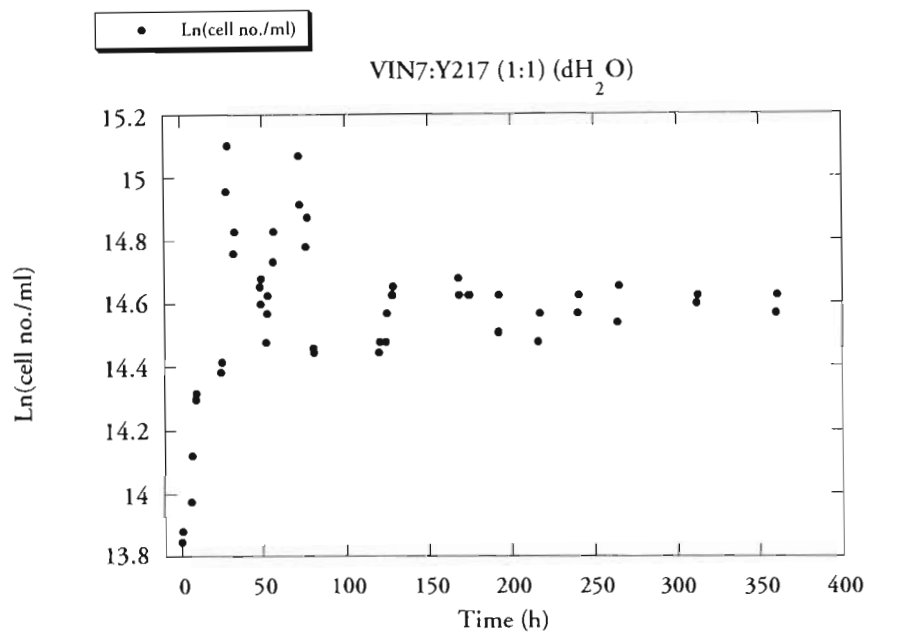

Figure **3.35** (a) Mean cell number per ml and % dead cells and (b) ln of cell number per ml of microscale batch growth in pure water (dH_2O) of mixed cultures of *Saccharomyces cerevisiae* sensitive strains, VIN7 (Sv) challenged by Y217 (Sy) at a Sv:Sy cell ratio of 1:1.

Cell counts and % dead cells were determined as described (section 3.2.2.6). The experimental error was estimated by averaging the readings and recording the minimum and maximum cell counts. The difference between the minimum and maximum and the average was assumed to represent the experimental error for the cell count. Since all the reading process extended over one half an hour period, the reading time was recorded within a 15 minutes margin of error.

Pure and mixed cell cultures grew actively, attaining the stationary phase by damped oscillations, yielding a strain-dependent cell concentration. For about $1x10^6$ initial cell concentration, pure cultures attained the stationary phase within a range of 2.0-4.5 $x10^7$ cells/ml growing in 5% grape juice (Figures **3.10**, **3.12**, **3.14** and **3.16**) and of 2.0-4.5 $x10^6$ cells/ml growing in pure water (Figures **3.11**, **3.13**, **3.15** and **3.17**). Growing in water at an initial concentration of about $1x10^7$ cells/ml, the strain-specific stationary phase cell concentration ranged between 1.3-1.8$x10^7$ per ml (Figures **3.22** and **3.23**). Mixed cultures of two strains of about $1x10^6$ initial cell/ml concentration attained the stationary phase within a range from 1.5 to 3.5 $x10^6$ cells/ml when grown in pure water (Figures **3.26** to **3.29**, **3.34** and **3.35**).

Oscillatory mode of growth was observed for both pure and mixed cultures. Growing in pure water, one inflection point and an over shooting of growth was clearly observed before reaching the stationary phase. Data of cells, growing in 5% grape juice, showed relatively rapid cell growth rate, reaching about one order of magnitude higher cell concentration than observed in pure water. This data also revealed more than one inflection point, possibly due to diauxic shifts occurring when grape juice sugars were depleted rapidly within 24 to 42 hours from inoculation. The rate of sugar assimilation in different strains was as follows in increasing order: Y217 < T206 ≤ T206q < VIN7. Both sugar and ammonium were simultaneously depleted (section 3.3.4.3). However, an over

shooting of the growth of cells in 5% grape juice could be attributed to the utilisation of other nutrients found in the medium as is in the case of most diauxic shifts.

Oscillatory modes of substance levels in cell media of ammonium (section *3.3.4.3.3*), ethanol (section *3.3.4.3.2*), acetic acid (section *3.3.4.3.4*), and glycerol (section *3.3.4.3.5*) were also observed. These metabolites could also be consumed by the cells as nutrients (Magasanik, 1992; Hinnebusch, 1992; Johnston and Carlson, 1992; Paltauf *et al.*, 1992).

Cells growing in the stressed media constantly sporulated as was revealed by spore staining (see Electron microscopy, Figure **3.54**). Although spores were not counted, it was clear that their numbers were many times more of those of the cells. It was estimated that the number of spores growing in pure water was substantially larger than their corresponding number associated with growth in 5% grape juice. Most of the sporulated *Saccharomyces cerevisiae* asci produced four ascospores, which upon release can germinate pending on environmental conditions. The availability of water, may be sufficient as the sole nutrient for germination (Dix and Webster, 1995).

Spores have several functions, such as the migration and distribution of genetic variabilities, bringing together compatible mating types for sexual reproduction. Spores may also function as survival structures and, thus, have particular selective advantages for cells, all of which can be affected by rapidly changing environmental conditions. In general, the main function of spores dictates their structure, such as the spore wall thickness and constituents as well as the reserved food types and amounts. Spores' wastage is high because food reserves are often insufficient to overcome the effects of severe antibiosis. Many also fail to germinate due to the effect of severe competition for the uptake of exogenouse nutrients (fungistasis). Ungerminated spores deplete food reserves by slow respiration, and as they age, membranes deteriorate and then become

progressively more leaky and more sensitive to fungistasis (Dix and Christie, 1974). The loss of metabolites brings on starvation and ultimately autolysis sets in. The process of deterioration is exacerbated by the activities of other cells whose growth can create a nutrient sink around the spore into which metabolites and metabolic substrates from the spores are drained (Ko and Lockwood, 1970). It is difficult to find any very precise information on the survival time of spores under natural conditions and for the majority the survival time may be relatively short. The enormous numbers that are produced compensates for the high wastage of spores.

A growth lag phase where the growth rate is by definition zero is not observed in both nutritionally stressed media (5% grape juice and pure water). The initial growth rate is relatively smaller than the subsequent growth at later times prior to the stationary phase for cells growing in 5% grape juice medium. This might be a period when cells adapt to the new environment and while using the "inertia" (1.3), they produce the enzymes which permit the absorption and the assimilation of the available nutrients in the new medium.

Growing in pure water, the log phase recovered ,is of a relatively uniform growth rate. Cells presumably use internal storage energy, therefore the active transport of nutrients from their surrounding into cells does not appear to limit the growth rate during the log phase.

The percentage of dead cells oscillated in pure cultures, reaching a maximum value between 20 to 25%. Larger amplitudes of dead cell concentrations were observed in pure water (between 0 to 12%) than in 5% grape juice (between 0 to 5%), when stabilised, for initial cell concentration of about 10^6 cells/ml.

Growing in water, when the initial cell concentration was about 10^7 cells/ml, the dead cell percentage decreased to about 5% or below, usually less than 0.5%. That could be due to

sporulation, mode of reproduction, budding, production of physical protective sheath structures and formation of large body of cell aggregates (see 3.3.5 Electron microscopy). Also, relatively higher discharge of possible nutrients to the environment, such as ethanol production, substrate that could be consumed as a carbon source (Johnston and Carlson, 1992).

The frequency of sampling and the mixing of cultures prior to counting positively affected the percentage of dead cells. Leaving cultures for a longer period of time without interruption yielded lower dead cell percentage readings, ranging between zero to 3 percent, usually less than 1%. This might be due to the degree of breakage of the protective mucoid structures (3.3.5) of the cells growing under extreme nutritional stress on mixing before drawing a sample (see 3.3.5 Electron microscopy).

It is evident that true flocculation of bottom yeast cells and cell aggregation due to incomplete separation of daughter cells from mother cells during proliferation (Dengis *et al.*, 1995) do not spread evenly throughout the medium space. These cells gradually sink to the bottom, as observed during the experimental work. Therefore, the cell concentration might be dependent more on total initial cell inoculum than on the medium volume after cells had sunk and aggregated. For purposes of cell counts or staining, it is necessary to re-suspend yeast flocs by agitation or swirling of the medium, as was practice here (3.2.2.6).

The killer effect was observed in mixed cultures when the killer strain (T206) challenged the sensitive strain. Few hours after exposure to the killer toxin (K_2), the dead cell percentage reached an extreme peak point of about 30%, less than half of that was found when the killer-cured derivative challenged the sensitive strains. Sensitive cells in the exponential growth phase are more susceptible to the killer toxin than in the stationary

growth phase (Woods and Bevan, 1968). The formation of cell protective structures observed under the scanning and transmission electron microscopes (section 3.3.5) physically blocked the toxin effects on the sensitive cells. Also the chemical changes in the medium may influence the toxin activity. Growth conditions can affect the copy number of L-dsRNAs per cell. Cells grown oxidatively on ethanol (section *3.3.4.3.2*), as a carbon source, have elevated levels of L-dsRNAs compared with those grown on glucose. During nitrogen starvation (section *3.3.4.3.3*), an extensive, but not complete, degradation of L-dsRNA takes place (Van Vuuren and Jacobs, 1992), which may affect the killer toxin production and activity. In this study, toxin levels were not quantified.

According to Bussey, (1974) and Carrau *et al.*, (1993) dead cells do not release any nitrogen source, such as ammonia, into the medium, causing killer cells to alter the fermentation prematurely on nutrient depletion. After ammonium addition, approximately 100% of the viable cells were composed of the killer yeast population, which suggested that nitrogen source could have been the killer growth - limiting factor. This may also affect the influence of the killer toxin on the sensitive cells.

Skipper and Bussey, (1977) showed that after toxin addition there is a lag period of about 40 minutes during which measurements of metabolic and macromolecular biosynthetic events effects are not seen, followed by a shut-off of macromolecular synthesis and plasma membrane damage which results in the loss of potassium ions and ATP. Maximum killing is attained after two or three hours depending on the strain.

Bussey, (1991) found that K_1 heterodimeric killer toxin is secreted into the growth medium during the exponential phase of growth. The K_1 toxin is active within a narrow pH range of 4.2 to 4.6, and causes rapid inhibition of the net proton extrusion and potassium uptake by sensitive cells. Soon the inside-outside differences in pH decreases

and, later potassium and ATP efflux are observed along with cell death and the cessation of macromolecular synthesis (Van Vuuren and Jacobs, 1992).

Pfeiffer and Radler, (1984) found that the K_2 toxin is a 16kD glycoprotein, active between pH 2.8 and 4.8, but optimally at pH range 4.2 to 4.4. In this study, although the concentrations of dead cells were relatively very low as described above, dead cell concentrations found to oscillate correlating to the pH levels, yielding an optimal pH range between 3.6 to 4.4 for the yeast strains used at the specified conditions (3.2.2.6). Cells grown in 5% grape juice medium, where the pH ranged between 3.0 to 3.8 (Vadasz, A.S., 1999, usually about 3.0-3.3) and in pure water, the pH oscillated between 4.2 to 6.9 (usually about 4.8-5.3). These pH ranges affected the toxin activity, and thus the damage induced by the killer toxin on the sensitive strains.

3.3.4.2 Cell survival in mixed cultures

The WLN plates (section 3.2.2.8) had grown strain typical colonies (section 3.3.2.2), and allowed to differentiate the relative survival of cells of the mixed cultures (Figure **3.36-3.46**). Because of the tedious, complex and time-consuming measurement process linked to the differentiation experiments, it was not possible to capture high-resolution data sets. But, observing the experimental data for the total viable cell concentration, which correspond to the ongoing cell count of total viable cells clearly reinforces results of the differentiation process that the strains growing in mixed cultures also yielded the same qualitative features of growth as those growing in pure cultures (3.3.4.1).

(a)

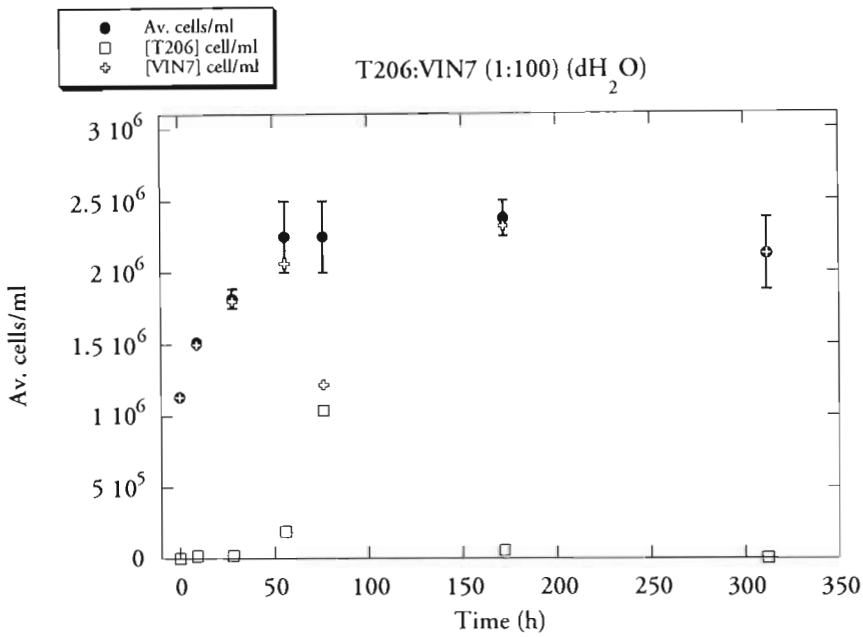

(b)

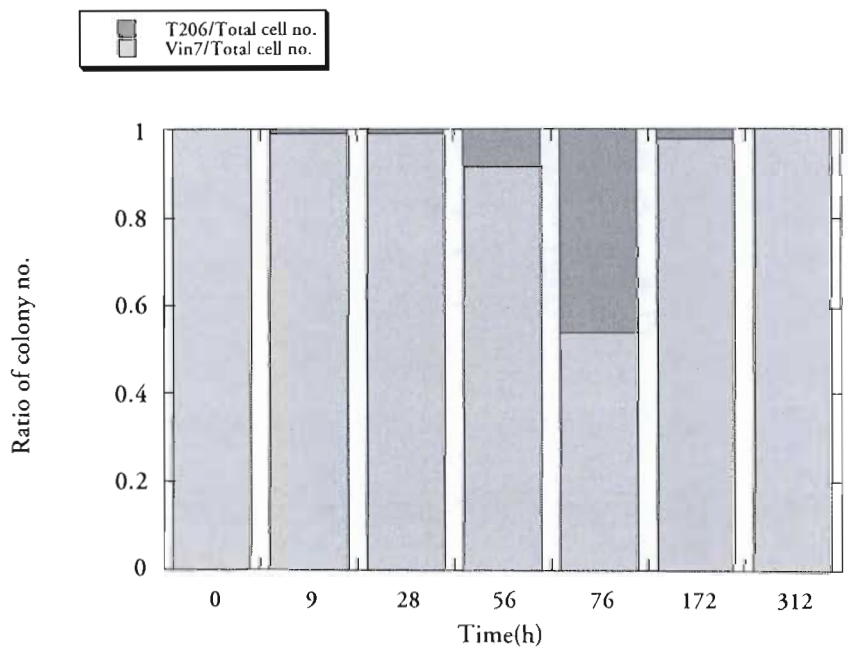

Figure **3.36** Relative survival of two strains of *Saccharomyces cerevisiae* growing in distilled water, following a challenge of a 9h culture of the sensitive strain (S), VIN7 by the killer strain (K), T206, at a K:S cell concentration of approximately 1:100, (a) Total and individual strain cell number per ml medium versus time; (b) Ratio of the number of colonies on WLN plates.

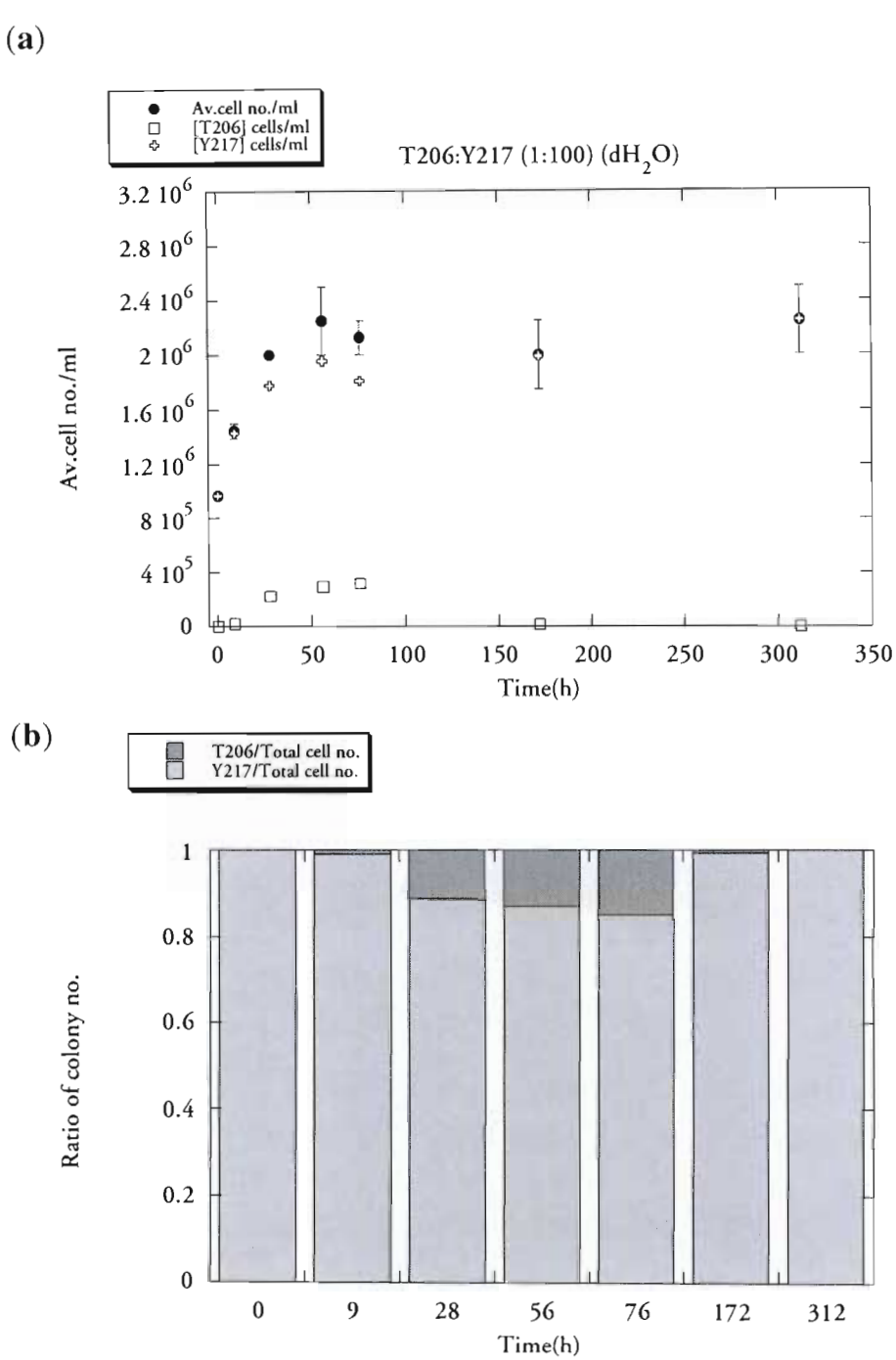

Figure **3.37** Relative survival of two strains *of Saccharomyces cerevisiae* growing in distilled water following a challenge of a 9h culture of the sensitive strain (S), Y217 by the killer strain (K), T206, at a K:S cell concentration of approximately 1:100, (a) Total and individual strain cell number per ml medium versus time; (b) Ratio of the number of colonies on WLN plates.

(a)

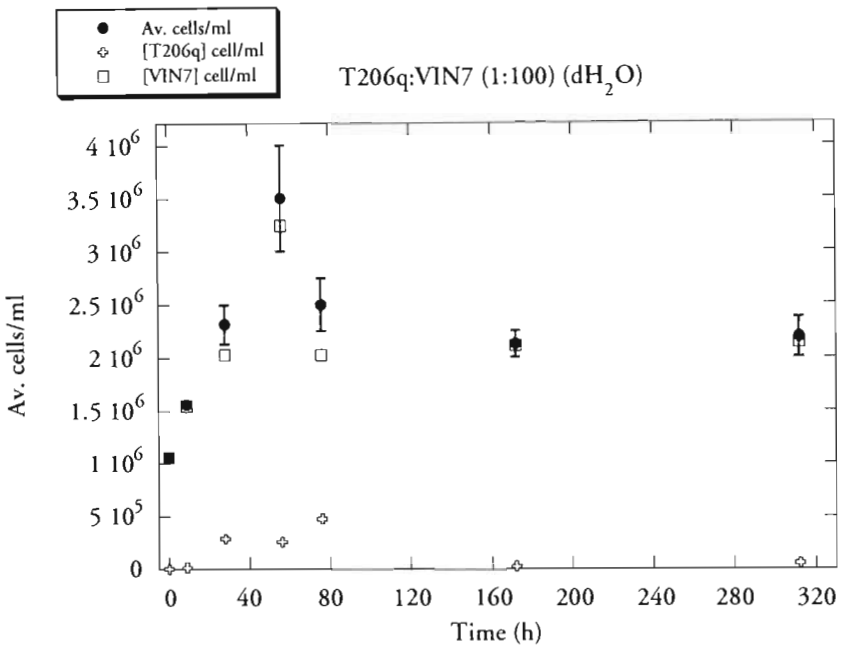

(b)

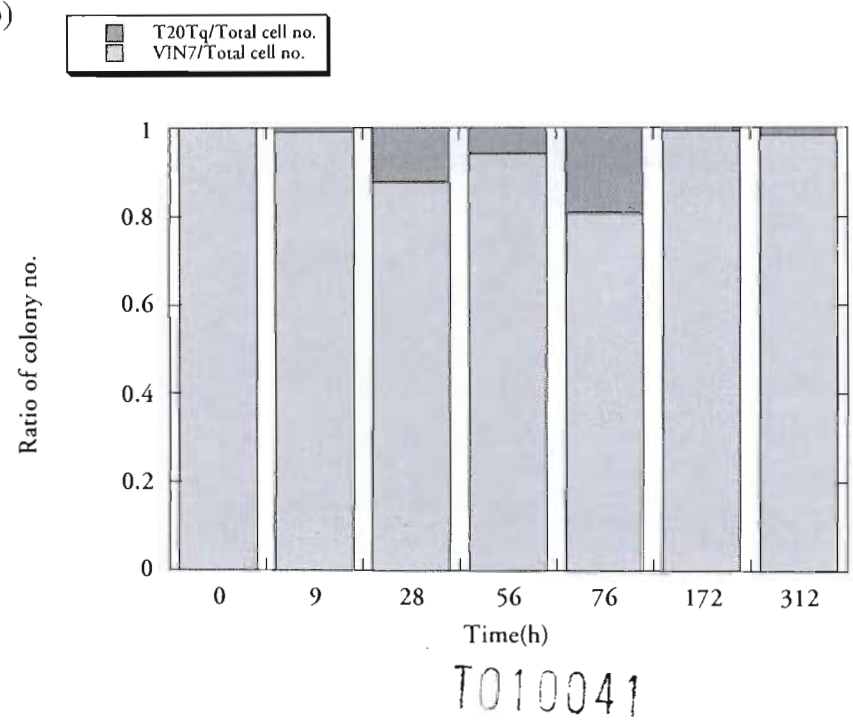

Figure **3.38** Relative survival of two strains of *Saccharomyces cerevisiae* growing in distilled water, following a challenge of a 9h culture of the sensitive strain (S), VIN7 by the killer-cured strain (Kq), T206q, at a Kq:S cell concentration of about 1:100, (a) Total and individual strain cell number per ml medium versus time; (b) Ratio of the number of colonies on WLN plates.

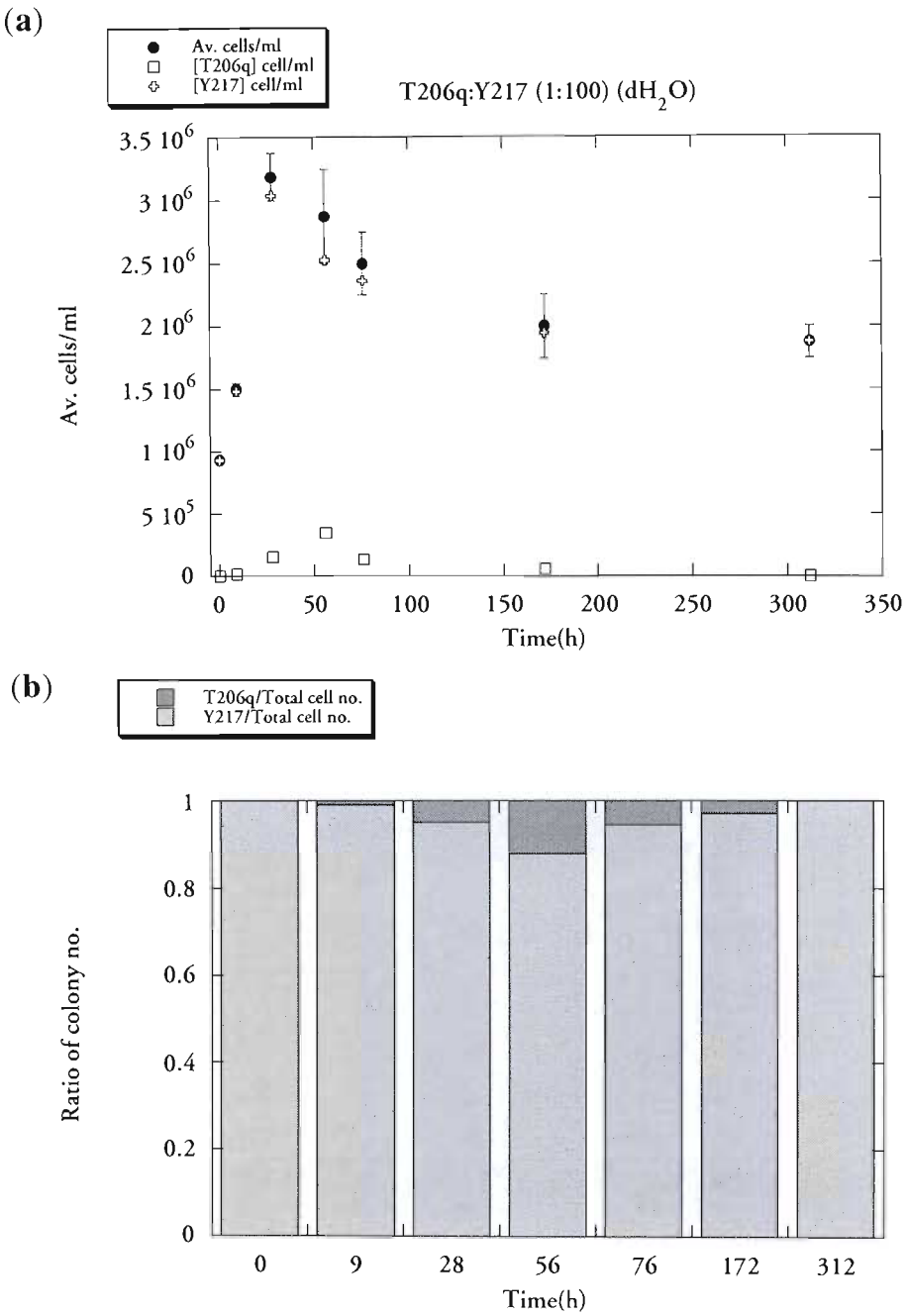

Figure **3.39** Relative survival of two strains of *Saccharomyces cerevisiae* growing in distilled water, following a challenge of a 9h culture of the sensitive strain (S), Y217 by the killer-cured strain (Kq), T206q, at a Kq:S cell concentration of about 1:100, (a) Total and individual strain cell number per ml medium versus time; (b) Ratio of the number of colonies on WLN plates.

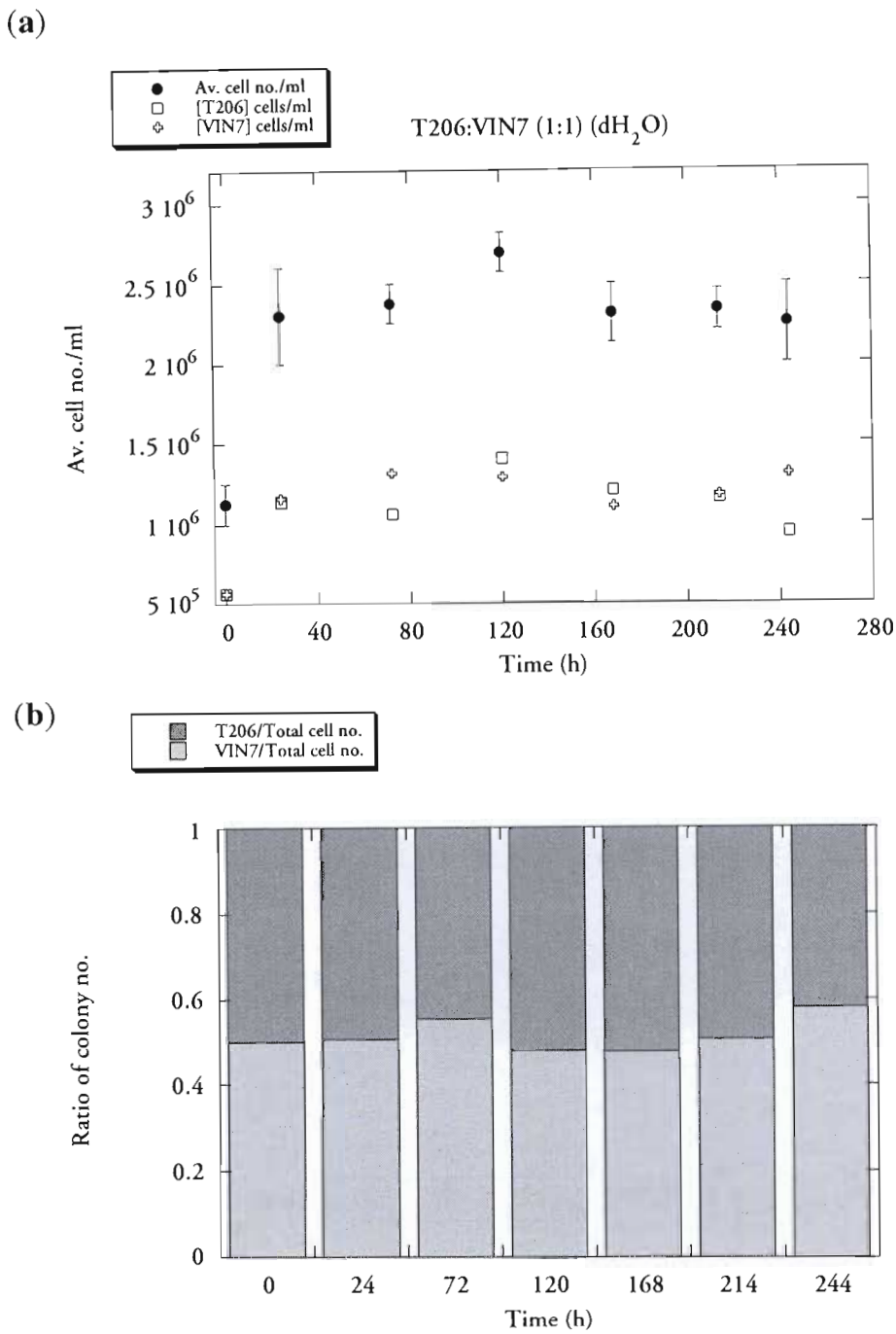

Figure **3.40** Relative survival of two strains of *Saccharomyces cerevisiae* growing in a mixed culture. Both killer strain (K), T206, and the sensitive strain (S), VIN7 were inoculated into distilled water, at K:S cell concentration ratio of about 1:1, (a) Total and individual strain cell number per ml medium versus time; (b) Ratio of the number of colonies on WLN plates.

(a)

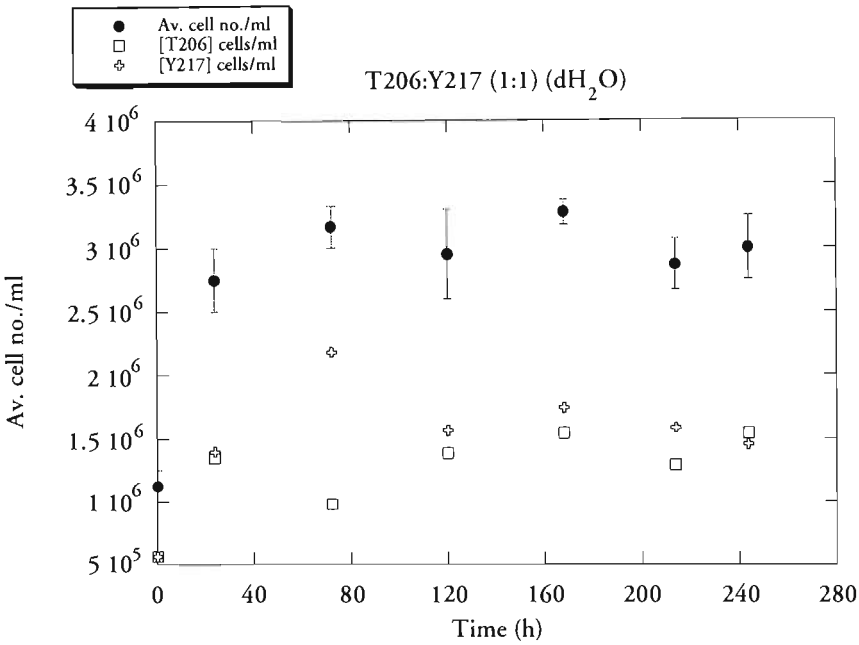

(b)

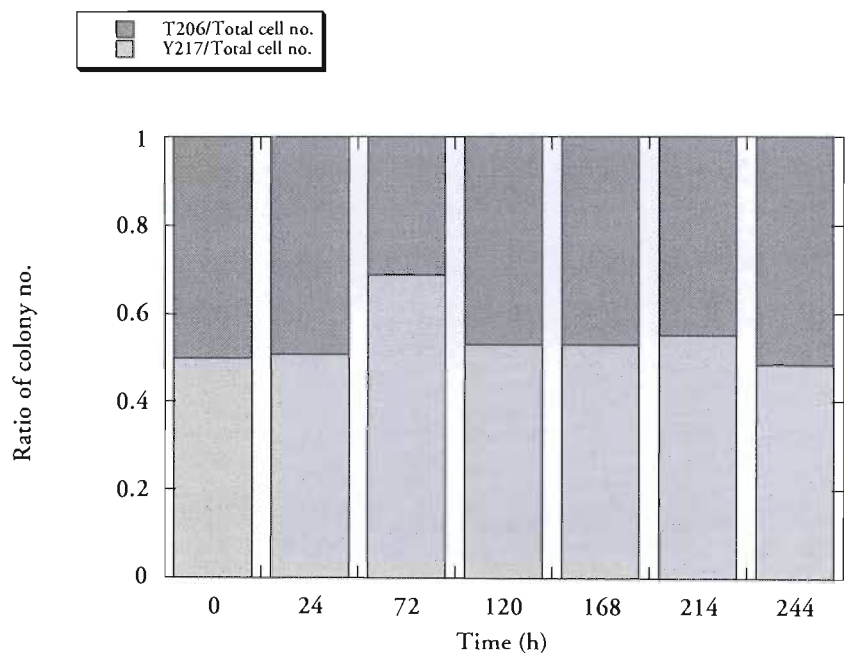

Figure **3.41** Relative survival of two strains of *Saccharomyces cerevisiae* growing in a mixed culture. Both killer strain (K), T206, and a sensitive strain (S), Y217 were inoculated into distilled water, at K:S cell concentration ratio of about 1:1, (a) Total and individual strain cell number per ml medium versus time; (b) Ratio of the number of colonies on WLN plates.

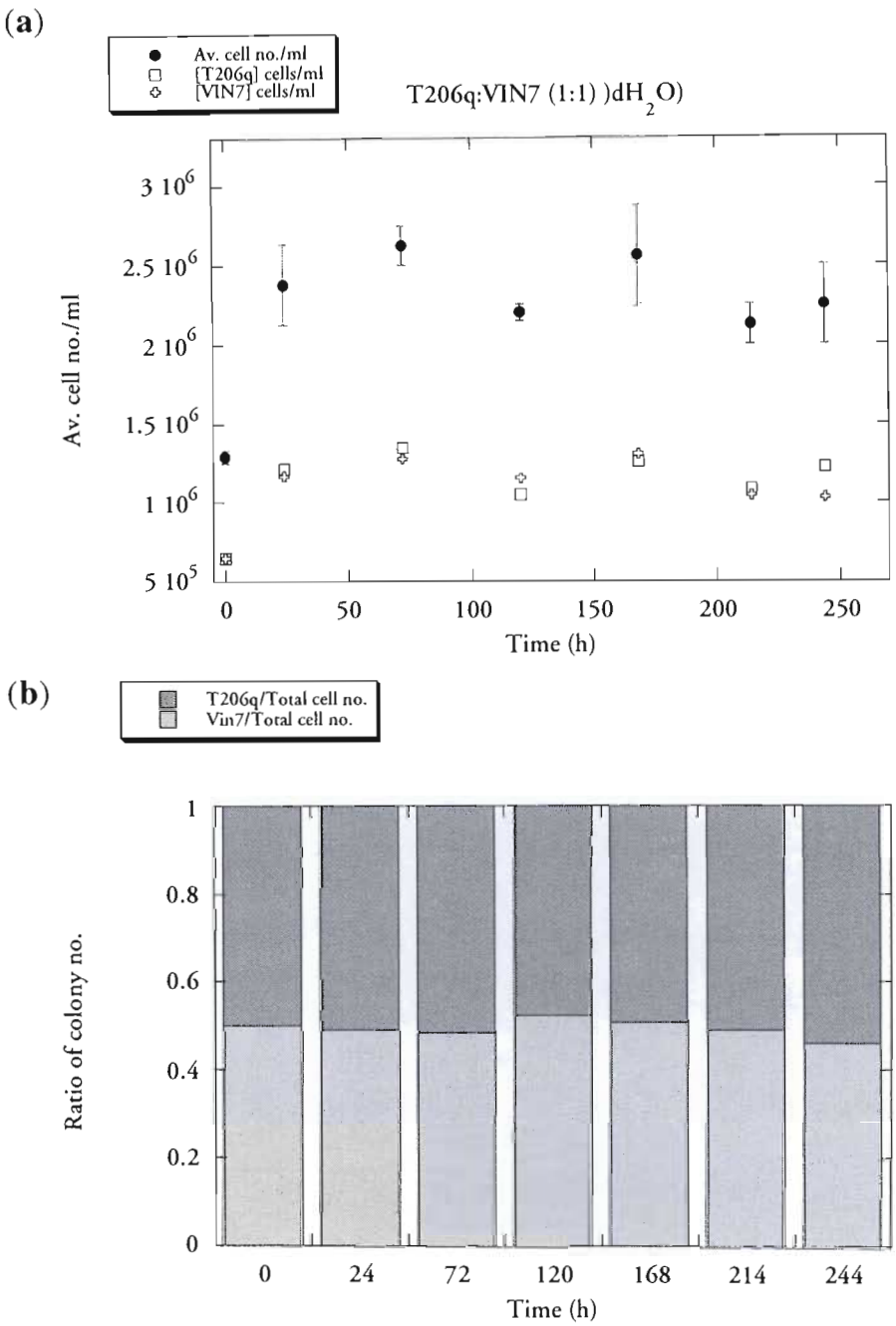

Figure **3.42** Relative survival of two strains of *Saccharomyces cerevisiae* growing in a mixed culture. Both killer-cured derivative (Kq), T206q, and the sensitive strain (S), VIN7 were inoculated into distilled water, at Kq:S cell concentration ratio of about 1:1 (a) Total and individual strain cell number per ml medium versus time; (b) Ratio of the number of colonies on WLN plates.

(a)

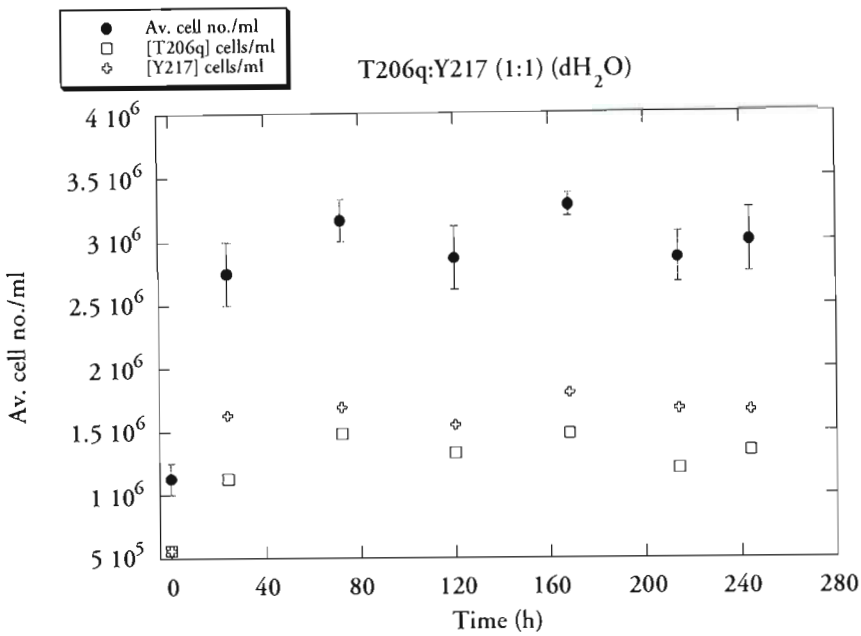

(b)

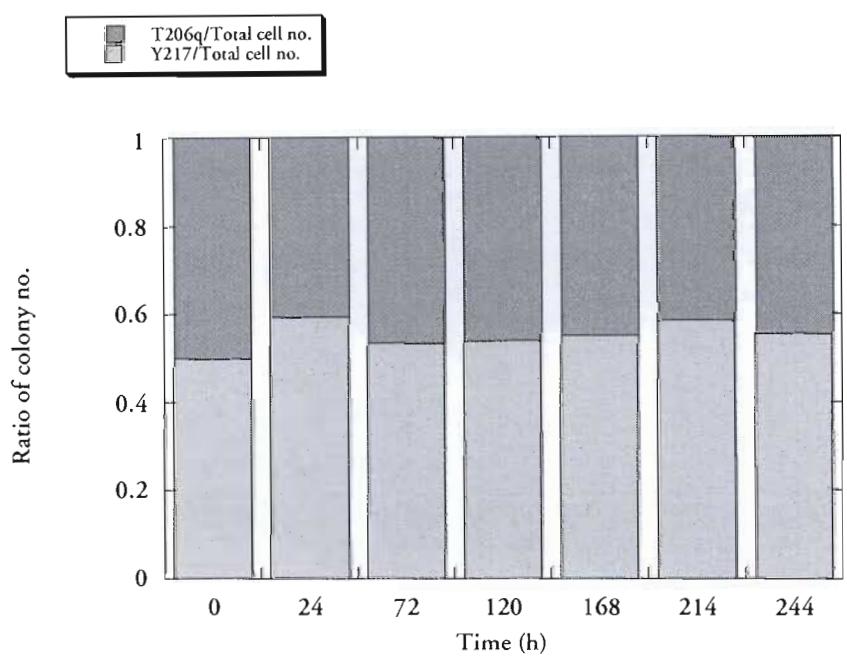

Figure **3.43** Relative survival of two strains of *Saccharomyces cerevisiae* growing in a mixed culture. Both killer-cured derivative (Kq), T206q, and the sensitive strain (S), Y217 were inoculated into distilled water, at Kq:S cell concentration ratio of about 1:1, (a) Total and individual strain cell number per ml medium versus time; (b) Ratio of the number of colonies on WLN plates.

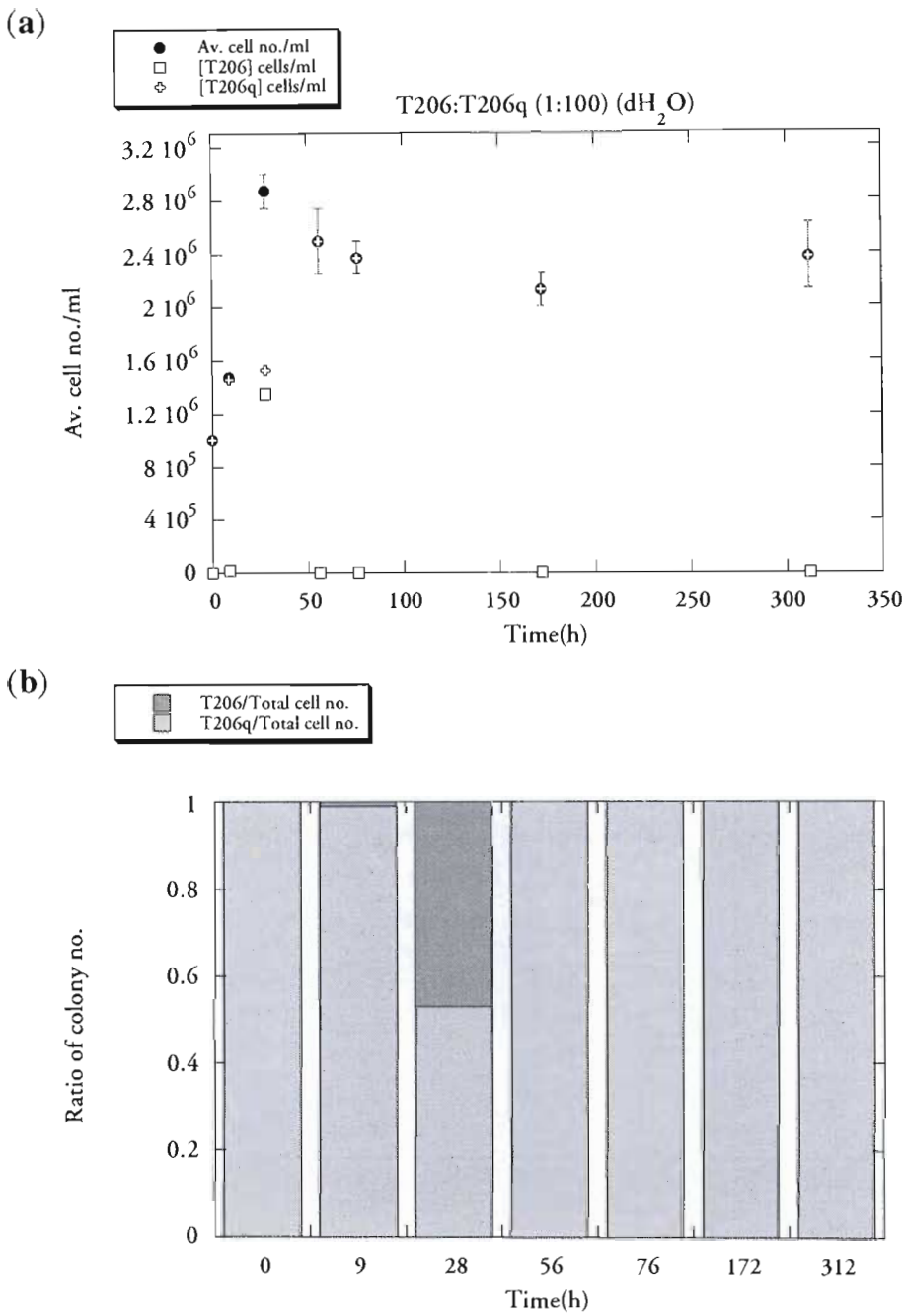

Figure **3.44** Relative survival of two strains of *Saccharomyces cerevisiae* growing in distilled water, following a challenge of a 9h culture of the killer-cured derivative (Kq), T206q, by its killer (K) progenitor, T206, at a K:Kq cell concentration ratio of about 1:100, (a) Total and individual strain cell number per ml medium versus time; (b) Ratio of the number of colonies on WLN plates.

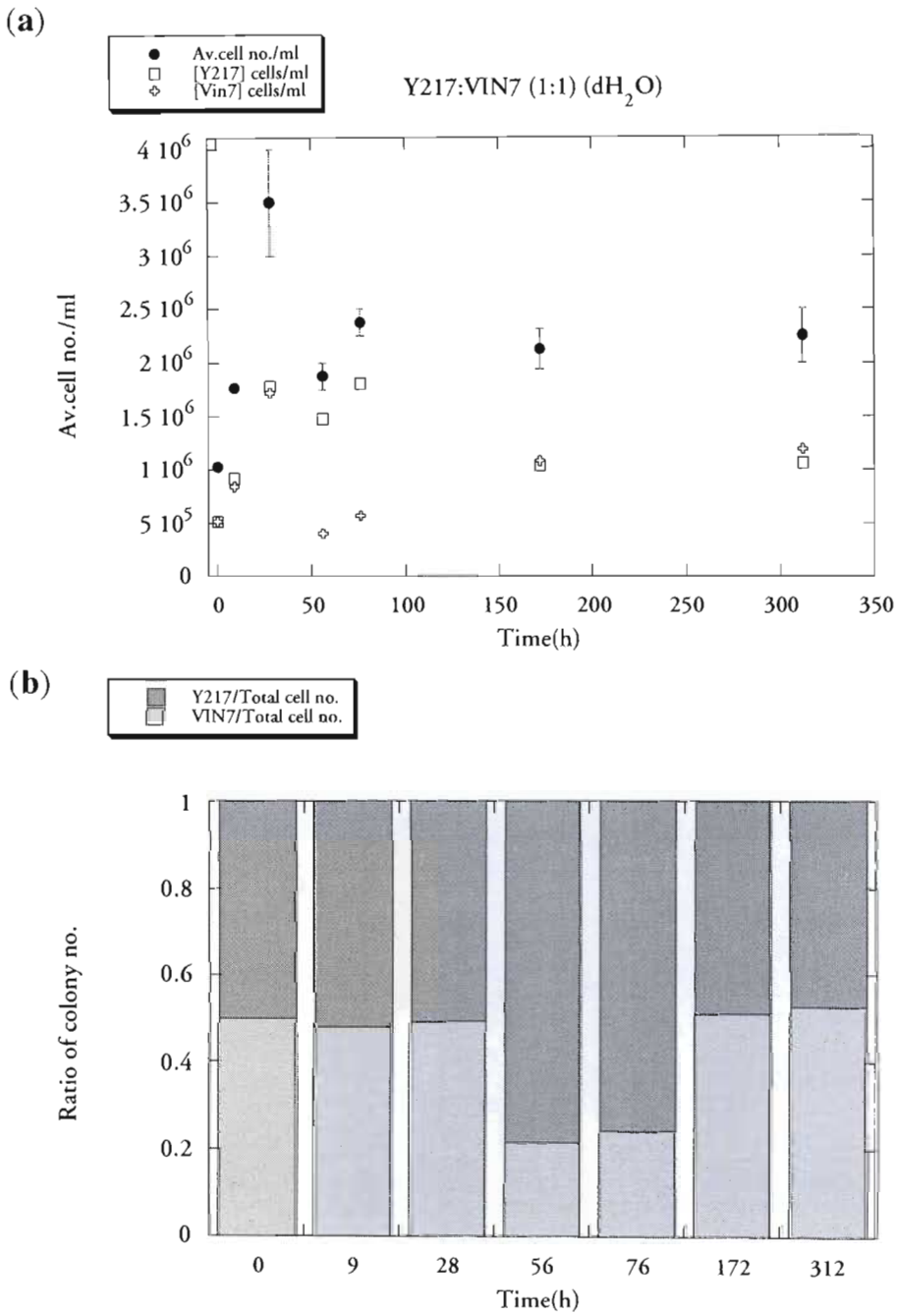

Figure **3.45** Relative survival of two strains of *Saccharomyces cerevisiae* growing in a mixed culture. Two sensitive strains VIN7 (Sv) and Y217 (Sy) were inoculated into distilled water, at an Sv:Sy cell concentration ratio of about 1:1, (a) Total and individual strain cell number per ml medium versus time; (b) Ratio of the number of colonies on WLN plates.

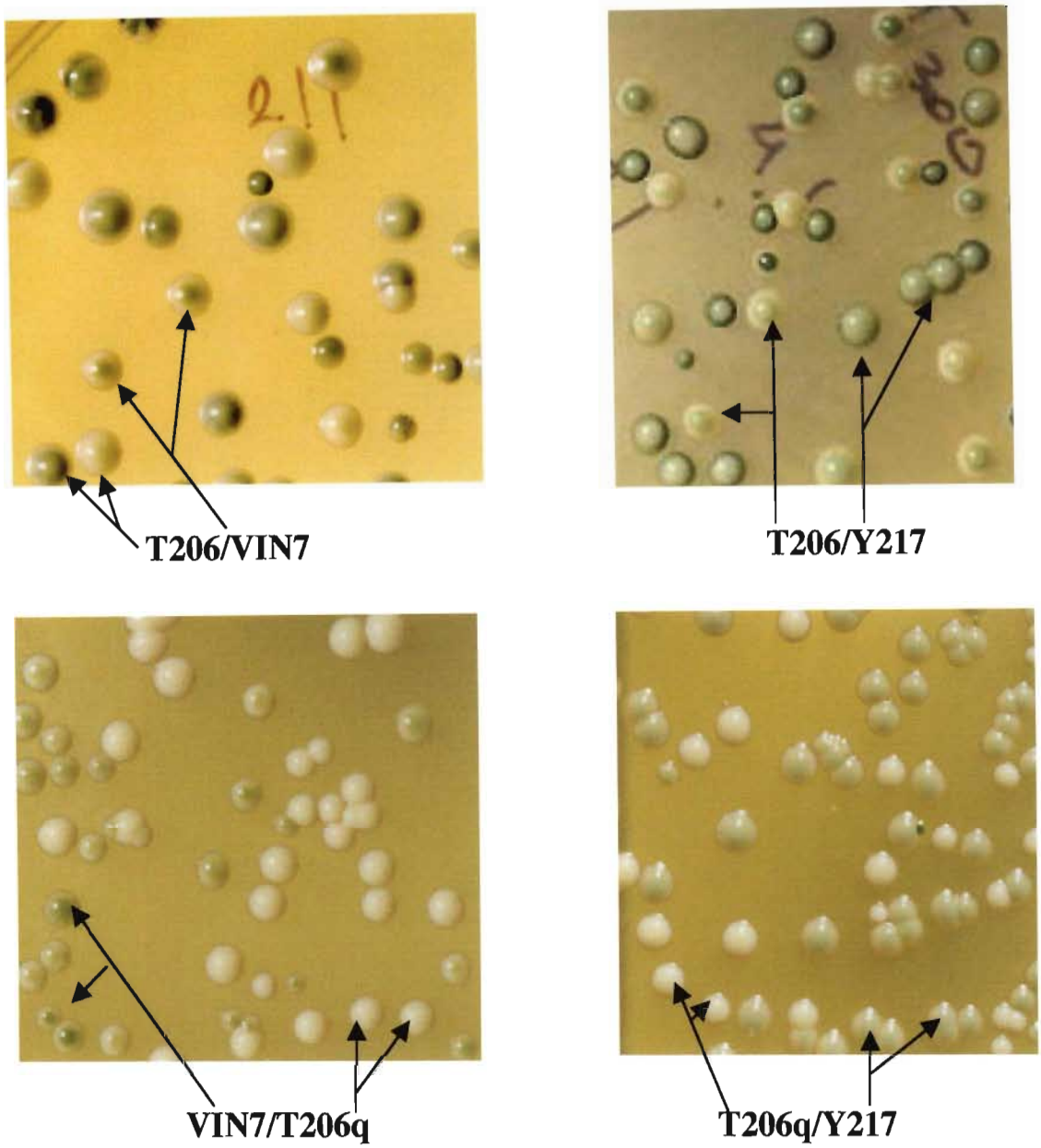

Figure **3.46** WLN agar plates reveal the relative survival of two strains growing in mixed cultures at cell concentration ratio of about 1:1. Samples of mixed cultures of *Saccharomyces cerevisiae* growing in distilled water; sensitive strains VIN7 and Y217, separately challenged by both the killer T206 and killer cured T206q, respectively, were inoculated on WLN plates. Individual cultures of each strain served as controls and for identification based on colony trait (Figure **3.5**).

T206 strain yields few types of colonies, one of these, although slightly darker at the colony top, characterised that of the killer-cured derivative (Figure **3.5**). Growing under extreme nutritional stress, it seemed that more typical killer colonies resembled those of the cured colonies. Therefore, it could be assumed that the amount of the VLPs (virus-like particles) per cell caused the multiple (or gradient) appearance of the killer strain colonies, and while growing in nutrient limiting medium, VLP reproduction presumably decreases and so the mycotoxin production. Inoculation of the stressed killer on methylene blue agar plates (3.3.2.1) revealed that killer phenomenon did not disappear, that is, no curing occurred.

The challenge of killer cured (Kq) cells by the killer (K) at a K:Kq ratio of 1:100 in pure water at (9h) early logarithmic phase (Figure **3.44**) revealed that the killer-cured phenotype dominated and the killer strain disappeared between 28 to 56 hours from inoculation, although after 9 hours of the challenge the number of the killer cells increased for a while. This could have happened due to the transfer of VLPs from the killer to the killer-cured strain. Transmission of yeast viruses has been thought to occur only by cytoplasmic mixing of cells (Figure **3.52**) during budding, mating, cytoduction or protoplast fusion (Wickner, 1986). Clearly, the killer strain T206 failed to kill its cured derivative, T206q.

Growing under nutritional stress, seemed to be a limiting factor in VLP reproduction, which might permit better survival of their host cells. VLPs that yeast cells contain per cell varies widely (Wickner, 1976), and although the basis for this variation is not understood (Van Vuuren and Jacobs, 1992) the extreme stressed environment could be one possible explanation.

Because strain T206 yielded a few types of colonies, it was harder to differentiate these growing in a mixed culture. A killer:sensitive cell ratio of 1:100 (Figures **3.36** and **3.37**) strongly revealed dominance of the sensitive strain and extinction of the killer strain, even though a short while after the challenge there was an increase in killer cell counts and sensitive dead cells. In this period (T_{76h}), VIN7 seemed to be more susceptible to the toxin or results present the onset of the oscillatory growth stage and the difference in growth rate at a particular time at the stationary phase. Samples of 312 hours, at the end of this work, revealed that the killer strain was extinct from the mixed cultures (Figures **3.36** and **3.37**). The latter is associated with the substantial difficulty that the killer strain has to grow in limited nutrient conditions and support the viral parasite that produces the killer toxin, which is necessary in order to overcome the competition with the sensitive strains. As a result, the efficiency of the killer system, yeast host- viral parasite relationship of symbiosis with the virus deteriorates, leading eventually to the extinction of the killer yeast, in some cases or coexistence with the sensitive strains in other.

The killer-cured derivative (Kq) which challenged Y217 (Sy) at a ratio of 1:100 (Kq:Sy) (Figure **3.39**), also seemed to be extinct at this time (T_{312h}). Relative growth rates of the yeast strains in the mixture or differences in the ability to sporulate due to the environmental conditions could mask the real ratio of surviving cells.

A ratio of killer:sensitive cells of 1:1 (Figures **3.40** and **3.41**) strongly supports the survival of the sensitive strains according to their relative growth rates. The killer did not dominate the mixed cultures, and in comparison with the killer-cured derivative (1:100 Kq:S ratio, Figures **3.38** and **3.39** and 1:1 Kq:S ratio, Figures **3.42** and **3.43**), it seemed to have a disadvantage while growing under nutritional stress. These might be due to the decrease in VLP reproduction, toxin production and activity, and the relative slower growth rate of the killer strain in comparison with the killer-cured strain's growth rate

and again the oscillatory stage at a particular time in the stationary phase. Both sensitive strains survived in these mixed cultures (Figure **3.40**, **3.41** and **3.46**) being, as expected, affected by their relative ability to adjust and to grow under extreme nutritional stress.

3.3.4.3 Metabolic analyses

Metabolic analyses (Appendix A.3) were performed throughout the cell growth (3.2.2.6) until reaching stable readings, for single and mixed 1:100 (K:S) and (Kq:S) ratio of cultures in 5% grape juice and pure water, separately. The T206 (K) and T206q (Kq) at a K:Kq cell ratio of 1:100, and between sensitive strains, VIN7 (Sv) and Y217 (Sy), at a Sv:Sy ratio of 1:1 were also examined in pure water. Trends of the yield of the different metabolites were as described by Vadasz, A.S. (1999).

3.3.4.3.1 Reducing sugar concentration

Sugar was always absent in pure the water growth medium. The initial concentration of sugar in the 5% grape-juice liquid medium was obtained from the standard curve (3.3.2.7) (approximately 0.56 g/l), (Vadasz, A.S., 1999). The different strains of *S. cerevisiae*, namely, VIN7, Y217, T206 and T206q utilised the sugar in this grape medium maximally but at different rates during the logarithmic phase of growth. VIN7 cells exhibited the relatively fast rate, whereas Y217 cells, showed the slowest rate of sugar assimilation. Using the DNS technique (3.3.2.7), revealed that total reducing sugar depleted from the medium (5% grape juice) between the 24 to 36 hours by the fermenting yeast strains T206, T206q and VIN7, separately, and between 36 to 42 hours when the fermenting strain was Y217. No trace of residual sugar was detected further. Challenged fermentation showed depletion of sugar between 24 to 33 hours in T206/VIN7 and

T206q/VIN7 cultures, and between 33 to 42 hours in T206/Y217 and T206q/Y217 cultures, respectively.

3.3.4.3.2 **Ethanol production**

Analyses of the fermenting media revealed that maximum ethanol concentrations produced by the killer and the killer-cured cells, growing in 5% grape juice, was about 1.58 and 1.63g/l, respectively, after about 150 hours. Afterwards, ethanol concentration decreased and fluctuated about 1.27 and 1.33g/l until the end of these fermentation experiments in about 280 hours. The sensitive strains, VIN7 and Y217, produced maximum ethanol concentrations of about 1.68 and 1.72g/l, respectively, in about 180 hours. Afterwards, ethanol concentrations decreased, reaching stable levels of about 1.53 and 1.52g/l. The rate of ethanol production seemed to correlate with the cell growth rate and concentration.

Growing in pure water, extracellular ethanol concentrations gradually reached maximum levels of approximately 1.5 $x10^{-2}$ g/l between 24 to 48 hours of inoculation. Afterwards, keeping a damped oscillatory mode, ethanol concentration decreased. Then, between 100 to 120 hours of inoculation, cultures reached stable oscillations between zero detection to about 5.0 $x10^{-3}$ g/l until the end of the experimental work in about 280 hours.

Challenges in pure water, involving a mixture of the two sensitive strains VIN7 and Y217 at a cell ratio of 1:1 seemed to be the best combination for ethanol production, followed by the 1:100 cell ratio challenges in decreasing order: T206q:VIN7 ≥ T206q:Y217 > T206:T206q > T206:VIN7 > T206:Y217.

In general, the rate of ethanol production seemed to increase at the logarithmic growth phase then gradually decrease to minimum oscillatory levels of ethanol concentrations.

Over short periods, the rate of ethanol production seemed to be constant with the concomitant to depletion of sugar and ammonium from the media (3.3.4.1). This was found to be more pronounced when using the killer and killer - cured strains than with the sensitive strains.

3.3.4.3.3 **Ammonium production**

Saccharomyces cerevisiae can utilise ammonia as the sole source of nitrogen. Analyses of fermenting media revealed that initially, the ammonium concentrations in 5% grape juice, both in controls and challenges were about 5.0 $x10^{-3}$ g/l, reaching a minimum level between 36 to 48 hours of inoculation. Ammonium levels, generally, increased after 48 hours, oscillated between zero to about 5.0 $x10^{-2}$ g/l. This increase could be linked to metabolism of other constituents in the medium such as amino acids.

In pure water medium, ammonium was absent, but later detected in concentrations that seemed to correlate with dead cell counts in a delay phase mode. Ammonium levels increased in 56 to 72 hours of inoculation to about 1.5 $x10^{-3}$/l, reaching a maximum levels in 100 to 120 hours of inoculation to about 4.5 $x10^{-3}$/l. Then, keeping an oscillatory mode of decrease, final stabilisation of levels recorded between zero to about 1.8 $x10^{-3}$ g/l.

3.3.4.3.4 **Acetic acid production**

In this study, levels of acetic acid were examined only in pure water medium, revealing that the single and mixed cultures produced minute amounts of acetic acid in an oscillatory mode. Acetic acid concentrations in pure and mixed cultures were detected about 48 and 24 hours of inoculation, respectively, reaching a maximum value of about 1.0 $x10^{-2}$g/l within a few hours. Then, gradually decreased in an oscillatory mode until stabilisation was achieved between zero to about 4.5 $x10^{-3}$g/l.

3.3.4.3.5 **Glycerol production**

In this study, levels of glycerol were examined only in pure water medium, revealing that the single and mixed cultures produced similar minute amounts of glycerol in an oscillatory mode. Glycerol was detected about 24 hours of inoculation, reaching a maximum value of about 1.8 $x10^{-2}$g/l within 72 hours. Then, concentrations gradually decreased, and reached stable oscillations between zero to about 1 $x10^{-2}$g/l.

3.3.5 Electron microscopy

Scanning electron microscopy (SEM *3.2.2.10.1*) and transmission electron microscopy (TEM *3.2.2.10.2*) produced typical images (Osumi, 1998) of unchallenged (control) *S. cerevisiae* cells from liquid and agar media, which revealed similar features. Undamaged cells bearing an intact cell wall (Vadasz *et al.*, 2000 Figure 2a; Figures **3.48**, **3.49, 3.50** and **3.52**) and smooth cell surface, interrupted by bud scars, usually located at the polar axes, were seen.

Yeast cells switched from the typical spheroidal to elongated shape (Figure **3.47** and **3.48a**), and also grew pseudohyphae on stress medium to presumably forage for scarce nutrients (Figure **3.48b**). Invasive growth (Figure **3.49**) and cell aggregation (Figures **3.48a**, **3.50** and **3.51**) could also be revealed using scanning electron microscopy (section *3.2.2.10.1*).

An attempt to use the methylene blue agar plates' material for the electron microscopy (Van Vuuren and Wingfield, 1986) failed. The methylene blue gave an undesirable reaction with the fixative, coupled with solubilization of the agar. Therefore, 3% grape juice agar was used for the challenge, coupling together the effects of limiting nutrients and the K_2 killer toxin.

(a)

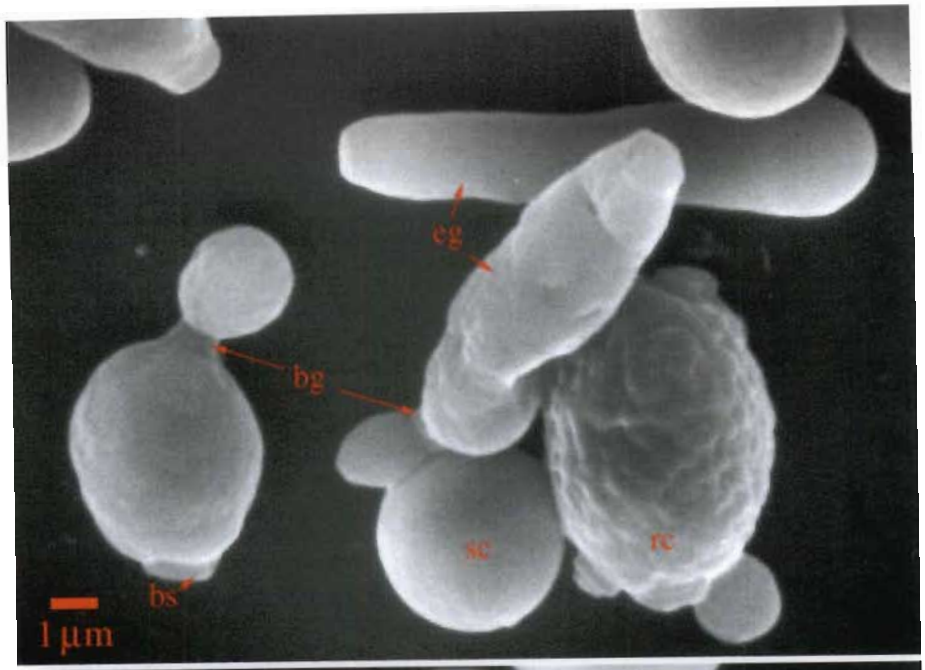

(b)

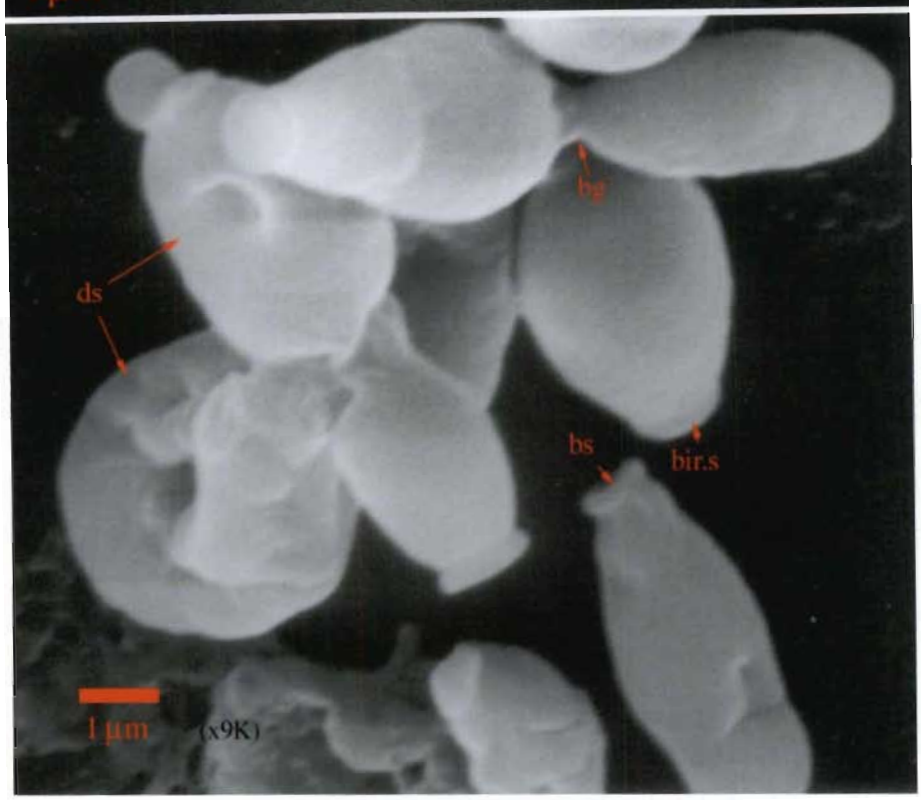

Figure **3.47** SEM images of several alternative morphologies of *Saccharomyces cerevisiae* wine strains growing under severe nutrient limitation, in (a) in 5% grape juice liquid and (b) on 3% grape juice agar media, of the sensitive strain VIN7 (Sv) challenged by the killer, T206.

Abbreviations: bg, budding; bir.s, birth scar; bs, bud scar; ds; doughnut shaped cell; eg elongated cell; rc, rippled cell; sc, smooth cell.

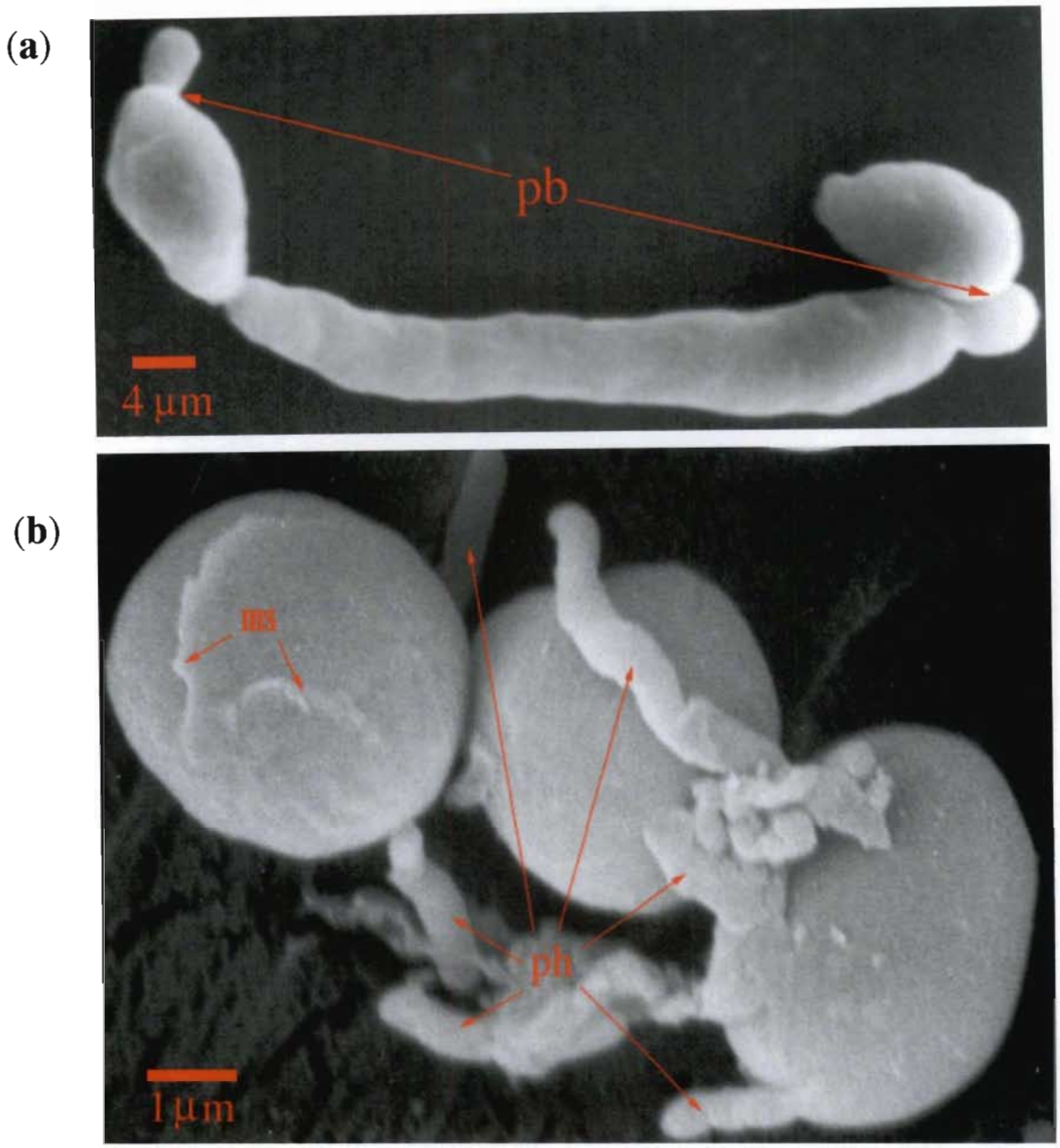

Figure **3.48** SEM images of *Saccharomyces cerevisiae* wine strains growing under severe nutrient limitation, (a) in 5% grape juice liquid and (b) on 3% grape juice agar media. (a) Bipolar budding (bp) of daughter cells, which stay attached to elongated mother cells, forming pseudohyphae; (b) Mucoid sheath (ms) on the outer cell surface of cells growing pseudohyphae (ph), which forage for limited nutrients.

(a)

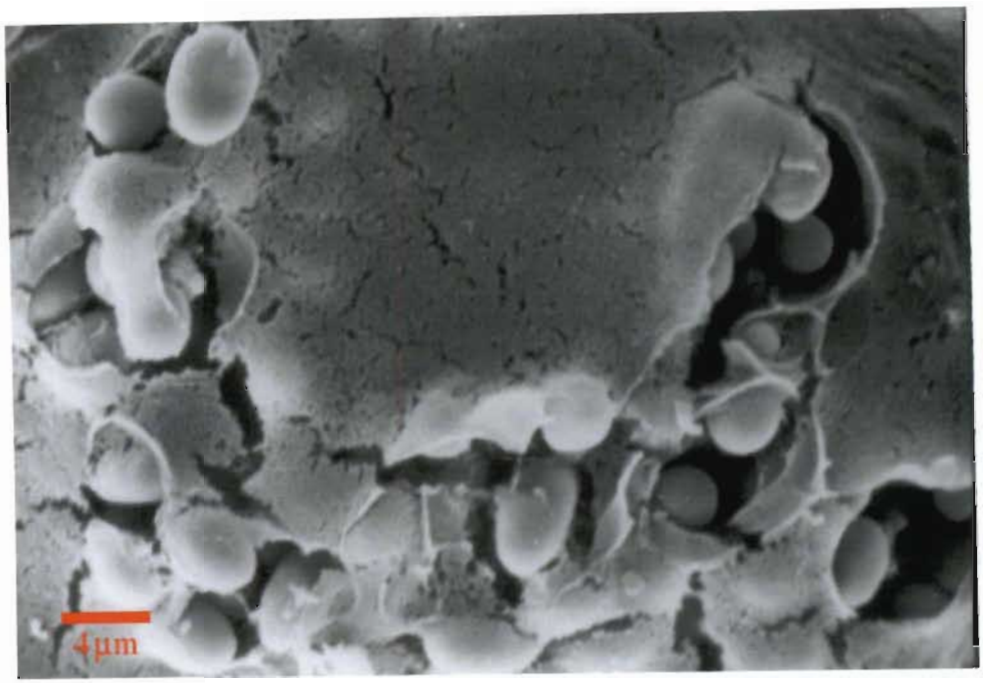

(b)

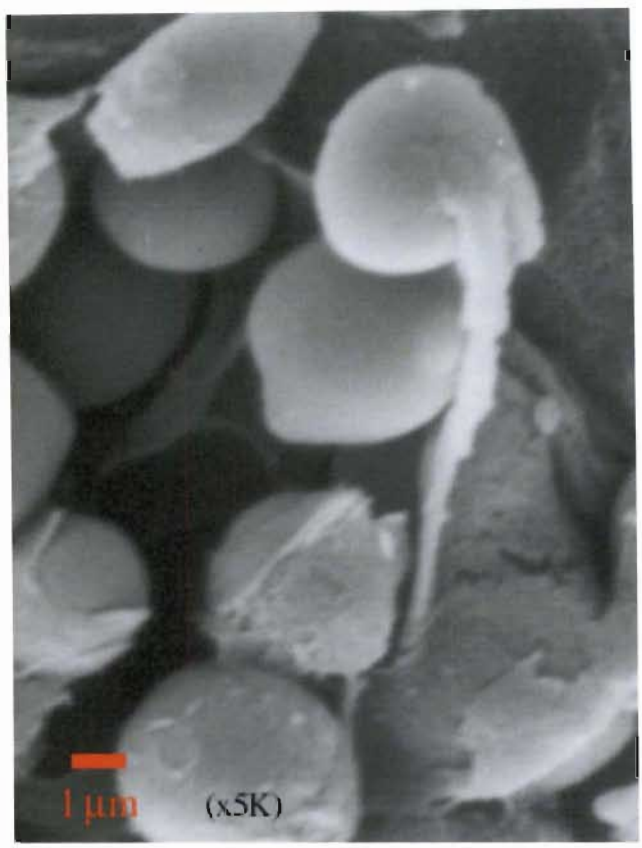

Figure **3.49** SEM images of *Saccharomyces cerevisiae* wine strains growing on 3% grape juice agar stress medium, revealing an invasive cell growth pattern (a and b).

(a)

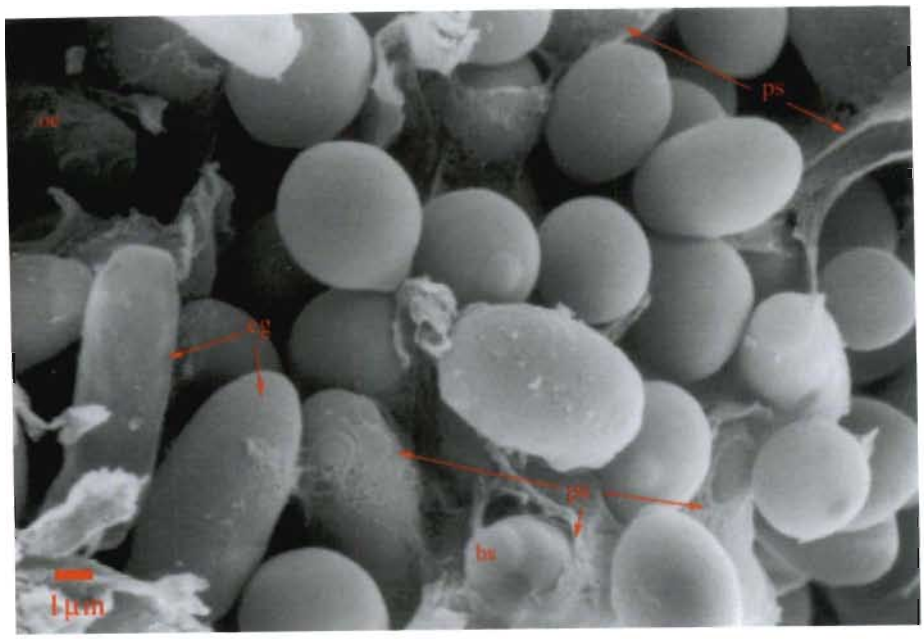

(b)

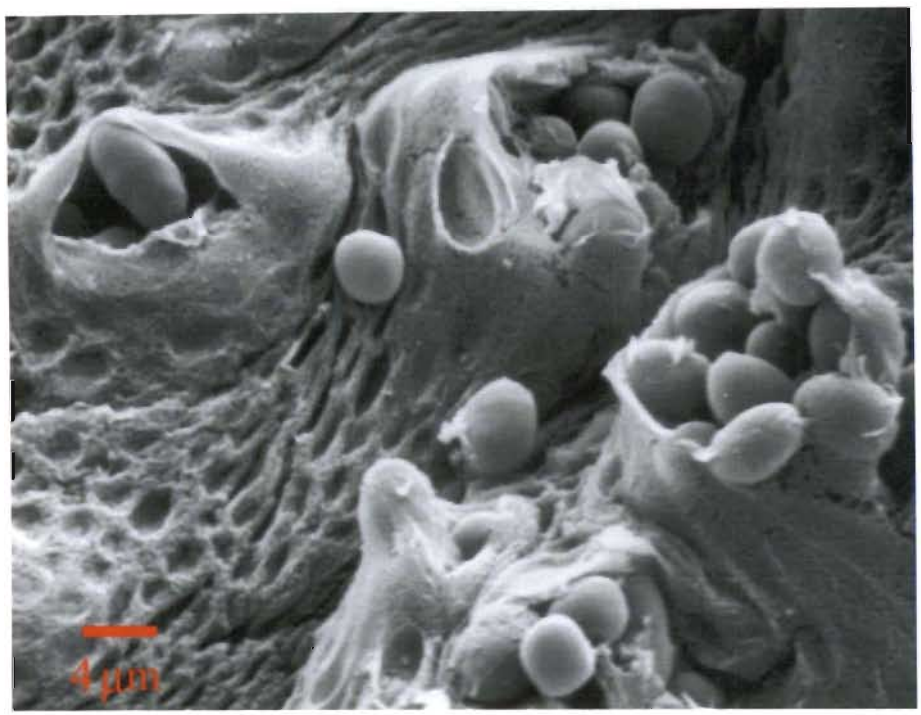

Figure **3.50** SEM images of *Saccharomyces cerevisiae* wine strains growing on 3% grape juice agar stress medium, showing that cells are covered by protective sheaths (ps) (a and b) and a mucoid matrix (b).

Abbreviations: bs, birth or bud scar; eg, elongated cell; oc, old cell.

(a)

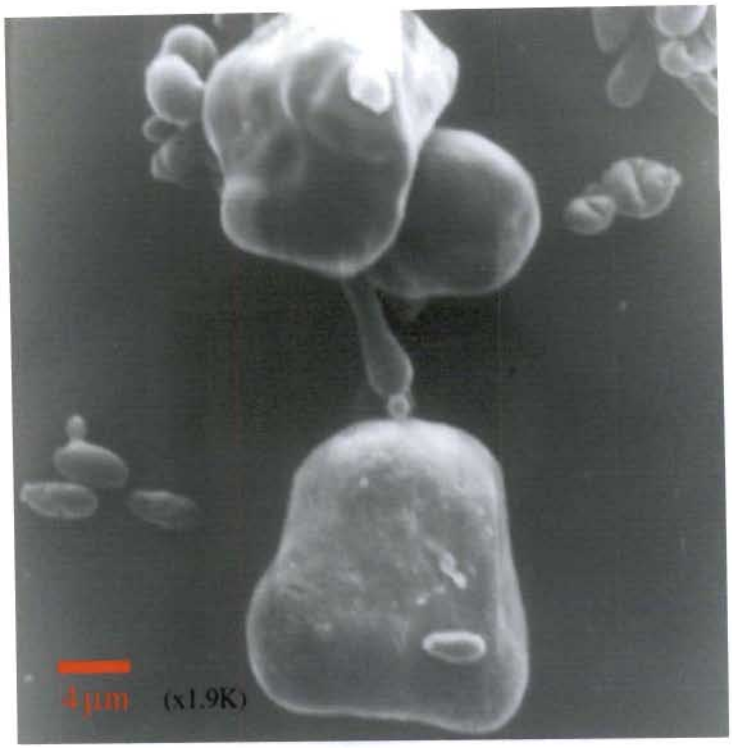

(b)

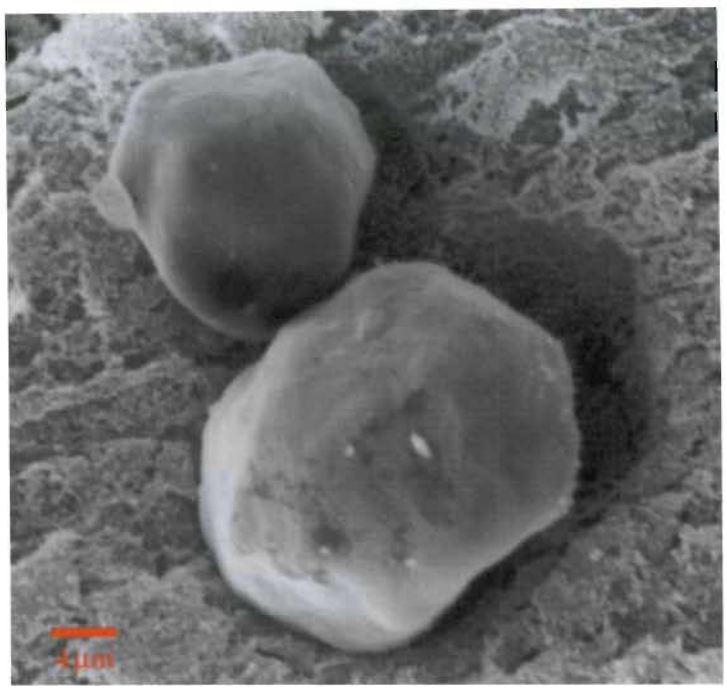

Figure **3.51** SEM images of *Saccharomyces cerevisiae* wine strains growing, (a) in 5% grape juice liquid medium and (b) on 3% grape juice agar stress media, respectively, showing formation of large bodies, which are aggregated cells surrounded by mucoid sheaths, presumably served as protective covers.

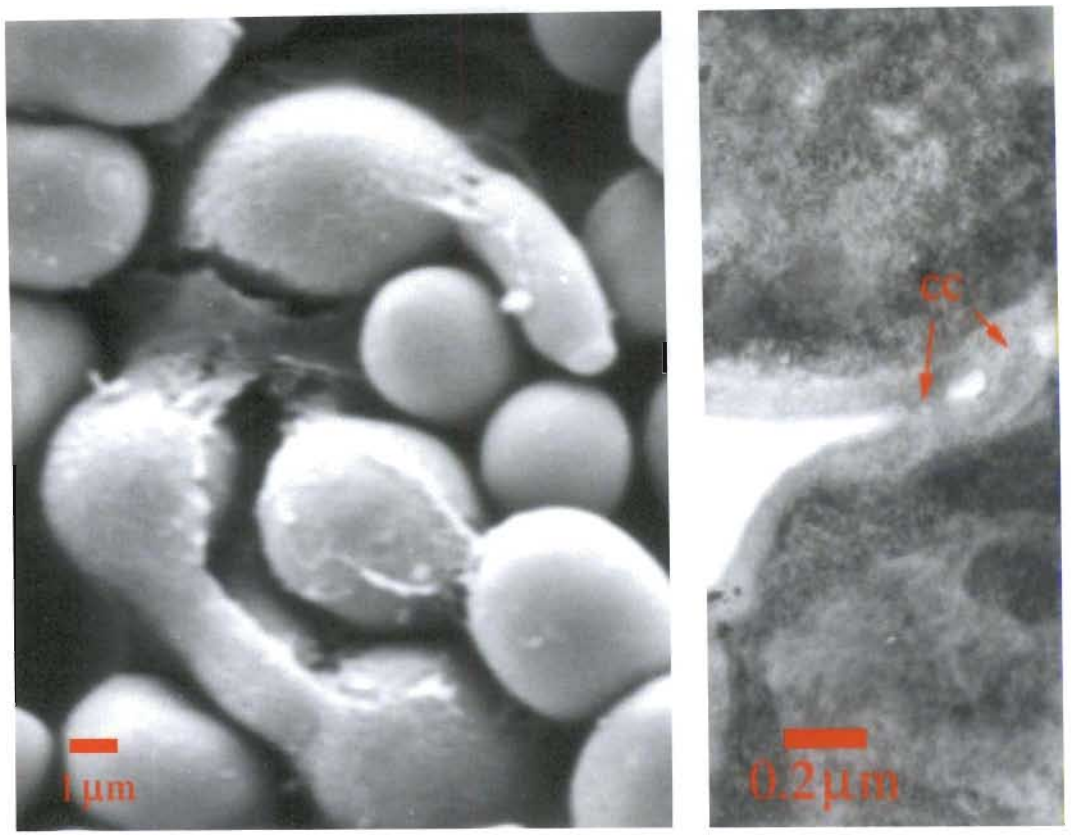

(a) **(b)**

Figure **3.52** SEM (a) and TEM (b) images of *Saccharomyces cerevisiae* wine strains growing on stress media, (a) 3% grape juice agar and (b) 5% grape juice liquid medium, respectively, revealing cell to cell "communication channels" (cc), or likely conjugation tubes facilitating the potential transfer of cytosolic elements.

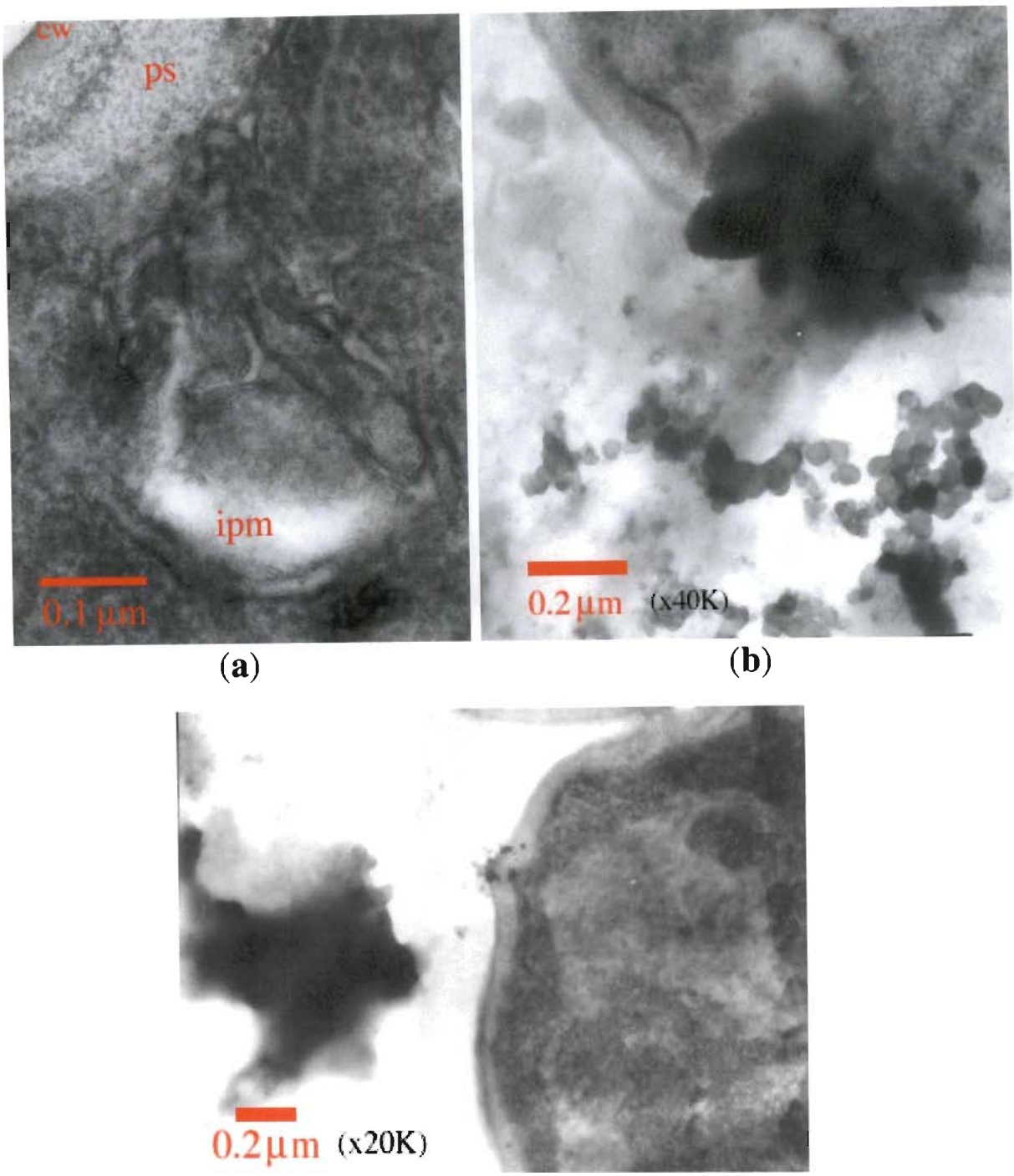

Figure **3.53** TEM images of *Saccharomyces cerevisiae* wine strains growing under nutrient limitation, (a) forming transport vesicles for the endocytosis or (b & c) exocytosis of materials, which are potential nutrients or/and toxins.

Abbreviations: cw, cell wall; ipm, invagination of the plasma membrane or fusion of Golgi cisternae of the plasma membrane; ps, periplasmic space.

(a)

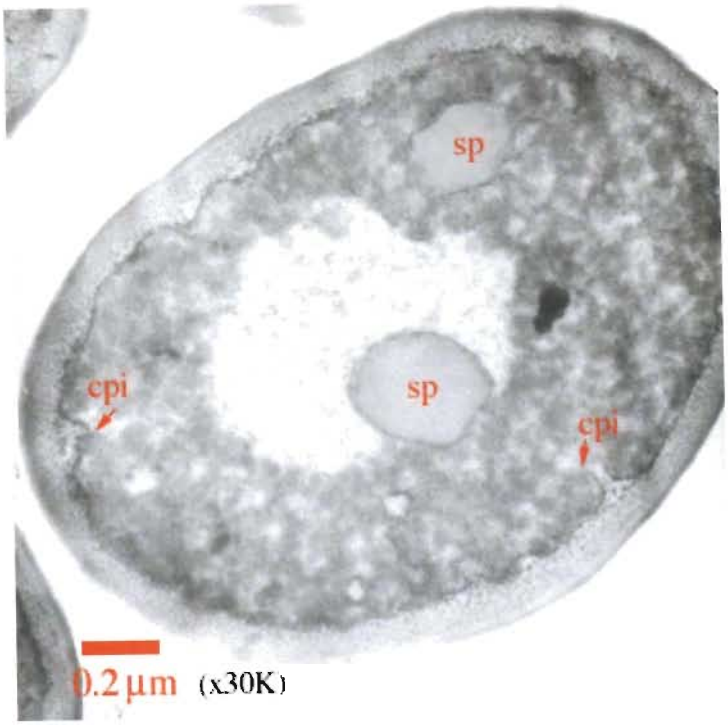

(b)

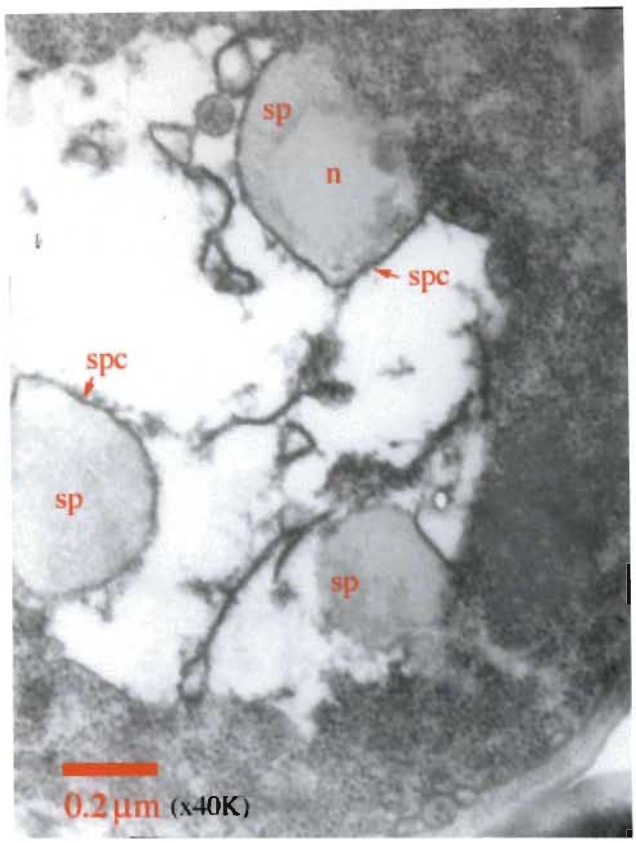

Figure **3.54** TEM images of *Saccharomyces cerevisiae* wine strains growing under severe nutritional stress condition, which induces ascospore formation.

Abbreviations: cpi, invagination of cytoplasmic membrane; n, nuclear material; sp, spore; spc, spore cortex.

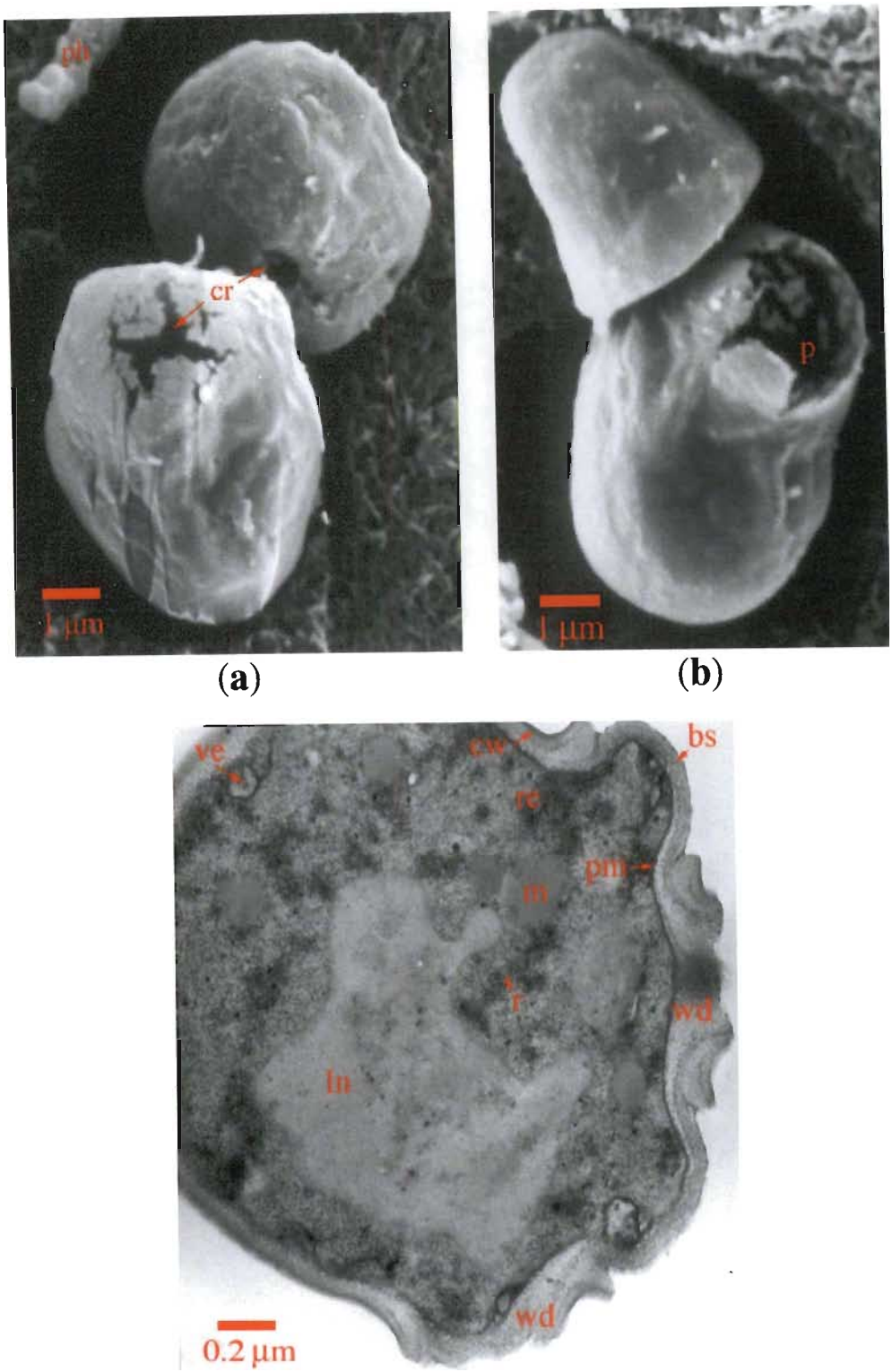

Figure **3.55** Micrographs of sensitive *S. cerevisiae* cells damaged by the K_2 killer toxin.

Abbreviations: bs, bud scar; cr, crack; cw, cell wall; ln, lobular nucleus; m, mitochondria; p, pore; pm, plasma membrane; r, ribosomes; re, rough endoplasmic reticulum; ve, plasma membrane-associated vesicle; wd, cell wall damage.

Sensitive wine yeast cells growing on the stressed media (section *3.2.2.10.*), produced a mucoid, sheath-like structure over some cells (Figure **3.50** and **3.51**). It is postulated that the mucoid secretion is mucin and that it masks the K_2 toxin from binding effectively to its cognate receptor. This would explain the poor killing of cells under stress conditions as the *FLO11* structural gene is induced to produce a mucin-like (flo11p) protein. This feature was also found on the agar wedges (*3.2.2.10.1*) taken away from the zone of clearing and superficial growth. Cells, taken at the perimeter of the concentric zone of inhibition, were damaged by the K_2 toxin (Figures **3.47** & **3.55**). Cells of normal yeast-like structure, which were embedded in the mucoid matrix or sheath, appeared to be physically protected from the toxin effects (Figure **3.50** and **3.51**). A closer examination of the mucoid matrix revealed imprints as if cells had been dislodged from the pits (Figure **3.50b**), perhaps during the preparatory steps for microscopy.

Scanning and transmission electron microscopy of K_2 - toxin damaged sensitive cells (Figure **3.55**) revealed cell shrinkage (also observed in pure culture subjected to extreme nutritional stress), characteristic of cytoplasmic efflux, and presumably the result of the interaction of the K_2 mycotoxin to specific cell wall receptors. This interaction is followed by formation (Martinac *et al.*, 1990) or activation of endogenous ion channels in the plasma membrane of the target cells, such as the *TOK1* potassium-selective ion channels in *S. cerevisiae* (Ahmed *et al.*, 1999). K_2 - toxin damaged cells (Vadasz *et al.*, 2000) were characterised by cell wall disruption at different positions, by way of cracks or/and pores, resulting in the extrusion of cytosol at these points (Figure **3.55**). However, disruption of a crenulated plasma membrane could not be proven.

Toxin - induced membrane damage is an energy (ATP) - dependent event (Skipper and Bussey, 1977). Shortly after the killer toxin binds to the receptor in the cell wall, this causes a decrease in the ion gradient across the membrane, interrupting the coupled

transport of protons and amino acids. This event may induce pore formation, allowing for the penetration of ions such as potassium and low-molecular weight metabolites. Hence, the formation of pores is assumed to be associated with the lethal effect of the killer toxin (Vadasz *et al.*, 2000; Van Vuuren and Jacobs, 1992).

Bussey, (1974) found that the membrane-damaged cells shrunk in volume owing to the loss of small metabolites through the large pores in the membrane, however, no cell lysis occurred. Carrau and co-workers, (1993) supported this showing that sensitive cells in the presence of K_1 did not lyse and that macromolecules were not released from the killed cells. However, the data presented in Figure **3.53** may suggest otherwise. Sensitive cells, damaged by the K_2 toxin, were not associated with a mucoid matrix but were characterised by the loss of turgidity and disruption of the cell (Figure **3.55**), resulting in the extrusion of the cytosol at these points. The K_2 toxin of T206 strain appears to resemble the K_1 mycotoxin, which is known to induce cytosolic efflux through pore formation (Bussey, 1991). The plasma membrane of toxin-damaged cells was retracted from the perimeter of the periplasmic space and irregular folds and 'pinocytotic type' vesicles were also associated with the plasma membrane. However, plasma membrane-associated vesicles (Figures **3.53a** and **3.55**), originating from Golgi cisternae, could be linked to the exocytosis of secretory compounds to the periplasmic space (Osumi, 1998). The well-defined cristae observed in mitochondria of unchallenged cells could not be easily detected in damaged cells. Also, toxin - affected cells showed the induction of a lobular nucleus. Ribosomes and most vacuoles in the cytosol stained darkly in both control and challenged cells. Ribosomes were arranged in clusters whilst attached to the rough endoplasmic reticula connecting between plasma membrane and the nucleus (Figure **3.55**).

The most intensively studied M-dsRNA species is M_1. *K1* killer heterodimeric toxin is secreted into the growth medium during the exponential phase of growth. As a pore-forming protein, which is processed from a precursor in the Golgi, it has allowed for identification of the KES2- and KES1- encoded proteases. The toxin binds to a β-1,6-glucan component of the receptor on the cell wall of the target yeast. This binding of the *K1* killer toxin is specific and has been used in its purification procedure. Both the α- and β- toxin subunits are implicated in receptor binding. The hydrophobic α-subunit - encoding region is the site controlling channel formation. It is still unknown if the α-subunit is sufficient to form a pore, or if the β-subunit is also involved (Bussey, 1991).

The resilient degree of a sensitive strain to the toxin might be attributed to differences in the structure of the yeast cell wall or properties of the K_2 toxin binding receptors (Hutchins and Bussey, 1983; Bussey, 1991) and flocculation properties (reviewed by Vadasz, A.S., 1999b).

Nutritionally-stressed media may negatively affect the copy number of VLPs in the killer cells (3.3.4.2), and thus influence the amount and degree of activity of the killer toxin. It is known that the depletion of nutrients in growth media potentially activates the *FLO11-MSS10* gene system in *S. cerevisiae* strains (Gagiano *et al.*, 1999). The decrease in both ammonium and sugar concentrations could induce the *FLO11* (*MUC1*) structural genes to produce a flocculin (flo11p) or mucin-like protein (muc1p) and manifest in pseudohyphae formation (Gagiano *et al.*, 1999; Lambrechts *et al.*, 1996). In this study, invasive growth (Figure **3.49**) and pseudohyphal formation (Figure **3.48**) was detected in all of the investigated *S. cerevisiae* strains (T206, T206q, VIN7 and Y217), subjected to nutritional stress. It is likely that yeast cells anchor to the agar medium, with the mucin-

like protein possibly promoting adhesion or aggregation of cells (Figure **3.50** and **3.51**), while pseudohyphae forage for the limited nutrients (Figure **3.48**).

Nitrogen starvation also induces morphological changes in haploid ellipsoidal cells of *S. cerevisiae* when the *GDH3* gene is partially deleted, forming a pseudohyphal growth pattern. The *GDH3* gene codes for the nicotinamide adenine dinucleotide ($NADP^+$, oxidised form)-linked glutamate dehydrogenase involved in the production of L-glutamate by the cell, which contributes to the fixed nitrogen present in cells. This gene might also be involved in the recognition of available nitrogen source. Haploids, bearing the partially deleted *GDH3* gene, form wrinkled colonies showing pseudohyphal growth patterns, when grown on either rich or stressed medium. Addition of glutamine to a yeast nitrogen-base medium increases the amount of pseudohyphae, which suggests that nitrogen starvation is not the only reason for the formation of the pseudohyphal phenotype (Wilkinson *et al.*, 1996).

3.4 Conclusions

This study aimed develop a new mathematical model simulating the dynamical interaction of killer and sensitive yeast strains in single and mixed cultures, in order to understand the macro qualitative features controlling the dynamics of these interaction. The growth pattern features of wine strains of *Saccharomyces cerevisiae* under extreme nutritional stress media (5% grape juice and pure water) were examined here. Genetic alteration of the viral dsRNA that inhabits a killer yeast, was induced by cycloheximide treatment (see 3.2.2.2; 3.3.1) in order to delete the ability of the killer yeast to produce its viral killer toxin, and therefore used as the killer control (see 3.2.2.9; 3.3.2.1; Figure **3.4**).

A lag phase of growth is not observed in both nutritional stressed media (5% grape juice and pure water), although the initial growth rate is relatively lower than the subsequent growth at later times prior to the stationary phase for cells growing in the 5% grape juice, but not in pure water. Oscillatory mode of growth, an over shooting and one or more inflection point(s) in the "ln curve" (3.3.4.1, 3.3.4.2, 3.3.4.3; Figures **3.10-3.25**) were observed for both pure and mixed cultures (see 3.3.4.1; 3.3.4.2). Oscillatory modes of pH and substance levels (3.3.4.3) in cell media of ethanol (*3.3.4.3.2*), ammonium (*3.3.4.3.3*), acetic acid (*3.3.4.3.4*), glycerol (*3.3.4.3.5*) were also observed. These substances were produced or/and released by the constant adapted cells (3.3.5, Figure **3.53**) and could be consumed by the cells as nutrients.

S. cerevisiae, under extreme nutritional stress, sporulate. Although spores were not counted (3.3.4.1; 3.3.5, Figure **3.54**), it was estimated that their number while grown in pure water was substantially larger than their corresponding number associated with growth in 5% grape juice. The spores survived the stressed environmental conditions, reproduced or/and germinated, others wasted and could be used as "nutrient sink" for the cells.

Growing in mixed cultures, the killer effect was observed only when the killer strain, not the killer-cured, challenged a sensitive strain (see 3.3.2.1, Figure **3.4**; 3.3.5, Figure **3.55**). Few hours after exposure to the killer toxin, dead cell percentage reached an extreme peak point less the half of that was found when the killer cured challenged a sensitive strain. The formation of cell protective structures observed under the scanning and transmission electron microscopes (section 3.3.5) physically blocked the toxin effects on the sensitive cells. Also, limited nutrient sources, possibly decreases VLP reproduction, and thus the toxin production and the chemical changes in the medium influence the toxin activity.

Growing on the WLN medium (3.2.2.8) of single (Figure **3.5**) and mixed of two (3.3.4.1; 3.3.4.2, Figure **3.46**) allowed to differentiate the relative survival of cells of the mixed cultures (Figure **3.36-3.45**). Killer-cured cells growing in pure water, challenged by the killer at a K:Kq cell ratio of 1:100 (Figure **3.44**) revealed that the killer-cured phenotype dominated and the killer strain phenotypes disappeared. A ratio of killer:sensitive 1:100 (Figures **3.36** and **3.37**) revealed dominance of the sensitive strain and extinction of the killer strain. A ratio of killer:sensitive 1:1 (Figures **3.40** and **3.41**) strongly support the survival of the sensitive strains according to their relative growth rates. The killer did not dominate the mixed cultures, and in comparison with the killer-cured (1:100 Kq:S ratio, Figures **3.38** and **3.39** and 1:1 Kq:S ratio, Figures **3.42** and **3.43**), it seemed to have a disadvantage while growing under nutritional stress.

CHAPTER 4

FORMULATION OF THE NEW MODEL

4.1 The conceptual model

The objective of the proposed new model is to address the following points:

- The new model is expected to recover a *Lag Phase* as a particular possibility.
- The new model is expected to recover an inflection point on the logarithm of the cell concentration curve as a particular possibility.
- The new model is expected to recover the Sigmoid Curve (LGM) as a special case.
- The new model is expected to recover an overshooting and an oscillatory mode of yeast growth.

To accomplish these goals a new model proposed and derived by Vadasz, (2000) is applied. This model that takes into account the reason for the limitation of the LGM, that might be its lack of kinetics is presented here. To clarify the matter one needs to emphasise accurately the definition of the terminology that is being used. In particular the term "kinetics" is at times used in misleading connotations. The correct meaning is related to its basic definition that is linked to the two branches of Dynamics, namely Kinematics and Kinetics. Kinematics is the study of the Dynamics of a system including *displacement* and *velocities* but without reference to the forces associated with this Dynamics. On the other hand, Kinetics is the branch of Dynamics which relates the action of *forces* and *accelerations* to their resulting *displacement* and *velocities*. Clearly, the LGM equation (2-1) and all its variations presented in Chapter 2 represent "rate equations" relating the growth *velocity* (growth rate) to its *displacement* (instantaneous

cell concentration) and is therefore a Kinematic model. As a matter of fact it was Pearl, (1927) who introduced the concept of forces in his classical paper. His paper starts by indicating that *"The primary biological variables involved in the growth of population are...: the* ***force*** *of natality, measured by the birth rate, on the one hand; and the* ***force*** *of mortality, measured by the death rate, on the other hand."* He later introduces a third factor affecting population growth in the form of *migration*. While Pearl, (1927) seems to be the first to introduce the concept of natural forces that affect the population growth, he did not translate the latter into a mathematical balance of forces in his proposed equation. The LGM as indicated above is a "rate equation" and therefore does not account for this balance of forces. One needs, therefore to extend the LGM in order to include a balance of forces and accelerations, representing therefore the Kinetics of the system.

4.2 Derivation of the new model

In order to mathematically present the "forces", which are involved in a population growth, the LGM equation (2-1) is used as the starting point, multiplying it by a coefficient c and introducing a change of momentum term, in the form (Vadasz, 2000)

$$\frac{\mathrm{d}}{\mathrm{d}t}\left(m\frac{\mathrm{d}x}{\mathrm{d}t}\right)+c\frac{\mathrm{d}x}{\mathrm{d}t}=c\mu\left[1-\frac{x}{\delta}\right]x \tag{4-1}$$

where c is now a "*damping coefficient*" and m is referred to as a "*virtual mass*". There is no evidence to suggest that m is in any way related to the cell average biomass or density although this possibility does not exclude and may serve as a future objective for study. In the most general case one need to allow both m as well as c to depend on the cell concentration x, i.e. $m \equiv m(x)$ and $c \equiv c(x)$. With these clarifications one can present equation (4.1) in the form

$$\frac{\mathrm{d}}{\mathrm{d}t}\left(m\frac{\mathrm{d}x}{\mathrm{d}t}\right)+c\frac{\mathrm{d}x}{\mathrm{d}t}-bx+K_o x^2=0 \tag{4-2}$$

where $b=c\mu$ and $K_o=c\mu/\delta$. The term $m(\mathrm{d}x/\mathrm{d}t)$ represents the *virtual momentum* of the cell growth and the first term in equation (4.2) is therefore the *virtual inertial force*. The second term is a *damping force* inhibiting growth if $c>0$. The third term represents a *central attracting force* (analogous to a *virtual magnetic force*) and the last term represents a *restoring force* of a non-linear *virtual hardening spring* with K_o as the "reference *virtual spring*'s stiffness" ($K_o x$ representing the *virtual hardening spring*'s stiffness). Equation (4.2) can be presented in the following form

$$m\ddot{x}+\left[\frac{\mathrm{d}m}{\mathrm{d}x}\dot{x}+c\right]\dot{x}-bx+K_o x^2=0 \tag{4-3}$$

where Newton's time derivative notation is introduced $\dot{x}=\mathrm{d}x/\mathrm{d}t$ and $\ddot{x}=\mathrm{d}^2x/\mathrm{d}t^2$, for simplicity. As previously indicated, both the virtual mass as well as the damping coefficient may in general be functions of concentration, i.e. $m\equiv m(x)$ and $c\equiv c(x)$. As a result, both coefficients affect the growth differently at different times during the cells' growth, but the time dependence is not explicit as proposed by Baranyi and Roberts, (1994) but only implicitly included via their dependence on the cell concentration $x(t)$. The consequence is that the model remains autonomous while preserving the advantages of Baranyi and Roberts, (1994) model that accounts for "*inertial*" effects. In addition, it is by far easier formulating for the new model an inverse problem that is sufficiently general, in order to establish the values of the coefficients as well as the accurate functional form of $m(x)$ and $c(x)$. In particular, interesting objectives for further studies relate to the fact that for $c\equiv c(x)$ there are additional stationary points of the system (4-1)

that correspond to $c(x)=0$. The existence of multiple stationary points is consistent with experimental results on yeast growth presented in section 3.3.4.1 Figures **3.10** to **3.25**.

4.3 Constitutive relationships and a simplified version of the new model

Since for this first presentation of the proposed new model there is no accurate form of these functions no formulation of the inverse problem yet, nor corresponding experiments performed, only an approximation for these functions is applied for demonstration purposes. Therefore, in the demonstrated examples to be presented in this study it is assumed following Vadasz, (2000) that $c=c_o=\text{constant}$, and a two-term Taylor expansion for $m(x)$, in the form

$$m=m_o\left[1+s(x-x_r)\right] \tag{4-4}$$

where $s=(1/m_o)(\mathrm{d}m/\mathrm{d}x)\approx\text{constant}$, and m_o is the value of m at $x=x_r$. In addition, it is assumed that m is a weak function of x, i.e. the value of s is small and can be expressed in the form $s=\varepsilon s_o$, where $\varepsilon<<1$ and s_o is another constant. Naturally, these assumptions are quite limiting and future research that may reveal the accurate forms of $m(x)$ and $c(x)$ will allow the relaxation of these limitations. Nevertheless, one will see that even with these limiting assumptions the model recovers a wide range of growth curves as well as a quite good fit with the experimental data of this study (Figures **3.10**-**3.35**). Substituting equation (4.4) and the weak-function assumption $s=\varepsilon s_o$ into equation (4.4) and dividing the whole equation by m_o yields

$$\left[1+\varepsilon s_o(x-x_r)\right]\ddot{x}+\left[\varepsilon s_o\dot{x}+\nu_o\right]\dot{x}-\alpha_o x+\sigma_o x^2=0 \tag{4-5}$$

where the following notation was used

$$v_o = \frac{c_o}{m_o} \quad ; \qquad \alpha_o = \frac{\beta}{m_o} = \frac{c_o \mu}{m_o} = v_o \mu \quad \text{and} \qquad \sigma_o = \frac{K_o}{m_o} = \frac{c_o \mu}{m_o \delta} = \frac{v_o \mu}{\delta} = \frac{\alpha_o}{\delta}$$

(4-6)

It is sensible to assume that $(x - x_r)$ is of a unit order of magnitude, i.e. $(x - x_r) = O(1)$, and therefore the term $\varepsilon s_o (x - x_r)$ is much smaller than the first term in the same brackets which is 1, because $\varepsilon << 1$. Hence the term $\varepsilon s_o (x - x_r)$ can be neglected at leading order. On the other hand, one can not apply the same argument to the term $(\varepsilon s_o \dot{x})$ because it is not sensible to speculate about the resulting order of magnitude of $\dot{x}$ that can be quite large, especially if very short time scales are involved. As a result the leading order form of equation (4-5) subject to these assumptions is

$$\ddot{x} + [s\dot{x} + v_o]\dot{x} - \alpha_o x + \sigma_o x^2 = 0 \qquad (4\text{-}7)$$

where the original parameter $\varepsilon s_o = s$ is reintroduced at this stage. Equation (4-7) was used in this study for demonstration of the proposed model subject to the limiting assumptions indicated above. Four constant parameters, namely s, v_o, α_o and σ_o, and two initial conditions, namely

$$x(0) = x_o \qquad \text{and} \qquad \dot{x}(0) = \dot{x}_o \qquad (4\text{-}8)$$

are needed as input data to solve the initial value problem. Equation (4-7) as well as its more general original form, equation (4.3), retain the same stationary points as the original LGM, i.e. $x_s = \delta$ and $x_s = 0$.

To solve the initial value problem (4-7) and (4-8) computationally, the second order ordinary differential equation (4-7) is firstly expressed in the form of the following two first order equivalent equations

$$\begin{cases} \dot{x} = y \\ \dot{y} = -\left[s\,y + v_o\right] y + \alpha_o x - \sigma_o x^2 \end{cases} , \tag{4-9}$$

that need to be solved subject to the following initial conditions

$$t = 0 : \; x(0) = x_o \quad \text{and} \quad y(0) = \dot{x}(0) = y_o \; . \tag{4-10}$$

yielding

$$\begin{cases} \dot{x} = y_{st} = 0 \\ \dot{y} = x(\alpha_0 - \sigma_0 x) \end{cases} \tag{4-11}$$

4.4 Derivation of the new model for two species competing over a common ecological niche

The experimental results of mixed wine yeast cultures presented in Chapter 3 (section 3.3.4.2) are being considered in order to establish whether they are consistent with the modified classical model analysis or not. The experimental results for the differentiation between the killer-strain T206 and the sensitive Y217 grown in mixed culture in water at an initial concentration ratio of 1:1 (Figure **3.41**) are presented in Figure **4.1a**, where a cubic-spline curve fitting (standard within the graphical software) was applied to the data. Because of the tedious and time consuming measurement process linked to the differentiation experiments there is no possibility of capturing a high-resolution data set. From Figure **4.1a** it is evident that both strains coexist and moderate oscillations of both strains concentration are observed, especially on the curve of the total viable cells. One may be even tempted to fit a logistic curve to these data. However, observing the experimental data for the total viable cell concentration that is presented in Figure **4.1b**, which corresponds to the ongoing cell count of total viable cells (i.e. not via the

differentiation process) clearly indicates that this is not the case. The data presented in Figure **4.1b** was captured at higher resolution. As a result, a cubic-spline curve fit (standard within the graphical software used) suggests wild oscillations in the total viable cell count. The extremely high spike between $t = 100$ hours and $t = 170$ hours is likely to be a curve-fitting artifact due to the lack of data during this long period of time. Similar results apply for competition between the two sensitive strains of yeast Y217 and VIN7 at an initial concentration ratio of 1:1 (Figure **3.45**), and are presented in Figure **4.2**. On the other hand, the experimental results presented in chapter 3 for the killer and sensitive strains (T206 and VIN7 or T206 and Y217) grown in a mixed culture in pure water, but at an initial concentration ratio of 1:100, respectively, show that the sensitive strains survive while the killer strain is subject to extinction (Figure **3.36** and **3.37**).

The major two conclusions are therefore: (1) Coexistence of both strains as well as extinction of one of them was recovered experimentally, and some results seem to depend on initial conditions, (2) Oscillations in the cell count of both the individual cell concentration as well as in the total viable cell count were recovered experimentally. The first conclusion is perfectly consistent with the analysis results pertaining to the Modified Classical Model, i.e. equations (2-8)-(2-9). The second conclusion is, however, inconsistent with the Modified Classical Model because the latter can not accommodate oscillations. A new model is required to recover the experimentally observed oscillatory growth.

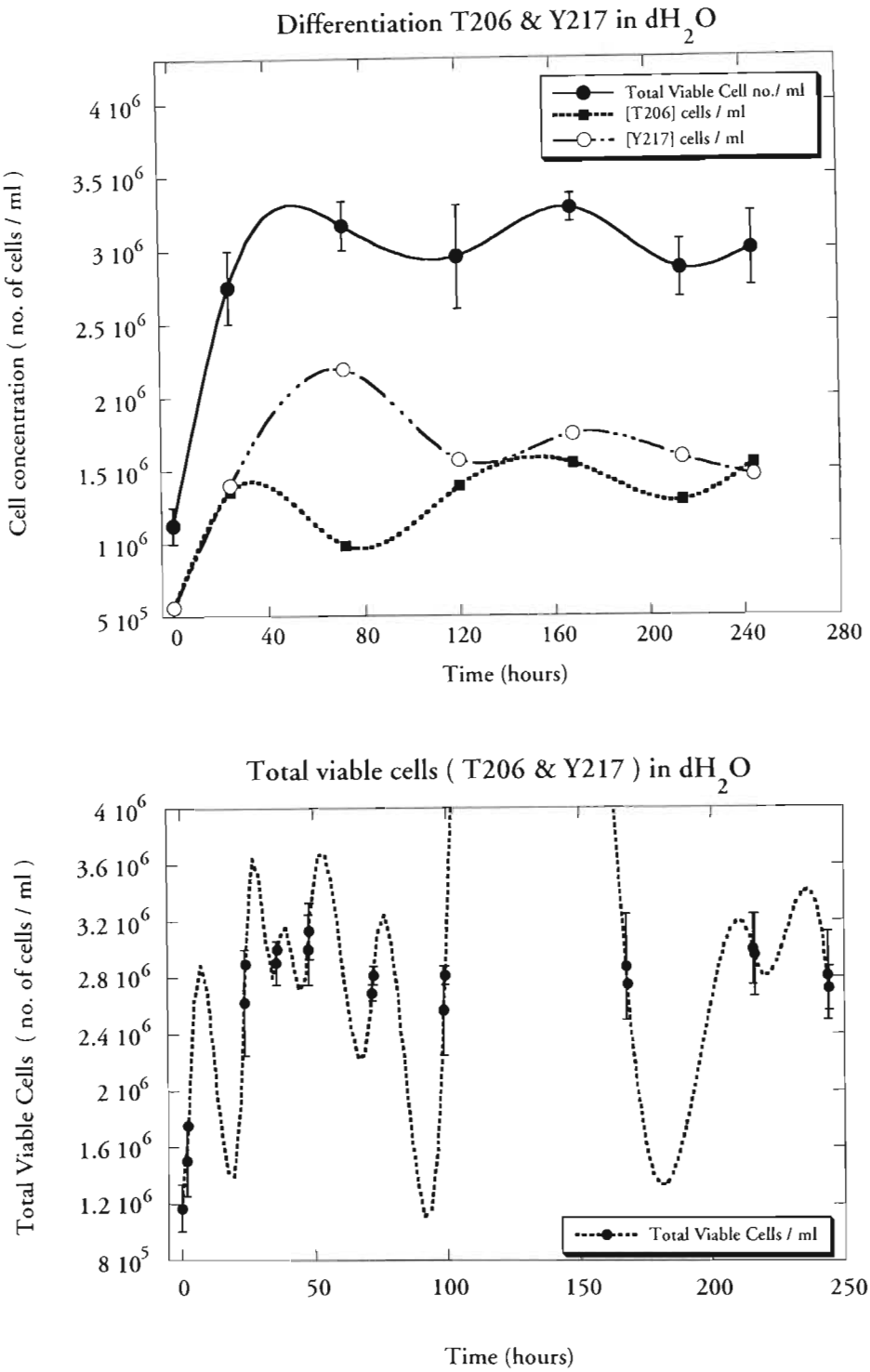

Figure **4.1** Experimental results of total viable cell concentration and differentiation between the killer T206 and the sensitive Y217 strains of yeast grown in mixed culture in pure water at an initial concentration ratio of 1:1. (a) Cell differentiation data; (b) Total viable cells. Aliquots of mixed cell population were plated onto WLN medium to determine the relative concentration of each as individual strains showed peculiar colony traits (Figure **3.46**).

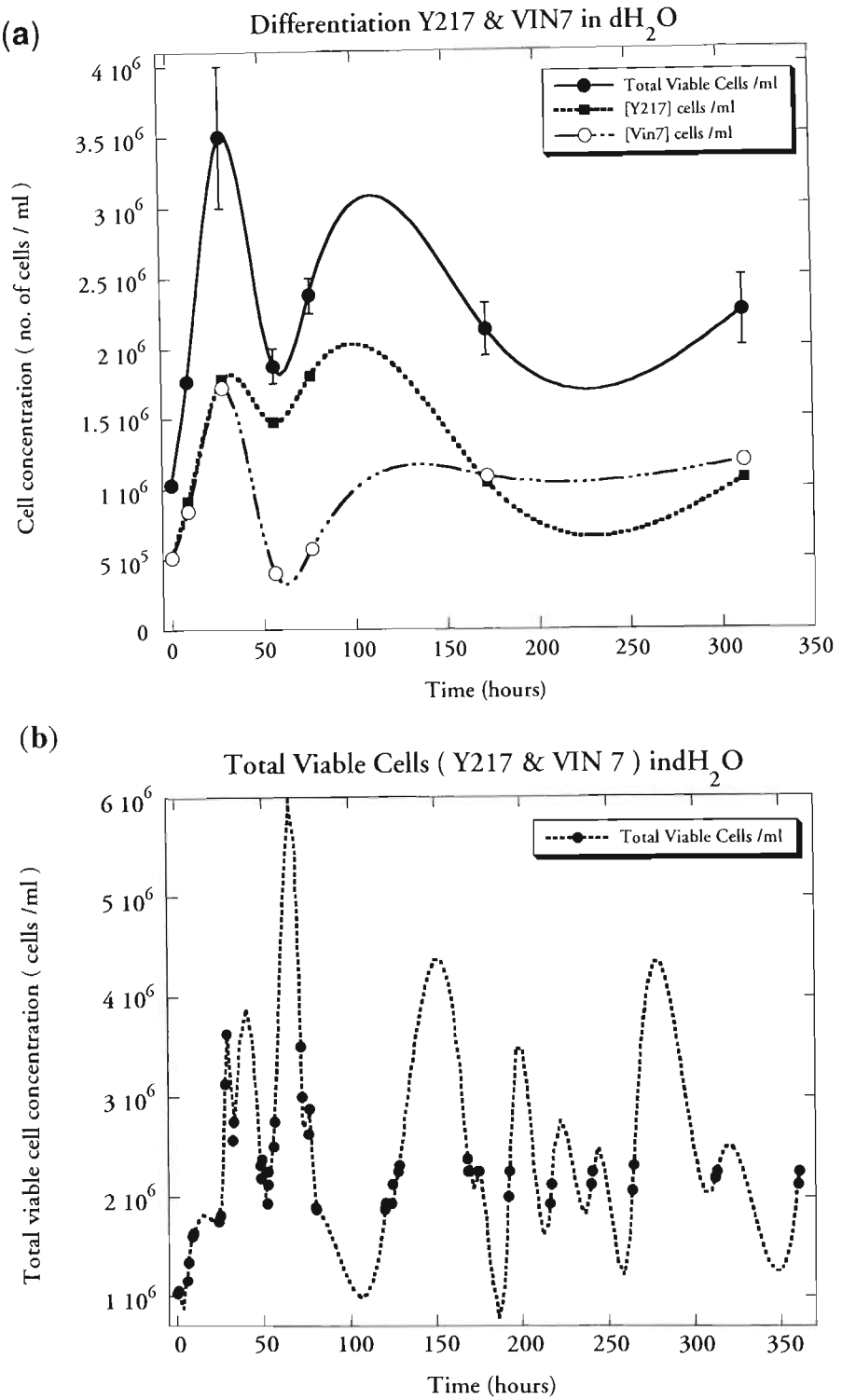

Figure **4.2** Experimental results of total viable cell concentration and differentiation between the two sensitive strains of yeast Y217 and VIN7 grown in mixed culture in pure water at an initial concentration ratio of 1:1. (a) Cell differentiation data; (b) Total viable cells. Aliquots of mixed cell population were plated onto WLN medium to determine the relative concentration of each as individual strains showed peculiar colony traits (Figure **3.46**).

4.5 The new model for two species competing over a common ecological niche

Extending the application of the new model that was developed (Vadasz, 2000) for a single species growing in isolation to apply for two species competing over a common ecological niche, by considering some of the analysis results from the modified classical model produces the following set of equations (Vadasz, 2000)

$$\frac{\mathrm{d}}{\mathrm{d}}\left(m_1\frac{\mathrm{d}x_1}{\mathrm{d}t}\right)+c_1\frac{\mathrm{d}x_1}{\mathrm{d}t}=c_1(\mu_1-\beta_{11}x_1-\beta_{12}x_2)x_1 \tag{4-11}$$

$$\frac{\mathrm{d}}{\mathrm{d}}\left(m_2\frac{\mathrm{d}x_2}{\mathrm{d}t}\right)+c_2\frac{\mathrm{d}x_2}{\mathrm{d}t}=c_2(\mu_2-\beta_{21}x_1-\beta_{22}x_2)x_2 \tag{4-12}$$

These equations can be presented in the form

$$\frac{\mathrm{d}}{\mathrm{d}}\left(m_1\frac{\mathrm{d}x_1}{\mathrm{d}t}\right)+c_1\frac{\mathrm{d}x_1}{\mathrm{d}t}-b_1x_1+K_{11}x_1^2+K_{12}x_1x_2=0 \tag{4-13}$$

$$\frac{\mathrm{d}}{\mathrm{d}}\left(m_2\frac{\mathrm{d}x_2}{\mathrm{d}t}\right)+c_2\frac{\mathrm{d}x_2}{\mathrm{d}t}-b_2x_2+K_{21}x_1x_2+K_{22}x_2^2=0 \tag{4-14}$$

where the following notation was used

$$b_1=c_1\mu_1\ ;\quad b_2=c_2\mu_2\ ;\quad K_{11}=c_1\beta_{11}\ ;\quad K_{12}=c_1\beta_{12}\ ;\quad K_{21}=c_2\beta_{21}\ ;\quad K_{22}=c_2\beta_{22} \tag{4-15}$$

Considering now $m_1\equiv m_1(x_1)$, $m_2\equiv m_2(x_2)$, $c_1=\text{constant}$ and $c_2=\text{constant}$, and assuming

$$m_1=m_{10}+\varepsilon m_{11}(x_1)=m_{10}\left[1+s_1(x_1-x_r)\right] \tag{4-16}$$

$$m_2=m_{20}+\varepsilon m_{21}(x_2)=m_{20}\left[1+s_2(x_2-x_r)\right] \tag{4-16}$$

then, for $s_1 << 1$ and $s_2 << 1$ one obtains from equations (4-13)-(4-14), after substituting (4-16)-(4-17) and dividing by m_{10} and m_{20} respectively a simplified version of the new model in the form

$$\ddot{x}_1 + (s_1\dot{x}_1 + v_1)\dot{x}_1 - \alpha_1 x_1 + \eta_{11}x_1^2 + \eta_{12}x_1x_2 = 0 \tag{4-17}$$

$$\ddot{x}_2 + (s_2\dot{x}_2 + v_2)\dot{x}_2 - \alpha_2 x_2 + \eta_{21}x_1x_2 + \eta_{22}x_2^2 = 0 \tag{4-18}$$

where

$$v_1 = \frac{c_1}{m_{10}}\ ; \qquad \alpha_1 = \frac{b_1}{m_{10}}\ ; \qquad \eta_{11} = \frac{K_{11}}{m_{10}}\ ; \qquad \eta_{12} = \frac{K_{12}}{m_{10}}\ ; \tag{4-20}$$

$$v_2 = \frac{c_2}{m_{20}}\ ; \qquad \alpha_2 = \frac{b_2}{m_{20}}\ ; \qquad \eta_{21} = \frac{K_{21}}{m_{20}}\ ; \qquad \eta_{22} = \frac{K_{22}}{m_{20}}\ ; \tag{4-21}$$

Converting each one of these equations into a pair of first order equations yields

$$\dot{x}_1 = y_1 \tag{4-22}$$

$$\dot{x}_2 = y_2 \tag{4-23}$$

$$\dot{y}_1 = -v_1y_1 - s_1y_1^2 + \alpha_1x_1 - \eta_{11}x_1^2 - \eta_{12}x_1x_2 \tag{4-24}$$

$$\dot{y}_2 = -v_2y_2 - s_2y_2^2 + \alpha_2x_2 - \eta_{21}x_1x_2 - \eta_{22}x_2^2 \tag{4-25}$$

The system of equations (4-22)-(4-24) was solved for different combinations of parameters and different initial conditions in an attempt to check whether the experimental results can be recovered qualitatively. There was no attempt to fit the experimental results quantitatively because the process involving the variation of 10 parameters and 2 additional unknown initial conditions for $y_1(0) = \dot{x}_1(0)$ and $y_2(0) = \dot{x}_2(0)$ becomes unmanageable by trial and error. A more systematic way is

needed along the lines of introducing an inverse problem, in order to establish accurately the values of the parameters.

CHAPTER 5

ANALYSIS OF THE PROPOSED MODEL

5.1 Linear stability analysis

The first step in applying the simplified version of the proposed new model for the solution of population growth is carrying out a linear stability analysis of the corresponding stationary points. The system of equations (4-9) has the general form $\dot{x} = f(x)$ and the stationary points x_{st} are defined by $f(x) = 0$, corresponding in this case to the trivial solution $x_{st1} = (x_{st} = 0;\ y_{st} = 0)$ and the non-trivial stationary solution $x_{st2} = (x_{st} = \alpha_0 / \sigma_0 = \beta / K_0 = \delta;\ y_{st} = 0)$.

Substituting $x = x_{st} + \varepsilon x_1$ and $y = y_{st} + \varepsilon y_1$ where $\varepsilon << 0$ into equation (4-9) yields

$$\begin{cases} \varepsilon \dot{x}_1 = y_{st} + \varepsilon y_1 \\ \varepsilon \dot{y}_1 = -\left[s(y_{st} + \varepsilon y_1) + v_0\right]\left(y_{st} + \varepsilon y_1\right) + \alpha_0(x_{st} + \varepsilon x_1) - \sigma_0(x_{st} + \varepsilon x_1)^2 \end{cases}$$

and after elimination of the basic solution of the set of equations (4.9) for $(x_{st}; y_{st})$, and ε^2 terms

$$\begin{cases} \varepsilon \dot{x}_1 = \varepsilon y_1 \\ \varepsilon \dot{y}_1 = -v_0 \varepsilon y_1 + \varepsilon x_1 \alpha_0 - \sigma_0 2 x_{st} \varepsilon x_1 \end{cases} \tag{5-1}$$

or

$$\begin{cases} \dot{x}_1 = y_1 \\ \dot{y}_1 = -\nu_0 y_1 + x_1(\alpha_0 - 2\sigma_0 x_{st}) \end{cases} \tag{5-2}$$

or

$$\begin{cases} \lambda x_1 = y_1 \\ \lambda y_1 = -\nu_0 y_1 + x_1(\alpha_0 - 2\sigma_0 x_{st}) \end{cases} \tag{5-3}$$

Substituting the first equation of (5-3) into the second equation yields

$$\lambda^2 x_1 + \nu_0 \lambda x_1 + x_1(\alpha_0 - \sigma_0 2x_{st}) = 0$$

or

$$\lambda^2 + \nu_0 \lambda - \alpha_0 - \sigma_0 2x_{st} = 0 \tag{5-4}$$

Substituting x_{st} values of equation (4-9) solutions into equation (5-4) yields the eigenvalues λ_i $(i = 1,2)$.

The linear stability of the trivial stationary point $x_{st1} = 0$ is controlled by

$$\lambda^2 + \nu_o \lambda - \alpha_o = 0 \quad . \tag{5-5}$$

Both eigenvalues are real as long as $\alpha_o > 0$, corresponding to positive specific growth rates and a positive damping coefficient, c_o, as well as a positive value of m_o. The first eigenvalue $\lambda_1 = -\nu_o \left[1 + \sqrt{1 + 4\alpha_o / \nu_o^2}\right] / 2$ is negative as long as $\nu_o > 0$. The second eigenvalue $\lambda_2 = -\nu_o \left[1 - \sqrt{1 + 4\alpha_o / \nu_o^2}\right] / 2$ is positive as long as $\nu_o > 0$. The trivial stationary point $x_{st1} = (x_{st} = 0;\ y_{st} = 0)$ is therefore an (unstable) saddle point if $\alpha_o > 0$.

The instability of the trivial stationary point is identical to the result obtained from the LGM. The type of instability is naturally different.

The linear stability of the other stationary point $x_{st2} = (x_{st} = \alpha_0 / \sigma_0 = \beta / K_0 = \delta$ is controlled by the following quadratic equation for the eigenvalues, λ_i $(i = 1,2)$

$$\lambda^2 + \nu_o \lambda + \alpha_o = 0 \quad . \tag{5-6}$$

For $\alpha_o > 0$ and $\nu_o > 0$ both eigenvalues are real if $\nu_o^2 > 4\alpha_o$, and they become a pair of complex conjugate eigenvalues if $\nu_o^2 < 4\alpha_o$. The former is associated with over-damping conditions, while the latter corresponds to under-damping. When the over-damping condition $\nu_o^2 > 4\alpha_o$ holds (and $\alpha_o > 0$, $\nu_o > 0$), the eigenvalues are $\lambda_{1,2} = -\nu_o \left[1 \mp \sqrt{1 - 4\alpha_o / \nu_o^2}\right] / 2 < 0$, and therefore the non-trivial stationary point is a stable node. For under-damping, $\nu_o^2 < 4\alpha_o$ (and $\alpha_o > 0$, $\nu_o > 0$), the eigenvalues become $\lambda_{1,2} = -\nu_o \left[1 \mp i\sqrt{4\alpha_o / \nu_o^2 - 1}\right] / 2 = \lambda_r + i\lambda_i$, and therefore the non-trivial stationary point is a stable spiral because the real part of the complex eigen values, $\lambda_r = -\nu_o / 2 < 0$, is negative.

5.2 Analysis of the corresponding Hamiltonian system

The results of the linear stability analysis apply in the neighbourhood of the corresponding stationary point. When the initial conditions or the solution deviate substantially from this neighbourhood the linear stability results are not anymore correct because of their local domain of validity implied in the linearisation of the equations. In order to obtain further information about the anticipated behaviour of the new model's simplified version we carried out an analysis of the corresponding Hamiltonian problem,

which is obtained by setting $v_o = s = 0$ in equation (4.9) leading to the Hamiltonian system

$$\begin{cases} \dot{x} = y \quad , & (5\text{-}7) \\ \dot{y} = \alpha_0 x - \sigma_0 x^2 \, . & (5\text{-}8) \end{cases}$$

The Hamiltonian energy of the system (5-7) and (5-8) can be obtained by dividing equation (5-8) by (5-7) to yield the following differential equation $\mathrm{d}y/\mathrm{d}x = \left(\alpha_o x - \sigma_o x^2\right)/y$, which can be integrated analytically to provide the result

$$H = \frac{\sigma_o}{3} x^3 - \frac{\alpha_o}{2} x^2 + \frac{1}{2} y^2 \qquad (5\text{-}9)$$

where H stands to represent the Hamiltonian energy. The phase diagram of the solution of the Hamiltonian system (5-7) and (5-8) is presented in Figure **5.1** for two sets of parameter values. Figure **5.1a** represents the phase diagram corresponding to $\sigma_o = 1$ and $\alpha_o = 2$. It is associated with a non-trivial stationary point located at $(x_s = \alpha_o/\sigma_o = 2; y_s = 0)$. Negative values of x are not consistent with population dynamics, as there is no physical meaning to negative population sizes. From the figure one can observe the existence of a homoclinic orbit associated with the equation $H_o = \sigma_o x^3/3 - \alpha_o x^2/2 + y^2/2 = 0$. Inside the closed domain embraced by the homoclinic orbit the solution remains finite moving on the limit cycles as described in the Figure **5.1a**. However, outside the homoclinic orbit the solution diverges, initially via physically non-acceptable negative values, and eventually towards $-\infty$. This suggests that the initial conditions as well as the parameters be constrained by physically realistic values. As the value of α_o decreases or the value of σ_o increases the non-trivial stationary point on Figure **5.1a** moves to the left towards the origin. At $\alpha_o = 0$ the two stationary points overlap at the origin as presented on Figure **5.1b**. At this point no realistically feasible

solutions are possible, except decay towards extinction. The latter applies for negative values of α_o as well. This result indicates that the possible set of initial conditions and parameters is constrained to a set that is compatible with physically feasible results. This, however, in no way limits the applicability of the model since in any case one has the limitation of positive values of x imposed on the system.

(a)

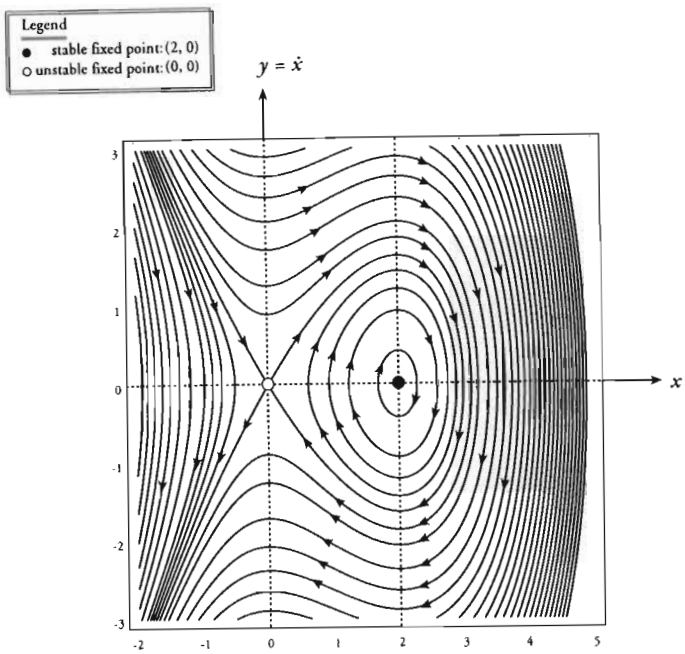

(b)

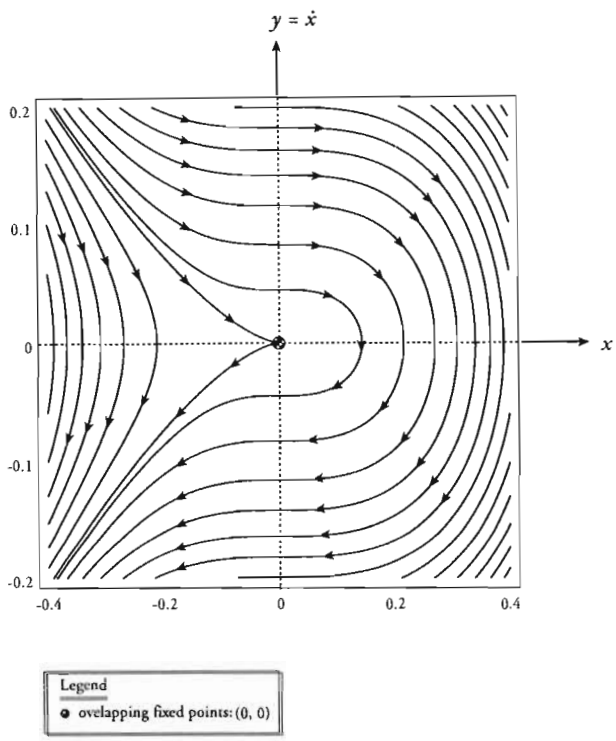

Figure **5.1** The phase diagram for the solution of the new model associated with the corresponding Hamiltonian problem.

(a) $\sigma_o = 1,\ \alpha_o = 2,\ \nu_o = s = 0,$ and (b) $\sigma_o = 1,\ \alpha_o = 0,\ \nu_o = s = 0.$

CHAPTER 6

NUMERICAL AND COMPUTATIONAL METHODS OF SOLUTIONS FOR THE NEW MODEL

Considering the two first order equations (4-9) and (4-10), which for reader convenience are repeated here

$$\begin{cases} \dot{x} = y \\ \\ \dot{y} = -\left[s\,y + \nu_o\right] y + \alpha_o x - \sigma_o x^2 \end{cases} \tag{4-9}$$

subject to the following initial conditions

$$t = 0 : \begin{cases} x(0) = x_o \\ \\ y(0) = \dot{x}(0) = y_o \end{cases} \tag{4-10}$$

Initially, some solutions of these equations were obtained by using a standard library package based on the Rung-Kutta method (IMSL Library, 1991). Eventually, the solution was accomplished by using Adomian's decomposition method of solution (Adomian, 1988, 1994) which was demonstrated to produce extremely accurate results in a substantial number of non-linear problems including cases which are extremely sensitive to initial conditions (see Vadasz and Olek, 1999, 2000 a, b). An algorithm developed originally by Olek, (1994) and modified by Vadasz and Olek, (1999, 2000 a, b) was used. Essentially, the method provides an accurate analytical solution in the form of an infinite

power series for each dependent variable. The solution follows Olek, (1994) and considers the following more general dynamical system of equations

$$\frac{\mathrm{d}X_i}{\mathrm{d}t} = \sum_{j=1}^{m} b_{ij} X_j + \sum_{l=1}^{m}\sum_{j=1}^{m} a_{ijl} X_j X_l \quad , \qquad \forall\ i = 1,2,....,m \tag{6-1}$$

given the initial conditions $X_i(0)$, $i = 1,2,...,m$. It can be easily observed that the system of equations (4-9) is just a particular case of equation (6-1). It provides the following analytical solution

$$X_i(t) = \sum_{n=0}^{\infty} c_{i,n} \frac{t^n}{n!} \qquad \forall\ i = 1,2,....,m \tag{6-2}$$

where

$$c_{i,0} = X_i(0) \qquad \forall\ i = 1,2,....,m \tag{6-3}$$

The convergence of the series (6.4) is difficult to assess *apriori*. Irrespective of this difficulty, the practical need to compute numerical values for the solution at different values of time requires the truncation of the series and, therefore, its convergence needs to be established in each particular case. To achieve this goal, the decomposition method can be used as an algorithm for the approximation of the dynamical response in a sequence of time intervals $[0,t_1)$, $[t_1,t_2)$, ..., $[t_{n-1},t_n)$ such that the solution at t_p is taken as initial condition in the interval $[t_p,t_{p+1})$, which follows. This approach has the following advantages: *(i)* in each time-interval one can apply a theorem proved by Répaci, (1990), which states that the solution obtained by the decomposition method converges to a unique solution as the number of terms in the series becomes infinite, and *(ii)* the approximation in each interval is continuous in time and can be obtained with the desired accuracy corresponding to the desired number of terms. For more details on

Adomian's decomposition method the reader is referred to Adomian, (1988, 1994), Olek, (1994), and Vadasz and Olek, (1999, 2000 a, b).

The latter procedure is adopted in the computation of the solution to equations (4-9). One can easily observe that this set of equations is just a particular case of equations (6-1) with $m=2$. The set of equations (4-9) provides the following non-zero coefficients for substitution in equation (6-1) $b_{12}=1$; $b_{21}=\alpha_o$; $b_{22}=-\nu_o$; $a_{211}=-\sigma_o$; $a_{222}=-s$. Except for these coefficients all others are identically zero. Therefore, the coefficients $c_{i,n}$ in equation (6-2) take the particular form

$$c_{1,n}=c_{2,(n-1)} \qquad \text{(a)}$$

(6-4)

$$c_{2,n}=\alpha_o\, c_{1,(n-1)}-\nu_o\, c_{2,(n-1)}-\sigma_o \sum_{k=0}^{n-1}\frac{(n-1)!\;\; c_{1,k}\; c_{1,(n-k-1)}}{k!\;(n-k-1)!}-s\sum_{k=0}^{n-1}\frac{(n-1)!\;\; c_{2,k}\; c_{2,(n-k-1)}}{k!\;(n-k-1)!} \qquad \text{(b)}$$

In all computations, 15 terms were used in the series, a time interval of $\Delta t=10^{-3}$ hours, and all computations were performed up to a value of $t=t_{\max}$ .of 280 or 350 hours (see Chapter 7). All computations were carried out to double precision on an Apple Power Macintosh G3 computer and the elapsed time for each computation was ~20 seconds. A few solution results obtained by using the present method were compared with corresponding numerical results obtained by using the fifth order Runge-Kutta-Verner method (IMSL Library, 1991) of solution with an error tolerance parameter equal to 10^{-6}. In all compared cases, the results between the two methods were identical to all significant digits of the double precision computations at all times.

The method of solution for the mixed cultures was identical to the one presented for the single species case, with the only necessary modifications related to the extension from two equations to four.

CHAPTER 7

RESULTS AND DISCUSSION

7.1 Pure cultures

To realise how the original non-Hamiltonian problem relates to the Hamiltonian system described in Chapter 5 (section 5.2) the simplified version of the new classical model, equations (4-9)-(4-10), was solved by using Adomian's decomposition method as presented in Chapter 6. The solution was sought for parameters values identical to the ones used for the Hamiltonian system in Chapter 5 (section 5.2), i.e. $\sigma_o = 1$ and $\alpha_o = 2$, but in addition in this case the values of ν_o and s did not vanish. The computational results corresponding to $\sigma_o = 1$, $\alpha_o = 2$, $s = 0.03$, $\nu_o = 0.1$, $x_o = 0.5$ and $y_o = 0$ are presented in Figure **7.1a** in the time domain and in Figure **7.1b** on a phase diagram. From Figure **7.1b** it is evident that the trajectory crosses the limit cycles presented in Figure **5.1a** for the corresponding Hamiltonian system and spirals towards the non-trivial stationary point ($x_s = \alpha_o/\sigma_o = 2$; $y_s = 0$). Furthermore, it is also evident that in this case $\nu_o^2 < 4\alpha_o$ ($\nu_o^2 = 0.01$ and $4\alpha_o = 8$) reinforcing the linear stability result, which suggests that the solution approaches the stationary point via damped oscillations. In general, as long as $\nu_o > 0$ and $s\dot{x} > 0$, the solution always moves towards the stationary point if it starts within the domain embraced by the homoclinic orbit associated with the Hamiltonian system. However, even if $\nu_o > 0$, the condition $s\dot{x} < 0$, which occurs whenever ($s > 0$ and $\dot{x} < 0$) or ($s < 0$ and $\dot{x} > 0$), may cause the solution to move momentarily away from the stationary point. This may occasionally cross the homoclinic orbit associated with the Hamiltonian system and still eventually restore the trajectory back within the domain embraced by the homoclinic orbit, as the value of $\dot{x}$ changes sign

in this process. However, this result suggest the real possibility that for some values of the parameters restoring the trajectory back within the realistically feasible domain does not occur and the solution diverges, initially via physically non-acceptable negative values, and eventually towards $-\infty$. This reinforces the previous conclusion regarding the existence of a set of initial conditions and parameters that is constrained by compatibility with physically feasible results, such as population saturation levels, etc.

For purposes of comparison of the simplified new model with experiments, one would be interested, ideally, to use experimental results obtained over a large period of time (300 to 600 hours) with a sufficient resolution as to capture all the substantial qualitative as well as quantitative features of the growth. Then, one could use the computational solution of the problem (4-9) – (4-10) in order to establish the values of the parameters in equations (4-9) that correspond to the performed experiment. To accomplish such a task one needs to formulate and analyse the corresponding inverse problem. In addition, it turns out that the formulation of the inverse problem dictates a particular experimental strategy that allows an accurate evaluation of these parameters, such as the need to capture three consecutive readings for each available data point in the experimental results. The latter is needed in order to approximate accurately the second derivative in equation (4-7). As the inverse problem was not yet formulated, nor analysed there is no systematic way to evaluate the parameters in equation (4-7), or its equivalent form (4-9). To make things worse, there is still no way of accurately specifying the derivative initial condition $y(0) = \dot{x}(0) = y_o$. The latter may be expected to be linked to the "*inertia*" of the cell growth in the previous environment, prior to being inoculated and grown in the actual environment. Therefore, at this stage the less systematic approach was adopted to determine the model's coefficients by trial and error. This process is extremely tedious, however for the purposes of the present demonstration it is sufficient for indicating a very

good match between the proposed new model and the experimental results, even for its simplified version. In this trial and error process the initial condition were treated for $y(0)=\dot{x}(0)=y_o$ as an unknown parameter to be determined. Based on the previous analysis one needs to reiterate that when the term $\left[s\dot{x}+\nu_o\right]$ in equation (4-7) becomes negative it may drive the solution to diverge (negative damping), i.e. by crossing the homoclinic orbit without the ability to recover back into the domain embraced by that orbit, lossing its stability. This fact and the consequent conditions that constrain the possible range of feasible parameter values make the trial and error process manageable.

The computational results corresponding to initial conditions: $x_o=1$ Mcell/ml and $y_o=0$ Mcell/(ml·h), are presented in Figure **7.2a** and compared with the experimental data (Figure **7.2b**) for growth of the T206 strain of *Saccharomyces cerevisiae* in a nutrient limited medium (5% grape juice).

The computational results obtained for the following set of parameters: $\sigma_o=0.0225$ (Mcell/ml)$^{-1}$h^{-2}, $\nu_o=0.01$ h^{-1}, $\alpha_o=0.0475$ h^{-2}, $s=-0.97$ (Mcell/ml)$^{-1}$, $x_o=1.46$ Mcell/ml and $y_o=0.04$ Mcell/(ml·h), are presented in Figure **7.3** and compared with the experimental data for yeast growth of the T206 strain of *Saccharomyces cerevisiae* in pure water.

It is evident from the figures that both the computational as well as the experimental results indicate a damped oscillation process that eventually tends to decay to the stationary point. The computational solutions according to the new proposed model presented in Figures **7.2a** and **7.3a** recovers very well the experimental results (Figures **7.2b** and **7.3a**) despite the simplifying assumptions in assuming a constant value of c in equation (4-3) and a small value of $|s|<<1$. From the parameter values listed above that were obtained via the trial and error process it is evident that $|s|=O(1)$, violating the

original assumption. Nevertheless, the computational results fit quite well with the experimental ones while the slight discrepancies may be associated with the violation of the latter assumption. Future work should be directed in establishing more accurate relationships for $m(x)$ and $c(x)$. The latter will allow an even better fit between the proposed model solution and experimental data. The spiralling approach of the solution towards the stationary point as observed in Figure **7.3b** is consistent with the linear stability condition for under-damping, i.e. $v_o^2 < 4\alpha_o$ ($v_o^2 = 10^{-4}$ h^{-2} and $4\alpha_o = 0.19$ h^{-2}).

In order to demonstrate the capability of the new model to capture different effects that were reported in previous growth experiments, numerous computations were performed representing solutions of the problem (4-9)-(4-10) within a wide range of parameter values. In particular, it was interesting to find out whether the model can recover the inflection point on the *"ln curve"* of the cell concentration and the "*Lag Phase*", the latter not being recovered in pure water growth for the reasons specified before (2.1). Typical computational results are presented in Figure **7.4** for $\ln(x)$ versus time, zooming into the initial time range of $0 < t < 40$ hours. It is evident from the figure that the curve is initially concave and at a later time it becomes convex, indicating the recovery of the inflection point on the *"ln curve"*. Two additional computational results corresponding to different combinations of parameters are presented in Figure **7.5**, where the "*Lag Phase*" is recovered by the proposed model. Figure **7.5a** shows the "*Lag Phase*" on a growth curve that stabilises at the stationary point via an overshooting, while in Figure **7.5b** the growth process decays to the stationary point via damped oscillations.

In addition, it may be observed from the proposed model represented by equation (4-3) that when the virtual mass vanishes, i.e. $m = 0$, the new model reduces to the special case of the Logistic Growth Model (LGM). An attempt was made to check if the computational results based on the new model could recover the LGM solution for the

case when m is not identically zero or when $m << 1$. The computational results representing the solution of the new model corresponding to the latter case are presented in Figure **7.6** for initial conditions compatible with the LGM solution for yeast growth presented by Pearl, (1927) and compared to experimental data based on Carlson, (1913). The parameter values and initial conditions used in these computations are: $\sigma_o = 4.5\,\mathrm{h}^{-2}$, $\nu_o = 8\,\mathrm{h}^{-1}$, $\alpha_o = 4.5\,\mathrm{h}^{-2}$, $s = 0.02$, $(x_o/\delta) = 0.0145$, $y_o = 0$. From Figure **7.6a** it is evident that a smooth logistic curve is recovered, identical to the one recovered by Pearl, (1927) when applying the LGM solution, the latter being presented in Figure **7.7**. Figure **7.6a** shows the resulting logistic curve, which fits well with the experimental data, while Figure **7.6b** shows that there is no inflection point on the *"ln curve"* of the cell concentration. Therefore, it may be concluded that in addition to recovering a wide spectrum of qualitative features that were identified in different experiments, such as overshooting and oscillations, a *"Lag Phase"* and an inflection point in the *"ln curve"* of the population size, the new model was shown to recover the Logistic Growth Curve as a special case.

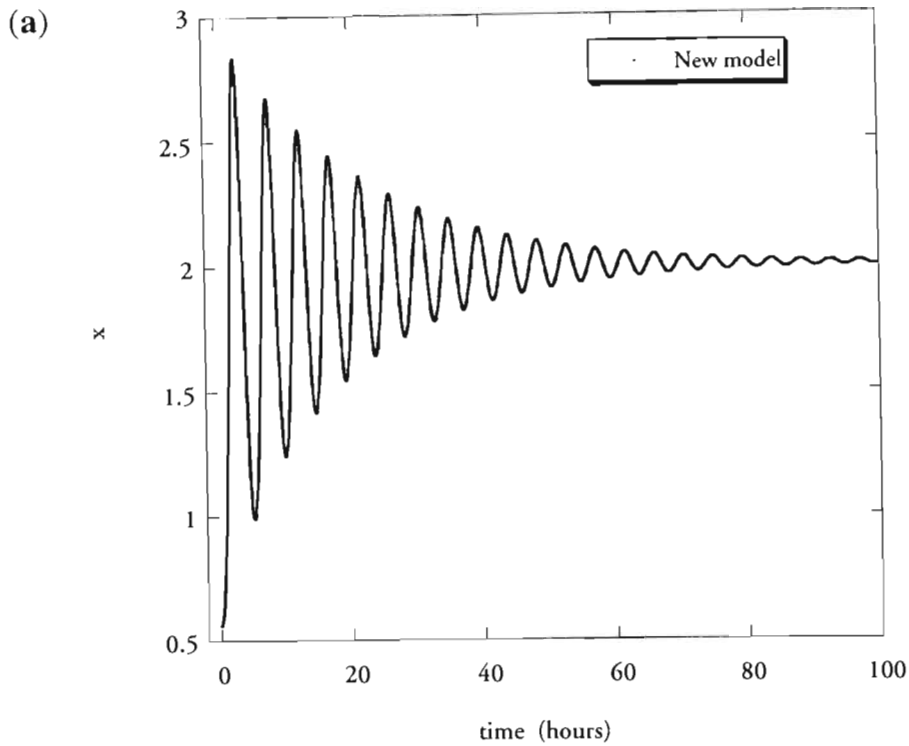

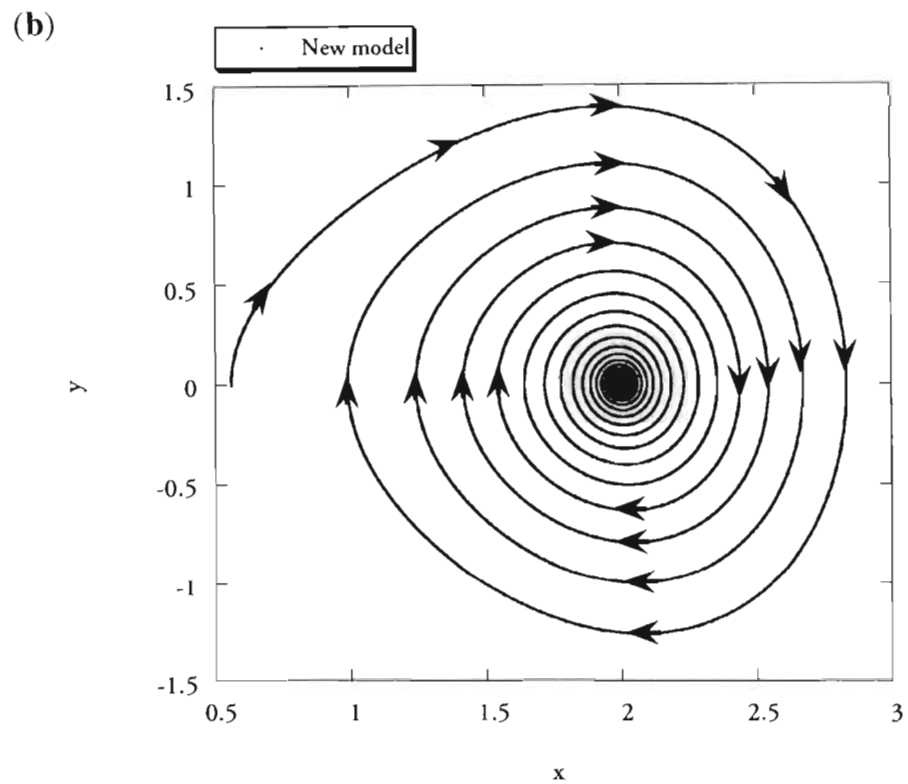

Figure **7.1** (a) Computational solution of equations (4-9)-(4-10) based on the new model. (b) The phase diagram corresponding to the computational solution of the new model. The model solution corresponds to the following data: σ_0=1, α_0=2, v_0=0.1, s=0.03, x_0=0.5, y_0=0.

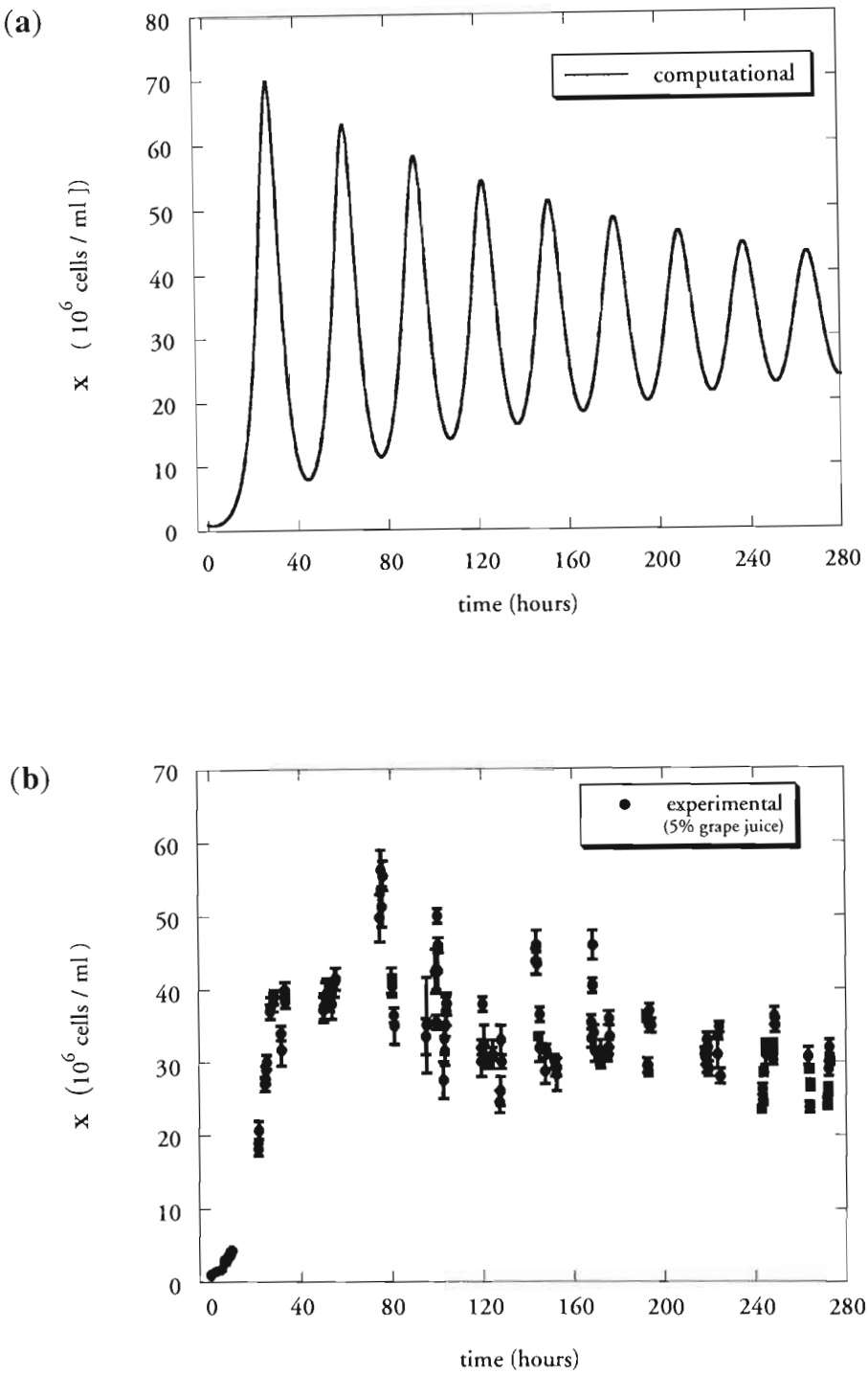

Figure **7.2** Computational solution (a) of equations (4-9)-(4-10) based on the proposed new model, in comparison with the new experimental results (b).
The model solution corresponds to the following initial conditions: x_0 =1Mcells/ml and y_0 =0Mcells/(ml

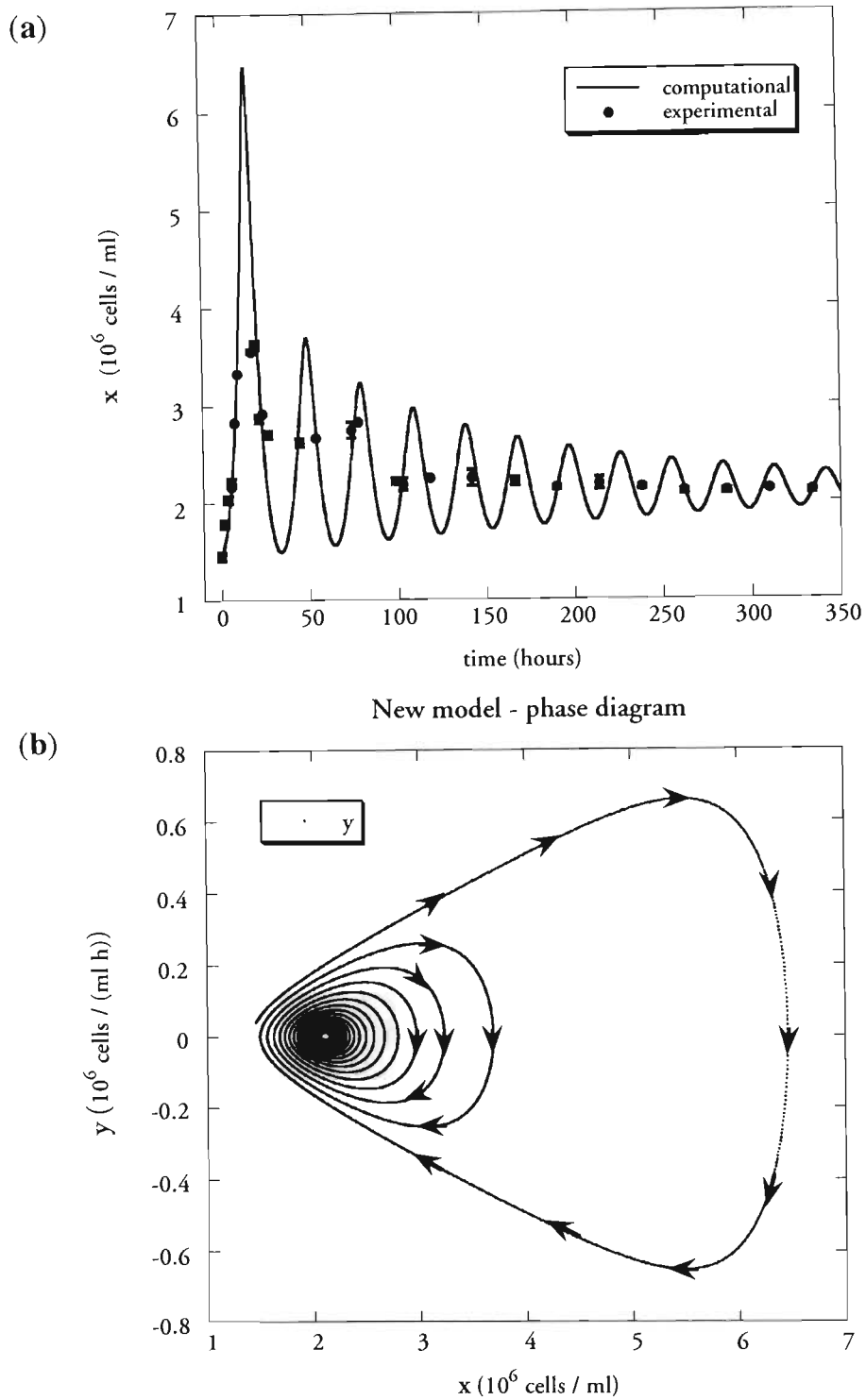

Figure **7.3** (a) Computational solution (—computational) of equations (4-9)-(4-10) based on the new model, in comparison with the new experimental results for yeast cells (• experimental). (b) The phase diagram corresponding to the computational solution of the newl model.

The model solution corresponds to the following data: s_0=0.0225 (Mcell/ml)$^{-1}$h^{-2}, n_0=0.01h^{-1}, a_0=0.0475h^{-2} s=-0.97(Mcell/ml)$^{-1}$, x_0=1.46Mcell/ml and y_0=0.04Mcell/(ml n).

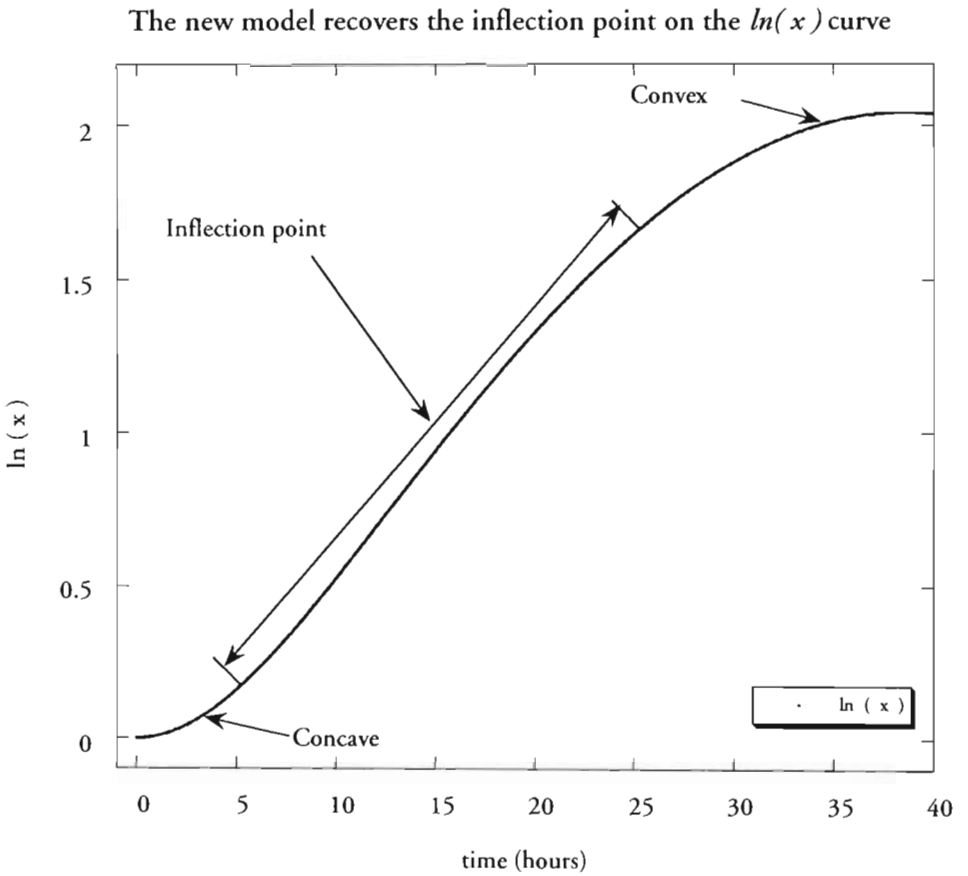

Figure **7.4** Computational results of the solution of equations (4-9)-(4-10) based on the new model indicating the recovery of an inflection point on the *ln of the cell concentration curve*.

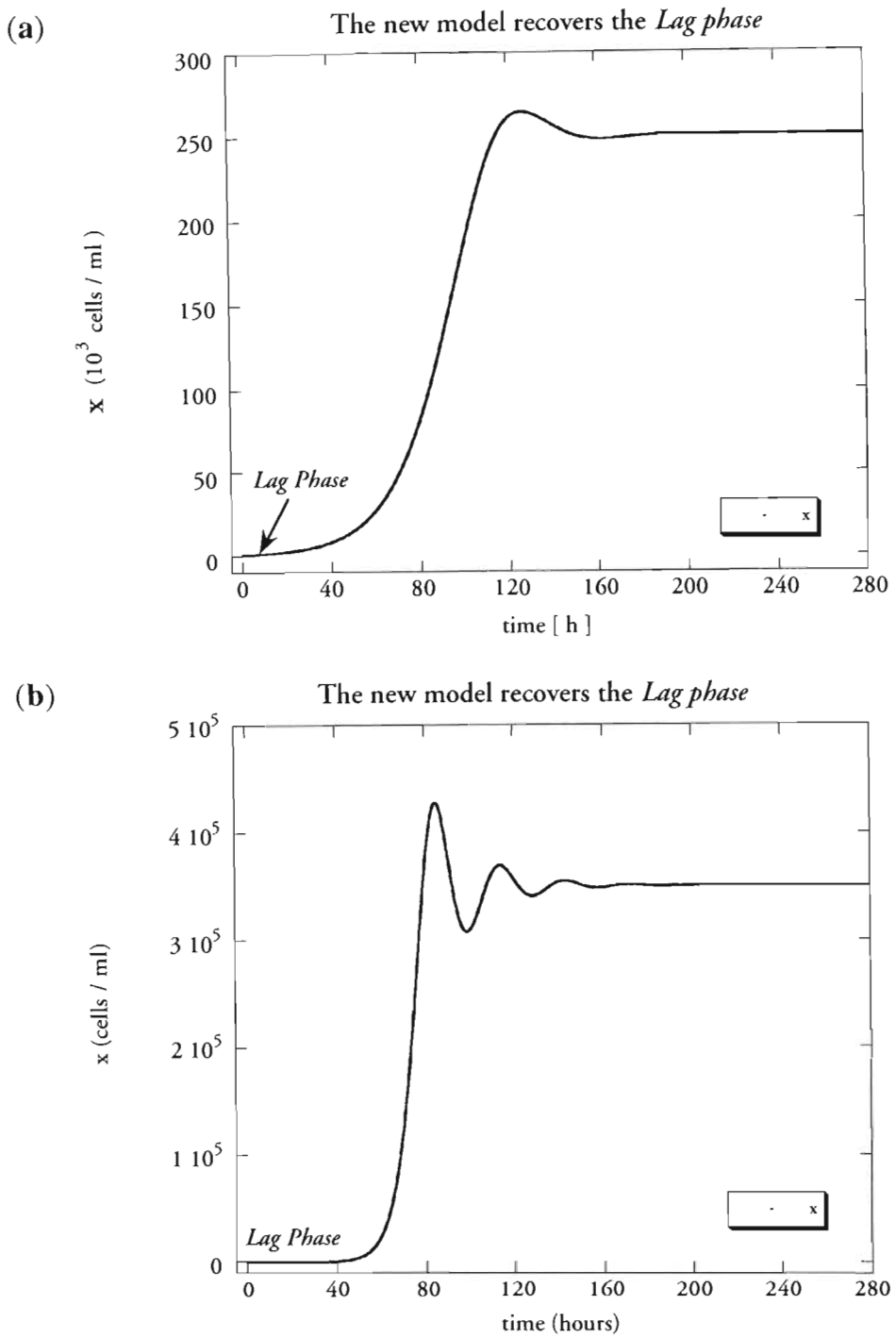

Figure **7.5** Computational results of the solution of equations (4-9)-(4-10) based on the new model indicating the recovery a *"Lag phase"*. (a) The solution stabilises to the stationary point via an overshooting. (b) The solution stabilises to the stationary point via damped oscillations.

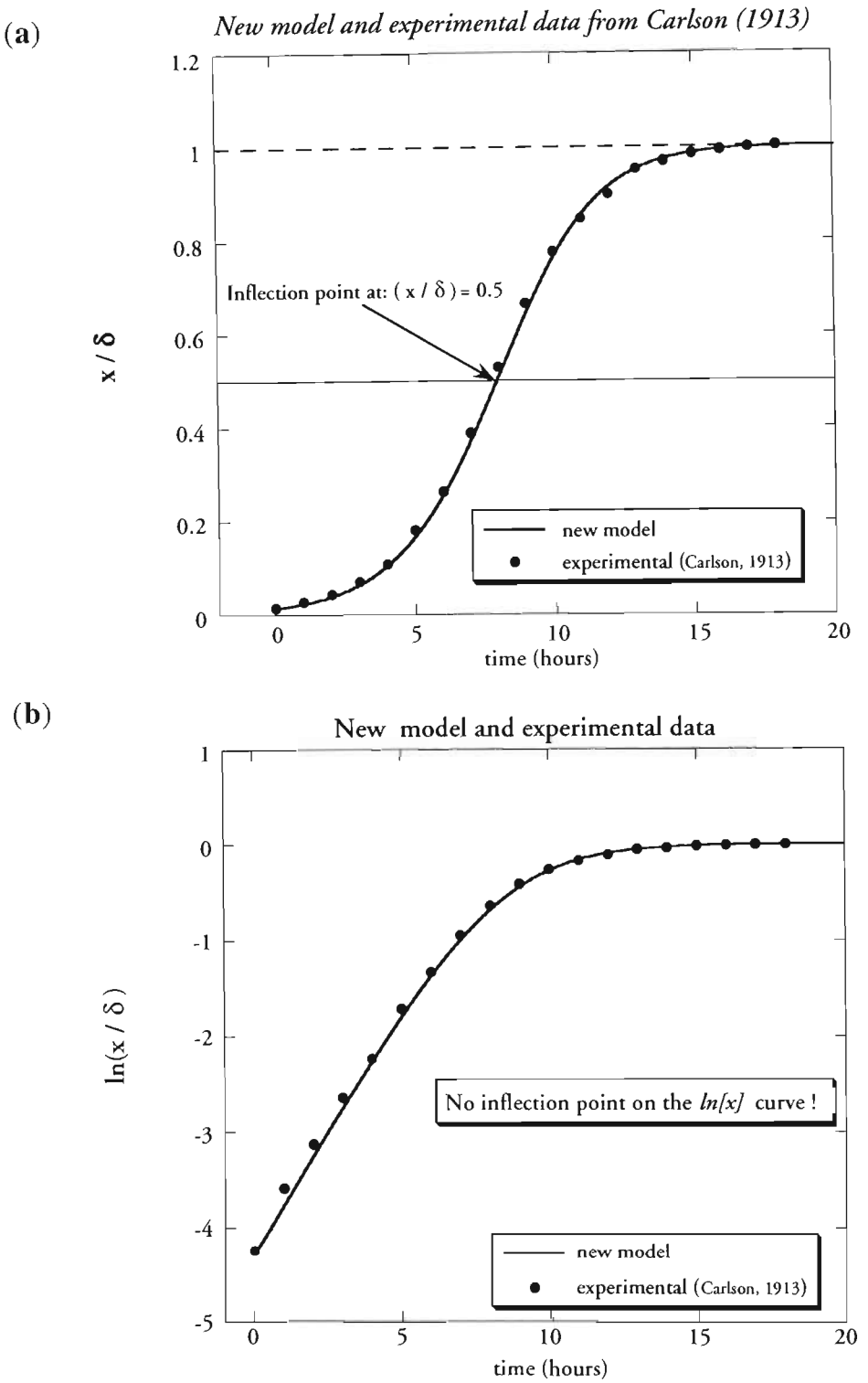

Figure **7.6** Computational results of the solution of equations (4-9)-(4-10) based on the new model indicating the recovery of the Logistic Growth Model solution as a special case, compared with the experimental data from Carlson, (1913). (a) Cell concentration (normalized and dimensionless) versus time. (b) The *ln curve* of the cell concentration versus time.

The model solution corresponds to the following data: s_0=4.5h^{-2}, n_0=8h-1, a_0=4.5h^{-2}, s=0.002, (x/d)=0.0145

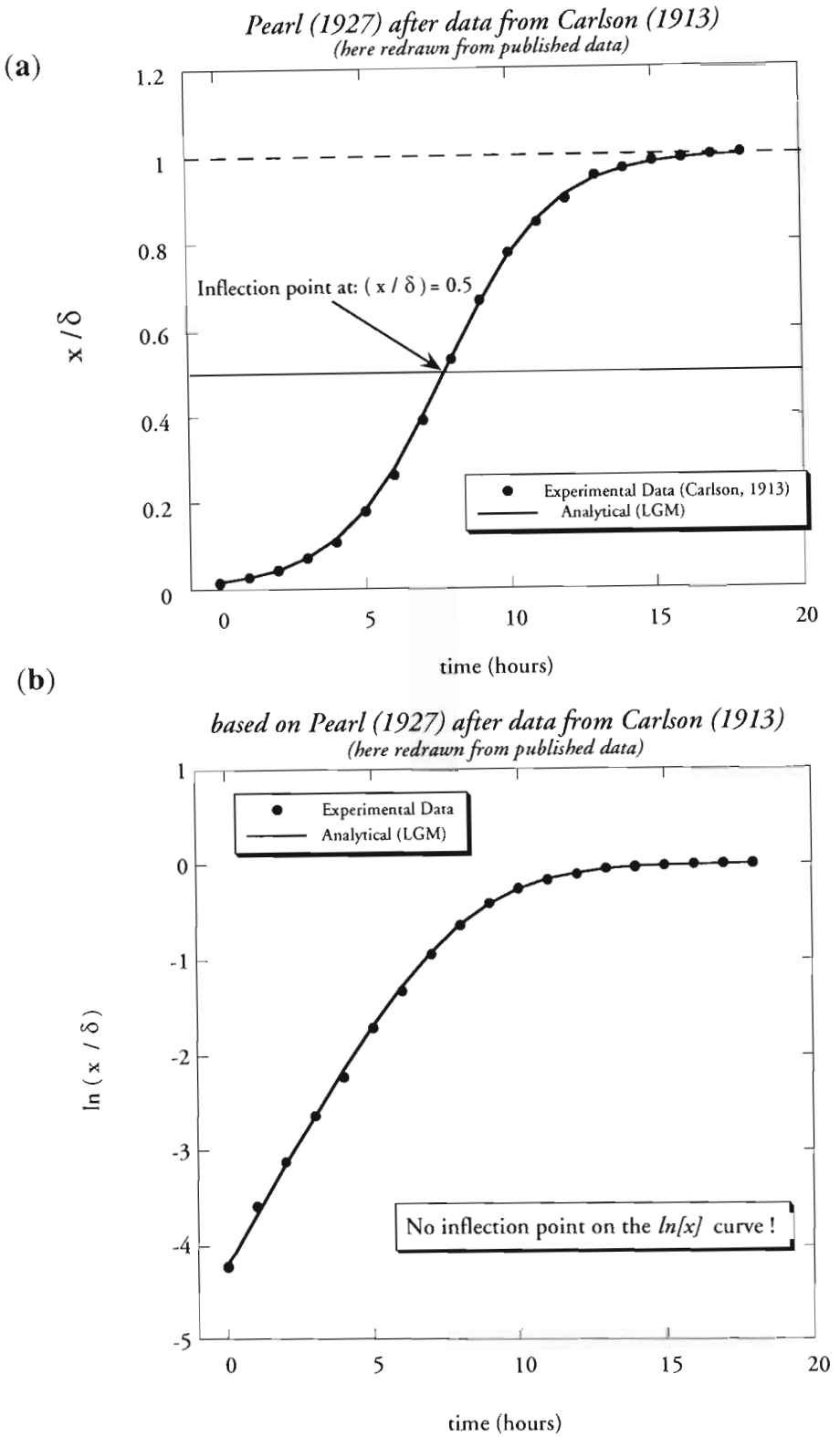

Figure **7.7** Comparison of the LGM solution with experimental results for yeast cells based on Pearl, (1927) after data from Carlson, (1913), (redrawn here using the tabulated data from Pearl, 1927). (a) Cell concentration (normalized and dimensionless) versus time. (b) The *ln curve* of the cell concentration versus time.

7.2 Mixed cultures

The presentation of the computational results from the simplified version of the new model is divided in two parts. The first part deals with parameter values unrelated to the experimental data, in order to demonstrate some qualitatively different type of results. In the second part, an attempt was made to fit at least the stationary points to the ones obtained experimentally.

The different qualitative features revealed by the computational solution of the new model of competition between two species are presented in Figures **7.8** to **7.12**. An example of a solution of coexistence between the two species is presented in Figure **7.8** showing also damped oscillations which are more pronounced in Figure **7.8b**, representing the curve of the total population size. Figure **7.9** shows an example of extinction of one of the species while the surviving species attains a steady state via damped oscillations. The extinction of one species is presented in Figure **7.10** as well, however in this case the surviving species grows and reaches steady state monotonically. Figure **7.11** presents a similar example of extinction of one species while the surviving species reaches steady state via damped oscillations, however, in this case the growth phase of the surviving species is linked to oscillations as well. Finally, in Figure **7.12** an example of a solution is presented where both species become extinct with positive values of their corresponding maximum specific growth rates, i.e. $\mu_1 > 0$, $\mu_2 > 0$ (or actually their corresponding values of $\alpha_1 > 0$ and $\alpha_2 > 0$).

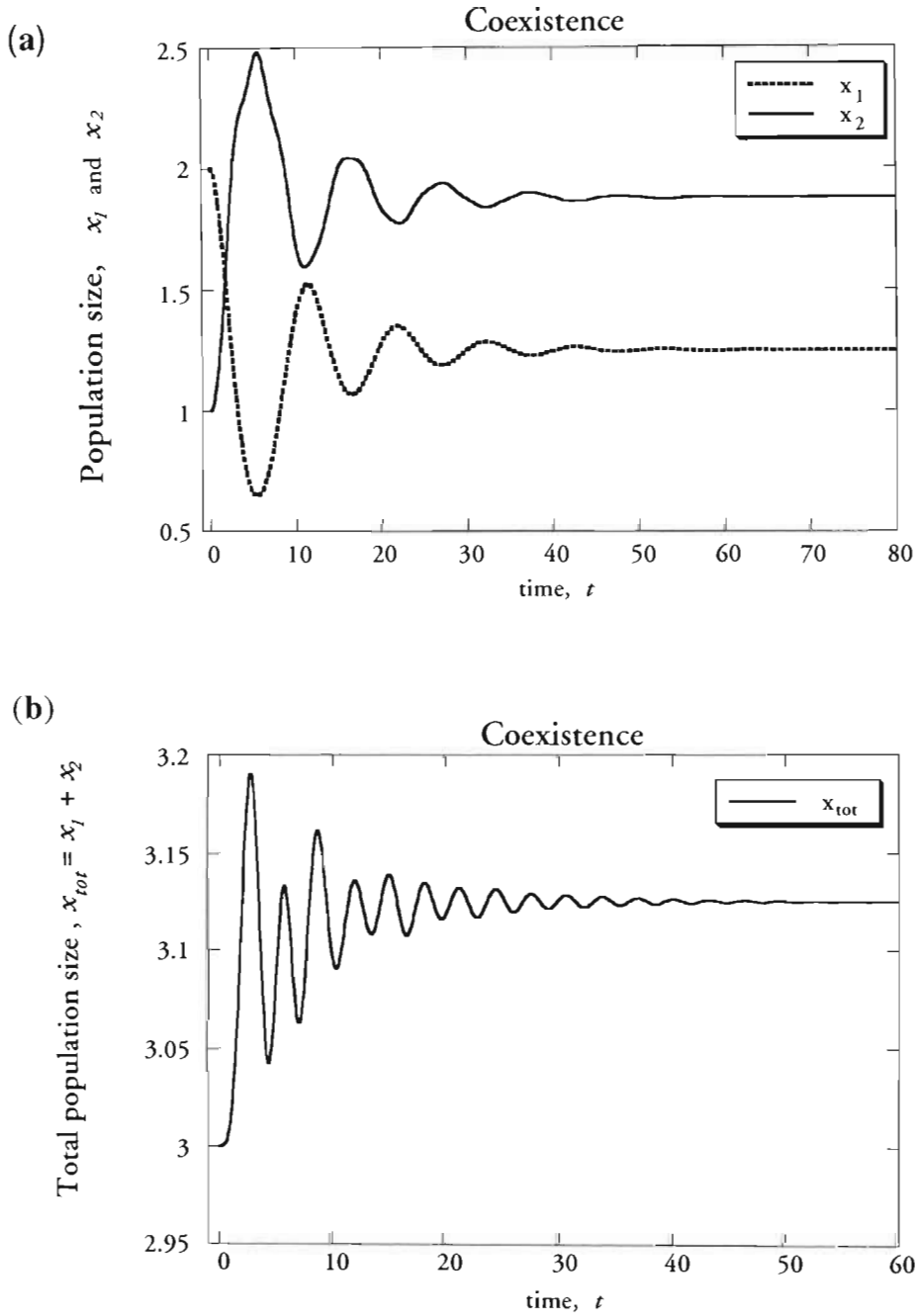

Figure **7.8** New model results for competition showing coexistence of both species and damped oscillations in their concentration.

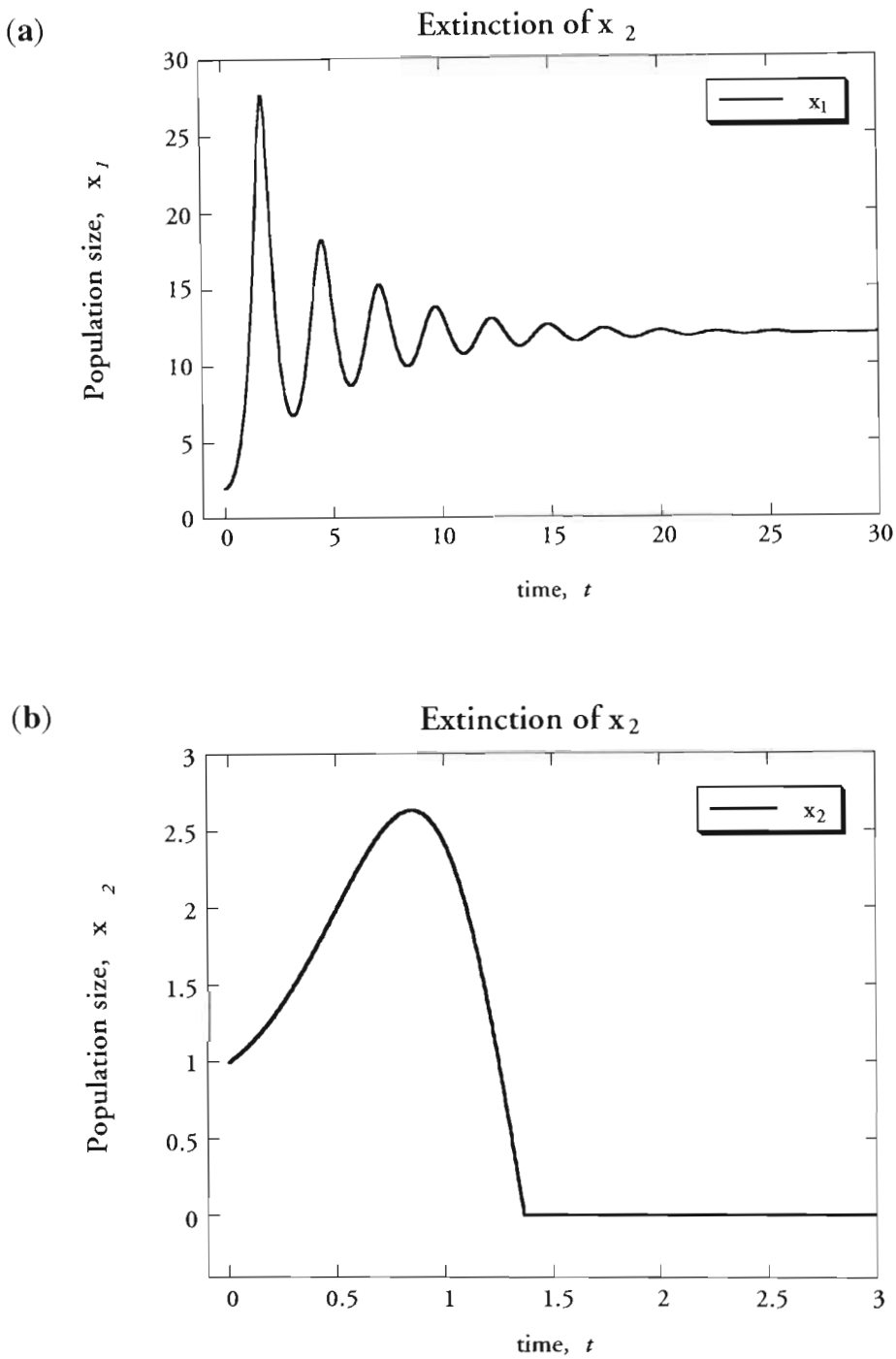

Figure **7.9** New model results for competition showing (a) damped oscillations in the concentration of the surviving species and (b) the extinction of the other species.

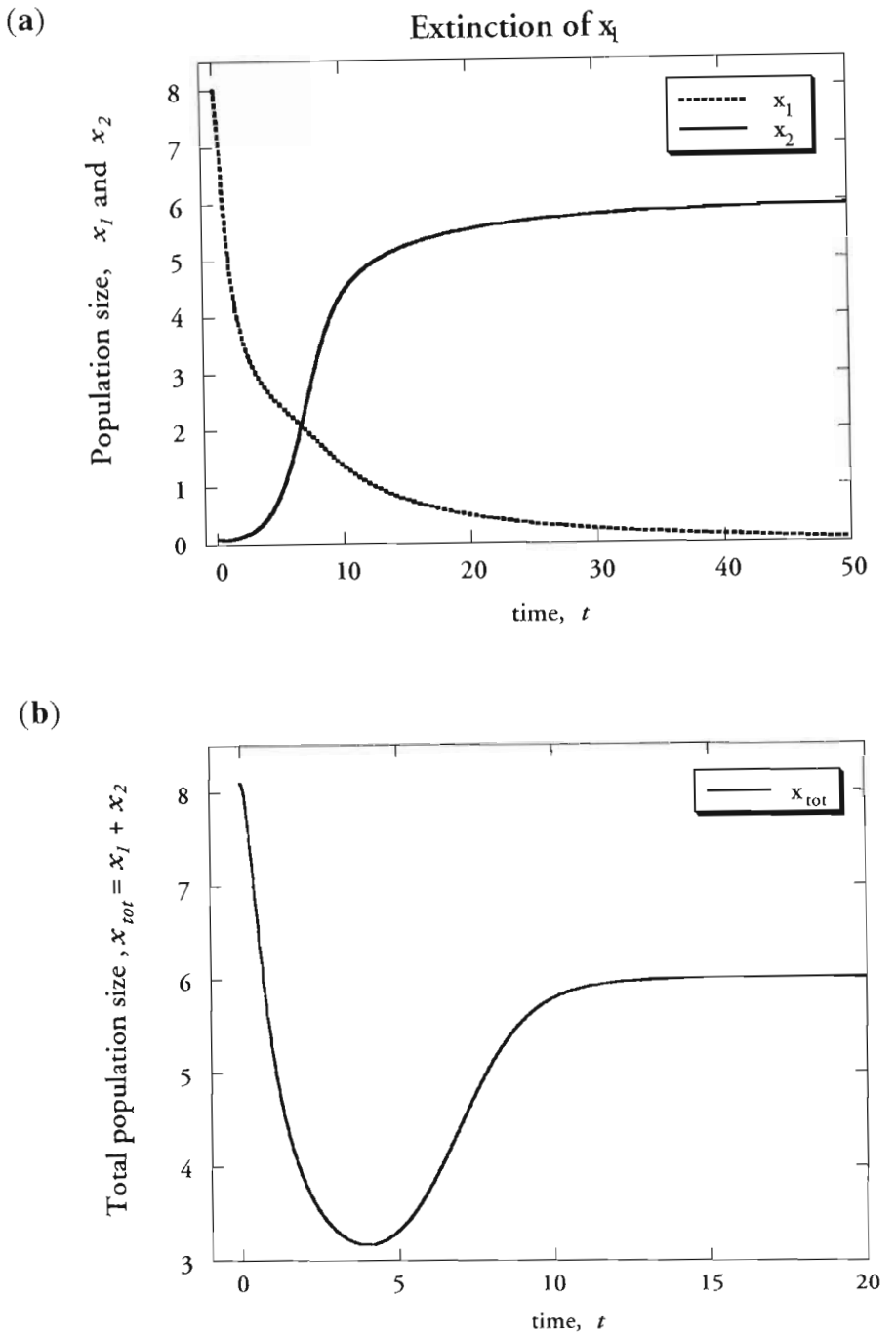

Figure **7.10** New model results for competition showing (a) the extinction of one species (x_1) and monotonic growth in the concentration of the surviving species (x_2) and (b) the concentration of both populations in the mixture.

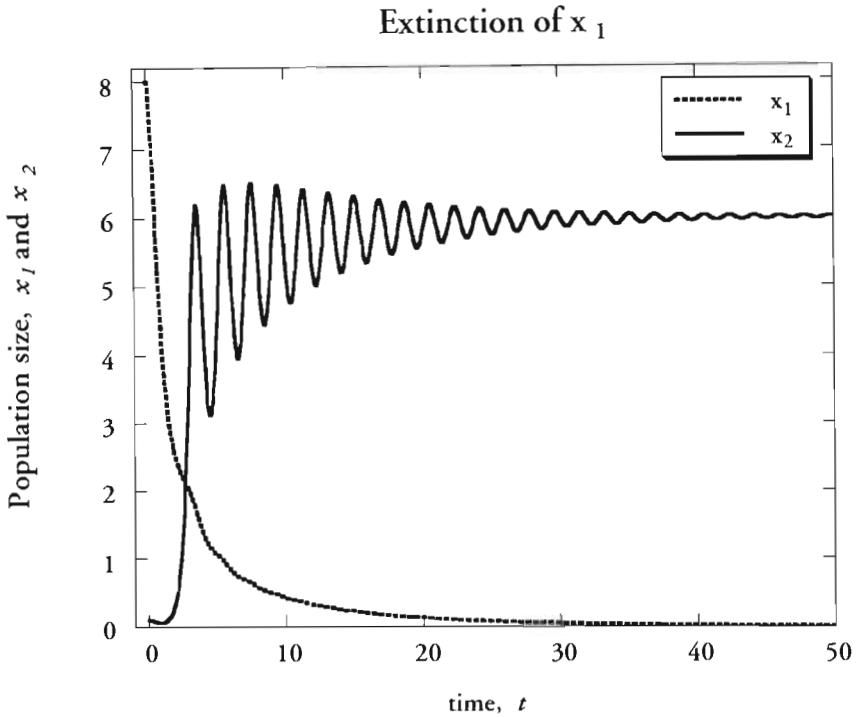

Figure **7.11** New model results for competition showing extinction of one species (x_1) and damped oscillation in the concentration of the surviving species (x_2).

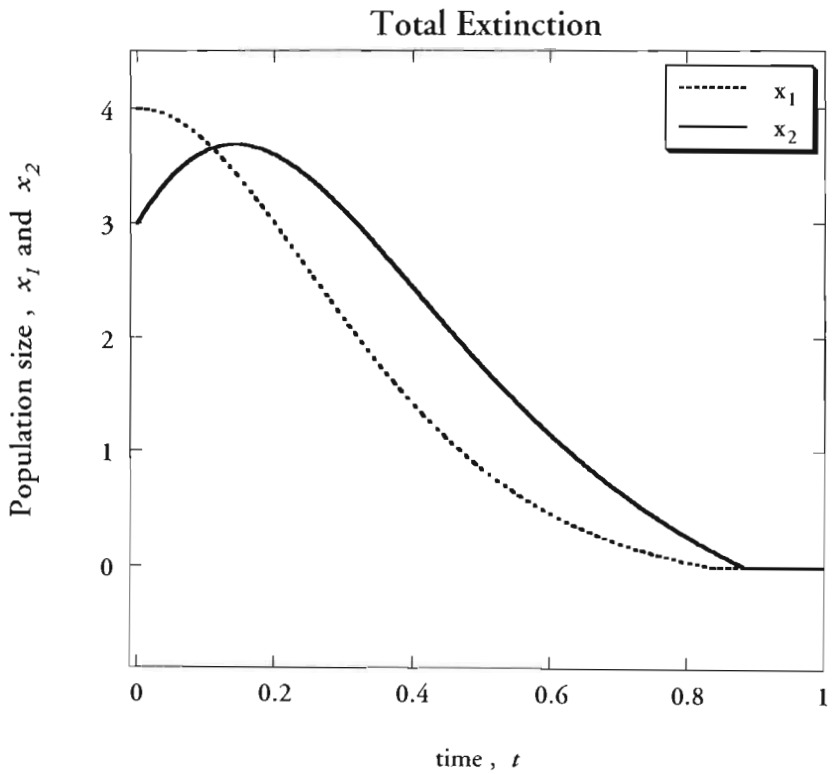

Figure **7.12** New model results for competition showing extinction of both species.

No attempt was made to fit the experimental results with the computational ones since it is futile to attempt to fit 10 parameter values and two unknown derivative initial conditions by trial and error. Nevertheless, from the experimental data it is possible to estimate the values of the stationary points and as a result to limit the trial and error process as far as reaching the neighbourhood of the stationary points is concerned. Furthermore, in order to be confident that the parameter values, which yield a computational solution that fits the experimental data, are indeed correct, one needs a much better resolution of experimental data points, at least for the total cell concentration. Therefore, the results presented here show a few computational results compared with the corresponding experimental data. For each set of experimental data one or more computational results corresponding to slightly different values of the parameters are presented.

The computational results related to the growth of the killer-T206 (carrying index 1) and sensitive Y-217 (carrying index 2) strains of yeast in a mixed culture with initial concentrations at a ratio of 1:1 are presented in Figures **7.13** to **7.15**. The set of parameter values corresponding to Figure **7.13** are $\nu_1 = 0.04\ \mathrm{h}^{-1}$, $\nu_2 = 0.002\ \mathrm{h}^{-1}$, $s_1 = -0.5\ (\mathrm{Mcell/ml})^{-1}$, $s_2 = -0.4\ (\mathrm{Mcell/ml})^{-1}$, $\alpha_1 = 0.2\ \mathrm{h}^{-2}$, $\alpha_2 = 0.264\ \mathrm{h}^{-2}$, $\eta_{11} = 0.1\ (\mathrm{MCell/ml})^{-1}\mathrm{h}^{-2}$, $\eta_{12} = 0.04115\ (\mathrm{MCell/ml})^{-1}\mathrm{h}^{-2}$, $\eta_{21} = 0.1\ \ (\mathrm{MCell/ml})^{-1}\mathrm{h}^{-2}$, $\eta_{22} = 0.08\ (\mathrm{MCell/ml})^{-1}\mathrm{h}^{-2}$, and the initial conditions are $x_1(0) = x_2(0) = 0.5625$ Mcell/ml and $\dot{x}_1(0) = \dot{x}_2(0) = 0$. Somewhat different computational results for the same set of experimental data are presented in Figure **7.14** corresponding to slightly less damping than in Figure **7.13** with the following parameter values $\nu_1 = 0.02\ \mathrm{h}^{-1}$, $\nu_2 = 0.002\ \mathrm{h}^{-1}$, $s_1 = -0.3\ (\mathrm{Mcell/ml})^{-1}$, $s_2 = -0.4\ (\mathrm{Mcell/ml})^{-1}$, $\alpha_1 = 0.2\ \mathrm{h}^{-2}$, $\alpha_2 = 0.264\ \mathrm{h}^{-2}$, $\eta_{11} = 0.1\ (\mathrm{MCell/ml})^{-1}\mathrm{h}^{-2}$, $\eta_{12} = 0.04115\ \ (\mathrm{MCell/ml})^{-1}\mathrm{h}^{-2}$, $\eta_{21} = 0.1$

$(\text{MCell/ml})^{-1}\text{h}^{-2}$, $\eta_{22} = 0.08\,(\text{MCell/ml})^{-1}\text{h}^{-2}$ and the same initial conditions, i.e. $x_1(0) = x_2(0) = 0.5625$ Mcell/ml and $\dot{x}_1(0) = \dot{x}_2(0) = 0$. A completely different set of parameters was used for the computational results presented in Figure **7.15** and compared to the same experimental data. The parameter values used in Figure **7.15** are $\nu_1 = 0.02\,\text{h}^{-1}$, $\nu_2 = 0.002\,\text{h}^{-1}$, $s_1 = -0.2\,(\text{Mcell/ml})^{-1}$, $s_2 = -0.35\,(\text{Mcell/ml})^{-1}$, $\alpha_1 = 0.03593\,\text{h}^{-2}$, $\alpha_2 = 0.528\,\text{h}^{-2}$, $\eta_{11} = 0.0179629\,(\text{MCell/ml})^{-1}\text{h}^{-2}$, $\eta_{12} = 0.0072394\,(\text{MCell/ml})^{-1}\text{h}^{-2}$, $\eta_{21} = 0.02\,(\text{MCell/ml})^{-1}\text{h}^{-2}$, $\eta_{22} = 0.016\,(\text{MCell/ml})^{-1}\text{h}^{-2}$ and the same initial conditions $x_1(0) = x_2(0) = 0.5625$ Mcell/ml and $\dot{x}_1(0) = \dot{x}_2(0) = 0$. The results presented in all figures compare well with the experimental data, certainly in the light of not attempting to undergo an extremely tedious process of trial and error for curve fitting.

The computational results related to the growth of the two sensitive strains of yeast Y-217 (carrying index 1) and VIN7 (carrying index 2) in a mixed culture with initial concentrations at a ratio of 1:1 are presented in Figures **7.16** and **7.17**. The set of parameter values corresponding to Figure **7.16** are $\nu_1 = 0.008\,\text{h}^{-1}$, $\nu_2 = 0.02\,\text{h}^{-1}$, $s_1 = -0.2\,(\text{Mcell/ml})^{-1}$, $s_2 = -0.35\,(\text{Mcell/ml})^{-1}$, $\alpha_1 = 0.028\,\text{h}^{-2}$, $\alpha_2 = 0.04\,\text{h}^{-2}$, $\eta_{11} = 0.018$ $(\text{MCell/ml})^{-1}\text{h}^{-2}$, $\eta_{12} = 0.007\,(\text{MCell/ml})^{-1}\text{h}^{-2}$, $\eta_{21} = 0.02\,(\text{MCell/ml})^{-1}\text{h}^{-2}$, $\eta_{22} = 0.016$ $(\text{MCell/ml})^{-1}\text{h}^{-2}$, and the initial conditions are $x_1(0) = x_2(0) = 0.515$ Mcell/ml and $\dot{x}_1(0) = \dot{x}_2(0) = 0$. A somewhat different set of parameters was used for the computational results presented in Figure **7.17**. Their values are $\nu_1 = 0.014\,\text{h}^{-1}$, $\nu_2 = 0.02\,\text{h}^{-1}$, $s_1 = -0.2\,(\text{Mcell/ml})^{-1}$, $s_2 = -0.35\,(\text{Mcell/ml})^{-1}$, $\alpha_1 = 0.07\,\text{h}^{-2}$, $\alpha_2 = 0.04\,\text{h}^{-2}$, $\eta_{11} = 0.045$ $(\text{MCell/ml})^{-1}\text{h}^{-2}$, $\eta_{12} = 0.0175\,(\text{MCell/ml})^{-1}\text{h}^{-2}$, $\eta_{21} = 0.02\,(\text{MCell/ml})^{-1}\text{h}^{-2}$, $\eta_{22} = 0.016$ $(\text{MCell/ml})^{-1}\text{h}^{-2}$, and the initial conditions are $x_1(0) = x_2(0) = 0.515$ Mcell/ml and $\dot{x}_1(0) = \dot{x}_2(0) = 0$. In this case of sensitive versus sensitive competition the results also

compare not badly with the experimental data given the lack of a substantial (or systematic) effort for curve fitting.

In all considered cases of mixed cultures with initial concentrations at a ratio of 1:1 both the experimental as well as the computational results recovered a mode of coexistence of both species.

The experimental results corresponding to the growth of two strains of yeast in mixed culture with initial concentrations at a ratio of 1:100 showed that one species survives while the other becomes extinct. The model results presented generally in Figures **7.9** and **7.10** recovered the possibility of extinction as well.

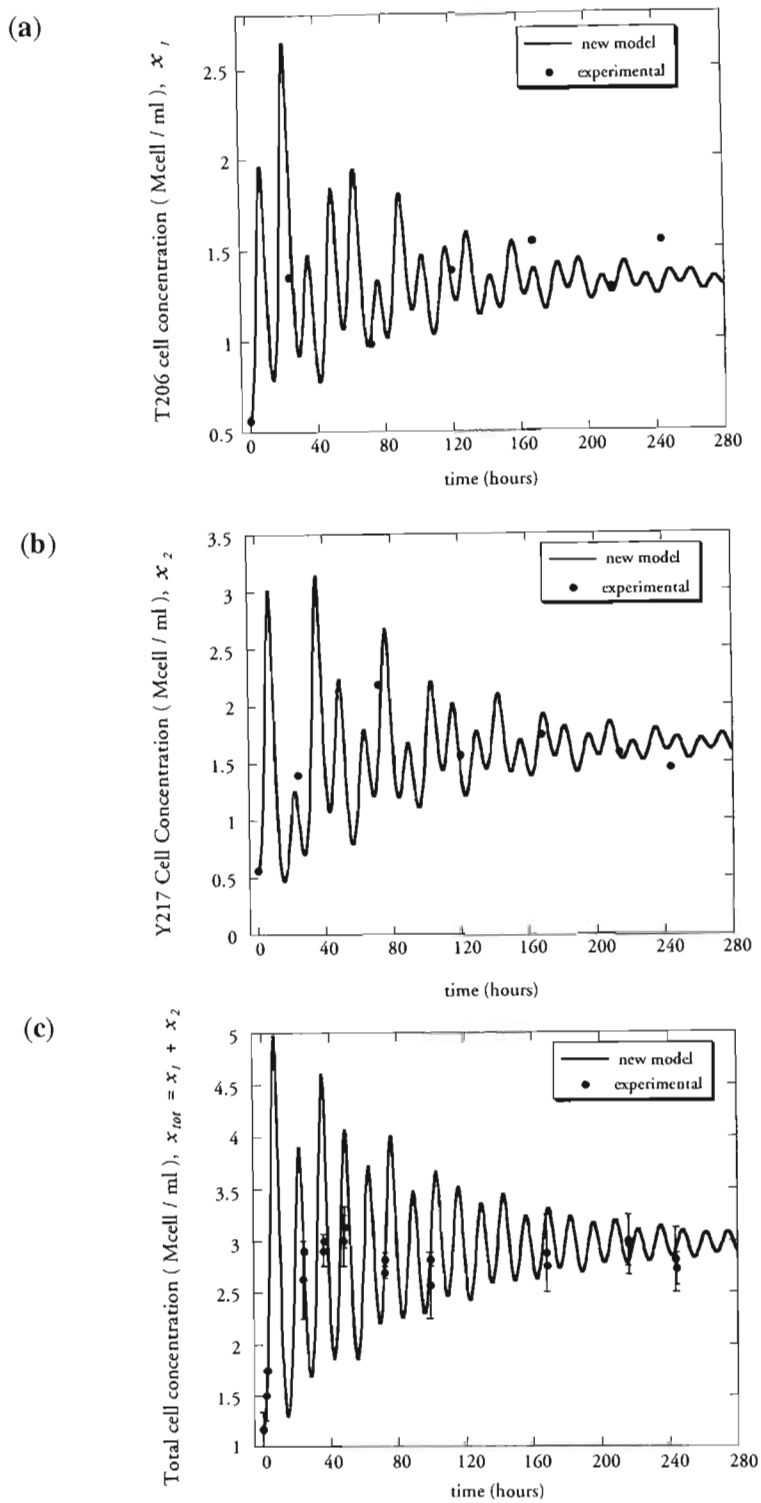

Figure **7.13** Computational results of the new model compared with experimental data for a mixed culture of killer-T206 and sensitive-Y217 strains of yeast. The parameter values are listed in the text.

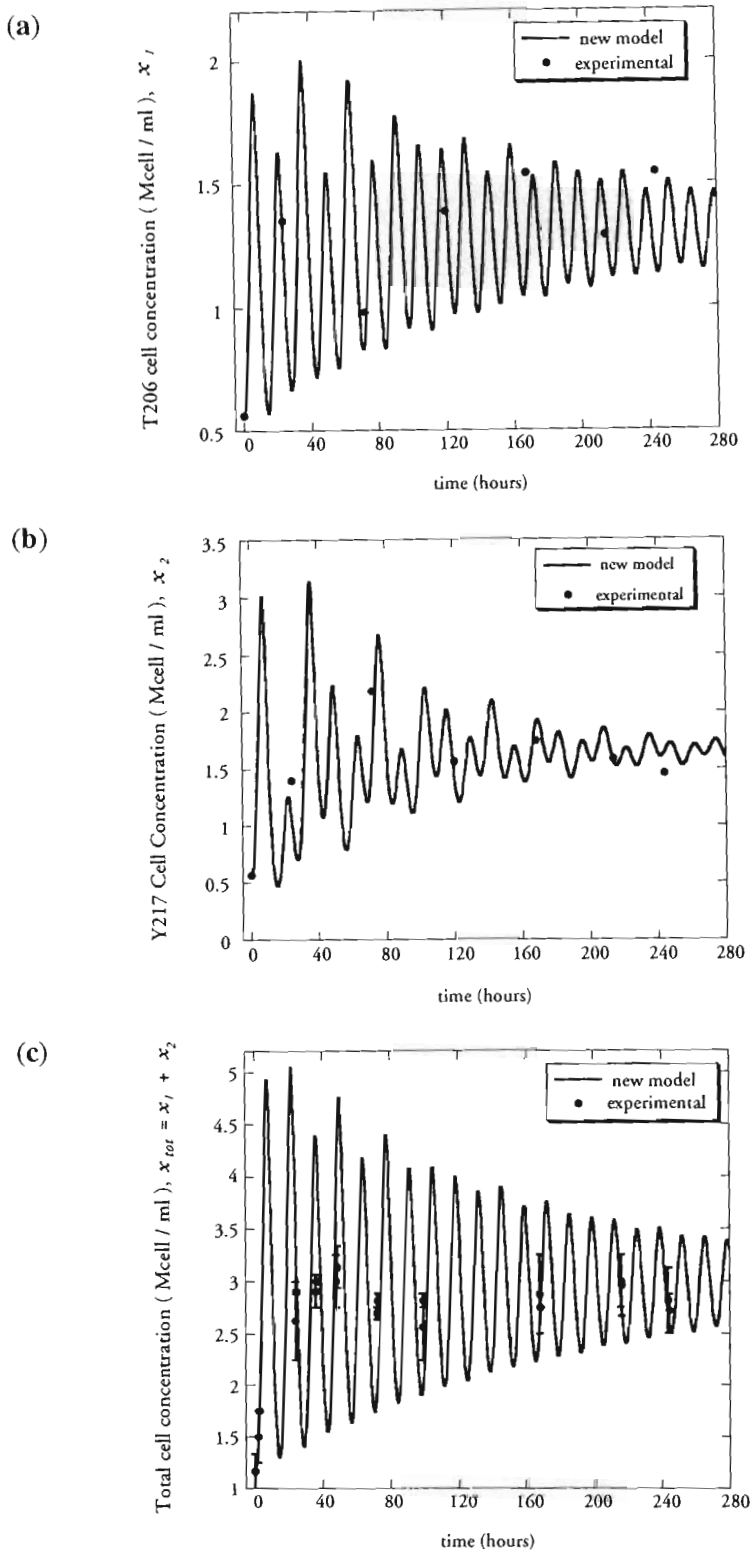

Figure **7.14** Computational results of the new model compared with experimental data for a mixed culture of killer-T206 and sensitive-Y217 strains of yeast. The parameter values are listed in the text.

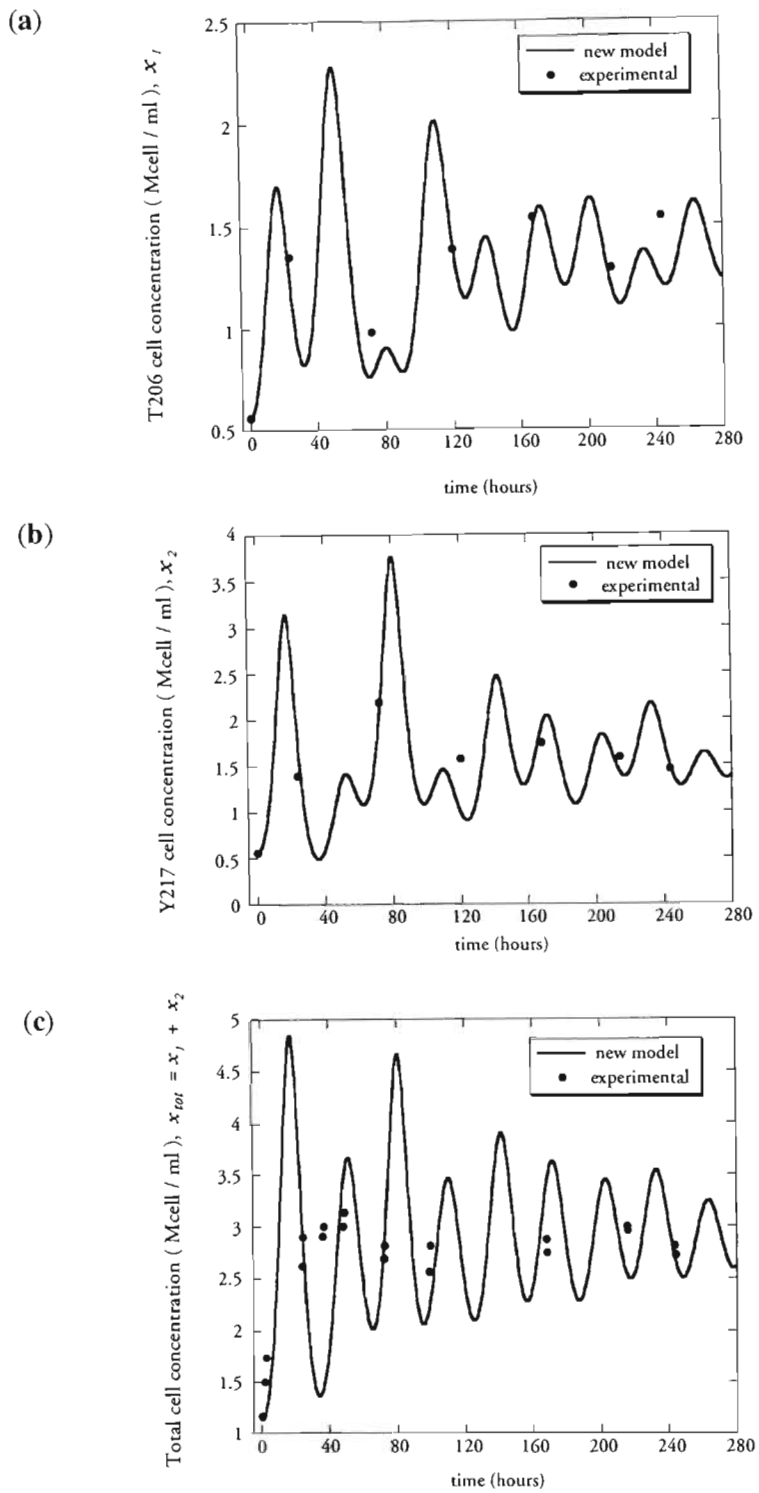

Figure **7.15** Computational results of the new model compared with experimental data for a mixed culture of killer-T206 and sensitive-Y217 strains of yeast. The parameter values are listed in the text.

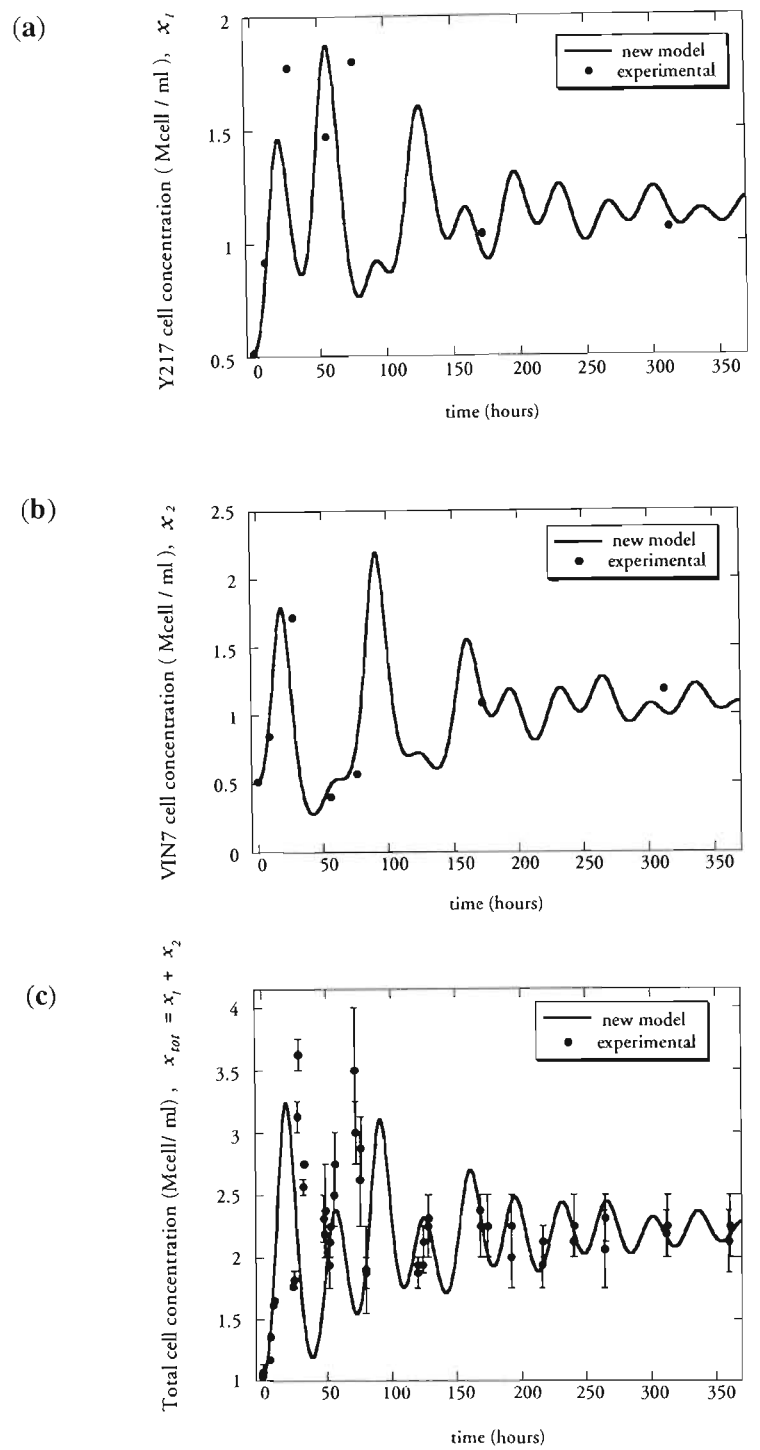

Figure **7.16** Computational results of the new model compared with experimental data for a mixed culture of two sensitive strains of yeast Y217 and VIN7. The parameter values are listed in the text.

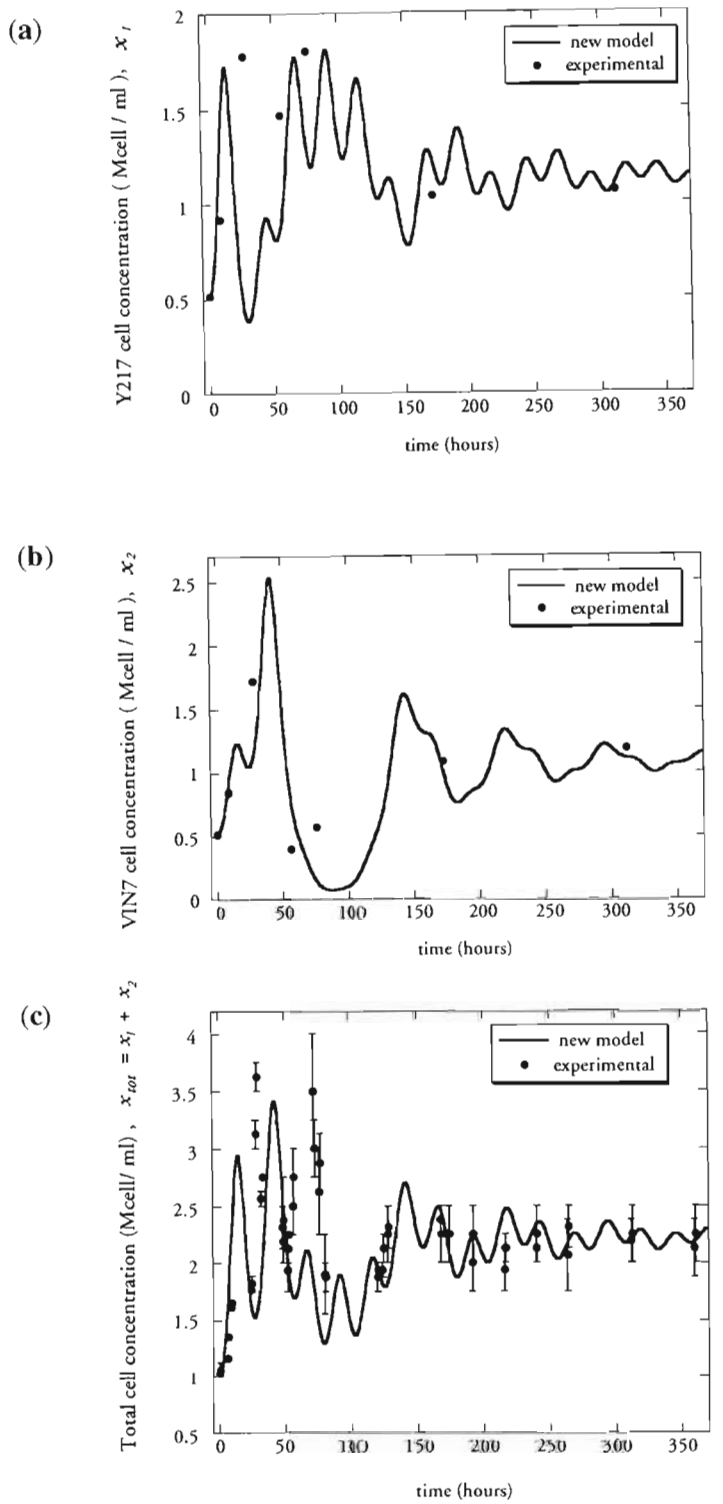

Figure **7.17** Computational results of the new model compared with experimental data for a mixed culture of two sensitive strains of yeast Y217 and VIN7. The parameter values are listed in the text.

CHAPTER 8

CONCLUSIONS

A new model that includes the complete cell growth dynamics was presented and showed to recover both qualitatively as well as quantitatively a wide variety of features that were captured experimentally from new experimental results of batch fermenting yeast in a limited nutrient media (5% grape juice and pure water). Both the experiments and the model results show that the growth of *Saccharomyces cerevisiae* strains, such as the killer T206 strain, in pure and mixed cultures is associated with damped oscillations. The proposed model also recovers effects that are frequently encountered in experiments, such as a "*Lag Phase*" as well as an inflection point in the "*ln curve*" of the cell concentration. The model also recovers the Logistic Growth Curve as a special case. The computational results presented were obtained for a simplified version of the proposed new model due to obvious reasons that were discussed. It is anticipated that further studies will reveal more accurate functional forms of the *"virtual mass"* as well as the *"damping coefficient"* a result that will enhance the accuracy as well as the ability of the proposed new model to recover a complete variety of growth curves. New experimental results for growth of yeast in pure water are presented and compared with results from the proposed dynamical model indicating a very good match.

Theoretical and experimental evidence of extinction and coexistence during batch interactions of two mixed strains of *Saccharomyces cerevisiae* (section 3.3.2.6) grown in pure water is provided. The experimental results show that in the limited nutrient conditions of growth, in pure water, the killer yeast was subjected to extinction when challenging the sensitive strain at 1:100 killer: sensitive concentration ratio, 9 hours from the sensitive strain inoculation (Figures **3.36** and **3.37**). However, if the initial

concentration ratio is 1:1 (Figures **3.40** and **3.41**), both strains in the mixed cultures coexist. Substantial oscillations are associated with the growth process in the mixed cultures. A new theoretical model that was originally developed for recovering the growth of single species in isolation was extended and applied for two species competing over a common ecological niche. The solutions of the model are shown to recover all the qualitative features captured in the experiments.

REFERENCES

Adomian, G. (1988). A review of the decomposition method in applied mathematics. *J. Math. Anal. Appl.* **135**: 501-544.

Adomian, G. (1994). *Solving frontier problems in physics: the decomposition method*, Kluwer Academic Publishers, Dordrecht.

Ahmed, A., Sesti, F., Ilan, N., Shih, T.M., Sturley, S.L. and Goldstein, S.A.N. (1999). A molecular target for viral killer toxin: TOK1 potassium channels. *Cell.* **99**: 283-291.

Baranyi, J., Roberts, T.A. and McClure, P.J. (1993). A non-autonomous differential equation to model bacterial growth. *Food Microbiology.* **10**: 43-59.

Baranyi, J. and Roberts, T.A. (1994). A dynamic approach to predicting bacterial growth in food. *International Journal of Food Microbiology.* **23**: 277-294.

Baranyi, J. and Roberts, T.A. (1995). Mathematics of predictive food microbiology. *International Journal of Food Microbiology.* **26**: 199-218.

Barton, J.K., Hollander, A.D., Hopfield, J.J. and Shulman, R.G. (1982). ^{13}C Nuclear magnetic resonance study of trehalose mobilisation in yeast spores. *Journal of Bacteriology.* **151.1**: 177-185.

Binder, M., Schanz, M. and Hartig, A. (1991). Vector-mediated overexpression of catalase A in the yeast *Saccharomyces cerevisiae* induced inclusion body formation. *European Journal of Cell Biology.* **54**: 305-312.

Blumberg, A.A. (1968). Logistic growth rate function. *J. Theoretical Biology.* **21**: 42-44.

Boiteaux, A. and Hess, B. (1978). Visualization of dynamic spatial structures in glycolyzing cell-free extracts of yeast, in *Frontiers of Biological Energetics*, P.L. Dutton, J. Leigh, A. Scarpa (Eds.). pp. 789-798. Academic Press, New York.

Boone, C., Bussey, H., Greene, D., Thomas, D.Y. and Vernet, T. (1986). Yeast killer toxin: site directed mutations implicate the precursor protein as the immunity component. *Cell.* **46**: 105-113.

Bussey, H. (1974). Yeast killer factor-induced turbidity changes in cells and sphaeroplasts of a sensitive strain. *J. Gen. Microbiol.* **82**: 171-179.

Bussey, H. (1991). K_1 killer toxin, a pore-forming protein from yeast. *Mol. Microbiol.* **5**: 2339-2343.

Carlson, T. (1913). Über Geschwindigkeit und Grösse der Hefevermerhrung in Würze, *Biochem. Ztschr.* **57**: 313-334.

Carrau, F.M., Neirotti, E and Gioia, O. (1993). Stuck wine fermentations: Effect of killer/sensitive yeast interactions. *Journal of Fermentation and Bioengineering.* **76**: 67-69.

Cheng, R.H., Caston, J.R., Wang, G.J., Gu, F., Smith, T.J., Baker, T.S., Bozarth, R.F., Trus, B.L., Cheng, N. and Wickner, R.B. (1994). Fungal virus capsids, cytoplasmic compartments for the replication of double-stranded RNA, formed as icosahedral shells of asymmetric *Gag* dimers. *J. Mol. Biol.* **244**: 255-258.

Davey, H.M., Davey, C.L., Woodward, A.M., Edmonds, A.N., Lee, A.W. and Kell, D.B. (1996). Oscillatory, stochastic and chaotic growth rate fluctuations in permittistatically controlled yeast cultures. *BioSystems* **39**: 43-61.

DeBach, P. (1966). "The Competitive Displacement and Coexistence Principles", *Ann. Rev. Ent.*, **11**: 183-212.

De la Fuente, I.M. (1999). Diversity of temporal self-organised behaviours in a biochemical system. *BioSystems*. **50**: 83-97.

Dengis, P.B., Nelissen, L.R. and Rouxhet, P.G. (1995). Mechanisms of yeast flocculation: Comparison of top and bottom-fermenting strains. *Appl. Environ. Microbiol.* **61**: 718-728.

Dix, N.J. and Christie, P. (1974). Changing sensitivity to soil fungistasis with age in *Drechslers rostrata* spores and associated permeability changes. *Transactions of the British Mycological Society*. **62**: 527-535.

Dix, N.J. and Webster, J. (1995). *Fungal Ecology*, Chapman & Hall, London, p.100.

Edelstein-Keshet, L. (1988). *Mathematical models in biology*, Random House, New York.

Fink, G.R. and Styles, C.A. (1972). Curing of a killer factor in *Saccharomyces cerevisiae*. *Proceeding of the National Academy of Science of the USA*. **69**: 2846-2849.

Franken, B.D., Ariatti, M., Pretorius, I.S. and Gupthar, A.S. (1998). Genetic and fermentation properties of the K_2 killer yeast, *Saccharomyces cerevisiae* T206. Antonie *van Leeuwenhoek*. **73**: 263-269.

Fried, H.M. and Fink, G.R. (1978). Electron microscopic heteroduplex analysis of "killer" double - stranded RNA species from yeast. *Proceeding of the National Academy of Science of the USA*. **75**: 4224-4228.

Gagiano, M., Van Dyk, D., Bauer, F.F., Lambrechts, M.G. and Pretorius, I.S. (1999). Msn1p / Mss10p, Mss11p and Muc1p / Flo11p are part of a signal transduction pathway downstream of Mep2p regulating invasive growth and pseudohyphal differentiation in *Saccharomyces cerevisiae*. *Mol Microbiol*. **31 (1)**: 103-116.

Gause, G.F. (1934). *The struggle for existence*, Hafner, New York (reprinted 1964).

Gupthar, A.S. (1987). Construction of a series of *Pichia stipitis* strains with increased cell DNA contents. *Current Genetics*. **12**: 605-610.

Haken, H. (1979). Pattern formation and pattern recognition – an attempt at a synthesis. in: *Pattern Formation by Dynamic Systems and Pattern Recognition*. Haken, H. (Ed.). pp. 2-13. Springer-Verlag, Berlin.

Hartig, A., Ogris, M., Cohen, G. and Binder, M. (1990). Fate of highly expressed proteins destined to peroxisomes in *Saccharomyces cerevisiae*. *Current Genetics*. **18**: 23-27.

Herring, A.J. and Bevan, E.A. (1974). Virus-like particles associated with the double stranded RNA species found in killer and sensitive strains of the yeast *Saccharomyces cerevisiae*. *J. Gen. Virol*. **22**: 387-394.

Herskowitz, I. and Oshima, Y (1981). Control of cell type in *Saccharomyces cerevisiae*:Mating type and mating-type interconversion. *In*: The molecular and cellular biology of the yeast *Saccharomyces cerevisiae*: Life cycle and inheritance. Strathern, J.N. *et al.* (Ed.). pp. 181-269. Cold Spring Harbor Laboratory Press, Cold Spring Harbor, New York.

Herskowitz, I., Rina, J. and Strathern, J. (1992). Mating type determination and mating-type interconversion in *Saccharomyces cerevisiae*. *In*: The molecular and cellular biology of the yeast *Saccharomyces cerevisiae*: Life cycle and inheritance. Strathern, J.N. *et al.* (Ed.). pp. 583-656. Cold Spring Harbor Laboratory Press, Cold Spring Harbor, New York.

Hinnebusch, A.J. (1992). General and pathway-specific regulatory mechanisms controlling the synthesis of amino acids biosynthetic enzymes in *Saccharomyces cerevisiae*. *In*: The molecular and cellular biology of the yeast *Saccharomyces cerevisiae*: Volume II - Gene expression. Jones, E.W., Pringle, J.R. and Broach, J.R. (Ed.). pp. 319-414. Cold Spring Harbor Laboratory Press, Cold Spring Harbor, New York.

Hutchins, K. and Bussey, H. (1983). Cell wall receptor for yeast killer toxin: involvement of β-1,6-D-glucan. *J. Bacteriol.* **154**: 161-168.

Hutchinson, G.E. (1948). Circular casual systems in ecology, *Ann. N.Y. Acad. Sci.* **50**: 211-246.

IMSL Library. (1991). Fortran subroutines for mathematical applications (DIVPRK), Version 2, Houston.

Johnston, M. and Carlson, M. (1992). Regulation of carbon and phosphate utilisation. *In*: The molecular and cellular biology of the yeast *Saccharomyces cerevisiae*: Volume II - Gene expression. Jones, E.W., Pringle, J.R. and Broach, J.R. (Ed.). pp. 193-281. Cold Spring Harbor Laboratory Press, Cold Spring Harbor, New York.

Klis, F.M. (1994). Cell wall assembly in yeast. *Yeast*. **10**, 851-869.

Ko, W.H. and Lockwood, J.L. (1970). Mechanism of lysis of fungal mycelia in soil. *Phytopathology*. **60**: 148-154.

Krebs, C.J. (1978). *Ecology: The experimental analysis of distribution and abundance*, 2nd edition, Harper and Row Publishers, New York.

Kreutzfeldt, C. and Witt, W. (1991). Structural Biochemistry. *In*: Tuite, M.F. and Oliver, S.G. (Eds.), *Saccharomyces*, *Biotechnology Handbooks* series - Atkinson, T. and Sherwood, R.F. (series Eds.). pp. 5-58. Plenum Publ. Corp.

Lambrechts, M.G., Bauer, F.F., Marmur, J and Pretorius, I.S. (1996). Muc1, a mucin – like protein that is regulated by *MSS10*, is critical for pseudohyphal differentiation in yeast. *Proc. Natl. Acad. Sci.* USA. **93**: 8419-8424.

Lemke, P.A. (1977). Double-stranded RNA viruses among filamentous fungi. *In*: Microbiology. Schessinger, D. (Ed.). pp. 568-570. Am. Soc.Microbiol.

Lillie, S.H. and Pringle, J.R. (1980). Reserve carbohydrate metabolism in *Saccharomyces cerevisiae*: responses to nutrient limitation. *Journal of Bacteriology*. **143.3**: 177-185.

MacArthur, R.H., (1968). "The Theory of the Niche", *In*: *Population Biology an Evolution*. R.C. Lewontin (Ed.). pp.159-176. Syracuse University Press, Syracuse.

Magliani, W., Conti, S.,Gerloni, M., Bertolotti, D. and Polonelli, L. (1997). Yeast killer systems.*Clinical Microbiology Reviews*. **10**: 369-400.

Magasanik, B. (1992). Regulation of nitrogen utilisation. *In*: The molecular and cellular biology of the yeast *Saccharomyces cerevisiae*: Volume II - Gene expression. Jones, E.W., Pringle, J.R. and Broach, J.R. (Ed.). pp. 283-318. Cold Spring Harbor Laboratory Press.

Martinac, B., Zhu, H., Kubalski, A., Zhou, X.L., Culbertson, M., Bussey, H. and Kung, C. (1990). Yeast K_1 killer toxin forms ion channels in sensitive yeast spheroplasts and in artificial liposomes. *Pro. Natl. Acad. Sci.* USA. **87**: 6228-6232.

May, M. Sir Robert, (1973). Time-delay versus stability in population models with two and three trophic levels. *Ecology*. **54**: 315-325.

May, M. Sir Robert, (1975). Mathematical aspects of the dynamics of animal populations, *In*: *Studies in Mathematical Biology – Part II: Populations and Communities*, Studies in Mathematics. Levin, S. A. (Ed.). Vol. **16**: 317-366. The Mathematical Association of America,

May, M. Sir Robert, (1981). Models for single populations, *In*: *Theoretical Ecology*, Sir Robert M. May (Ed.). pp. 5-29. Blackwell Scientific Publications, Oxford.

May, Sir Robert M. (1981b). "Models for Two Interacting Populations". *In*: *Theoretical Ecology – Principles and Applications*May. Sir Robert M. (Ed.). 2nd edition. pp.78-104. Blackwell Scientific Publications, Oxford,

May, M. Sir Robert, (1995). Necessity and change: deterministic chaos in ecology and evolution, *Bulletin of the American Mathematical Society*. **32** (3): 291-308.

Miller, G.L. (1959). Effects of ethanol and other alkanols on the temperature relations of glucose transport and fermentation in *Saccharomyces cerevisiae*. *Appl. Microbiol. Biotechnol*. **22**: 265.

Olek, S. (1994). An Accurate Solution to the Multispecies Lotka-Volterra Equations. *SIAM Review*. **36**: 480-488.

Osumi, M. (1998). The ultrastructure of yeast: cell wall structure and formation. *Micron*. **29**: 207-233.

Paltauf, F., Kohlwein, S.P. and Henry, S.A. (1992). Regulation and compartmentalisation of lipid synthesis in yeast. *In*: The molecular and cellular biology of the yeast *Saccharomyces cerevisiae*: Volume II - Gene expression. Jones, E.W., Pringle, J.R. and Broach, J.R. (Ed.). pp 415-500. Cold Spring Harbor Laboratory Press, Cold Spring Harbor, New York.

Pasteur, L. (1866). *Etudes sur la Vin, ses Maladies, Causes qui les Provoquent.* Imprimerie Imperial, Paris.

Pearl, R. 1927 The growth of populations. *The Quarterly Review of Biology* II. **4**: 532-548.

Pettoello-Mantovani, M. Nocerino, A., Polonelli, L., Morace, G., Conti, S., Di Martino, L., De Ritis, G., Iafusco, M. and Guandalini, S. (1995). *Hansenula anomala* killer toxin induces secretion and severe acute injury in the rat intestine. *Gastroentrology*. **109**: 1900-1906.

Pfeiffer, P. and Radler, F. (1984). Purification and characterisation of extracellular and intracellular killer toxin of *Saccharomyces cerevisiae*. *J. Gen. Microbiol.* **128**:2699-2706.

Pianka, E.R. (1981). "Competition and Niche Theory", *In*: *Theoretical Ecology – Principles and Applications*. May, Sir Robert M. (Ed.). 2nd edition. pp.167-196. Blackwell Scientific Publications, Oxford.

Pielou, E.C. (1969). *An introduction to mathematical ecology*, John Wiley and Sons, New York.

Polonelli, L., Lorenzini, R., Dr Bernardis, F. and Morace, G. (1986). Potential effect of yeast killer toxin. *Mycopathologia*. **96**: 103-107.

Radler, F. and Knoll, C. (1988). Die bildung von killertoxin und die beeinflussung der garung durch apiculatus-hefen. *Vitis*. **27**: 111-132.

Radler, F., Herzberger, S., Schonig, I. and Schwarz, P. (1992). Investigation of a killer strain of *Zygosaccharomyces bailii*. *Journal of General Microbiology*. **139**: 495-500.

Ramon-Portugal, F., Delia-Dupuy, M.L., Pingaud, H., Carrilo-Leroux, G.A. and Riba, J.P. (1997). Kinetic study and mathematical modelling of killer and sensitive *S. cerevisiae* strains growing in mixed culture. *Bioprocess Engineering*. **17**: 375-381.

Répaci, A. (1990). Non-Linear Dynamical Systems: On the Accuracy of Adomian's Decomposition Method. *Appl. Math. Lett.* **3**: 35-39.

Reynolds, E.S. (1963). The use oflead citrate at high pH as an electron opaque stain in electron mycroscopy. *J. Cell. Biol.* **17**: 208-212.

Roberts, T.A. (1995). Microbial growth and survival: developments in predictive modelling. *International Biodeterioration & Biodegradation.* **36**: 297-309.

Skipper, N. and Bussey, H. (1977). Mode of action of yeast toxins: energy requirements for *Saccharomyces cerevisiae* killer toxin. *J. Bacteriol.* **129**: 668-677.

Sprague, Jr. G.F. and Thorner, J.W. (1992). Pheromone response and signal transduction during the mating process of *Saccharomyces cerevisiae*. *In*: The molecular and cellular biology of the yeast *Saccharomyces cerevisiae*: Life cycle and inheritance. Strathern, J.N. *et al.* (Ed.). pp 657-744. Cold Spring Harbor Laboratory Press, Cold Spring Harbor, New York.

Spurr, A.R. (1969). A low viscosity epoxy resin embedding medium for electron microscopy. *J. Ultrastruct. Res.* **26**: 31-34.

Stratford, M. (1992). Yeast flocculation: Reconciliation of physiological and genetic viewpoints. *Yeast.* **8**: 25-38.

Starmer, W.T., Ganter, P.F., Aberdeen, V., Lachance, M.A. and Phaff, H.F. (1992). The ecological role of killer yeasts in natural communities of yeast. *Can. J. Microbiol.* **33**:783-796.

Strogatz, S.H. (1994). *Nonlinear Dynamics and Chaos.* pp. 19-20. Perseus Books, Reading MA.

Tipper, D.J. and Bostian, K.A. (1984). Double-stranded ribonucleic acid killer systems in yeasts. *Microbiol. Rev.* **48**: 125-156.

Vadasz, A.S. (1999). Microscale vinifications challenged by a k_2 killer yeast. BSc Honour thesis. Department of Biochemistry, University of Durban-Westville, Durban, South-Africa.

Vadasz, A.S. (1999b). Regulation of flocculation and pseudohyphae formation in beverage strains of *Saccharomyces cerevisiae*. Seminar for BSc Honours. Department of Biochemistry, University of Durban-Westville, Durban, South-Africa.

Vadasz, A.S., Jagganath, D,B., Pretorius, I.S. and Gupthar, A.S. (2000). Electron microscopy of the K_2 killer effect of *Saccharomyces cerevisiae* T206 on a mesophilic wine yeast. Antonie *van Leeuwenhoek*. **78**: 117-122.

Vadasz, A.S., Vadasz, P., Gupthar, A.S. and Abashar, M.E. (2000a). The recovery of an oscillatory mode of batch yeast growth in water for a pure culture. *Submitted for publication.*

Vadasz, A.S., Vadasz, P., Gupthar, A.S. and Abashar, M.E. (2000b). Theoretical and experimental recovery of oscillations during batch yeast growth in a pure culture subject to nutritional stress. *Submitted for publication.*

Vadasz, A.S., Vadasz, P., Gupthar, A.S. and Abashar, M.E. (2000c). Multiple stationary points of batch yeast growth in water for a pure culture. *Submitted for publication.*

Vadasz, P. (2000). Derivations of the new model of population dynamics. Communication notes, Westville.

Vadasz, P. and Olek, S. (1999). Weak Turbulence and Chaos for Low Prandtl Number Gravity Driven Convection in Porous Media. *Transport in Porous Media.* **37**: 69-91.

Vadasz, P. and Olek, S. (2000a). Convergence and Accuracy of Adomian's Decomposition Method for the Solution of Lorenz Equations. *International Journal of Heat and Mass Transfer.* **43**: 1715-1734.

Vadasz, P. and Olek, S. (2000b) Route to Chaos for Moderate Prandtl Number Convection in a Porous Layer Heated from Below. *Transport in Porous Media.* **41**: 211-239.

Vadasz, P. and Vadasz, A.S. (2000). Extinction and Coexistence in Population Dynamics for Two Species Competing over a Common Ecological Niche, submitted for publication.

Van Vuuren, H.J.J. and Jacobs, C.J. (1992). Killer yeasts in the wine industry: A review. *Am. Enol. Vitic.* **43**: 119-128.

Van Vuuren, H.J.J. and Wingfield, B.D. (1986). Killer yeast-cause of stuck fermentations in a wine cellar. *S. Afr. J. Enol. Vitic.* **7**: 113-118.

Verhulst, P.F. (1838). Notice sur la loi que la population suit dans son accroissement. *Corr. Math. et Phys. Publ. par A. Quetelet.* T. **X**: 113-121.

Wangersky, P.J. and Cunningham, W.J. (1957). Time lag in population models. *Cold Spring Harb. Symp. Quant. Biol.* **22**: 329-338.

Waterham, H.R., Titorenko, V.I., Swaving, G.J., Harder, W. and Veenuis, M. (1993). Peroxisomes in the methylotrophic yeast *Hansenula polymorpha*do not necessarily derive from pre-existing organelles. *EMBO Journal.* **12**: 4785-4794.

Wickerham, L.J. (1951). Taxonomy of yeasts. Technical Bulletin 1029. United States Department of Agriculture. Washington D.C., USA.

Wickner, R.B. (1976). Killer of *Saccharomyces cerevisiae* double-stranded ribonucleic acid plasmid. *Bacteriol. Rev.* **40**: 757-773.

Wickner, R.B. (1986). Double-stranded RNA replication in yeast: the killer system. *Ann. Rev. Biochem.* **55**: 373-395.

Wickner, R.B. (1992). Yeast RNA virology: The killer system. *In*: The molecular and cellular biology of the yeast *Saccharomyces cerevisiae*: Volume I - Genome dynamics, protein synthesis, and energetics. Jones, E.W., Pringle, J.R. and Broach, J.R. (Ed.). pp 263-296. Cold Spring Harbor Laboratory Press, Cold Spring Harbor, New York.

Wickner, R.B. (1996). Prions and RNA viruses of *Saccharomyces cerevisiae*. *Annual Reviews of Genetics*. **30**: 109-139.

Wilkinson, B.M., James, C.M. and Walmsley, R.M. (1996). Partial deletion of the *Saccharomyces cerevisiae* GDH3 gene results in novel starvation phenotypes. *Microbiology*. **142**: 1667-1673.

Wolf, J. and Heinrich, R. (1997). Dynamics of two-component biochemical systems in interacting cells; synchronization and desynchronization of oscillations and multiple steady states. *BioSystems*. **43**: 1-24.

Woods, D.R. and Bevan, E.A. (1968). Studies on the nature of the killer factor produced by *Saccharomyces cerevisiae*. *J. Gen. Microbiol.* **51**: 115-121.

APPENDICES

Appendix A.1 Linear stability analyses

A.1.1 Linear stability analysis of the logistic growth model (LGM) (1.2.2.1.2)

The LGM Equation (1-11) $dx/dt = (\mu - \beta x)x$ has the general form $\dot{x} = f(x)$ and the stationary points x_{st} are defined by $f(x) = 0$, corresponding in this case to the solutions $x_{st1} = 0$ and $x_{st2} = \mu/\beta$.

Equation (1-11) can be presented as

$$\frac{d}{dt}x - \mu x + \beta x^2 = 0 \qquad \text{(A.1.1-1)}$$

Substituting $x = x_{st} + \varepsilon x_1$ where $\varepsilon << 0$ into equation (A.1.1-1) yields

$$\frac{dx}{dt}(x_{st} + \varepsilon x_1) - \mu(x_{st} + \varepsilon x_1) + \beta(x_{st} + \varepsilon x_1)^2 = 0 \qquad \text{(A.1.1-2)}$$

$$\frac{dx}{dt}(x_{st}) + \frac{dx}{dt}(\varepsilon x_1) - \mu(x_{st}) - \mu\varepsilon x_1 + \beta(x_{st})^2 + 2x_{st}\varepsilon x_1 + \beta\varepsilon^2 x_1^2 = 0 \qquad \text{(A.1.1-3)}$$

The term $\beta\varepsilon^2 x_1^2 << 0$ and therefore it may be neglected.

Also, $dx_{st}/dt - \mu(x_{st}) + \beta(x_{st})^2 = 0$ because it is equal to the basic solution (A.1.1-1) for $x = x_{st}$. Equation (A.1.1-3) becomes

$$\varepsilon\left(\frac{d}{dt}x_1 - \mu x_1 + 2\beta x_{st} x_1\right) = 0 \qquad \text{(A.1.1-4)}$$

or

$$\frac{d}{dt}x_1 - \mu x_1 + 2\beta x_{st} x_1 = 0, \qquad \text{(A.1.1-5)}$$

yielding the characteristic equation for the eigenvalue, λ

$$\lambda + 2\beta x_{st} - \mu = 0 \qquad \text{(A.1.1-6)}$$

and

$$\lambda = \mu - 2\beta x_{st} \qquad \text{(A.1.1-7)}$$

The eigenvalue obtained from Equation (A.1.1-7) is $\lambda = \mu$ for $x_{st1} = 0$ and $\lambda = -\mu$ for $x_{st2} = \mu / \beta$. The growth rate value μ may obtain positive or negative values.

$$x_1 = Ae^{\lambda t}$$

or

$$x_1 = Ae^{-(2\beta x_{st} - \mu)t}$$

Assuming that the constant $\beta > 0$ when $\mu > 0$ and $\beta < 0$ when $\mu < 0$ in order to eliminate the possibility of non-feasible negative stationary values one concludes from the linear stability analysis as follows. For $x_{st1} = 0$, when $\mu > 0$, $\lambda > 0$, the solution at this stationary point grows exponentially and therefore is unstable, and when $\mu < 0$ (and $\beta < 0$), $\lambda < 0$, this point is stable. For $x_{st2} = \mu / \beta$, $\lambda = -\mu$, therefore, when $\mu > 0$, $\lambda < 0$, yielding a stable point, and when $\mu < 0$ (and $\beta < 0$), $\lambda > 0$, the solution becomes unstable. When both stationary points equal to zero, at $\mu / \beta = 0$ or $\mu = 0$, the solutions overlap at a critical point, yielding a transcritical bifurcation (see Figure A.1.1).

Global stability analysis of (1-11) $dx / dt = (\mu - \beta x)x$ (Figure A.1.2) yields the same solutions.

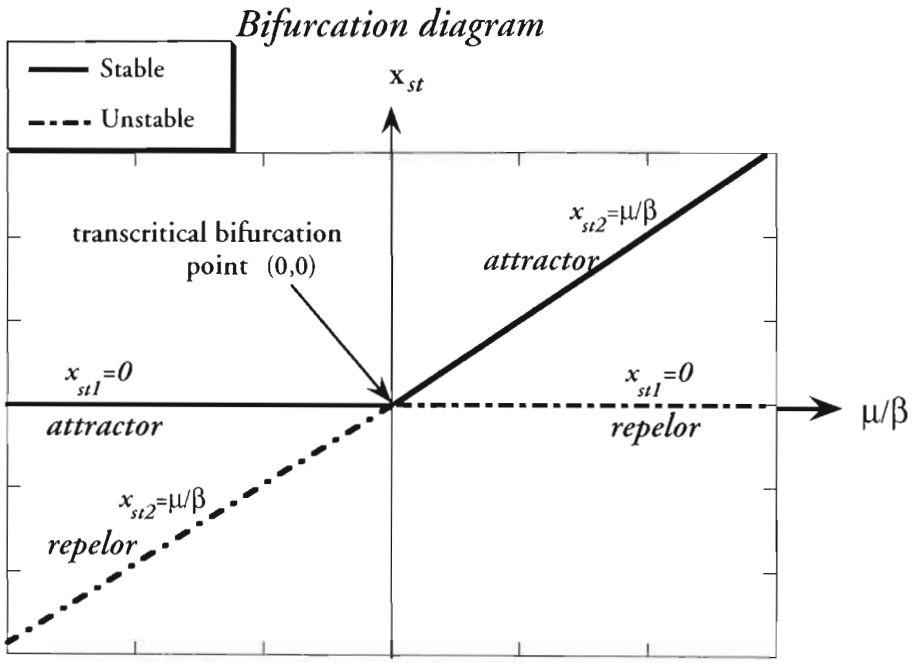

Figure **A.1.1** Bifurcation diagram and linear stability analysis of equation (1-11) $dx / dt = (\mu - \beta x)x$.

(a)

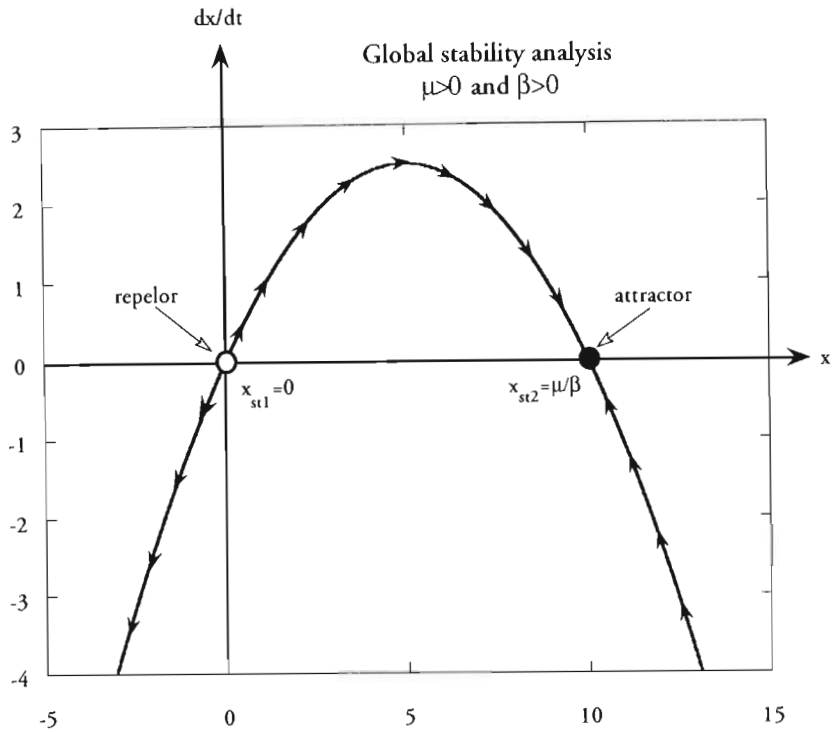

(b)

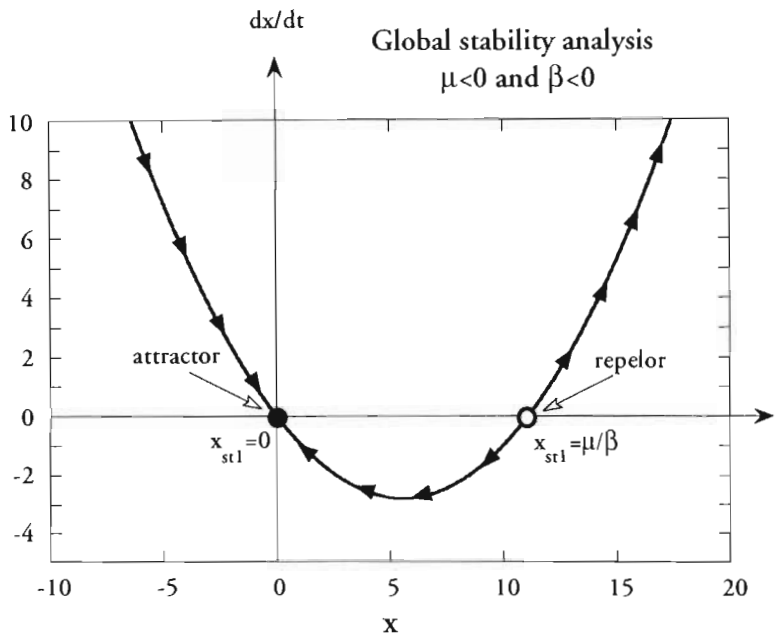

Figure **A.1.2** Global stability analysis of equation (1-11) $dx/dt=(\mu-\beta x)x$ for (a) $\mu>0$ and (b) $\mu<0$.

A.1.2 Linear stability analysis of the classical model for two species competing over a common ecological niche (1.2.2.2.1)

The classical model for two species competing over a common ecological niche was introduced as an extension of the Logistic Growth Model (LGM), which applies for one species in isolation. The classical model Equations (1-31) $\frac{\mathrm{d}x_1}{\mathrm{d}t} = \left[\mu_1 - \gamma_1\left(h_1 x_1 + h_2 x_2\right)\right] x_1$ and (1-32) $\frac{\mathrm{d}x_2}{\mathrm{d}t} = \left[\mu_2 - \gamma_2\left(h_1 x_1 + h_2 x_2\right)\right] x_2$ have the general form $\dot{x} = f(x)$ and the stationary points x_{st} are defined by $f(x) = 0$, corresponding in this case to the following solutions:

S1 $x_{st1} = 0$ and $x_{st2} = 0$

S2 $x_{st1} = 0$ and $x_{st2} \neq 0$. In this case $x_{st2} > 0$, therefore, $\mu_2 - \gamma_2(h_2 x_{st2}) = 0$, and thus $x_{st2} = \mu_2 / (\gamma_2 h_2)$

S3 $x_{st2} = 0$ and $x_{st1} \neq 0$. In this case $x_{st1} > 0$, therefore, $\mu_1 - \gamma_1(h_1 x_{st1}) = 0$, and thus $x_{st1} = \mu_1 / (\gamma_1 h_1)$

S4 $x_{st1} \neq 0$ and $x_{st2} \neq 0$, and both $x_{st1} > 0$ and $x_{st2} > 0$, therefore,

$\mu_1 - \gamma_1(h_1 x_{st1} + h_2 x_{st2}) = 0 = \mu_2 - \gamma_2(h_1 x_{st1} + h_2 x_{st2})$ and

$\mu_1 / \gamma_1 = h_1 x_{st1} + h_2 x_{st2} = \mu_2 / \gamma_2 = \mu / \gamma$, yielding $x_{st1} = (\mu / \gamma - h_2 x_{st2}) / h_1$ and

$x_{st2} = (\mu / \gamma - h_1 x_{st1}) / h_2$.

Naturally, $x_{st} \geq 0$, therefore, $x_{st} = 0$, denote the absence of cells, and $x_{st} > 0$, denote any other cell concentration.

Equations (1-31) and (1-32) can be presented as

$$\mu_1 x_1 - \gamma_1 h_1 x_1^2 - \gamma_1 h_2 x_2 x_1 - \dot{x}_1 = 0 \quad \text{(a)}$$

$$\mu_2 x_2 - \gamma_2 h_2 x_2^2 - \gamma_2 h_1 x_1 x_2 - \dot{x}_2 = 0 \quad \text{(b)} \qquad \text{(A.1.2-1)}$$

where $\dot{x} = dx / dt$.

Substituting $x_1 = x_{st1} + \varepsilon x_{11}$ and $x_2 = x_{st2} + \varepsilon x_{21}$ where $\varepsilon << 0$ into equation A.1.2-1 yields

$$\mu_1(x_{st1} + \varepsilon x_{11}) - \gamma_1 h_1 (x_{st1} + \varepsilon x_{11})^2 - \gamma_1 h_2 (x_{st2} + \varepsilon x_{21})(x_{st1} + \varepsilon x_{11}) - (\dot{x}_{st1} + \varepsilon \dot{x}_{11}) = 0 \quad \text{(a)}$$

$$\mu_2(x_{st2} + \varepsilon x_{21}) - \gamma_2 h_2 (x_{st2} + \varepsilon x_{21})^2 - \gamma_2 h_1 (x_{st1} + \varepsilon x_{11})(x_{st2} + \varepsilon x_{21}) - \dot{x}_{st2} - \varepsilon \dot{x}_{21} = 0 \quad \text{(b)} \qquad \text{(A.1.2-2)}$$

Reducing the basic solutions from (A.1.2-1) (a) for x_{st1} and (b) for x_{st2} from (A.1.2-2) (a) and (b), respectively, and cancelling ε^2 terms

Both sides of Equation (A.1.2-3) are divided by ε

$$\dot{x}_{11} + x_{11}(2\gamma_1 h_1 x_{st1} + \gamma_1 h_2 x_{st2} - \mu_1) + x_{21}(\gamma_1 h_2 x_{st1}) = 0 \quad \text{(a)}$$

$$\dot{x}_{21} + x_{21}(2\gamma_2 h_2 x_{st2} + \gamma_2 h_1 x_{st1} - \mu_2) + x_{11}(\gamma_2 h_1 x_{st2}) = 0 \quad \text{(b)} \qquad \text{(A.1.2-3)}$$

or

$$x_{11}(\lambda + 2\gamma_1 h_1 x_{st1} + \gamma_1 h_2 x_{st2} - \mu_1) + x_{21}(\gamma_1 h_2 x_{st1}) = 0 \quad \text{(a)}$$

$$x_{21}(\lambda + 2\gamma_2 h_2 x_{st2} + \gamma_2 h_1 x_{st1} - \mu_2) + x_{11}(\gamma_2 h_1 x_{st2}) = 0 \quad \text{(b)} \qquad \text{(A.1.2-4)}$$

Equation (A.1.2-4) can be presented as

$$ax_{11} + bx_{21} = 0 \quad \text{(a)}$$

(A.1.2-5)

$$cx_{11} + dx_{21} = 0 \quad \text{(b)}$$

where

$$a = \lambda + 2\gamma_1 h_1 x_{st1} + \gamma_1 h_2 x_{st2} - \mu_1$$

$$b = \gamma_1 h_2 x_{st1}$$

(A.1.2-6)

$$c = \gamma_2 h_1 x_{st2}$$

$$d = \lambda + 2\gamma_2 h_2 x_{st2} + \gamma_2 h_1 x_{st1} - \mu_2.$$

From (A.1.2-5) (a) $x_{21} = -ax_{11}/b$, therefore (A.1.2-5) (b) can be equal to $cx_{11} + d(-ax_{11}/b) = 0$ or $x_{11}(c - da/b) = 0$. $x_{11} \neq 0$, therefore, $c - da/b = 0$, and thus, $cb = da$.

$$\mathbf{Sx} = \begin{bmatrix} a;b \\ c;d \end{bmatrix} \begin{bmatrix} x_{11} \\ x_{21} \end{bmatrix} = 0$$

$$\det[\mathbf{S}] = ad - cb = 0$$

or

$$\det[\mathbf{S}] =$$
$$(\lambda + 2\gamma_1 h_1 x_{st1} + \gamma_1 h_2 x_{st2} - \mu_1)(\lambda + 2\gamma_2 h_2 x_{st2} + \gamma_2 h_1 x_{st1} - \mu_2) - (\gamma_2 h_1 x_{st2})(\gamma_1 h_2 x_{st1}) = 0$$

(A.1.2-7)

$$\begin{cases} x_{11} = A_1 e^{\lambda_1 t} + A_2 e^{\lambda_2 t} \\ \\ x_{21} = B_1 e^{\lambda_1 t} + B_2 e^{\lambda_2 t} \end{cases} \qquad \text{(A.1.2-8)}$$

therefore, the linear stability condition is achieved when both $\lambda_1 < 0$ and $\lambda_2 < 0$. Substituting each solution into (A.1.2-8) reveals the linear stability condition for each of the four possible solutions, as are presented in Table **A.1.2.1**.

Table **A.1.2.1** Linear stability analyses of the steady state solutions for the classical model of two species competing over a common ecological niche (1.2.2.2.1)

	Steady State Solutions	**Linear Stability Conditions**
S1	$x_{st1} = 0$ and $x_{st2} = 0$	$\lambda_1 = \mu_1 < 0$ and $\lambda_2 = \mu_2 < 0$
S2	$x_{st1} = 0$ and $x_{st2} = \mu_2 / (\gamma_2 h_2)$	$\lambda_1 = \mu_1 - (\gamma_1 / \gamma_2)\mu_2 < 0 \rightarrow \mu_1 / \gamma_1 < \mu_2 / \gamma_2$ and $\lambda_2 = -\mu_2 < 0 \rightarrow \mu_2 > 0$
S3	$x_{st2} = 0$ and $x_{st1} = \mu_1 / (\gamma_1 h_1)$	$\lambda_1 = -\mu_1 < 0 \rightarrow \mu_2 > 0$ and $\lambda_2 = \mu_2 - (\gamma_2 / \gamma_1)\mu_1 < 0 \rightarrow \mu_2 / \gamma_2 < \mu_1 / \gamma_1$
S4	$x_{st1} = (\mu / \gamma - h_2 x_{st2}) / h_1$ and $x_{st2} = (\mu / \gamma - h_1 x_{st1}) / h_2$	Globally Stable if $\mu_1 > 0$ & $\mu_2 > 0$ subject to $h_1 x_{st1} = h_2 x_{st2}$.

Appendix A.2 Materials and Solutions

Filter sterilisation: Passing through 0.22µm pore size filter (Millex-GS, Millipore).

Autoclave sterilisation: 20 minutes at 1.2 kg/cm^2, with rapid exhausting.

DNS reagent (Miller, 1959)

250ml 2.13N sodium potassium tartrate

100ml NaOH containing 0.21M 3,5 dinitrosalicylic acid

150ml distilled water (autoclaved)

All components were mixed aseptically and stored in a dark bottle for not more than 30 days at room temperature.

Growth media

G – medium

100ml white Hanepoot grape juice (*Ceres*, SA) (filter sterilised)

1g yeast extract in 50ml distilled water (autoclaved)

0.1g $(NH_4)_2 HPO_4$ in 50ml distilled water (autoclaved)

All components were mixed aseptically at room temperature

pH 4.02.

Grape juice agar

10ml *Ceres* Hanepoot white grape juice (filter sterilised)

2.0g agar in 90ml distilled water (autoclaved)

The 10ml juice was filtered aseptically into the autoclaved cooled (45^0C) agar medium.

The medium was thoroughly mixed, aseptically poured into sterile petri dishes and left to solidify for about an hour at room temperature in the laminar flow.

Adjusting the amounts of the *Ceres* Hanepoot white juice (3ml) and distilled water (97ml) produces the 3% (v/v) grape juice agar.

Grape juice liquid medium

5% (v/v): 15ml *Ceres* Hanepoot white juice (filter sterilised) was mixed with cool 285ml distilled, autoclaved water.

Methylene blue medium

Solution a: Methylene blue agar medium:

Yeast extract	0.6g
Malt extract	0.6g
D – glucose	1.0g
Peptones	1.0g
Agar	4.0g

All components were mixed in 120ml distilled water, adjusted to pH 4.6 and autoclaved.

Solution b: Citric-phosphate buffer:

0.1M Citric acid

0.2M NaH_2PO_4

All components were mixed in 60ml distilled water, adjusted to pH 4.6 and autoclaved.

Solutions a and b were mixed together.

Methylene blue of 10mg (Loeffer's methylene blue, BDH, UK) was added into autoclaved cooled 20ml distilled water, and filtered aseptically into the autoclaved cooled agar - citric phosphate buffer. The medium was thoroughly mixed, aseptically poured into sterile petri dishes, and left to solidify for about an hour at room temperature in the laminar flow.

WLN (Bacto W.L. Nutrient) medium

WLN - powder was mixed in distilled water in ratio of 8g powder to 100ml water and then autoclaved. The clear evergreen medium was cooled (45^0C), aseptically poured into sterile petri dishes, and left to solidify for about an hour at room temperature in the laminar flow.

YMA (Yeast malt agar) (Wickerham, 1951)

Yeast extract	0.6g
Malt extract	0.6g
D – glucose	1.0g
Peptones	1.0g
Agar	3.0g

All components were mixed in 200ml distilled water and autoclaved. The medium was cooled (45^{0}C), thoroughly mixed, aseptically poured into sterile petri dishes, and left to solidify for about an hour at room temperature in the laminar flow.

YMB (Yeast malt broth)

YMB medium (200ml) was made up of all YMA medium components except the agar and autoclaved.

YMA_{cyc}

Cycloheximide was filtered aseptically into the cooled (45^{0}C) YMA medium, at ratios of 1, 2, 3 and 4µg cycloheximide per 4 ml YMA volume, thoroughly mixed and aseptically poured into sterile petri dishes. A single YMA_{cyc} petri dish contained a maximum volume of 20ml medium.

Reagents used for RNA islolation

Agarose gel electrophoresis buffer (x10)

Tris - HCl	0.39M
Na_2HPO_4	0.3M
EDTA	0.1M

These components were mixed in distilled water, adjusted to pH 7.5 with 10% (v/v) HCl, then autoclaved.

Gel loading buffer

50% (v/v) Glycerol

0.05% Bromophenol blue

0.05% Xylene cyanol

These components were mixed in distilled water, adjusted to pH 7.5 with 10% (v/v) HCl.

Phenol

Melted phenol crystals of 70% (v/v), were mixed in cooled - autoclaved TE buffer (pH 7.5), and kept in a tightly closed dark bottle in a fume cupboard.

Sea sand (grade GR)

The sea-sand was thoroughly washed with sterile distilled water, followed by TE buffer (pH 7.5), then covered with the buffer and autoclaved in a foiled beaker. On setting, the repeated washing ensured that the pH of the suspension was 7.5.

TE buffer

Tris - HCl	10mM
EDTA	1mM

These components were mixed in distilled water, adjusted to pH 7.5 with 10% (v/v) HCl, then autoclaved.

Tris - H_2SO_4

Tris - H_2SO_4	50mM

This was mixed in distilled water and adjusted to pH 9.3 with 10% (v/v) H_2SO_4 , then autoclaved.

Tris - mercaptoethanol buffer

Tris - HCl	100mM

2.5% (v/v) 2-β- mercaptoethanol (99% v/v)

97.5% v/v distilled water

These components were mixed and adjusted to pH 8.7 with 10% (v/v) HCl, then autoclaved.

TSE buffer

Tris - H_2SO_4	10mM
NaCl	0.1M
EDTA	1mM

These components were mixed in distilled water, adjusted to pH 7.5 with 10% (v/v) H_2SO_4 , then autoclaved.

TSE + SDS buffer

Tris - H_2SO_4	10mM
NaCl	0.1M
EDTA	1mM
SDS	0.2% (w/v)

These components were mixed in distilled water, adjusted to pH 7.5 with 10% (v/v) H_2SO_4 , then autoclaved.

Sample-preparation solutions for electron microscopy

Lead citrate stain solution (Reynolds, 1963)

In a 50ml volumetric flask were weighed:

Lead nitrate	1.33g
Sodium citrate	1.76g
Distilled water	30ml

The mixture was shaken vigorously for 1 minute then intermittently for 30 minutes, allowing the formation of lead citrate. After addition of 8ml NaOH (1M), the solution was mixed by inversion until all precipitations dissolved, brought to 50ml total volume by addition of distilled water, decanted into a tightly-closed bottle and stored in an undisturbed place at 4^0C. This stain was used by pipetting it from the centre, not touching bottle sides and bottom, where precipitation might have occurred.

Osmium tetroxide (1% v/v)

4% solution from sealed vial	2ml
Distilled water	6ml

This was prepared in a fume cupboard. The used solution was discarded and washed into a bottle found in a fume cupboard for re-cycling.

Spurr (1967) standard resin mixture

(S024 Spurr's resin kit)

ERL 4206 (VCD)	10g
DER	6g
NSA	26g
S_1	0.4g

These solutions weighed directly into a 50ml ointment-jar and stirred for 30 minutes. The magnetic stirrer was dropped into acetone immediately after it was used, then washed with soap and water. The jar was covered and stored at -20^{0}C. In order to avoid moisture from the resin solution, it was defrosted before opening the jar.

Uranyl acetate (2% w/v)

Uranyl acetate	2g
Distilled water	100ml

The solution was stored in a dark bottle at 4^{0}C.

Appendix A.3 Kits specifications

Acetic acid detection test

Acetic acid

Biochemical analysis
Food analysis

1 UV-method

for the determination of acetic acid in foodstuffs and other materials

Not for use in *in vitro* diagnostic procedures for clinical diagnosis.

Cat. No. 148261

Test-Combination for ca. 3 x 10 determinations

Recommendations to methods and standardized procedures see references.

Principle (Ref. 1-3)

Acetic acid (acetate) is converted in the presence of the enzyme acetyl-CoA synthetase (ACS)[1] with adenosine-5'-triphosphate (ATP) and coenzyme A (CoA) to acetyl-CoA (1).

(1) Acetate + ATP + CoA $\xrightarrow{ACS^1}$ acetyl-CoA + AMP[2] + pyrophosphate

Acetyl-CoA reacts with oxaloacetate to citrate in the presence of citrate synthase (CS) (2).

(2) Acetyl-CoA + oxaloacetate + H_2O $\xrightarrow{CS}$ citrate + CoA

The oxaloacetate required for reaction (2) is formed from malate and nicotinamide-adenine dinucleotide (NAD) in the presence of malate dehydrogenase (MDH) (3). In this reaction NAD is reduced to NADH.

(3) Malate + NAD^+ $\xrightarrow{MDH}$ oxaloacetate + NADH + H^+

The determination is based on the formation of NADH measured by the increase in absorbance at 340, 334 or 365 nm. Since a preceding indicator reaction is used, the amount of NADH formed is not linearly proportional to the acetic acid concentration (for calculations, see below).

The Test-Combination contains

1. Bottle 1 with approx. 32 ml of solution, consisting of: triethanolamine buffer, pH 8.4; L-malic acid, 134 mg; magnesium chloride, 67 mg; stabilizers.
2. Bottle 2 with approx. 280 mg lyophilisate, consisting of: ATP, 175 mg; CoA, 18 mg; NAD, 86 mg; stabilizers.
3. Bottle 3 with approx. 0.4 ml of enzyme suspension, consisting of: malate dehydrogenase, 1100 U; citrate synthase, 270 U.
4. 3 Bottles 4, with lyophilisate acetyl-CoA-synthetase, 5 U each.
5. Standard solution.

Preparation of solutions

1. Use solution of bottle 1 undiluted.
2. Dissolve contents of bottle 2 with 7 ml redist. water.
3. Use suspension of bottle 3 undiluted.
4. Dissolve contents of one bottle 4 with 0.25 ml redist. water.

Stability of solutions

Solution 1 is stable for 1 year at +4°C.
Bring solution 1 to 20–25°C before use.
Solution 2 is stable for 4 weeks at +4°C.
Contents of bottle 3 are stable for 1 year at +4°C.
Solution 4 is stable for 5 days at +4°C.

Procedure

Wavelength[3]: 340 nm, Hg 365 nm or Hg 334 nm
Glass cuvette[4]: 1 cm light path
Temperature: 20–25°C
Final volume: 3.23 ml
Read against air (without a cuvette in the light path) or against water.
Sample solution: 1–30 µg acetic acid/cuvette[5] (in 0.1–2.0 ml sample volume).

Pipette into cuvettes	blank	sample
solution 1	1.00 ml	1.00 ml
solution 2	0.20 ml	0.20 ml
redist. water	2.00 ml	1.90 ml
sample solution*	–	0.10 ml
mix** and read absorbances of the solutions (A_0). Addition of		
suspension 3	0.01 ml	0.01 ml
mix** and read absorbances of the solutions (A_1) after approx. 3 min. Start reaction by addition of		
solution 4	0.02 ml	0.02 ml
mix**, wait until the reaction has stopped (approx. 10–15 min) and read the absorbances of the solutions (A_2). If the reaction has not stopped after 15 min, continue to read the absorbances at 2 min intervals until the absorbance increases constantly for 2 min.		

* Rinse the enzyme pipette or the pipette tip of the piston pipette with sample solution before dispensing the sample solution.
** For example, with a plastic spatula or by gentle swirling after closing the cuvette with Parafilm® (registered trademark of the American Can Company, Greenwich, Ct., USA).

If the absorbance A_2 increases constantly, extrapolate the absorbance to the time of the addition of solution 4.

Determine the absorbance differences (A_1-A_0) and (A_2-A_0) for the blank and the sample.

With preceding indicator reactions, there is no linear proportionality between the measured absorbance difference and the acetic acid concentration.

The following formula, which should generally be used for preceding indicator reactions, serves to calculate the $\Delta A_{acetic\ acid}$ (see Ref. 2).

$$\Delta A_{acetic\ acid} = \left[(A_2-A_0)_{sample} - \frac{(A_1-A_0)^2_{sample}}{(A_2-A_0)_{sample}}\right] - \left[(A_2-A_0)_{blank} - \frac{(A_1-A_0)^2_{blank}}{(A_2-A_0)_{blank}}\right]$$

The absorbance differences measured should as a rule be at least 0.100 absorbance units to achieve sufficiently accurate results (see "Instructions for performance of assay").

Calculation

According to the general equation for calculating the concentration:

$$c = \frac{V \times MW}{\varepsilon \times d \times v \times 1000} \times \Delta A\ [g/l], \text{ where}$$

V = final volume [ml]
v = sample volume [ml]
MW = molecular weight of the substance to be assayed [g/mol]
d = light path [cm]
ε = absorption coefficient of NADH at:
340 nm = 6.3 [l x mmol^{-1} x cm^{-1}]
Hg 365 nm = 3.4 [l x mmol^{-1} x cm^{-1}]
Hg 334 nm = 6.18 [l x mmol^{-1} x cm^{-1}]

It follows for acetic acid:

$$c = \frac{3.23 \times 60.05}{\varepsilon \times 1 \times 0.1 \times 1000} \times \Delta A = \frac{1.940}{\varepsilon} \times \Delta A\ [g\ acetic\ acid/l\ sample\ solution]$$

If the sample has been diluted during preparation, the result must be multiplied by the dilution factor F.

When analyzing solid and semi-solid samples which are weighed out for sample preparation, the result is to be calculated from the amount weighed:

$$content_{acetic\ acid} = \frac{c_{acetic\ acid}\ [g/l\ sample\ solution]}{c_{sample}\ [g/l\ sample\ solution]} \times 100\ [g/100\ g]$$

1 ACS, also known as acetate thiokinase
2 AMP = adenosine-5'-monophosphate
3 The absorption maximum of NADH is at 340 nm. On spectrophotometers, measurements are taken at the absorption maximum; when spectralline photometers equipped with a mercury vapour lamp are used, measurements are taken at a wavelength of 365 nm or 334 nm.
4 If desired, disposable cuvettes may be used instead of glass cuvettes.
5 See instructions for performance of assay.

Instructions for performance of assay

The amount of acetic acid present in the cuvette should range between 2 µg and 30 µg (measurement at 365 nm) or 1 µg and 15 µg (measurement at 340, 334 nm), respectively. The sample solution must therefore be diluted sufficiently to yield an acetic acid concentration between 0.02 and 0.3 g/l or 0.01 and 0.15 g/l, respectively.

Dilution table

estimated amount of acetic acid per liter measurement at 340 or 334 nm	365 nm	dilution with water	dilution factor F
< 0.15 g	0.3 g	—	1
0.15–1.5 g	0.3–3.0 g	1 + 9	10
1.5–15 g	3.0–30 g	1 + 99	100
> 15 g	> 30 g	1 + 999	1000

If the absorbance difference measured (ΔA) is too low (e. g. < 0.100), the sample solution should be prepared anew (weigh out more sample or dilute less strongly) or the sample volume to be pipetted into the cuvette can be increased up to 2.0 ml. The volume of water added must then be reduced so as to obtain the same final volume for the sample and blank in the cuvettes. The new sample volume v must be taken into account in the calculation.

1. Instructions for sample preparation

1.1. Liquid foodstuffs

Filter turbid solutions and dilute to obtain an acetic acid concentration of less than 0.3 g/l. The diluted solution can be used for the assay, even if it is slightly colored. When intensely colored juices are used undiluted for the assay because of their low acetic acid concentration, they must be decolorized by means of activated charcoal, polyamide or polyvinylpoly-pyrrolidone (PVPP).

Examples:

Determination of acetic acid in fruit juices

a) Fruit juices with a high acetic acid content (for example, in the range of approx. 0.3 g/l): Dilute the sample with water 1 + 1; use 0.1 ml for the assay.

b) Fruit juices with a low acetic acid content (less than approx. 0.02 g/l):

Decolorize colored juices:

Add 1% (w/v) activated charcoal to the sample, stir for approx. 30 s and filter. Use 0.5 ml for the assay (take into account the altered sample volume v in the calculation).

In certain situations (when using a large sample volume), adjust acid juices to pH 8.

Determination of acetic acid in wine (Ref. 6)

Use 0.1 ml of white wine undiluted for the assay (this volume may be increased up to 2.0 ml, if necessary).

Use 0.1 ml of red wine containing about 0.2 g of acetic acid/l undiluted for the assay without decolorizing.

To red wine containing less than 0.1 g acetic acid/l add 1% (w/v) polyamide or PVPP, stir for approx. 1 min and filter. Adjust an aliquot volume of the largely decolorized sample to pH 8 (indicator paper) with sodium hydroxide (0.1 mol/l), dilute with water to give double the volume. Use up to 2.0 ml, if necessary, for the assay (take into account the altered sample volume v in the calculations).

High alcohol concentrations in the sample may delay the acetate reaction. The absorbances A_2 should therefore be read after 20 min.

Determination of acetic acid in vinegar

Dilute the sample according to the dilution table and use 0.1 ml for the assay.

Determination of acetic acid in sour dressings and sauces

Separate solids from the sample and place into a refrigerator for 20 min to obtain separation of fat. Filter, adjust filtrate to room temperature and dilute according to the dilution table, if necessary.

Determination of acetic acid in beer (Ref. 9, 10)

To remove the carbonic acid stir approx. 5–10 ml of beer for 30 s with a glass rod or filter. The largely CO_2-free sample is used for the assay without further dilution.

1.2. Solid foodstuffs (Ref. 4, 8)

Homogenize solid and semi-solid samples (e.g. vegetable and fruit products, yogurt and leaven) in an electric mixer, meat grinder or mortar, extract or dissolve with water, and filter, if necessary.

Extract fat-and protein-containing samples (e.g. meat products) with water of about 60°C (condenser), allow to cool, fill up to a certain volume in the volumetric flask and keep it in a refrigerator for 20 min to obtain separation of fat, and filter.

Add perchloric acid (1 mol/l) to protein-containing sample solutions in a ratio of 1 : 3 (1 + 2), centrifuge, neutralize an aliquot volume of the supernatant solution with KOH (2 mol/l) (measure the volume of KOH used for neutralization), keep it in a refrigerator for 20 min in order to precipitate the $KClO_4$ and filter. Use the clear solution, which may be diluted, if necessary, adjusted to room temperature, for the assay.

For calculating the content (in g/100 g) according to the above-mentioned formula (see calculation) the content of the sample in the sample solution is needed. When applying the above-mentioned sample preparation and considering the water content of the sample the concentration of the sample is calculated according to the following furmula:

$$c_{sample} = \frac{a \times 1000 \times d}{(b + a \times w) \times (d + e)} \quad [g/l]$$

It is:
a: the weighed sample in g
b: volume of perchloric acid in ml
d: volume of supernatant in ml
e: volume of KOH in ml
w: water content of the sample (%; w/w : 100)
1000: factor for g expressed in mg
(The specific gravity of water from the sample at room temperature is approx. 1 g/ml. It can be neglected for the calculation.)

Examples:

Determination of acetic acid in hard cheese

Weigh approx. 2 g of ground cheese accurately into a 100 ml volumetric flask, add about 70 ml water and incubate at approx. 60°C for 20 min. Shake flask from time to time. After cooling to room temperature, dilute to 100 ml with water. For separation of fat, place the flask in a refrigerator for 20 min, filter, discard the first few ml of the filtrate. Use the clear solution, which may also be slightly opalescent, adjusted to room temperature, for the assay.

Determination of acetic acid in mayonnaise or yogurt

Weigh approx. 5 g of sample accurately into a 100 ml volumetric flask, add approx. 50 ml redist. water and heat for 20 min in a water-bath at 50–60°C; shake from time to time. After cooling to room temperature, fill up to 100 ml with redist. water. For separation of fat, place the mixture for 20 min in a refrigerator. Filter solution and use the clear or slightly turbid solution, adjusted to room temperature, for the assay.

2. Specificity

The method is specific for acetic acid.

3. Further applications

The method may also be used in the examination of paper, pharmaceuticals (e. g. infusion solutions, acetylsalicylic acid preparations) emulsifiers (after alkaline hydrolysis) and in research when analyzing biological samples.

For details of sampling, treatment and stability of the sample see Bergmeyer, H. U. & Möllering, H. (1974) in Methods of Enzymatic Analysis (Bergmeyer, H. U., ed.) 2nd ed., Vol. 3, p. 1523–1525, Verlag Chemie, Weinheim, Academic Press, Inc. New York and London; Holz, G. & Bergmeyer, H. U. (1974) in Methods of Enzymatic Analysis (Bergmeyer, H. U., ed.) 2nd ed., Vol. 3, p. 1530, Verlag Chemie, Weinheim, Academic Press, Inc. New York and London; Lundquist, F. (1974) in Methods of Enzymatic Analysis (Bergmeyer, H. U., ed.) 2nd ed., Vol. 3, p. 1534–1535, Verlag Chemie, Weinheim, Academic Press, Inc. New York and London.

3.1. Determination of acetic acid in serum and plasma (Ref. 3)

Serum and plasma can be used directly for the determination of acetic acid.

Dilute dialysate (from hemodialysis) with water in the ratio 1 : 10 (1 + 9) (dilution factor F = 10).

Pipette into centrifuge tubes	reagent blank	sample
solution 1	1.00 ml	1.00 ml
solution 2	0.20 ml	0.20 ml
sample solution	–	0.50 ml
redist. water	1.50 ml	1.00 ml
Mix contents of the tubes thoroughly and centrifuge for approx. 5 min. Pipette into cuvettes		
supernatant sample	–	1.00 ml
supernatant reagent blank	1.00 ml	–
read absorbances of the solutions (A_0). Add		
suspension 3	0.01 ml	0.01 ml
mix thoroughly; read the absorbances of the solutions (A_1) after approx. 3 min. Add		
solution 4	0.02 ml	0.02 ml
mix thoroughly; read the absorbances of the solutions (A_2) after approx. 15 min.		

$$\Delta A_{\text{acetic acid}} = [(A_2-A_0)_{\text{sample}} - \frac{(A_1-A_0)^2_{\text{sample}}}{(A_2-A_0)_{\text{sample}}}] - [(A_2-A_0)_{\text{blank}} - \frac{(A_1-A_0)^2_{\text{blank}}}{(A_2-A_0)_{\text{blank}}}]$$

Calculation:

$$c = \frac{0.3340 \times \Delta A \times F}{\varepsilon} \text{ [g acetic acid/l sample]}$$

$$c = \frac{5.562 \times \Delta A \times F}{\varepsilon} \text{ [mmol acetic acid/l sample]}$$

Wavelength	Hg 365 nm	340 nm	Hg 334 nm
c [g/l]	0.0982 x ΔA x F	0.0530 x ΔA x F	0.0541 x ΔA x F
c [mmol/l]	1.636 x ΔA x F	0.8829 x ΔA x F	0.9000 x ΔA x F

3.2. Determination of acetic acid in fermentation samples and cell culture media

Place the sample, after centrifugation, if necessary, in a water-bath of 80°C (cover the tube because of the volatility of acetic acid) to stop enzymatic reactions. Centrifuge and use the supernatant, diluted according to the dilution table, if necessary, for the assay. Alternatively, deproteinization can be carried out with perchloric acid. See the abovementioned examples.

Homogenize gelatinous agar media with water and treat further as described.

4. Interferences

Esters of acetic acid may be saponified under test conditions (examples: ethylacetate in wine; acetylsalicylic acid in pharmaceuticals). Acetic acid formed is responsible for creep reactions which have to be drawn into consideration when calculating results (extrapolation of A_2 to the time of the addition of ACS = solution 4).

Detection of interferences of the test system

When the enzymatic reaction is complete after the time given in "Procedure" it can be concluded in general that the reaction is not interfered. For assurance of results a re-start of the reaction (qualitatively or quantitatively) by the addition of 'standard material' (e.g. sodium acetate) can be done: a further change of absorbance proves suitability of measurements.

For the detection of gross errors when performing the assays and of interfering substances in the sample material it is recommended to analyze a sample solution in a double determination with two different sample volumes (e.g. 0.10 ml and 0.20 ml): the measured absorbance differences have to be proportional to the sample volumes.

When analyzing solid samples it is recommended to weigh in two different amounts (e.g. 1g and 2g) into 100 ml volumetric flasks and to perform the determinations with the same sample volume: the absorbance differences have to be proportional to the amounts weighed in.

References

1 Bergmeyer, H. U. & Möllering, H. (1974) in Methoden der enzymatischen Analyse (Bergmeyer, H. U., Hrsg.) 3. Aufl., Bd. 2, S. 1566-1574; Verlag Chemie, Weinheim, and (1974) in Methods of Enzymatic Analysis (Bergmeyer, H. U., ed.) 2nd ed., vol. 3, p. 1520-1528, Verlag Chemie, Weinheim, Academic Press, Inc. New York and London.

2 Bergmeyer, H. U. (1974) in Methoden der enzymatischen Analyse (Bergmeyer, H. U., Hrsg.) 3. Aufl., Bd. 1, S. 119-125; Verlag Chemie, Weinheim, and (1974) in Methods of Enzymatic Analysis (Bergmeyer, H. U., ed.) 2nd ed., vol. 1, p. 112-117, Verlag Chemie, Weinheim, Academic Press, Inc. New York and London.

3 Beutler, H.-O. (1984) in Methods of Enzymatic Analysis (Bergmeyer, H. U., ed.) 3rd ed., vol. VI, pp. 639-645, Verlag Chemie, Weinheim, Deerfield Beach/Florida, Basel.

4 Amtliche Sammlung von Untersuchungsverfahren nach §35 LMBG: Untersuchung von Lebensmitteln: Bestimmung von Essigsäure (Acetat) in Fleischerzeugnissen, 07.00/14, (November 1981). Bestimmung von Essigsäure (Acetat) in Wurstwaren, 08.00/16, (November 1981). Bestimmung der Essigsäure in Tomatenketchup und vergleichbaren Erzeugnissen, 52.01.01/16, (November 1983). Bestimmung von Essigsäure (Acetat) in Brot einschließlich Kleingebäck aus Brotteigen, 17.00/16, (Juni 1990).

5 Gombocz, E., Hellwig, E., Vojir, F. & Petuely, F. (1981) Deutsche Lebensmittel-Rundschau 77, 13-14.

6 Junge, Ch. & Spadinger, Ch. (1979) Die flüchtigen Säuren des Weines, Deutsche Lebensmittel-Rundschau 75, 12-15.

7 Müller, H. & Horbach, A. (1981) Bestimmung von Acetylengruppen in Poly-ε-caprolactam durch Hydrolyse und enzymatische Essigsäure-Analyse. Die Angewandte Makromolekulare Chemie 96, 37-41.

8 Spicher, G. & Rabe, E. (1981) Die Mikroflora des Sauerteiges: XII. Mitteilung: Der Einfluß der Temperatur auf die Lactat-/Acetatbildung in mit homofermentativen Milchsäurebakterien angestellten Sauerteigen, Z. Lebensm. Unters. Forsch. 172, 20-25.

9 Piendl, A. & Wagner, I. (1983) Physiologische Eigenschaften der organischen Säuren des Bieres; 1. Acetat, Brauindustrie 68, 862-864 und 866.

10 Klopper, W.J., Angelino, S.A.G.F., Tuning, B. & Vermeire, H.A. (1986) Organic acids and glycerol in beer, J. Inst. Brew. 92, 225-228.

Acetic acid standard solution

for the Test-Combination Acetic acid
UV-method, Cat. No. 148 261

Concentration: see bottle label.
Acetic acid standard solution is a stabilized aqueous solution of acetic acid. It serves as standard solution for the enzymatic analysis of acetic acid in foodstuffs and other materials.

Application

1. Addition of acetic acid standard solution to the assay mixture:
Instead of sample solution the standard solution is used for the assay.

2. Restart of the reaction, quantitatively:
After completion of the reaction with sample solution and measuring of A_2, add 0.05 ml standard solution to the assay mixture. Read absorbance A_1 after the end of the reaction (approx. 20 min.). An increase of absorbance is observed.

A calculation of results is not possible because of the preceding equilibrium reaction with MDH (3).

3. Internal standard
The standard solution can be used as an internal standard in order to check the determination for correct performance (gross errors) and to see whether the sample solution is free from interfering substances:

Pipette into cuvettes	blank	sample	standard	sample + standard
solution 1	1.00 ml	1.00 ml	1.00 ml	1.00 ml
solution 2	0.20 ml	0.20 ml	0.20 ml	0.20 ml
redist. water	2.00 ml	1.90 ml	1.90 ml	1.90 ml
sample solution	–	0.10 ml	–	0.05 ml
standard solution	–	–	0.10 ml	0.05 ml
mix, and read absorbances of the solutions (A_0). Continue as described in the pipetting scheme under "Procedure". Follow the instructions given under "Instructions for performance of assay" and the footnotes.				

The recovery of the standard is calculated according to the following formula:

$$\text{recovery} = \frac{2 \times \Delta A_{\text{sample + standard}} - \Delta A_{\text{sample}}}{\Delta A_{\text{standard}}} \times 100\ [\%]$$

BOEHRINGER MANNHEIM

992.105 1523716

With coutesy: Boehringer Mannheim, FRG.

Ammonia detection test

Urea/Ammonia

Enzymatic BioAnalysis
Food Analysis

1 UV method

for the determination of urea and ammonia in foodstuffs and other materials and for the determination of nitrogen after Kjeldahl digestion (see pt. 12.2)

Not for use in diagnostic procedures for clinical purposes
FOR *IN VITRO* USE ONLY

Cat. No. 542946

Test-Combination for approx. 25 determinations each

For recommendations for methods and standardized procedures see references (2)

Principle (Ref. 1)
Urea is hydrolyzed to ammonia and carbon dioxide in the presence of the enzyme urease (1).

(1) $Urea + H_2O \xrightarrow{urease} 2\,NH_3 + CO_2$

In the presence of glutamate dehydrogenase (GlDH) and reduced nicotinamide-adenine dinucleotide (NADH), ammonia reacts with 2-oxoglutarate to L-glutamate, whereby NADH is oxidized (2).

(2) $2\text{-Oxoglutarate} + NADH + NH_4^+ \xrightarrow{GlDH} L\text{-glutamate} + NAD^+ + H_2O$

The amount of NADH oxidized in the above reaction is stoichiometric to the amount of ammonia or with half the amount of urea, respectively. NADH is determined by means of its light absorbance at 334, 340 or 365 nm.

The Test-Combination contains:
1. Bottle 1 with approx. 60 ml solution, consisting of: triethanolamine buffer, pH approx. 8.0; 2-oxoglutarate, 220 mg; stabilizers
2. Bottle 2 with approx. 50 tablets; each tablet contains: NADH, approx. 0.4 mg; stabilizers
3. Bottle 3 with approx. 0.7 ml urease solution, approx. 80 U
4. Bottle 4 with approx. 1.2 ml glutamate dehydrogenase solution, approx. 1000 U

Preparation of solutions
1. Use contents of bottle 1 undiluted.
2. Dissolve **one tablet** of bottle 2 with **one ml** solution of bottle 1 in a beaker or in a reagent tube for each assay (blank and samples) depending on the number of determinations. Use forceps for taking the tablets out of bottle 2. This results in reaction mixture 2*.
3. Use contents of bottle 3 undiluted.
4. Use contents of bottle 4 undiluted.

Stability of reagents
Solution 1 is stable at +4°C (see pack label).
Bring solution 1 to 20–25°C before use.
Tablets 2 are stable at +4°C (see pack label).
Reaction mixture 2 is stable for 3 days at +4°C.
Bring reaction mixture 2 to 20–25°C before use.
The contents of bottle 3 and 4 are stable at +4°C (see pack label).

Procedure
Wavelength[1]: 340 nm, Hg 365 nm or Hg 334 nm
Glass cuvette[2]: 1.00 cm light path
Temperature: 20–25°C
Final volume: 3.040 ml
Read against air (without a cuvette in the light path) or against water
Sample solution: 0.3–14 µg urea/cuvette[3] or
0.2– 8 µg ammonia/cuvette[3]
(in 0.100–2.000 ml sample volume)

Pipette into cuvettes	Blank urea	Urea sample	Blank ammonia	Ammonia sample
reaction mixture 2*	1.000 ml	1.000 ml	1.000 ml	1.000 ml
sample solution**	–	0.100 ml	–	0.100 ml
solution 3	0.020 ml	0.020 ml	–	–
redist. water	2.000 ml	1.900 ml	2.020 ml	1.920 ml
Mix***, and read absorbances of the solutions (A_1) after approx. 5 min at 20–25°C. Start reaction by addition of:				
solution 4	0.020 ml	0.020 ml	0.020 ml	0.020 ml
Mix***, wait for completion of the reaction (approx. 20 min) and read absorbances of the solutions (A_2). If the reaction has not stopped after 20 min, read absorbances at 2 min intervals until the absorbances decrease constantly over 2 min.				

If the absorbance A_2 decreases constantly, extrapolate the absorbance to the time of the addition of solution 4.

Determine the absorbance differences (A_1–A_2) for both, blanks and samples. Subtract the absorbance difference of the blank from the absorbance difference of the corresponding sample.

$$\Delta A = (A_1 - A_2)_{sample} - (A_1 - A_2)_{blank}$$

This results in $\Delta A_{urea + ammonia}$ (from urea sample) and

$\Delta A_{ammonia}$ (from ammonia sample).

The difference of these values results in ΔA_{urea}.

The measured absorbance differences should, as a rule, be at least 0.100 absorbance units to achieve sufficiently accurate results (see "Instructions for performance of assay").

If the absorbance differences of the samples (ΔA_{sample}) are higher than 1.000 (measured at 340 nm or Hg 334 nm respectively) or 0.500 (measured at 365 nm), the concentration of urea (or ammonia, respectively) in the sample solution is too high. The sample is to be diluted according to the dilution table in that case.

Calculation
According to the general equation for calculating the concentration:

$$c = \frac{V \times MW}{\varepsilon \times d \times v \times 1000} \times \Delta A \; [g/l]$$

V = final volume [ml]
v = sample volume [ml]
MW = molecular weight of the substance to be assayed [g/mol]
d = light path [cm]
ε = extinction coefficient of NADH at
340 nm = 6.3 [l x mmol^{-1} x cm^{-1}]
Hg 365 nm = 3.4 [l x mmol^{-1} x cm^{-1}]
Hg 334 nm = 6.18 [l x mmol^{-1} x cm^{-1}]

It follows for urea:

$$c = \frac{3.040 \times 60.06}{\varepsilon \times 1.00 \times 0.100 \times 2 \times 1000} \times \Delta A_{urea} = \frac{0.9129}{\varepsilon} \times \Delta A_{urea}$$

[g urea/l sample solution]

for ammonia:

$$c = \frac{3.040 \times 17.03}{\varepsilon \times 1.00 \times 0.100 \times 1000} \times \Delta A_{ammonia} = \frac{0.5177}{\varepsilon} \times \Delta A_{ammonia}$$

[g ammonia/l sample solution]

If the sample has been diluted on preparation, the result must be multiplied by the dilution factor F.

---

1 The absorption maximum of NADH is at 340 nm. On spectrophotometers, measurements are taken at the absorption maximum; if spectralline photometers equipped with a mercury vapor lamp are used, measurements are taken at a wavelength of 365 nm or 334 nm.
2 If desired, disposable cuvettes may be used instead of glass cuvettes
3 See instructions for performance of the assay

* For simplification of the assay performance it is also possible to pipette directly 1.000 ml of solution 1 into the cuvette and add 1 tablet from bottle 2. After dissolution of the tablet with the aid of a spatula continue working as described in the procedure. The difference in volume of ca. 1% (increase of volume by 1 tablet per 3.040 ml assay volume) has to be taken into account in the calculation by multiplication of the result with 1.01.

** Rinse the enzyme pipette or the pipette tip of the piston pipette with sample solution before dispensing the sample solution.

*** For example, with a plastic spatula or by gentle swirling after closing the cuvette with Parafilm® (registered trademark of the American Can Company, Greenwich, Ct., USA)

When analyzing solid and semi-solid samples which are weighed out for sample preparation, the result is to be calculated from the amount weighed:

$$\text{Content}_{urea} = \frac{c_{urea}\ [\text{g/l sample solution}]}{\text{weight}_{sample}\ \text{in g/l sample solution}} \times 100\ [\text{g/100 g}]$$

$$\text{Content}_{ammonia} = \frac{c_{ammonia}\ [\text{g/l sample solution}]}{\text{weight}_{sample}\ \text{in g/l sample solution}} \times 100\ [\text{g/100 g}]$$

1. Instructions for performance of assay

The amount of urea (ammonia) present in the cuvette has to be between 0.3 µg and 14 µg (0.2 µg and 8 µg). In order to get a sufficient absorbance difference, the sample solution is diluted to yield an urea (ammonia) concentration between 0.02 and 0.14 g/l (0.01 and 0.08 g/l).

Dilution table

Estimated amount of urea (ammonia) per liter	Dilution with water	Dilution factor F
< 0.14 g (< 0.08 g)	—	1
0.14–1.4 g (0.08–0.8 g)	1 + 9	10
1.4–14 g (0.8–8.0 g)	1 + 99	100

If the measured absorbance difference (ΔA) is too low (e.g. < 0.100), the sample solution should be prepared again (weigh out more sample or dilute less strongly) or the sample volume to be pipetted into the cuvette can be increased up to 2.000 ml. The volume of water added must then be reduced so as to obtain the same final volume in the cuvettes for the sample and blank. The new sample volume v must be taken into account in the calculation.

2. Technical information

2.1 Use only freshly distilled water for the assay.

2.2 Work in an atmosphere free from ammonia (ban smoking in the laboratory).

3. Specificity (Ref. 1)

The method is specific for urea and ammonia.

In the analysis of commercial urea and ammonium sulfate, results of approx. 100% have to be expected.

4. Sensitivity and detection limit (Ref. 1.4)

The smallest differentiating absorbance for the procedure is 0.005 absorbance units. This corresponds to a maximum sample volume v = 2.000 ml and measurement at 340 of a ammonia concentration of 0.02 mg/l sample solution, resp. of an urea concentration of 0.04 mg/l (if v = 0.100 ml, this corresponds to 0.4 mg ammonia/l, resp. 0.8 mg urea/l sample solution).

The detection limit of 0.08 mg ammonia/l, resp. 0.15 mg urea/l is derived from the absorbance difference of 0.020 (as measured at 340 nm) and a maximum sample volume v = 2.000 ml.

5. Linearity

Linearity of the determination exists from approx. 0.2 µg ammonia/assay (0.08 mg ammonia/l sample solution; sample volume v = 2.000 ml) to 8 µg ammonia/assay (0.08 g ammonia/l sample solution; sample volume v = 0.100 ml), resp. from 0.3 µg urea/assay (0.15 mg urea/l sample solution; sample volume v = 2.000 ml) to 14 µg urea/assay (0.14 g urea/l sample solution; sample volume v = 0.100 ml).

6. Precision

Ammonia:

In a double determination using one sample solution, a difference of 0.005 to 0.010 absorbance units may occur. With a sample volume of v = 0.100 ml and measurement at 340 nm, this corresponds to an ammonia concentration of approx. 0.4–1 mg/l. (If the sample is diluted during sample preparation, the result has to be multiplied by the dilution factor F. If the sample is weighed in for sample preparation, e.g. using 1 g sample/100 ml = 10 g/l, a difference of 0.004–0.01 g/100 g can be expected.)

The following data for the determination of ammonia have been published in the literature:

CV = 1.6%	(plasma)	(Ref. 1.2)
CV = 0.88–1.16%	(ammonium chloride solutions)	(Ref. 1.4)
CV = 0.34%	(ammonium chloride solutions)	
CV = 0.36–0.96%	(meat samples)	(Ref. 3.2)

Urea:

In a double determination using one sample solution, a difference of 0.005 to 0.015 absorbance units may occur. With a sample volume of v = 0.100 ml and measurement at 340 nm, this corresponds to an urea concentration of approx. 0.7–2 mg/l. (If the sample is diluted during sample preparation, the result has to be multiplied by the dilution factor F. If the sample is weighed in for sample preparation, e.g. using 1 g sample/100 ml = 10 g/l, a difference of 0.007–0.02 g/100 g can be expected.)

The following data for the determination of urea have been published in the literature:

CV = 2.7%	(serum)	(Ref. 1.1)
CV = 3%	(serum)	(Ref. 1.3)

Analysis of swimming-pool water (Lit. 3.7):

x = 0.611 mg/l	r = 0.1854 mg/l	$s_{(r)} = \pm 0.066$ mg/l
	R = 0.2145 mg/l	$s_{(R)} = \pm 0.076$ mg/l
x = 2.323 mg/l	r = 0.1247 mg/l	$s_{(r)} = \pm 0.044$ mg/l
	R = 0.1883 mg/l	$s_{(R)} = \pm 0.067$ mg/l
x = 5.749 mg/l	r = 0.0707 mg/l	$s_{(r)} = \pm 0.025$ mg/l
	R = 0.1707 mg/l	$s_{(R)} = \pm 0.060$ mg/l

7. Interference/sources of error

During protein precipitation with perchloric acid which is to be carried out in foodstuffs, protein fragments are occasionally obtained. These protein fragments are kept in solution and can gradually form ammonia in alkaline buffer systems leading to creep reactions. This formation of ammonia is very low and can be differentiated and calculated from the ammonia content of the sample by extrapolation of the absorbance A_2.

The common ingredients of foodstuffs do not interfere with the assay of urea and ammonia. Only high concentrations of tannins in fruit juices can cause an inhibition of the GIDH reaction. Fruit juices should therefore always be treated with PVPP.

As high concentrations of heavy metals cause turbidity they make also a reliable determination of urea and ammonia difficult. In most cases high concentrations of metal ions can be removed as hydroxides by alkalization of the sample solution (pH > 7.5).

Sodium thiosulfate, occasionally added to samples of swimming-pool water, does not interfere with the assay up to 1 mg per cuvette.

8. Recognizing interference during the assay procedure

8.1 If the conversion of urea and ammonia has been completed according to the time given under 'determination', it can be concluded in general that no interference has occurred.

8.2 On completion of the reaction, the determination can be restarted by adding urea and/or ammonium chloride or ammonium sulfate (qualitative or quantitative): if the absorbance is altered subsequent to the addition of the standard material, this is also an indication that no interference has occurred.

8.3 Operator error or interference of the determination through the presence of substances contained in the sample can be recognized by carrying out a double determination using two different sample volumes (e.g. 0.100 ml and 0.200 ml): the measured differences in absorbance should be proportional to the sample volumes used.

When analyzing solid samples, it is recommended that different quantities (e.g. 1 g and 2 g) be weighed into 100 ml volumetric flasks. The absorbance differences measured and the weights of sample used should be proportional for identical sample volumes.

8.4 Possible interference caused by substances contained in the sample can be recognized by using an internal standard as a control: in addition to the sample, blank and standard determinations, a further determination should be carried out with sample **and** standard solution in the same assay. The recovery can then be calculated from the absorbance differences measured.

8.5 Possible losses during the determination can be recognized by carrying out recovery tests: the sample should be prepared and analyzed with and without standard material. The additive should be recovered quantitatively within the error range of the method.

9. Reagent hazard

The reagents used in the determination of urea and ammonia are not hazardous materials in the sense of the Hazardous Substances Regulations, the Chemicals Law or EC Regulation 67/548/EEC and subsequent alteration, supplementation and adaptation guidelines. However, the general safety measures that apply to all chemical substances should be adhered to.

After use, the reagents can be disposed of with laboratory waste, but local regulations must always be observed. Packaging material can be disposed of in waste destined for recycling.

10. General information on sample preparation

In carrying out the assay:

Use **clear, colorless and practically neutral liquid samples** directly, or after dilution according to the dilution table, and of a volume up to 2.000 ml;

Filter **turbid solutions**;

Degas **samples containing carbon dioxide** (e.g. by filtration);

Adjust **acid samples** to approx. pH 7–8 by adding sodium or potassium hydroxide solution;

Adjust **acid and weakly colored samples** to approx. pH 7–8 by adding sodium or potassium hydroxide solution and incubate for approx. 15 min;

Treat **'strongly colored' samples** that are used undiluted or with a higher sample volume with polyvinylpolypyrrolidone (PVPP), e.g. 2.5–5 g/100 ml;

Crush or homogenize **solid or semi-solid samples,** extract with water or dissolve in water and filter if necessary;

Deproteinize **samples containing protein** with perchloric acid or with trichloroacetic acid;

Extract **samples containing fat** with hot water (extraction temperature should be above the melting point of the fat involved). Cool to allow the fat to separate, make up to the mark, place the volumetric flask in an ice bath for 15 min and filter;

Break up **emulsions** with trichloroacetic acid.

Important note

The Carrez-clarification should not be used in the sample preparation for urea/ammonia determination due to a too low recovery rate (adsorption of urea/ammonia).

11. Application examples

Determination of ammonia in fruit juices

Add 0.5–1.0 g polyvinylpolypyrrolidone (PVPP) to 10 ml fruit juice (clear, turbid or colored juices) – when the sample volume is increased, neutralize, if necessary, and fill up to 20 ml with water – into a beaker and stir for 1 min (magnetic stirrer). Filter sample solution immediately and use it for the assay.

In the assay, only "blank ammonia" and "sample ammonia" are measured.

Determination of urea and ammonia in water (swimming-pool water)

Dilute the clear sample solution according to the dilution table or use up to v = 2.000 ml sample volume for the assay.

Determination of urea in milk

Mix 1 ml milk with 4 ml trichloroacetic acid (0.3 mol/l). After approx. 5 min centrifuge for separation of the precipitate (for 3 min, ca. 4000 rpm). Use 0.100 ml of the supernatant clear solution for the assay.

Determination of ammonia in milk

Mix 1 ml milk with 4 ml trichloroacetic acid (0.3 mol/l). After approx. 5 min centrifuge for separation of the precipitate. Decant the supernatant and neutralize with KOH (10 mol/l) (dilution factor can be neglected due to the high concentration of KOH), filter and use 1.000–2.000 ml sample solution for the assay.

In the assay, only "blank ammonia" and "sample ammonia" are measured.

Determination of ammonia in bakery products

Accurately weigh approx. 10 g of the minced sample into a homogenizer beaker, add approx. 20 ml perchloric acid (1 mol/l) and homogenize for approx. 2 min. Proceed as stated under "meat and meat products". Use at most 1.000 ml for the assay.

In the assay only "blank ammonia" and "sample ammonia" are to be measured.

Determination of urea and ammonia in meat and meat products

Accurately weigh approx. 5 g of the homogenized sample (from a sample of 100 g, that has been ground and homogeneously mixed in a mixer) into a homogenizer beaker, add approx. 20 ml perchloric acid (1 mol/l) and homogenize for approx. 2 min. Transfer the contents quantitatively with approx. 40 ml water into a beaker. Adjust to pH 7.0 (< 7.5) first with potassium hydroxide (5 mol/l) and then exactly with potassium hydroxide (2 mol/l). Transfer the contents quantitatively with water into a 100 ml volumetric flask, fill up to the mark with water, whereby care must be taken that the fatty layer is above the mark and the aqueous layer is at the mark.

For separation of fat and for precipitation of the potassium perchlorate refrigerate for 20 min. Afterwards filter. Discard the first few ml. Use the clear, possibly slightly turbid solution for the assay.

Calculation of the amount of urea and ammonia according to the aforementioned calculation formula, whereby it must be multiplied with the volume displacement factor K = 0.98.

12. Further applications

The method may also be used in the examination of fertilizers, pharmaceuticals, cosmetics, paper (Ref. 2.1) and in research when analyzing biological samples. For details of sampling, treatment and stability of the sample see Ref. 1.1–1.4.

Examples:

12.1 Determination of urea and ammonia in fertilizers

Grind approx. 10 g of the sample and mix thoroughly. Accurately weigh approx. 100 mg of the homogeneous material into a 100 ml beaker and add approx. 50 to 60 ml water. Adjust to pH 7–8 with diluted hydrochloric acid (1 mol/l) or in the case of acidic fertilizer with diluted sodium hydroxide (1 mol/l). Warm on a heatable magnetic stirrer for approx. 10 min to 60–70°C. Allow to cool, transfer quantitatively into a 100 ml volumetric flask and fill up to the mark with water. Mix the solution and filter, if necessary.

Use 0.100 ml of the clear solution diluted, if necessary, for the assay.

12.2 Determination of nitrogen after Kjeldahldigestion

The determination of total nitrogen can be obtained via the ammonia determination in a sample mineralized according to the Kjeldahl-method. Normally, the samples have to be incinerated wet (sulfuric acid). The ammonia, formed from nitrogen, is determined according to the procedure as follows.

Accurately weigh approx. 2 g of the ground and homogenized sample into a 100 ml Kjeldahl-flask, add 20 ml sulfuric acid (specific gravity = 1.84 g/ml) and approx. 30 mg catalyst mixture (e.g. acc. to Wieninger) or one Kjeldahl tablet, heat for approx. 2–3 h until the sample is disintegrated (yellowish or blue-greenish solution). Allow the sample to cool and carefully (protective glasses) transfer quantitatively into a beaker filled with 600 ml ice-cold water while stirring all the time (magnetic stirrer, icebath). Neutralize with approx. 60 ml KOH (10 mol/l) (pH 6–8). Transfer the neutralized solution quantitatively into a 1 l volumetric flask, fill up to the mark with water and mix. If necessary, filter the mixture (sometimes necessary after disintegration with Kjeldahl tablets); discard the first few ml. Use the solution diluted, if necessary, for the assay.

Calculation:

Nitrogen content of the sample (in %)

$$= \frac{\Delta A \times V \times MW \times 100}{\varepsilon \times d \times v \times 1000 \times \text{amount weighed [g]}}$$

$$= \frac{\Delta A \times 3.04 \times 14.01 \times 100}{\varepsilon \times 1.00 \times 0.100 \times 1000 \times \text{amount weighed [g]}}$$

12.3 Determination of urea in urine

Dilute urine according to the dilution table with physiological sodium chloride solution (dilution factor = F).

12.4 Determination of urea in serum and plasma (Ref. 1.1, 1.3)

Dilute serum or plasma, respectively, according to the dilution table with physiological sodium chloride solution (dilution factor = F) and use for the assay.

Calculation:

$$c = \frac{0.9129 \times \Delta A \times F}{\varepsilon} \text{ [g urea/l sample]}$$

$$c = \frac{15.2 \times \Delta A \times F}{\varepsilon}\ [\text{mmol urea/l sample}]$$

Wavelength	Hg 365 nm	340 nm	Hg 334 nm
c [g/l]	0.2685 x ΔA x F	0.1449 x ΔA x F	0.1477 x ΔA x F
c [mmol/l]	4.471 x ΔA x F	2.413 x ΔA x F	2.460 x ΔA x F

12.5 Determination of urea and ammonia in fermentation samples and cell culture media

Place the sample (after centrifugation, if necessary) in a waterbath at 80 °C for 15 min to stop enzymatic reactions. Centrifuge and use the supernatant (diluted according to the dilution table, if necessary) for the assay. Alternatively, deproteinization can be carried out with perchloric acid. See the above-mentioned examples.

Homogenize gelatinous agar media with water and treat further as described.

References

1.1 Gutmann, I. & Bergmeyer, H. U. (1974) in Methoden der enzymatischen Analyse (Bergmeyer, H. U. Hrsg.) 3. Aufl., Bd. 2, S. 1842–1845, Verlag Chemie, Weinheim and (1974) in Methods of Enzymatic Analysis (Bergmeyer, H. U. ed.) 2nd ed., vol. 4, pp. 1794–1798, Verlag Chemie, Weinheim/Academic Press, Inc., New York and London

1.2 da Fonseca-Wollheim, F., Bergmeyer, H. U. & Gutmann, I., (1974) in Methoden der enzymatischen Analyse (Bergmeyer, H. U. Hrsg.) 3. Aufl., Bd. 2, S. 1850–1853, Verlag Chemie, Weinheim and
(1974) in Methods of Enzymatic Analysis (Bergmeyer, H. U. ed.) 2nd ed., vol. 4, pp. 1802–1806, Verlag Chemie, Weinheim/Academic Press, Inc., New York and London

1.3 Kerscher, L. & Ziegenhorn, J. (1985) in Methods of Enzymatic Analysis (Bergmeyer, H. U., ed.) 3rd. ed., vol. VIII, pp. 444–453, Verlag Chemie Weinheim, Deerfield Beach/Florida, Basel

1.4 Bergmeyer, H. U. & Beutler, H.-O. (1985) in Methods of Enzymatic Analysis (Bergmeyer, H. U., ed.) 3rd ed., vol. VIII, pp. 454–461, Verlag Chemie Weinheim, Deerfield Beach/Florida, Basel

2.1 Untersuchung von Papieren, Kartons und Pappen für die Lebensmittelverpackungen (gem. Empfehlungen XXXVI der Kunststoffkommission des Bundesgesundheitsamtes) Kapitel 8 (Methoden) Pkt. 3.4.2 (Ammoniak) und Pkt. 3.5.2. (Harnstoff); März 1979

2.2 Gornbocz, E., Hellwig, E., Vojir, F. & Petuely, F. (1981) Deutsche Lebensmittel-Rundschau 77, 9 (Harnstoff)

2.3 Brautechnische Analysenmethoden, Band III, S. 597–599 (1982), Bestimmung von Ammoniak, Methodensammlung der Mitteleuropäischen Brautechnischen Analysenkommission (MEBAK), herausgegeben von F. Drawert im Selbstverlag der MEBAK, Freising

2.4 Nederlandse Norm, Water: Enzymatische bepaling van het gehalte aan ureum in zwemwater, NEN 6494, Juni 1984 (Water-Enzymatic determination of urea in swimming water)

3.1 Höpner, Th. (1977) Enzymatische Methoden in der Wasseranalytik – Möglichkeiten und Grenzen, Vom Wasser 49, 173–182

3.2 Gerhardt, U. & Quang, T. D. (1979) Methoden zur Ammoniakbestimmung in Fleisch und Fleischerzeugnissen, Fleischwirtschaft 59, 946–948

3.3 Erbersdobler, H. & Zucker, H. (1980) Harnstoff-Gehalt der Milch – ein Indikator der Proteinversorgung von Milchkühen, Kraftfutter 63, 10–12

3.4 Wolfschoon-Pombo, A., Klostermeyer, H., Buchberger, J. & Graml, R. (1981) Harnstoff in der NPN-Fraktion der Kuhmilch – Bestimmung, Vorkommen und Beeinflussung, Milchwissenschaft 36, 462–466

3.5 Barchietto, G., Cantoni, C., Frigerio, R. & Provera, D. (1984) Esame comparativo dei prodotti di autolisi nella carne di maiale (Azoto non proteico, Urea, Ammoniaca), Conservazione degli Alimenti 3, 12–17

3.6 Cheuk, W. L. & Finne, G. (1984) Enzymatic Determination of Urea and Ammonia in Refrigerated Seafood Products, J. Agric. Food Chem. 32, 14–18.

3.7 Kohler, P. (1985) Ringversuch für die enzymatische Bestimmung von Harnstoff in Badewasser, Mitt. Gebiete Lebensm. Hyg. 76, 470–477

3.8 Pasquier, J.-M. & Grandjean, L. (1985) Méthode de dosage de l'urée dans l'eau de piscine, Trav. chim. aliment. hyg. 76, 464–469

3.9 Buchberger, J., Weiß, G. & Graml, R. (1988) Untersuchungen zum Orotsäure- und Harnstoffgehalt der Milch; I. Teil: Orotsäuregehalt, dmz deutsche molkerei-zeitung 37, 1128–1133; II. Teil: Harnstoffgehalt, dmz deutsche molkerei-zeitung 38, 1167–1169

3.10 Bartels, U. (1991) Die enzymatische Bestimmung von Ammonium im Niederschlagswasser, CLB Chemie in Labor und Biotechnik 42, 377–382

Urea standard solution

The standard solution serves as a control for the enzymatic determination of urea in foodstuffs and other materials.

Reagents
Urea, AR grade

Preparation of the standard solution
Accurately weigh approx. 140 mg urea to the nearest 0.1 mg into a 1000 ml volumetric flask, fill up to the mark with redist. water, and mix thoroughly.

Prepare standard solution freshly before use. The standard solution may be frozen in portions.

Application
1. Addition of urea solution to the assay mixture:
Instead of sample solution the standard solution is used for the assay.

2. Restart of reaction, quantitatively:
After completion of the reaction with sample solution and measuring A_2, add 0.050 ml standard solution to the assay mixture. Read absorbance A_3 after the end of the reaction (approx. 20 min).
Calculate the concentration from the difference $(A_2 - A_1)$ according to the general equation for calculating the concentration. The altered total volume must be taken into account. Because of the dilution of the assay mixture by the addition of the standard solution, the result differs insignificantly from the result got according to pt. 1.

3. Internal standard:
The standard solution can be used as internal standard in order to check the determination for correct performance (gross errors) and to see whether the sample solution is free from interfering substances:

Pipette into cuvettes:	Blank	Sample	Standard	Sample + Standard
reaction mixture 2	1.000 ml	1.000 ml	1.000 ml	1.000 ml
sample solution	–	0.100 ml	–	0.050 ml
standard solution	–	–	0.100 ml	0.500 ml
solution 3	0.020 ml	0.020 ml	0.020 ml	0.020 ml
redist. water	2.000 ml	1.900 ml	1.900 ml	1.900 ml

Mix, and read absorbances of the solutions (A_1) after approx. 5 min. Continue as described in the pipetting scheme under „Procedure". Follow the instructions given under „Instructions for performance of assay" and the footnotes.

The recovery of the standard is calculated according to the following formula:

$$\text{recovery} = \frac{2 \times \Delta A_{\text{sample + standard}} - \Delta A_{\text{sample}}}{\Delta A_{\text{standard}}} \times 100\ [\%]$$

BOEHRINGER MANNHEIM

0698.3045.1 748 530 13

With coutesy: Boehringer Mannheim, FRG.

Ethanol

1 UV-method

for the determination of ethanol in foodstuffs and other materials

Simplified procedure for the determination of ethanol in alcoholic beverages see pt. 1.2.

0
3
5

Cat. No. 176 290

Test-Combination for ca. 30 determinations

Enzymatic BioAnalysis
Food Analysis

Not for use in *in vitro* diagnostic procedures for clinical diagnosis.

Recommendations to methods and standardized procedures see references.

Principle (Ref. 1,2)
Ethanol is oxidized to acetaldehyde in the presence of the enzyme alcohol dehydrogenase (ADH) by nicotinamide-adenine dinucleotide (NAD) (1).

(1) Ethanol + NAD$^+$ $\xrightleftharpoons{\text{ADH}}$ acetaldehyde + NADH + H$^+$

The equilibrium of this reaction lies on the side of ethanol and NAD. It can, however, be completely displaced to the right at alkaline conditions and by trapping of the acetaldehyde formed. Acetaldehyde is oxidized in the presence of aldehyde dehydrogenase (Al-DH) quantitatively to acetic acid (2).

(2) Acetaldehyde + NAD$^+$ + H_2O $\xrightarrow{\text{Al-DH}}$ acetic acid + NADH + H$^+$

NADH is determined by means of its absorbance at 334, 340 or 365 nm.

The Test-Combination contains

1. Bottle 1 with approx. 100 ml solution, consisting of: potassium diphosphate buffer, pH 9.0; stabilizers.
2. Bottle 2 with approx. 30 tablets, each tablet contains: NAD, approx. 4 mg; aldehyde dehydrogenase, 0.8 U; stabilizers.
3. Bottle 3 with approx. 1.6 ml enzyme suspension, consisting of: ADH, 7000 U; stabilizers.
4. Ethanol standard solution.

Preparation of solutions

1. Use contents of bottle 1 undiluted.
2. Dissolve one tablet of bottle 2 with 3 ml solution of bottle 1 in a beaker or in a centrifuge tube for each assay (blank or samples) depending on the number of determinations. Use forceps for taking the tablets out of bottle 2. This results in reaction mixture 2*.
3. Use contents of bottle 3 undiluted.

Stability of solutions

Solution 1 is stable for one year at +4°C.
Bring solution 1 to 20–25°C before use.
Reaction mixture 2 is stable for one day at +4°C.
Bring reaction mixture 2 to 20–25°C before use.
Contents of bottle 3 are stable for one year at +4°C.

Procedure

Wavelength[1]: 340 nm, Hg 365 nm or Hg 334 nm
Glass cuvette[2]: 1 cm light path
Temperature: 20–25°C
Final volume: 3.15 ml
Read against air (without a cuvette in the light path), against water or against blank[3].
Sample solution: 0.5–12 µg ethanol/cuvette[4] (in 0.1–0.5 ml sample volume)

Pipette into cuvettes	blank	sample
reaction mixture 2*	3.00 ml	3.00 ml
redist. water	0.10 ml	–
sample solution**	–	0.10 ml
mix***, after approx. 3 min read absorbances of the solutions (A_1). Start reaction by addition of		
suspension 3	0.05 ml	0.05 ml
mix***, after completion of the reaction (approx. 5–10 min) read absorbances of the solutions immediately one after another (A_2).		

It is absolutely necessary to stopper the cuvettes, e.g., with Parafilm*, during measurement (see "Instructions for performance of assay").

* For simplification of the assay performance it is also possible to pipette directly 3 ml of solution 1 into the cuvette. Afterwards add 1 tablet of bottle 2 and dissolve it (for solubilization crush the tablet with a glass rod, if necessary). Continue as described in the scheme. The volume error of approx. 1% (the increase of volume caused by one tablet/3.15 ml final volume) has to be taken into account in the calculation by multiplication of the result with 1.01.

** Rinse the enzyme pipette or the pipette tip of the piston pipette with sample solution before dispensing the sample solution.

*** For example, with a plastic spatula or by gentle swirling after closing the cuvette with Parafilm* (registered trademark of the American Can Company, Greenwich, Ct., USA).

Determine the absorbance differences (A_2–A_1) for both blank and sample. Subtract the absorbance difference of the blank from the absorbance difference of the sample.

$$\Delta A = \Delta A_{sample} - \Delta A_{blank}$$

The absorbance differences measured should as a rule be at least 0.100 absorbance units to achieve sufficiently accurate results (see "Instructions for performance of assay").

Calculation
According to the general equation for calculating the concentration in reactions in which the amount of NADH formed is stoichiometric with half the amount of substrate:

$$c = \frac{V \times MG}{\varepsilon \times d \times v \times 2 \times 1000} \times \Delta A \text{ [g/l], where}$$

V = final volume [ml]
v = sample volume [ml]
MW = molecular weight of the substance to be assayed [g/mol]
d = light path [cm]
ε = absorption coefficient of NADH at:
340 nm = 6.3 [l x mmol^{-1} x cm^{-1}]
Hg 365 nm = 3.4 [l x mmol^{-1} x cm^{-1}]
Hg 334 nm = 6.18 [l x mmol^{-1} x cm^{-1}]

It follows for ethanol:

$$c = \frac{3.15 \times 46.07}{\varepsilon \times 1 \times 0.1 \times 2 \times 1000} \times \Delta A = \frac{0.7256}{\varepsilon} \times \Delta A \text{ [g ethanol/l sample solution]}$$

If the sample has been diluted during preparation, the result must be multiplied by the dilution factor F.

When analyzing solid and semi-solid samples which are weighed out for sample preparation, the result is to be calculated from the amount weighed:

$$\text{content}_{ethanol} = \frac{c_{ethanol} \text{ [g/l sample solution]}}{c_{sample} \text{ [g/l sample solution]}} \times 100 \text{ [g/100 g]}$$

1 The absorption maximum of NADH is at 340 nm. On spectrophotometers, measurements are taken at the absorption maximum; when spectralline photometers equipped with a mercury vapour lamp are used, measurements are taken at a wavelength of 365 nm or 334 nm.
2 If desired, disposable cuvettes may be used instead of glass cuvettes.
3 For example, when using a double-beam photometer.
4 See instructions for performance of the assay

Instructions for performance of assay

The amount of ethanol present in the cuvette should range between 1 µg and 12 µg (measurement at 365 nm) or 0.5 µg and 6 µg (measurement at 340, 334 nm), respectively. The sample solution must therefore be diluted sufficiently to yield an ethanol concentration between 0.01 and 0.12 g/l or 0.005 and 0.06 g/l, respectively.

Because of the high sensitivity of the method it has to be taken care that ethanol free water is used and it is worked in an ethanol free atmosphere.

Dilution table

estimated amount of ethanol per liter measurements at		dilution with water	dilution factor F
340 or 334 nm	365 nm		
< 0.06 g	< 0.12 g	–	1
0.06–0.6 g	0.12–1.2 g	1 + 9	10
0.6 –6.0 g	1.2 –12 g	1 + 99	100
6.0 –60 g	12 –120 g	1 + 999	1000
> 60 g	> 120 g	1 + 9999	10000

Because of the volatility of ethanol, the dilution of samples should be carried out as follows:

Fill the volumetric flask half with water and pipette the sample with an enzyme test pipette or a piston type pipette under the surface of the water. Fill up to the mark with water and mix.

If the absorbance difference measured (ΔA) is too low (e.g. < 0.100), the sample solution should be prepared anew (weigh out more sample or dilute less strongly) or the sample volume to be pipetted into the cuvette can be increased up to 0.5 ml. The volume of solution 1 or reaction mixture 2, respectively, remains the same (3.00 ml). The volume of water pipetted into the blank cuvette must then be increased so as to obtain the same final volume for the sample and blank in the cuvettes. The new sample volume (v) and the new final volume (V) must be taken into account in the calculation.

1. Instructions for sample preparation

1.1. Liquid foodstuffs

Use clear, colorless or slightly colored solutions directly or after dilution according to the dilution table for the assay. Filter turbid solutions or clarify with Carrez reagents. Strongly colored solutions, which are used undiluted for the assay because of their low ethanol concentration, are to be decolorized with polyamide or polyvinylpolypyrrolidone (PVPP). Carbonic acid containing beverages are to be degassed, beverages with low ethanol content should be adjusted to the alkaline pH range. During the whole procedure it is to be taken care that the ethanol is not evaporated. For example, when diluting an ethanol containing sample, it is to be pipetted under the surface of the water.

Examples:

Determination of ethanol in fruit juices

a) Use clear light juices after neutralization or dilution, depending on the ethanol content, for the assay (see dilution table).

b) Decolorize intensely colored juices by addition of 2% polyamide or polyvinylpolypyrrolidone (PVPP) (e.g. 5 ml juice + 100 mg polyamide or PVPP), stir for 2 min (vessel must be stoppered) and filter. Use the mostly clear solution after neutralization for the assay. Decolorization can often be omitted on dilution.

c) Filter turbid juices and clarify with Carrez-solutions, if necessary: Pipette 10 ml of juice into a 25 ml volumetric flask, add 1.25 ml Carrez-I-solution (3.60 g potassium hexacyanoferrate-II, $K_4[Fe(CN_6)] \cdot 3\ H_2O$/100 ml), 1.25 ml Carrez-II-solution (7.20 g zinc sulfate, $ZnSO_4 \cdot 7\ H_2O$/100 ml) and 2.50 ml NaOH (0.1 mol/l), shake vigorously after each addition, dilute to 25 ml with water, filter (dilution factor F = 2.5). Use the clear sample solution, which may be weakly opalescent, for the assay directly or diluted, if necessary.

Determination of ethanol in alcohol-deficient and alcohol-free beer

Add solid potassium hydroxide or solid sodium hydroxide to approx. 100 ml sample in a beaker while stirring carefully until a pH value of approx. pH 8–9 is obtained. Use solution, diluted according to the dilution table, if necessary, for the assay.

Determination of ethanol in vinegar

Filter, if necessary and neutralize vinegar. Neutralization can be omitted on dilution.

Determination of ethanol in alcoholic beverages

a) *Wine* (Ref. 14): Dilute wine with redist. water to the appropriate concentration (see dilution table). Decolorization and neutralization are not necessary.

b) *Beer:* To remove carbonic acid, stir approx. 5–10 ml of beer in a beaker for approx. 30 s using a glass rod or filter. Dilute the sample 1 : 1000 (1 + 999) with water and use the diluted sample solution for the assay.

c) *Liqueur:* Pipette liquid liqueurs for dilution into an appropriate volumetric flask and fill up with water to the mark. Weigh approx. 1 g of viscous liqueurs (e.g. egg liqueur) accurately into a 100 ml volumetric flask, fill up to the mark with redist. water, keep it in a refrigerator for separation of fat, and filter. Dilute the clear solution 1 : 100 (1 + 99) with water and use it for the assay.

d) *Brandy:* Take care as mentioned for taking the sample of alcoholic beverages and dilute to a certain concentration (e.g. 1 + 9999). Convert the measured values (g ethanol/l solution) into volume percentage (v/v) with the aid of conversion tables.

1.2. Simplified determination of ethanol in beer, wine (Ref. 14) and brandy

Sample preparation

Dilute beer, wine and brandy according to the dilution table.

Reagent solution for 10 determinations

Dissolve 10 tablets of bottle 2 with 30 ml solution from bottle 1, add 0.5 ml suspension from bottle 3, and mix.
(Attention: Prepare reagent solution with alcohol-free water in alcohol-free atmosphere. Store in a container tightly stoppered.)

Stability

The reagent solution is stable for 8 h at 20°C.

Procedure

Pipette 3.00 ml reagent solution into the cuvette and read absorbance A_1. Start reaction by addition of 0.1 ml diluted sample. On completion of the reaction (approx. 5 min) read absorbance A_2. Determine absorbance difference of $A_2 - A_1 = \Delta A$.

Calculation

$$c = \frac{0.714}{\varepsilon} \cdot \Delta A \cdot F \text{ [g ethanol/l sample]}$$

F = dilution factor

1.3. Pasty foodstuffs

Homogenize semi-solid samples, extract with water or dissolve, respectively, and filter, if necessary. Clarify with Carrez-solutions or decolorize.

Examples:

Determination of ethanol in chocolates, sweets and other alcoholcontaining chocolate products

Chocolates with liquid filling compound (brandy balls, brandy cherries):

Open, e.g., one brandy ball carefully, pipette 0.50 ml of the liquid filling into a 50 ml volumetric flask filled with approx. 25 ml water, taking care that the tip of the pipette dips into the water. Fill up to the mark with water, stopper and mix. Dilute the solution with water in a ratio of 1 : 20 (1 + 19). Use 0.1 ml of the diluted solution for the assay (dilution factor F = 2000).

Chocolate products with highly viscous filling:

Weigh accurately the filling of one or several sweets or chocolates into a 50 ml volumetric flask filled with approx. 5 ml water (when the sample is weighed by means of a pipette, the tip of the pipette must **not** touch the water surface). Fill up to the mark with water, mix, filter, if necessary, and dilute until the alcohol content of the sample is less than 0.12 g/l.

Determination of ethanol in jam

Homogenize sample thoroughly (mixer, etc.) and weigh approx. 10–20 g into a beaker. Add some water, mix and neutralize the mixture with KOH, if necessary. Transfer the mixture quantitatively into a 100 ml volumetric flask and fill up to the mark with redist. water.

Decolorize solution with 2% polyamide or PVPP, if necessary (see "Instructions 1.1.b") and filter. Use the filtrate for the assay undiluted.

Determination of ethanol in honey

Weigh approx. 20 g honey accurately into a 100 ml volumetric flask and dissolve with some water under slightly agitation at approx. 50 °C (ascending tube!), cool to room temperature and fill up to the mark with redist. water. Use the solution for the assay, clarify with Carrez-solutions (see "Instructions 1.1.c"), if necessary (dilution factor F = 2.5). Use the clear solution for the assay after filtration.

Determination of ethanol in dairy products (e.g. curds, kefir)

Weigh approx. 10 g of the homogenized sample accurately into a 100 ml volumetric flask, add approx. 50 ml water and keep the flask (ascending tube!) at 50°C for 15 min under slightly agitation. For protein precipitation add 5 ml Carrez-I-solution, 5 ml Carrez-II-solution and 10 ml NaOH (0.1 mol/l) (see "Instructions 1.1.c"), shake vigorously after each addition. Allow to cool to room temperature and fill up to the mark with water. Mix and filter. Use the clear, possibly slightly turbid solution for the assay.

1.4. Solid foodstuffs

Homogenize solid or semi-solid samples (using a mortar, etc.), extract with water or dissolve; filter, if necessary.

Extract fat-containing samples with warm water (approx. 50°C) in a small flask with ascending tube. Allow to cool for separation of fat, rinse the ascending tube with water and filter.

Deproteinize protein-containing sample solutions with perchloric acid (1 mol/l) in a ratio of 1 : 3 (1 + 2) and centrifuge. Neutralize with KOH (2 mol/l).

2. Specificity

The influence of aldehydes and ketones is eliminated by the order of reagent addition during the assay. Methanol is not converted because of the unfavourable K_m-values of the used enzymes.
n-Propanol and n-butanol is quantitatively converted under assay conditions, higher primary alcohols lead to sample dependent creep reactions. Secondary, tertiary and aromatic alcohols do not react. Even higher concentrations of glycerol do not disturb the assay.

3. Sources of error

The presence of ethanol in the used redist. water or in air results in increased blanks or in creep reactions, respectively. Therefore it is necessary to cover the cuvette during the assay.

Detection of interferences of the test system

When the enzymatic reaction is complete after the time given in "Procedure" it can be concluded in general that the reaction is not interfered. For assurance of results a re-start of the reaction (qualitatively or quantitativeiy) by the addition of 'standard material' can be done: a further change of absorbance proves suitability of measurements.

For the detection of gross errors when performing the assays and of interfering substances in the sample material it is recommended to analyze a sample solution in a double determination with two different sample volumes (e.g. 0.10 ml and 0.20 ml): the measured absorbance differences have to be proportional to the sample volumes.

When analyzing solid samples it is recommended to weigh in two different amounts (e.g. 1 g and 2 g) into a 100 ml volumetric flask and to perform the determinations with the same sample volume: the absorbance differences have to be proportional to the amounts weighed in.

4. Further applications (s. References)

The method may also be used in the examination of cosmetics, pharmaceuticals, and in research when analyzing biological samples.

For details of sampling, treatment and stability of the sample see Bernt, E. & Gutmann, I. (1974) in Methods of Enzymatic Analysis (Bergmeyer, H. U., ed.) 2nd ed. vol. 3, p. 1500, Verlag Chemie, Weinheim, Academic Press, Inc. New York and London.

Examples:

4.1. Determination of ethanol in blood, plasma or serum, respectively (Ref. 2)

Mix 0.5 ml blood with 4.0 ml ice-cold perchloric acid (0.33 mol/l) and centrifuge. Use 0.1 ml for the assay.

The dilution factor F (depending on sample preparation) is obtained from the sample volume (0.5 ml), the perchloric acid volume (4.0 ml), the specific gravity of the sample material (1.06 g/ml blood, 1.03 g/ml plasma or serum) and the fluid content (0.80 in case of blood and 0.92 in case of plasma or serum):

$$F_{blood} = \frac{0.5 \times 1.06 \times 0.80 + 4.0}{0.5} = 8.85$$

$$F_{plasma,\ serum} = \frac{0.5 \times 1.03 \times 0.92 + 4.0}{0.5} = 8.95$$

Calculation:

$$c = \frac{0.7256 \times \Delta A \times F}{\varepsilon}\ [\text{g ethanol/l sample}]$$

$$c = \frac{15.75 \times \Delta A \times F}{\varepsilon}\ [\text{mmol ethanol/l sample}]$$

Ethanol in blood:

Wavelength	Hg 365 nm	340 nm	Hg 334 nm
c [g/l]	1.889 x ΔA	1.019 x ΔA	1.039 x ΔA
c [mmol/l]	41.00 x ΔA	22.13 x ΔA	22.55 x ΔA

Ethanol in plasma or serum, respectively:

Wavelength	Hg 365 nm	340 nm	Hg 334 nm
c [g/l]	1.910 x ΔA	1.031 x ΔA	1.051 x ΔA
c [mmol/l]	41.46 x ΔA	22.38 x ΔA	22.81 x ΔA

4.2. Determination of ethanol in urine (Ref. 12)

Dilute urine with bidest. water according to the dilution table. Use the diluted sample for the assay (dilution factor = F).

Calculation:

$$c = \frac{0.7256 \times \Delta A \times F}{\varepsilon}\ [\text{g ethanol/l sample}]$$

$$c = \frac{15.75 \times \Delta A \times F}{\varepsilon}\ [\text{mmol ethanol/l sample}]$$

Wavelength	Hg 365 nm	340 nm	Hg 334 nm
c [g/l]	0.2134 x ΔA x F	0.1152 x ΔA x F	0.1174 x ΔA · F
c [mmol/l]	4.632 x ΔA x F	2.500 x ΔA x F	2.549 x ΔA x F

4.3. Determination of ethanol in fermentation samples and cell culture media

Place the sample (after centrifugation, if necessary) into a waterbath at 80°C for 15 min (cover the tube because of the volatility of ethanol) to stop enzymatic reactions. Centrifuge and use the supernatant (diluted according to the dilution table, if necessary) for the assay. Alternatively, deproteinization can be carried out with perchloric acid or with Carrez-solutions. See the above-mentioned examples.

Homogenize gelatinous agar media with water and treat further as described.

5. Technical instructions

1. Ethanol is very volatile. Therefore it is necessary to be very careful when handling ethanol containing samples, diluting samples and pipetting sample solutions into the assay system.

When filtering solutions the filtrate should not drop into the container but rinse down the wall.

When dispensing ethanol containing solutions, always pipette these solutions under the surface of water (when diluting) or of buffer (when performing the assay).

2. When pipetting highly diluted sample solutions into the assay system, rinse measuring glass pipet (enzyme test pipet) at least 5 times. The tip of the piston type pipet should be rinsed 3 times.

3. Do not use the same piston type pipet for diluting the sample and pipetting the sample solution into the assay system.

4. Always work in alcohol-free atmosphere with ethanol-free water.

References

1 Beutler, H.-O. & Michal, G. (1977) Neue Methode zur enzymatischen Bestimmung von Ethanol in Lebensmitteln, Z. Anal. Chem. **284**, 113–117.
2 Beutler, H. O. (1984) in Methods of Enzymatic Analysis (Bergmeyer, H.U., ed.) 3rd ed., vol. VI, pp. 598–606, Verlag Chemie, Weinheim, Deerfield Beach/Florida, Basel.
3 Schweizerisches Lebensmittelbuch (1981) Kapitel 61B/2.1.
4 Gondorf, F., Hellwig, E., Vojir, F. & Petuely, F. (1981) Deutsche Lebensmittel Rundschau **77**, 8.
5 Bucher, T. & Redetzki, H. (1951) Eine spezifische photometrische Bestimmung von Ethylalkohol auf fermentativem Wege, Klinische Wochenschrift **29**, 615–616.
6 Tanner, H. & Brunner, F. M. (1965) Zur Bestimmung des in alkoholfreien Getränken und in Aromadestillaten enthaltenen Ethylalkohols, Mitt. Gebiete Lebensm. Unters. u. Hyg. **56**, 480–487.
7 Quast, P. (1978) Weitere Notwendigkeiten und Möglichkeiten der Fruchtanalyse beim Apfel, Mitt. Obstbauversuchsring des Alten Landes **9**, 293–301.
8 Henniger, G. & Boos, H. (1978) Anwendung der enzymatischen Analyse bei der Untersuchung kosmetischer Präparate dargestellt an einigen Beispielen, Seifen - Öle - Fette - Wachse **104**, 159–164.
9 Henniger, G. & Hoch, H. (1981) Enzymatische Substratbestimmungen in der pharmazeutischen Analytik, dargestellt an den Bestimmungen von L-Ascorbinsäure, Ethanol und Lactose, Deutsche Apotheker Zeitung **121**, 643–649.
10 Kohler, P. (1982) Enzymatische Ethanol-Bestimmung in Glace- und Schokoladeprodukten, Mitt. Gebiete Lebensm. Hyg. **73**, 44–49.
11 Jung, G. & Férard, G. (1978) Enzyme-coupled measurement of ethanol in whole blood and plasma with a centrifugal analyzer, Clin. Chem. **24**, 873–876.
12 Beutler, H.-O. (1985) unpublished results.
13 Pfandl, A. & Menschig, D. (1984) Ein Beitrag zur enzymatischen Glycerin- und Ethanolbestimmung, Pharm. Ind. **46**, 403–407.
14 Die Methode ist zugelassen bei der Untersuchung von Wein im Rahmen der Qualitätsweinprüfung in Rheinland-Pfalz (1985; Landwirtschaftskammer Bad Kreuznach) und in Hessen (1986; Ministerium für Landwirtschaft und Forsten). The use of the method is admitted for the investigation of wine within quality wine examination in Rheinland-Pfalz (1985; Landwirtschaftskammer Bad Kreuznach) and in Hessen (1986; Ministerium für Landwirtschaft und Forsten).
15 Buckee, G.K. & Baker, C.D. (1986) Enzymatic Determination of Ethanol in Alcohol-Free and Low Alcohol Beers, Monatsschrift für Brauwissenschaft **39**, 257–259.

Ethanol-standard solution

for the Test-Combination Ethanol
UV-method, Cat. No. 176290

Concentration
see bottle label.
Ethanol standard solution is a stabilized aqueous solution of ethanol. It serves as standard solution for the enzymatic analysis of ethanol in foodstuffs and other materials.

Application
1. Addition of ethanol standard solution to the assay mixture:
Instead of sample solution the standard solution is used for the assay.

2. Restart of the reaction, quantitatively:
After completion of the reaction with sample solution and measuring of A_2, add 0.05 ml standard solution to the assay mixture. Read absorbance A_3 after the end of the reaction (approx. 5 min). Calculate the concentration from the difference of (A_3-A_2) according to the general equation for calculating the concentration. The altered total volume must be taken into account. Because of the dilution of the assay mixture by addition of the standard solution, the result differs insignificantly from the data stated on the bottle label.

3. Internal standard
The standard solution can be used as an internal standard in order to check the determination for correct performance (gross errors) and to see whether the sample solution is free from interfering substances:

Pipette into cuvettes	blank	sample	standard	sample + standard
reaction mixture 2	3.00 ml	3.00 ml	3.00 ml	3.00 ml
redist. water	0.10 ml	–	–	–
sample solution	–	0.10 ml	–	0.05 ml
standard solution	–	–	0.10 ml	0.05 ml
mix, and read absorbances of the solutions (A_1) after approx. 3 min. Continue as described in the pipetting scheme under "Procedure". Follow the instructions given under "Instructions for performance of assay" and the footnotes.				

The recovery of the standard is calculated according to the following formula:

$$\text{recovery} = \frac{2 \times \Delta A_{\text{sample + standard}} - \Delta A_{\text{sample}}}{\Delta A_{\text{standard}}} \times 100\ [\%]$$

BOEHRINGER MANNHEIM

992.203 668 559 id

With coutesy: Boehringer Mannheim, FRG.

Glycerol detection test

Glycerol

1 UV-method

for the determination of glycerol in foodstuffs and other materials

Determination of glycerol and dihydroxyacetone in cosmetics see under Pt. 5.

Determination of triglycerides: see separate instructions

0 3 5 **Cat. No. 148270**

Test-Combination for ca. 3 x 10 determinations

Biochemical Analysis
Food Analysis

Not for use in *in vitro* diagnostic procedures for clinical diagnosis.

Recommendations to methods and standardized procedures see references.

Principle (Ref. 1)

Glycerol is phosphorylated by adenosine-5'-triphosphate (ATP) to L-glycerol-3-phosphate in the reaction catalyzed by glycerokinase (GK) (1).

(1) Glycerol + ATP $\xrightarrow{GK}$ L-glycerol-3-phosphate + ADP

The adenosine-5'-diphosphate (ADP) formed in the above reaction is reconverted by phosphoenolpyruvate (PEP) with the aid of pyruvate kinase (PK) into ATP with the formation of pyruvate (2).

(2) ADP + PEP $\xrightarrow{PK}$ ATP + pyruvate

In the presence of the enzyme lactate dehydrogenase (L-LDH) pyruvate is reduced to L-lactate by reduced nicotinamide-adenine dinucleotide (NADH) with the oxidation of NADH to NAD (3).

(3) Pyruvate + NADH + H$^+$ $\xrightarrow{L\text{-}LDH}$ L-lactate + NAD$^+$

The amount of NADH oxidized in the above reaction is stoichiometric with the amount of glycerol. NADH is determined by means of its absorption at 334, 340 or 365 nm.

The Test-Combination contains

1. Three bottles 1, with approx. 2 g coenzyme/buffer mixture each, consisting of:
   glycylglycine buffer, pH 7.4; NADH, 7 mg; ATP, 22 mg; PEP, 11 mg; magnesium sulfate; stabilizers.
2. Bottle 2 with 0.4 ml enzyme suspension, consisting of:
   pyruvate kinase, approx. 240 U; lactate dehydrogenase, approx. 220 U.
3. Bottle 3 with 0.4 ml glycerokinase suspension, approx. 34 U.
4. Standard solution.

Preparation of solutions for 10 determinations

1. Dissolve contents of one bottle 1 with 11 ml redist. water. Before use allow the solution to stand for approx. 10 min at room temperature.
2. Use contents of bottle 2 undiluted.
3. Use contents of bottle 3 undiluted.

Stability of solutions

Solution 1 is stable for 4 days at +4°C.
Bring solution 1 to 20–25°C before use.
Suspension of bottles 2 and 3 are stable for 1 year at +4°C.

Procedure

Wavelength[1]: 340 nm, Hg 365 nm or Hg 334 nm
Glass cuvette[2]: 1 cm light path
Temperature: 20–25°C
Final volume: 3.02 ml
Read against air (without a cuvette in the light path) or against water.
Sample solution: 3–40 µg glycerol/cuvette[3] (in 0.1–2.0 ml sample volume).

Pipette into cuvettes	blank	sample
solution 1	1.00 ml	1.00 ml
redist. water	2.00 ml	1.90 ml
sample solution*	–	0.10 ml
suspension 2	0.01 ml	0.01 ml
mix**, wait for completion of the reaction[4] (approx. 5–7 min) and read absorbances of the solutions (A_1). Start reaction by addition of:		
suspension 3	0.01 ml	0.01 ml
mix**, wait for completion of the reaction (approx. 5–10 min) and read the absorbances of blank and sample immediately one after another (A_2). If the reaction has not stopped after 15 min, continue to read the absorbances at 2 min intervals until the absorbance decreases constantly over 2 min.		

* Rinse the enzyme pipette or the pipette tip of the piston pipette with sample solution before dispensing the sample solution.

** For example, with a plastic spatula or by gentle swirling after closing the cuvette with Parafilm® (registered trademark of the American Can Company, Greenwich, Ct., USA).

If the absorbance A_2 decreases constantly, extrapolate the absorbances to the time of the addition of suspension 3.

Determine the absorbance differences (A_1–A_2) for both, blank and sample. Subtract the absorbance difference of the blank from the absorbance difference of the sample.

$$\Delta A = \Delta A_{sample} - \Delta A_{blank}$$

The absorbance differences measured should as a rule be at least 0.100 absorbance units to achieve sufficiently accurate results (see "Instructions for performance of assay").

If the absorbance difference of the sample (ΔA_{sample}) is higher than 1.000 (measured at 340 nm, Hg 334 nm resp.) or 0.500 (measured at Hg 365 nm) respectively, the concentration of glycerol in the sample solution is too high. The sample is to be diluted according to the dilution table in that case.

Calculation

According to the general equation for calculating the concentration:

$$c = \frac{V \times MW}{\varepsilon \times d \times v \times 1000} \times \Delta A \text{ [g/l], where}$$

V = final volume [ml]
v = sample volume [ml]
MW = molecular weight of the substance to be assayed [g/mol]
d = light path [cm]
ε = absorption coefficient of NADH at
340 nm = 6.3 [l x mmol^{-1} x cm^{-1}]
Hg 365 nm = 3.4 [l x mmol^{-1} x cm^{-1}]
Hg 334 nm = 6.18 [l x mmol^{-1} x cm^{-1}]

It follows for glycerol:

$$c = \frac{3.02 \times 92.1}{\varepsilon \times 1 \times 0.1 \times 1000} \times \Delta A = \frac{2.781}{\varepsilon} \times \Delta A \text{ [g glycerol/l sample solution]}$$

If the sample has been diluted during preparation, the result must be multiplied by the dilution factor F.

When analyzing solid and semi-solid samples which are weighed out for sample preparation, the result is to be calculated from the amount weighed:

$$\text{content}_{glycerol} = \frac{c_{glycerol} \text{ [g/l sample solution]}}{c_{sample} \text{ [g/l sample solution]}} \times 100 \text{ [g/100 g]}$$

1 The absorption maximum of NADH is at 340 nm. On spectrophotometers, measurements are taken at the absorption maximum; when spectralline photometers equipped with a mercury vapour lamp are used, measurements are taken at a wavelength of 365 nm or 334 nm.

2 If desired, disposable cuvettes may be used instead of glass cuvettes

3 See instructions for performance of the assay

4 It is necessary to wait for completion of this pre-reaction (ADP in ATP and pyruvate in PEP react), otherwise the results will be too high.

Instructions for performance of assay
The glycerol content present in the cuvette should range between 3 µg and 40 µg. The sample solution must therefore be diluted sufficiently to yield a glycerol concentration between 0.03 and 0.4 g/l.

Dilution table

estimated amount of glycerol per liter	dilution with water	dilution factor F
< 0.4 g	–	1
0.4–4.0 g	1 + 9	10
4.0–40 g	1 + 99	100
> 40 g	1 + 999	1000

If the absorbance difference measured (ΔA) is too low (e. g., < 0.100), the sample solution should be prepared anew (weigh out more sample or dilute less strongly) *or* the sample volume to be pipetted into the cuvette can be increased up to 2.0 ml. The volume of water added must then be reduced so as to obtain the same final volume for the sample and blank in the cuvettes. The new sample volume v must be taken into account in the calculation.

1. Instructions for sample preparation

1.1. Liquid foodstuffs

Use clear, colorless or slightly colored solutions directly or after dilution for the assay. Filter turbid solutions or clarify with Carrez reagents. Strongly colored solutions which are used undiluted for the assay because of their low glycerol concentration are to be decolorized with polyamide or polyvinylpolypyrrolidone (PVPP). Carbonic acid containing beverages are to be degassed.

Examples:

Determination of glycerol in fruit juices
Dilute the sample to yield a glycerol concentration of less than 0.5 g/l (see dilution table).
Filter turbid juices. Use the clear solution for the assay, even if it is slightly colored.
When analyzing **strongly** colored juices (e.g., sour cherry juice, grape juice), decolorize the sample as follows:
Mix 10 ml of juice and approx. 0.1 g of polyamide powder or polyvinylpolypyrrolidone (PVPP), stir for 1 min and filter. Use the clear solution, which may be slightly colored, for the assay.

Determination of glycerol in wine
Dilute the sample according to the dilution table.
In general, red wine can also be analyzed without decolorization.

Determination of glycerol in beer
To remove the carbonic acid, stir about 5–10 ml of beer for approx. 1 min using a glass rod or filter; dilute the largely CO_2-free sample according to the dilution table.

1.2. Solid foodstuffs

Mince the sample (using a morfar, meat grinder or homogenizer) and mix thoroughly. Weigh out the sample and extract with water heated to 60°C, if necessary. Transfer to a volumetric flask and fill up to the mark with water. Filter and use the clear solution for the assay. Dilute the solution, if necessary (see dilution table).

Examples:

Determination of glycerol in marzipan
Remove chocolate coating of the marzipan if necessary. Weigh approx. 1 g of marzipan accurately into a small porcelain cup containing approx. 2 g sea-sand, grind thoroughly, mix with approx. 50 ml water and incubate at approx. 60°C for 20 min. Pour supernatant solution into a 100 ml volumetric flask. Wash the residue (sea-sand) twice with portions of 10 ml water each and transfer the wash solution into the volumetric flask. Allow the solution in the volumetric flask to cool to room temperature and fill up to the mark with water. For separation of fat, place in a refrigerator for 15 min. Filter the solution, centrifuge, if necessary, at 3000 rpm. Use the largely clear solution for the assay, dilute, if necessary (see dilution table).

Determination of glycrol in tobacco products
Mix and mince sample thoroughly (grain size max. 0.2 mm). Weigh approx. 1 g accurately into a 100 ml volumetric flask. After addition of approx. 70 ml water stir vigorously (magnetic stirrer) for approx. 1 h at room temperature. Fill up to the mark with water, mix and filter. Pipette 25 ml filtrate into a 50 ml volumetric flask, add successively and stir vigorously after each addition: 5 ml Carrez-I-solution (3.60 g $K_4[Fe(CN_6)] \cdot 3H_2O$/100 ml), 5 ml Carrez-II-solution (7.20 g $ZnSO_4 \cdot 7\,H_2O$/100 ml) and 10 ml NaOH (0.1 mol/l). Fill up to the mark with water, mix and filter. Use the filtrate for the assay (0.1–0.5 ml).

2. Specificity
The method is specific for glycerol. Dihydroxyacetone is not converted under the given conditions (see also pt. 5).

3. Sources of error
The slow hydrolysis of ATP and phosphoenolpyruvate as well as the air oxidation of NADH results in a slow creep reaction which can be taken into account by extrapolation. An extrapolation is not absolutely necessary if the absorbance of blank and sample are measured immediately one after another.

Detection of interferences of the test system
When the enzymatic reaction is complete after the time given in "Procedure" it can be concluded in general that the reaction is not interfered. For assurance of results a re-start of the reaction (qualitatively or quantitatively) by the addition of 'standard material' can be done: a further change of absorbance proves suitability of measurements.

For the detection of gross errors when performing the assays and of interfering substances in the sample material it is recommened to analyze a sample solution in a double determination with two different sample volumes (e. g., 0.10 ml and 0.20 ml): the measured absorbance differences have to be proportional to the sample volumes.

When analyzing solid samples it is recommened to weigh in two different amounts (e. g., 1 g and 2 g) into 100 ml volumetric flasks and to perform the determinations with the sample volume: the absorbance differences have to be proportional to the amounts weighed in.

4. Further applications
The method may also be used in the examination of paper (Ref. 3), cosmetics (Ref. 9) and in research when analyzing biological samples. For details of sampling, treatment and stability of the sample see Ref. 1.

4.1 Determination of glycerol in cosmetics

Determination of glycerol in skin tonic
Dilute sample as far as the glycerol concentration lies under 0.4 g/l. Use undiluted or diluted sample for the assay.

Determination of glycerol in pre-shave, after-shave
If the after-shave is mixable with water without the occurance of a turbidity, proceed according to skin tonic.

If a turbidity occurs after diluting the after-shave with water, this turbidity has to be removed with polyamide or activated charcoal (Clarocarbon® F; registered trademark of E. Merck, Darmstadt, W.-Germany):

Mix 1.0 ml after-shave with 9.0 ml water, add 100 mg polyamide or activated charcoal, mix again and filter (dilution factor: 10).

If the glycerol concentration in the filtrate is lower than 0.02 g/l, the sample volume which has to be pipetted into the cuvette, can be increased up to 2.0 ml. The quantity of water which has to be added must be reduced accordingly.

Determination of glycerol in skin cream
Weigh approx. 1 g skin cream accurately into a 100 ml volumetric flask, add approx. 70 ml water and keep at 60°C for 30 min, while occasionally shaking. After cooling to room temperature, fill up to the mark with water. Place volumetric flask in a refrigerator or better in an ice-bath for 15 min. Filter or centrifuge solution.
If necessary dilute filtrate or supernatant and use for the assay.

Determination of glycerol in toothpaste
Weigh approx. 1 g toothpaste accurately into 100 ml beaker, add approx. 70 ml water and extract for 30 min at 60°C while stirring (heatable magnetic stirrer). Transfer suspension into centrifuge tube. Pour the clear supernatant into a 250 ml volumetric flask after centrifugation. Rinse precipitate with water into a beaker and repeat extraction one to two times. Fill up the volumetric flask to the mark, filter, if necessary.
Depending on the glycerol concentration use clear solution, respectively the filtrate directly or after dilution with water for the determination. If the glycerol concentration in the clear solution or in the filtrate is lower than 0.02 g/l the sample volume, which has to be pipetted into the cuvette, can be increased up to 2.0 ml. The water quantity, to be added, has to be reduced accordingly.

Determination of glycerol in soap
Weigh approx. 1 g grated soap accurately into a beaker, add approx. 50 ml HCl (0.1 mol/l) and while stirring vigorously incubate on a heatable magnetic stirrer until boiling. Transfer aqueous phase with a pipette into a 100 ml volumetric flask. Repeat extraction with approx. 30 ml HCl (0.1 mol/l). Bring volumetric flask to room

temperature and fill up to the mark with redist. water. Place volumetric flask in an ice-bath or refrigerator for 15 min. Filter through a fluted filter. Use filtrate, depending on the expected glycerol concentration, diluted or undiluted for the determination.

If the glycerol concentration is lower than 0.02 g/l, the volume which has to be pipetted into the cuvette can be increased up to 2.0 ml. In this case the volume of the water quantity to be added has to be reduced accordingly.

4.2 Determination of glycerol in plasma and serum (Ref. 1,2)

Mix 1.0 ml of plasma or serum with 4.0 ml of redist. water in a centrifuge tube and incubate in a boiling water-bath for 5 min, centrifuge. Use 0.5 ml of the supernatant for the assay.

The dilution factor F (depending on sample preparation) is obtained from the sample volume (1.0 ml), the volume of redist. water (4.0 ml), the specific gravity of the sample material (1.03 g/ml plasma or serum) and the fluid content (0.92 in case of plasma or serum):

$$F = \frac{1.0 \times 1.03 \times 0.92 + 4.0}{1.0} = 4.95$$

Calculation:

$$c = \frac{0.5563 \times \Delta A \times F}{\varepsilon} \text{ [g glycerol/l sample]}$$

$$c = \frac{6.040 \times \Delta A \times F}{\varepsilon} \text{ [mmol glycerol/l sample]}$$

Wavelength	Hg 365 nm	340 nm	Hg 334 nm
c [g/l]	0.8099 x ΔA	0.4371 x ΔA	0.4456 x ΔA
c [mmol/l]	8.794 x ΔA	4.746 x ΔA	4.838 x ΔA

4.3 Determination of "total glycerol" (= free and esterified glycerol; Ref. 10) in serum

Mix 0.2 ml of serum with 0.5 ml of ethanolic potassium hydroxide (0.5 mol/l; free of glycerol!) in a centrifuge tube. Cover the tube with Parafilm® (registered trademark of American Can Co., Greenwich, Ct., USA) and incubate for 30 min at 55°C (or for 60 min at 37°C, respectively) in a water-bath. Allow to cool to room temperature, add 1.0 ml of magnesium sulfate solution (0.15 mol/l; free of glycerol), mix and centrifuge. Use 0.5 ml of the clear supernatant for the assay.

The dilution factor F (depending on sample preparation) is obtained from the sample volume (0.2 ml), the volume of the ethanolic potassium hydroxide (0.5 ml), the specific gravity of the sample material (1.03 g/ml serum), and the fluid content (0.92 in case of serum):

$$F = \frac{0.2 \times 1.03 \times 0.92 + 0.5 + 1.0}{0.2} = 8.45$$

Calculation:

$$c = \frac{0.5563 \times \Delta A \times F}{\varepsilon} \text{ [g "total glycerol"/l sample]}$$

$$c = \frac{6.040 \times \Delta A \times F}{\varepsilon} \text{ [mmol "total glycerol"/l sample]}$$

Wavelength	Hg 365 nm	340 nm	Hg 334 nm
c [g/l]	1.383 x ΔA	0.7462 x ΔA	0.7606 x ΔA
c [mmol/l]	15.01 x ΔA	8.101 x ΔA	8.259 x ΔA

4.4 Determination of glycerol in fermentation samples and cell culture media

Place the sample (after centrifugation, if necessary) into a water-bath at 80°C for 15 min to stop enzymatic reactions. Centrifuge and use the supernatant (diluted according to the dilution table, if necessary) for the assay. Alternatively, deproteinization can be carried out with perchloric acid or with Carrez-solutions. See the above-mentioned examples.

Homogenize gelantinous agar media with water and treat further as described.

4.5 Determination of triglycerides by means of glycerol after enzymatic hydrolysis

An especially advantageous method of analyzing the fat content in dairy products, such as milk, yogurt or fresh cheese, is effected by means of glycerol determination after enzymatic hydrolysis of the triglycerides. The assay is carried out without sample preparation and does, in particular, not include preceding isolation of fat in the diluted sample. Using this method, it is possible to determine the fat content in milk, even in low-fat products (see separate instructions "Triglycerides").

5. Determination of glycerol and dihydroxyacetone (Ref. 13, 14) in cosmetics

In the enzymatic reaction catalyzed by GK, dihydroxyacetone is also phosphorylated (4) by ATP to dihydroxyacetone phosphate (DAP).

(4) Dihyroxyacetone + ATP $\xrightarrow{GK}$ DAP + ADP

The ADP formed hereby is converted according to the reactions (2, 3). Also here NADH is determined by means of its absorbance.
The actually consumed NADH amount is stoichiometric with the dihydroxyacetone amount.

Because both reactions are catalyzed by GK, a differentiation between glycerol and dihydroxyacetone can only be made by different GK activities in the assay. A slight GK activity is necessary for the conversion of glycerol. Glycerol is converted with approx. 0.2 U GK/assay in approx. 10 min whereas dihydroxyacetone is converted practically not at all. After completion of the glycerol reaction, dihydroxyacetone is also converted entirely by increase in activity of GK (4 U) in approx. 40 min.

Reagents

1. Test-Combination Glycerol, Cat. No. 148 270[5]
2. Glycerokinase, Cat. No. 127 795[5]
3. Ammonium sulfate, $(NH_4)_2SO_4$, A. R.
4. Dihydroxyacetone (for standard solution only)

Preparation of solutions

I. **Buffer coenzyme solution**
Dissolve contents of one bottle 1 of the Test-Combination Glycerol with 11 ml redist. water. Leave approx. 10 min at room temperature before use.

II. **Pyruvate kinase/Lactate dehydrogenase, PK/LDH**
Use contents of bottle 2 of the Test-Combination undiluted.

III. **Glycerokinase, GK, diluted**
(0,25 mg/ml):
Mix 0.1 ml of the contents of bottle 3 of the Test-Combination with 0.3 ml ammonium sulfate solution (V).
The diluted suspension is stable for 6 months at +4°C.

IV. **Glycerokinase, GK, concentrated**
(5 mg/ml):
Use suspension undiluted.
The suspension is stable for 1 year at +4°C.

V. **Ammonium sulfate solution**
(3.2 mol/l):
Dissolve 42.3 g $(NH_4)_2SO_4$ in a 100 ml volumetric flask with approx. 80 ml redist. water, afterwards fill up to 100 ml with redist. water.
The solution is stable for 1 year at 20–25°C.

VI. **Standard solution**
(0.40 g Dihydroxyacetone/l):
Dissolve 40 mg dihydroxyacetone with 100 ml redist. water. Prepare freshly before use.
The measuring of the standards is only necessary for checking the procedure.

Pipette into cuvettes	blank	sample
solution (I)	1.00 ml	1.00 ml
suspension (II)	0.01 ml	0.01 ml
redist. water	2.00 ml	1.90 ml
sample solution	–	0.10 ml
Mix, after approx. 5–7 min read absorbances of the solutions (A_1). Start reaction by addition of		
suspension (III)	0.01 ml	0.01 ml
mix, wait for completion of the reaction (approx. 10–15 min) and read the absorbances of the solutions (A_2). If the reaction has not stopped after 15 min (e. g., with high concentrations of dihydroxyacetone), continue to read the absorbances at 2 min intervals until the absorbances decrease constantly over 2 min. Further addition of		
suspension (IV)	0.01 ml	0.01 ml
mix, after completion of the reaction (approx. 40–45 min) read absorbances of the solutions (A_3).		

* The reaction is finished when sample and blank show the same absorbance change.

5 Available from Boehringer Mannheim GmbH.

If the absorbance of A_2 decreases constantly, the absorbance is extrapolated to the addition of suspension III. Determine the absorbance differences (A_1–A_2) for both blank and sample. Substract the absorbance difference of the blank from the absorbance difference of the sample, thereby obtaining $\Delta A_{glycerol}$.

Determine the absorbance differences for both blank and sample (extrapol. A_2–A_1). Subtract the absorbance difference of the blank from the absorbance difference of the sample, thereby obtaining $\Delta A_{dihydroxyacetone}$.

Calculation

It follows for glycerol:

$$c = \frac{3.02 \times 92.1}{\varepsilon \times 1 \times 0.1 \times 1000} \times \Delta A = \frac{2.781}{\varepsilon} \Delta A \text{ [g glycerol/l sample solution]}$$

for dihydroxyacetone:

$$c = \frac{3.03 \times 90.1}{\varepsilon \times 1 \times 0.1 \times 1000} \times \Delta A = \frac{2.730}{\varepsilon} \Delta A \text{ [g dihydroxyacetone/l sample solution]}$$

If the sample has been diluted during preparation, the result must be multiplied by the dilution factor F.

Instructions for sample preparation

Cosmetics in emulsion form

(milk, oil in water emulsion)

Weigh approx. 5 g of the sample material accurately into a 250 ml volumetric flask, add approx. 200 ml water and keep at approx. 60°C for 15 min. Swirl flask frequently. After cooling to room temperature fill up to 250 ml with water, mix. Filter the solution through a fluted filter. Discard the first few ml. Mix 10 ml of the frequently opalescent solution with 10 ml trichloroacetic acid solution (30 mmol/l), centrifuge after 5 min (10 min, 5000 rpm). Use the clear solution, diluted if necessary, for the assay.

Cosmetics in lotion form

(Lotion, solid particles suspended in water)

Weigh approx. 5 g sample material accurately into a 250 ml volumetric flask, add approx. 200 ml water and keep at 60°C for 15 min. Further procedures see "emulsions".

Cosmetics in ointmentform

(Ointments, creams, water in oil emulsions)

Weigh approx. 2 g sample accurately into a 250 ml volumetric flask, add approx. 200 ml water and keep at 60°C for 15 min. Swirl flask frequently. After cooling to room temperature fill up to the mark with water, mix. Place inside refrigerator for 20 min in order to separate the fat, filter. Discard the first few ml. Mix 10 ml of the possibly still opalescent solution with 10 ml trichloroacetic acid solution (30 mmol/l), and centrifuge after 5 min (10 min at 5000 rpm). Use the clear solution for assay.

References

1 Eggstein, M. & Kuhlmann, E. (1974) in Methoden der enzymatischen Analyse (Bergmeyer, H. U., Hrsg.) 3. Aufl., Bd. 2, S. 1871-1877, Verlag Chemie, Weinheim, and (1974) in Methods of Enzymatic Analysis (Bergmeyer, H. U., ed.) 2nd ed., vol. 4, pp. 1825-1831; Verlag Chemie, Weinheim/Academic Press, Inc., New York and London.
2 Wieland, O. H. (1984) in Methods of Enzymatic Analysis (Bergmeyer, H. U. ed.) 3rd ed., vol. VI, pp. 504-510, Verlag Chemie, Weinheim, Deerfield Beach/Florida, Basel.
3 Untersuchung von Papieren, Kartons und Pappe für Lebensmittel-Verpackungen (gem. Empf. XXXVI der Kunststoffkommission des Bundesgesundheitsamtes) Kapitel 8 (Methoden), Pkt. 3.5.2. (März 1979).
4 Gombocz, E., Hellwig, E., Vojir, F. & Petuely, F. (1981) Deutsche Lebensmittel-Rundschau 77, 8.
5 Holbach, B. & Woller, R. (1976) Uber den Zusammenhang zwischen Botrytisbefall von Trauben und den Glycerin- sowie Gluconsäuregehalt von Wein, Weinwissenschaft 31, 202-214.
6 Holbach, B. & Woller, R. (1977) Vergleichende Glycerinbestimmung im Wein nach der Methode Rebelein und der enzymatischen Methode, Weinwissenschaft 32, 212-218.
7 Wagner, K. & Kreutzer, P. (1978) Beitrag zur Glycerinbestimmung in Wein, Likörwein und weinhaltigen Getränken, Weinwissenschaft 33, 109-113.
8 Michal, G. (1976) Enzymatische Analyse in der Pharmazie, Acta Pharmaceutica Technologica, Suppl. 1, S. 151-162.
9 Henninger, G. & Boos, H. (1978) Anwendung der enzymatischen Analyse bei der Untersuchung kosmetischer Präparate, dargestellt an einigen Beispielen; Seifen – Öle – Fette – Wachse 104, 159-164.
10 Schmidt, F. H. & von Dahl, K. (1968) Zur Methode der enzymatischen Neutralfettbestimmung in biologischem Material, Z. Klin. Chem. Klin. Biochem. 6, 156-159.
11 Pfandl, A. & Menschig, D. (1984) Ein Beitrag zur enzymatischen Glycerin- und Ethanolbestimmung, Pharm. Ind. 46, 403-407.
12 Walter, E. & Kohler, P. (1985) Ringversuch für die enzymatische Bestimmung von Glycerin, Z. Lebensm. Unters. Forsch. 180, 121-125.
13 Wieland, O. (1957) Biochem. Z. 329, 313.
14 Wieland, O. & Witt, I. (1974) in Methoden der enzymatischen Analyse (Bergmeyer, H. U., Hrsg.) 3. Auflage, S. 1487, Verlag Chemie, Weinheim, und Wieland, O. (1974) in Methods of Enzymatic Analysis (Bergmeyer, H. U., ed.) 2nd ed., vol. 4, pp 1404; Verlag Chemie, Weinheim/Academic Press, Inc., New York and London.
15 Schweizerisches Lebensmittelbuch (1985); Kapitel 61B/2.2
16 Klopper, W. J., Angelino, S.A.G.F., Tuning, B. & Vermeire, H. A. (1986) Organic acids and glycerol in beer, J. Inst. Brew. 92, 225-228.

3. Internal standard

The standard solution can be used as an internal standard in order to check the determination for correct performance (gross errors) and to see whether the sample solution is free from interfering substances:

Pipette into cuvettes	blank	sample	standard	sample + standard
solution 1	1.00 ml	1.00 ml	1.00 ml	1.00 ml
suspension 2	0.01 ml	0.01 ml	0.01 ml	0.01 ml
redist. water	2.00 ml	1.90 ml	1.90 ml	1.90 ml
sample solution	–	0.10 ml	–	0.05 ml
standard solution	–	–	0.10 ml	0.05 ml
mix, and read absorbances of the solutions (A_1) after approx. 7 min. Continue as described in the pipetting scheme under "Procedure". Follow the instructions given under "Instructions for performance of assay" and the footnotes.				

The recovery of the standard is calculated according to the following formula:

$$\text{recovery} = \frac{2 \times \Delta A_{sample + standard} - \Delta A_{sample}}{\Delta A_{standard}}$$

BOEHRINGER MANNHEIM

Glycerol standard solution

for Test-Combination Glycerol

UV-method, Cat. No. 148 270

Concentration: see bottle label.

Glycerol standard solution is a stabilized aqueous solution of glycerol. It is used as standard solution for enzymatic determination of glycerol in foodstuffs and other sample materials.

Application

1. Addition of glycerol standard solution to the assay mixture:
The standard solution is used for the determination instead of the sample solution.

2. Restart of the reaction, quantitatively:
After completion of the reaction with sample solution and measuring of A_2, add 0.02 ml standard solution to the assay mixture. Read absorbance A_3 after the end of the reaction (approx. 15 min). Calculate the concentration from the difference of (A_2–A_3) according to the general equation for calculating the concentration. The altered total volume must be taken into account. Because of the dilution of the assay mixture by addition of the standard solution, the result differs insignificantly from the data stated on the bottle label.

02.93.151 249 041 10

Spurr' resin

TAAB LABORATORIES EQUIPMENT LIMITED

3 MINERVA HOUSE CALLEVA INDUSTRIAL PARK
ALDERMASTON BERKSHIRE ENGLAND RG7 4QW

TEL 0734 817775 FAX 0734 817881 TELEX 847928

SPURR'S RESIN

This low viscosity embedding resin developed for electron microscopy has proved very popular for more than 20 years but more recently has been the subject of much speculation over its toxicity. This has resulted in an increase in the use of TAAB premix resin kits which limit the handling of the components and unused resin mixture can be left in the containers to harden before disposal eliminating the need for washing up with its associated risks. Full details of the resin are obtained from the paper referenced below.

The suggested standard embedding medium is formulated as follows:-

ERL 4206 resin	10.0ml
DER 736 (flexibiliser)	6.0ml
NSA hardener	26.0ml
'S1 accelerator	0.4ml

This mixture has a pot-life of 3-4 days and should be cured for 8 hours at 70°C. Harder or softer blocks can be obtained by *varying* the quantity of DER 736 between 4.0ml and 8.0ml, *increasing* the quantity of DER 736 giving softer blocks.

A *rapid* cure may be effected in 3 hours by increasing the quantity of S1 to 1.0ml, but this reduces the pot-life to 2 days.

The component in Spurr resin giving most concern over its toxicity is ERL 4206. There have also been claims regarding the carcinogenicity. It should be assumed therefore that ERL 4206 is both toxic and carcinogenic and extreme caution should always be exercised when using the chemical and its users should be restricted to competent technicians only, a *recommendation* we would give with the use of *all* resins.

We are now supplying S1 in quantities of 25ml in the S024 Spurr kit. Since the material has limited shelf life of up to 6 months, we feel that our decision will prevent the inadvertent use of old material, thereby preventing inconsistent results.

Arthur R. Spurr, J.Ultrastructure Research, 26,31-43 (1969).

HANDLING PRECAUTIONS:

All epoxy resins *may* cause dermatitis and therefore care *should* be taken to avoid skin or eye contact. Skin may be washed with soap and plenty of water. Eyes should be irrigated with copious quantities of water. Contaminated clothing should be changed immediately. Cured resins are inert although resin dust should be avoided. Always wear gloves and use a fumehood whenever possible.

Catalogue reference

S024 Spurr's resin kit

S031 Spurr Premix kit, hard

S032 Spurr Premix kit, medium

S033 Spurr Premix kit, soft

All components are available separately and in varying quantities.

A full range of embedding moulds and capsules, together with safety and protection equipment, chemicals and clothing are listed in TAAB's full 232 page catalogue No.4.

With coutesy:TAAB laboratories equipment limited, England.